CORROSION INHIBITION IN FLOWING AQUEOUS MEDIA.

A Thesis for the Degree of

Doctor of Philosophy

presented by

Martin Robert Berry. B.Sc. (Tech.)

University of Manchester Institute of Science & Technology,
Department of Chemical Engineering.

October, 1967.

ProQuest LLC.
789 East Eisenhower Parkway
P.O. Box 1346
Ann Arbor, MI 48106 – 1346

A C K N O W L E D G M E N T S.

The author wishes to express his gratitude to the following -

Professor F.Morton and Professor T.K.Ross for the provision of reseach facilities within the Department of Chemical Engineering.

Professor T.K.Ross for his continued interest, encouragement, and supervision throughout the reseach.

The Geigy Company Limited for the provision of a reseach grant.

His mother for typing the thesis.

Thanks are also conveyed to the technical and laboratory staff of the Department.

D E C L A R A T I O N.

The work reported in this thesis is original. No part of the work has been submitted for a degree at any other University.

B I O G R A P H I C A L N O T E.

The author graduated with a 2nd.Class Division II Honours degree in Chemical Engineering in I964 in the University of Manchester Institute of Science and Technology. The present reseach has been carried out in the Corrosion Science section of the Department of Chemical Engineering during the period October I964 to October I967.

ABSTRACT.

The reseach contains a brief literature survey of corrosion and inhibition, both in static and flowing media. Preliminary work was carried out in static medium before employing the flow system. The experimental techniques used were weight loss, potential, capacitance, and polarisation measurements.

Pretreated copper, and also pretreating the medium with benzotriazole within certain concentration limits, greatly increases the corrosion resistance of copper in static media. This confirms previous findings.

In flowing media the protective power of the inhibitor is reduced. A theory has been put forward to account for this. The degree of attack depends on the ratio of cuprous to cupric benzotriazoles present at the metal surface.

The experiments also showed that the fraction of area of surface coverage by the inhibitor (determined by capacitance measurements) cannot be the sole criterion for determining inhibitor efficiency in flowing medium. In fact in a static medium, the area of surface coverage very closely followed the inhibitor efficiency, but not so in a flowing medium.

The results confirmed the findings of other workers that results from static experiments cannot be applied to flowing media.

CONTENTS.

C H A P T E R I.

Literature Survey.

1. 1. General Introduction.

Corrosion has been described as one of the scourges of civilization (1) as it is a universal phenomenon. In Britain alone, the annual cost of corrosion is well over £600M, being incurred by the replacement of materials in maintenance costs, and in lost production (2).

The corrosion scientist tries to eliminate, or greatly reduce, the metal loss due to corrosion. He does so for two reasons - conservation of metals and economics (3).

(1) **Conservation of Metals.**

As the metal resources of the world are limited, unnecessary loss or wastage of metals must be minimised.

(2) **Economics.**

This may be subdivided into two categories - (i) direct and (ii) indirect losses.

(i) **Direct Losses.**

(a) Cost of replacement.

(b) Maintenance.

(ii) **Indirect Losses.**

These losses are far more difficult to assess, but they may be many times more costly than the direct losses.

(a) Shutdown.

(b) Loss of product.

(c) Loss of efficiency.

(d) Contamination.

(e) Overdesign.

(f) Deterioration.

(g) Explosion, Fire Risk, etc.

These are the main problems the corrosion scientist is trying to deal with in his efforts to combat corrosion.

1. 1. Corrosion and Corrosion Principles.

In the study of corrosion over the years, several theories have been advanced to account for certain observed phenomena. These include the Acid Theory, Hydrogen Peroxide Theory, Colloid Theory, and Direct Oxygen Attack Theory, but it is now accepted that corrosion and aqueous solution is a purely electrochemical phenomena. (4,5,6).

In a simple corrosion process, the overall chemical reaction is made up of two elementary reactions - the anodic and cathodic reactions.

The anodic reaction is metal dissolution.

$$M \longrightarrow M^{z+} + ze \qquad (1)$$

This reaction will bein equilibrium at a characteristic potential for this metal, the potential being governed by the relative free energies of the atoms in the lattice and the ions in solution.

For electrical neutrality to prevail, the anodic reaction will be balanced by the cathodic reaction. Two typical cathodic reactions encountered in the corrosion processes are -

$$2H^{+} + 2e \longrightarrow H_2 \qquad (2)$$

$$\text{or} \qquad O_2 + 2H_2O + 2e \longrightarrow 4OH^{-} \qquad (3)$$

These two reactions will have their own characteristic equilibrium potentials dependant on their respective free energy relationships.

When a metal is immersed in solution, some of the metal surface becomes anodic and others cathodic. The formation of anodic areas is favoured by a lack of dissolved

oxygen in the immediate region, or the absence of any protective coating on the metal surface. Electrons, liberated by reaction (I), will transfer via the metal to the cathodic sites to take part in reactions (2) or (3). Normally, if no oxygen is present, the hydrogen evolution reaction (reaction (2)) occurs, but in the presence of oxygen, the oxygen reduction reaction (reaction (3)) takes place.

The standard electrode potential of a metal (E°_{m}) is given for a metal in a solution of metal cations at unit activity. It is often important to know how these values vary with changes in activity, as one metal may be anodic to another metal at one concentration, but when the concentration of ions is altered, the reverse may be true. The relationship is given by the Nernst equation which can be derived from thermodynamic considerations (b):-

$$E_m = E^{\circ}_{m} + \frac{RT}{nF} \ln a_{Me^{n+}}$$

where E_m = electrode potential of metal, M, in a solution of a activity $a_{Me^{n+}}$

Each anodic and cathodic reaction has its unique potential which may be shifted in either direction by the presence or absence of other chemical species, and is a function of the reaction rate. A change in potential with a change in reaction rate is termed polarization. Anodic reactions always polarize in the anodic direction, whereas cathodic reactions polarize cathodically. The causes of electrode polarisation are activation polarisation, concentration polarisation, and IR drop.

(I) Activation Polarization.

This is caused by the fact that the reaction at the electrode requires a certain energy (the activation energy) to initiate it. This polarization is characteristic of metal ion dissolution or deposition. It is small for non-transition metals (eg. Pu, Ca., or Zn). The degree of polarization is also influenced by the anion associated with the metal in solution. In some cases the controlling step is the slow rate of hydration of the metal ion as it leaves the lattice, or the dehydration of the hydrated ion as it enters the metal lattice.

When equilibrium between the metal and the solution is obtained, the anodic dissolution and the cathodic deposition are proceeding at the same rate. (Fig.1.)

$$M \text{ (in lattice)} \rightleftharpoons M^{z+} \text{ (hydrated in solution)} + ze.$$

The exchange current density, i_o, is then given by -

$$i_o = L_a \exp\left(\frac{-\Delta G_A^*}{RT}\right) = L_c \exp\left(\frac{-\Delta G_c^*}{RT}\right)$$

where La and Lc are parameters containing dimensional constants.

If a potential is now applied so that the metal becomes an anode, the equilibrium will be upset. The value of the increase in anodic potential is termed the anodic overpotential (η_A). The displacement of the energies is divided between the anodic and cathodic reactions in the ratio $\alpha/1-\alpha$ where α is the ratio of the distance between the transition state and the lattice energy well to the total distance between the lattice and solution energy

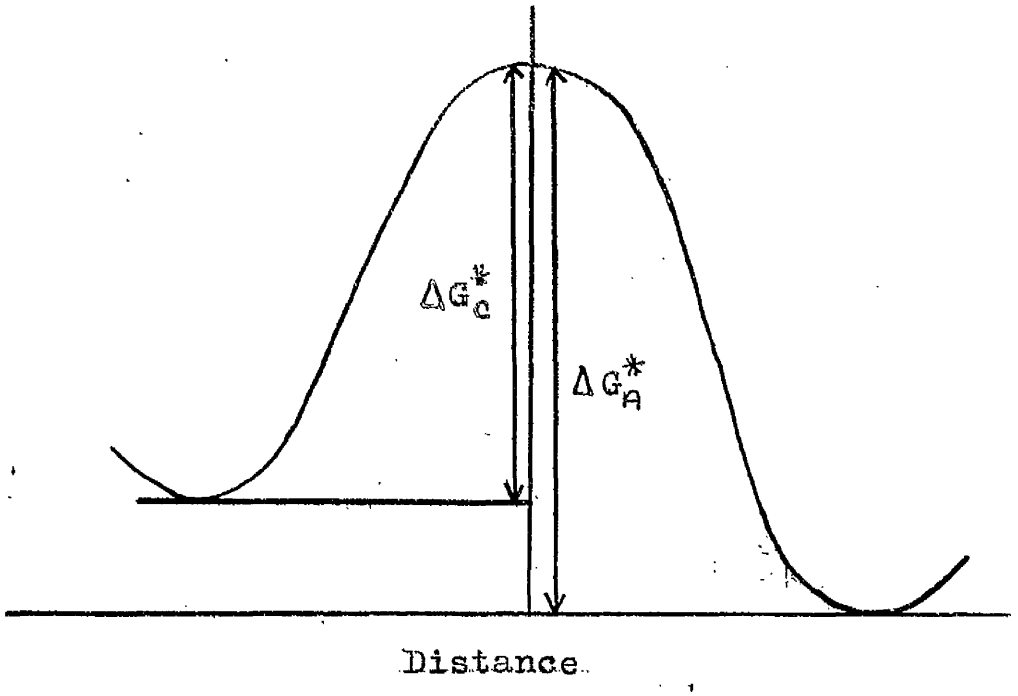

Fig.I Energy/Distance Relationship at a Metal/Solution Interface under Equilibrium Conditions.

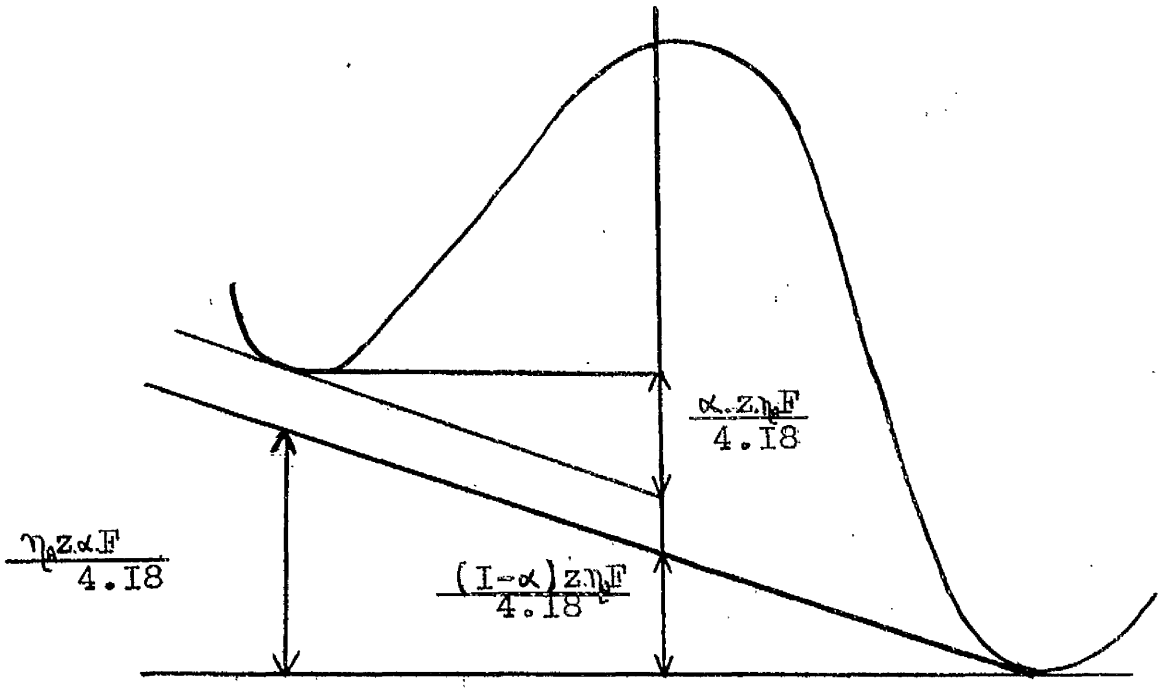

Fig.2 Energy/Distance Relationship at a Metal/Solution Interface Subjected to an Anodic Overpotential, η_A.

wells (Fig.2.) The applied anodic current density is then given by:-

$$i_a = i_o \left[\exp.\left(\frac{\alpha z \eta_A F}{RT}\right) - \exp.\left(\frac{-(1-\alpha) z \eta_A F}{RT}\right) \right]$$

A similar expression may be obtained for the corresponding cathodic process. This equation may be simplified in two cases.

Case 1. When the irreversibility of the electrode process is small and the overpotential is less than 0.02V, the expression may be expanded as $e^x = 1 + x$

$$i_A = i_o . \frac{\eta_A z F}{RT}$$

The anodic current is proportional to the overpotential.

Case 2. When the overpotential is greater than 0.05V and the rate of reaction opposed by the overpotential is small, the second term in the expression may be neglected. This gives, on rearranging the expression -

$$\eta_A = \frac{2.303RT}{F} \log \frac{i_a}{i_o}$$

$$\eta_A = a + b \log. i$$

where a and b are characteristic constants of each electrode process. This equation is known as the Tafel Equation.

η_A is sometimes termed the activation over-potential and is a measure of the extent of the interference with equilibrium at the metal electrode.

(2) Concentration Polarization.

If a metal M is placed in a solution of its ions and made the cathode, the concentration polarization, in the absence of any external current, is given by the Nernst equation -

$$E_1 = E^{\circ}_M - \frac{0.059}{z} \log (M^{z+})$$

When the external current flows, metal is deposited on the electrode and so decreases the concentration of metal ions to $(M^{z+})s$. The oxidation polarization is now -

$$E_2 = E^{\circ}_m - \frac{0.059}{z} \log (M^{z+})s.$$

As $(M^{z+})s < (M^{z+})$, the potential of the polarized cathode is less noble (more active) in the presence of the external current. The value $(E_2 - E_1)$ is the concentration polarization and equals -

$$\frac{0.059}{z} \log \frac{(M^{z+})}{(M^{z+})s}.$$

The larger the current, the smaller the value of $(M^{z+})s$ and the larger the concentration polarization.

When $(M^{z+})s$ approaches zero at the metal electrode, the concentration polarization approaches infinity. The value of the current density is termed the limiting current density (i_L). If the applied current density is i, it can be shown that $E_2 - E_1 = \frac{2.303RT}{zF} \log \frac{i_L}{i_L - i}$.

(3) IR Drop.

This is due to the electrical resistance of a film or the electrolyte. When the current density is i and the film or electrolyte resistance is R, the contribution to the polarization is iR.

Concentration polarization is decreased with electrolyte motion, but activation polarization and IR drop are not significantly affected.

The rate of the overall reaction is controlled by the rate of the slowest elementary step in one of the

reactions. For example, the hydrogen discharge may consist of the following steps -

(a) The hydrogen ion, existing as the hydroxonium ion, diffuses to the metal surface

$$H_3O^+ \longrightarrow \text{Cathode}.$$

(b) H_3O^+ adsorbs to a cathodic point on the metal surface.

(c) An electron is transferred from the metal to the adsorbed hydrogen ion.

(d) The adsorbed hydrogen atom combines with another hydrogen atom in its vicinity, forming hydrogen molecule.

(e) The hydrogen molecule diffuses from the surface.

The slowest of the above reactions determines the overall rate of the hydrogen discharge.

Generally, there are four types of reaction control which are governed by the relative resistances of the anodic, cathodic, and electrolytic reactions. These are easily illustrated by polarization (current/potential) diagrams.

When the two resistances are equal, the corrosion is under mixed control (Fig.3a). If the resistance of the anode is much higher than the cathodic one, anodic control takes place (Fig.3c.) Fig.3b. shows the case of cathodic control. Resistance control (Fig.3d.) occurs when the electrolyte resistance is so high that the resultant current is not sufficient to polarize the anodes or cathodes appreciably.

Inhibitors act by interfering with either the anodic (anodic inhibitors), cathodic (cathodic inhibitors), or both (mixed inhibitors) electrode reactions. Very few

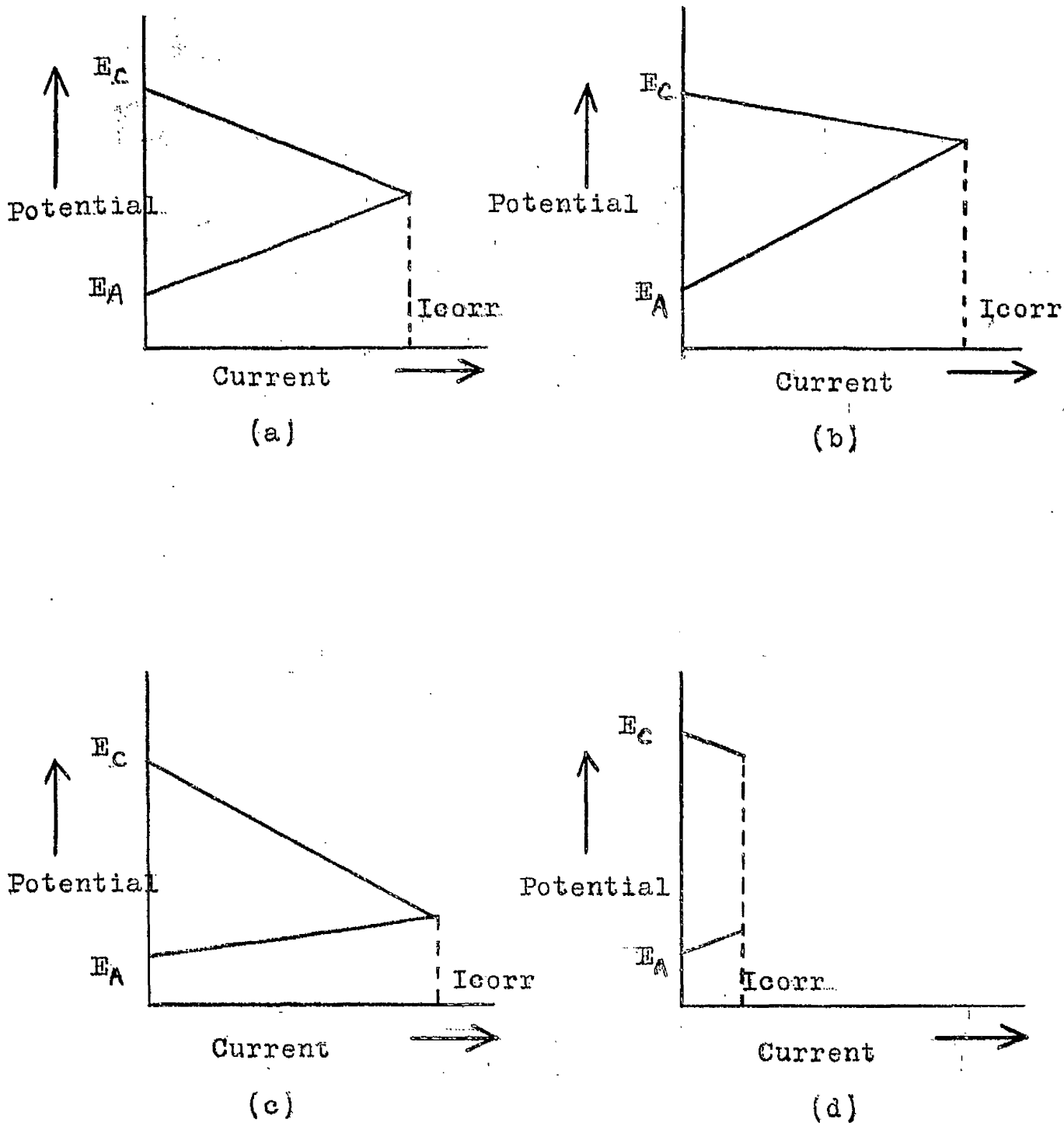

Fig.3 Schematic Representation of the Various Types of Reaction Control.

inhibitors act purely by altering the resistance of the electrolyte.

I.2. Corrosion Prevention.

Some of the methods used by industry to prevent corrosion are outlined here. It is estimated (8) that they cost Britain £500M. per year. For ease of discussion, the methods used may be placed into two categories - kinetic and thermodynamic..

I) Thermodynamic Methods.

(a) Alloying.

Effectively the alloying of a metal in this way increases its nobility and so reduces the driving E.M.F. in the corrosion cell.. The nobility of a metal is a function of its sublimation energy, ionization energy, and solvation energy, which is a function of lattice stability, by increasing the strength of the metallic bonding. As the magnitudes of the ionization or solvation energies cannot be significantly changed, the nobility increases.

Care must be taken when alloying certain metals, as their physical properties may change.

(b) Cathodic Protection.

This form of protection may be effected in two ways - (i) by galvanic action and (ii) by impressed polarization by an external battery or generator, the latter being more easy to control and cheaper to use.

Both these methods employ the same basic principle. The metal to be protected is connected to a source of electrons and is flooded with a high electron concentration.

Consequently metal ions are hindered from crossing the double layer into solution by the adverse electrical potential gradient and the scrap metal, not the metal being protected, dissolves. (Fig. 4.)

This method has some disadvantages -

i) Excessive alkali can be produced causing corrosion products to coat the anode and stifle any protective action.

ii) Any stray currents could affect other metal structures in the vicinity.

2) Kinetic Methods.

(a) Poisons.

Normally the most commonly occurring cathodic reactants are hydrogen ions and dissolved oxygen (not so with Redox reactions).

$$2H^+ + 2e \longrightarrow H_2\,(g) \qquad (1)$$

$$O_2\,(dis) + 2H_2O + 4e \longrightarrow 4OH^- \qquad (2)$$

Poisons operate by preventing one or both of these reactions.

Eg. Hydrazine poisons reaction (2) by reacting with the dissolved oxygen before it reaches the metal surface.

$$N_2H_4 + {}^5\!/_2 O_2 \longrightarrow 2\,NO_2^- + 2\,H^+ + H_2O.$$

Arsenous oxide prevents reaction (1) by converting hydrogen adsorbed on the metal surface to water.

$$As_2O_3 + 6H(ads.) \longrightarrow 2\,As + 3\,H_2O.$$

(b) Anodic Protection.

Some metals have stable and insoluble corrosion products. If these products coat the metal with a layer impermeable to the corroding media, the metal will be

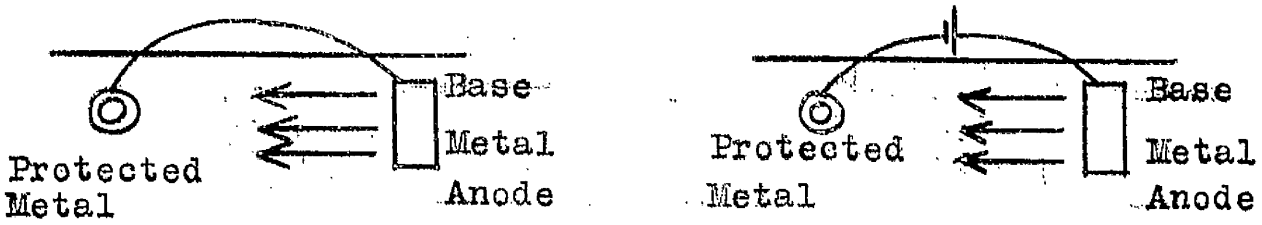

Galvanic Method

Generator Method

Fig.4 Schematic Representation of Cathodic Protection.

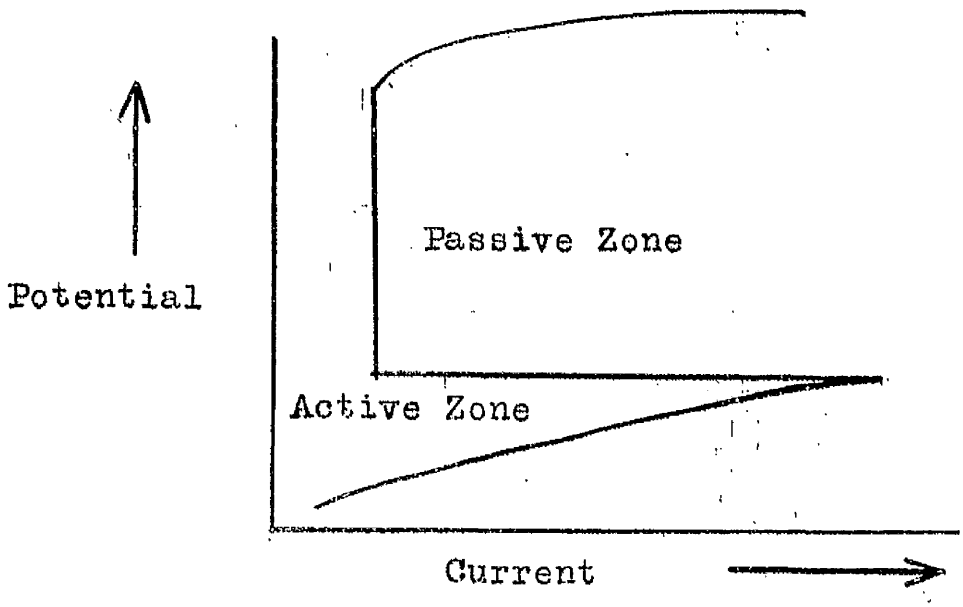

Fig.5 Diagram showing the Passive Zone for Anodic Protection.

protected against further effective corrosion. This phenomena is termed passivity.

Anodic protection induces this state of passivity (cf. cathodic protection where immunity is induced) on the metal. An electric current is passed which brings the metal to its passive zone (Fig. 5) where no effective current flows. If the passive film breaks down, it must be renewed very quickly, otherwise severe pitting corrosion will occur.

This method has the disadvantage that in some cases very large initial currents need to be passed to induce passivity.

(c) Metall and other coatings.

Metall coatings fall into anodic or cathodic categories.

(i) Cathodic Metal Coatings - the base metal is coated with a more noble metal (eg. tin or chromium plating).

This has the disadvantage that unless the coating is 100% effective, very severe pitting will take place. Hence the cathodic coating must be uniform, non-porous, and must not be subjected to treatment likely to cause cracking of the coating.

(ii) Anodic Metal Coatings - in this case the metal is coated with a more active metal (eg. Zn-coated iron). If a crack appears in the coating, the coating dissolves and no pitting results.

The same principles apply to metallic-based paints.

Apart from chemical conversion coatings (eg. the metal oxide, chromate or phosphate), the most common coatings are plastics, glass enamels, bitumens, to which may be added fillers such as asbestos, grease, paint, etc.

These coatings operate simply by interposing a large resistance (ca. 10^6 ohms) between the anodic and cathodic sites so that no current flows. It also excludes water and oxygen from the metal surface.

(d) Filming Inhibitors.

These inhibitors form a barrier, isolating the metal from its environment. Again they fall into two types - anodic and cathodic.

(i) Anodic Inhibitors - these inhibitors de-activate the active (anodic) sites by producing a passivating oxide film on the metal surface where cations are formed. These inhibitors are gradually used up and must be replenished, because below a certain critical concentration of inhibitor, severe pitting will take place. Examples of this type are nitrite and chromate ions.

(ii) Cathodic Inhibitors - this type relies on general coverage of the metal surface and stifling the reaction at the cathode. Eg. bicarbonate ion HCO_3^- leads to the precipitation of a carbonate film under the alkaline cathode conditions.

$$O_2 + 2H_2O + 4e \longrightarrow 4OH^-$$

$$HCO_3^- + OH^- \longrightarrow \downarrow CO_3^{--} + H_2O$$

A third smaller class of filming inhibitors exists - the mixed type whose action is both anodic and cathodic

(eg. benzoate ion).

(e) Vapour-Phase Inhibitors.

When the corrosive environment is atmospheric and not so amenable to soluble inhibitors, air-borne or vapour-phase inhibitors are used. Normally these are used for protecting metals being transported. They are essentially soluble filming inhibitors consisting of nitrite, benzoate, or carbonate anions attached to "parachutes" of a suitable heavy organic cation. The inhibitor slowly evaporates and protection is afforded from both the anion and cation.

(f) Adsorption Inhibitors.

These substances, when added to the corrodent, protect the metal by adsorbing on to the metal surface. A large number of organic inhibitors fall into this category and the complete mechanism of protection is not yet fully understood. It is with this class of inhibitors that this thesis deals.

I.3. Theories and Mechanisms of Inhibition.

Inhibitors of acidic corrosion were known as far back as the middle-ages (9) when master armourers added organic products (eg. flour and yeast) to acid to remove scale from metal articles. Baldwin (10) took out the first patent when he proposed a mixture of molasses and vegetable oil as an additive during the pickling of iron sheets. In 1872 Marangoni and Stephenelli (11) said that the corrosion of iron in acid solutions could be reduced by addition of bran, glue and gelatine to the acid.

After this time there have been many reports of compounds which act in a similar way. The list includes sulphides, sulphonides, sulphodes, sulphonic acids, esters, amines, alcohols, aldehydes, organic bases, quinolines, and thioureas. These inhibitors range from simple structural ones (formic acid) to the very complex ones (dextrose). Colloidal inhibitors (egg albumen, tannin) have also been reported.

As the range of inhibitors is so large, it is not surprising that no single mechanism has been postulated for all working inhibitors.

Putilova et al (9) distinguished between the types of inhibitors -

(i) Type A - those which acted at the metal surface.

(ii) Type B - those which affected the media, eg. sulphites deactivate the corrodent by combining with the dissolved oxygen.

Type A. can be categorised still further -

(a) Passivators - these act by assisting in the formation of a protective coating (eg. phosphates).

(b) Immunisers - these usually delay the onset of corrosion by acting with the corrodent in some way. After being consumed, corrosion can occur.

(c) Adsorption Inhibitors - this is the largest group and it is with this class that this thesis deals.

These three prerequisites of an electrochemical corrosion process are a conduction path, a potential difference, and the availability of electrode reactions for

carrying charges across the metal/solution interface. (12.13). So an inhibitor may act by increasing the true ohmic resistance, or by interfering with the electrochemical reactions.

The first adsorption theory of inhibitor action was proposed by Sieverts and Lueg (14) after studying organic inhibitors (eg. amines) in HCl and H_2SO_4. They said that, at constant temperature, the protective power (z) resembled the adsorption isotherm.

$$z = a.C^b.$$

where C = concentration of the inhibitor in the acid

a and b are constants.

This could not, however, explain why certain inhibitors only operate within certain limits (15.16).

Kreutzfeld and Valpert maintained that inhibitors formed a continuous adsorbed insulating layer on the metal surface. Schunbert (17) concluded, from his studies of lyophilic colloids, that adsorption took place on the anodic regions of the metal, retarding the transfer of metal ions to the solution.

Hackerman et al (18.19) conceded that organic inhibitors are effective by virtue of their attachment to the metal surface, adhering either by physical or by chemisorption. In the case of physical adsorption, the inhibiting effects would result from the decreased ability of the corrosive medium to reach the metal surface. This may show itself as an increase in film resistance, hydrogen overvoltage, or a diffusion controlling step. The chemisorbed species would

access of
also impede the corrosive media, but also decrease the tendency of the metal ion to leave the metal surface (20). They also proposed that the non-polar molecules can be included in the composition of the adsorbed layer, producing a more complete coating on the metal surface. This could explain the enhanced protective power of technical inhibitors over the same chemically pure inhibitors (21).

Chappell, Roetheli, and McCarthy (22) after studying the effect of quinoline ethiodide on the cathodic and anodic polarization of iron and steel in N H_2SO_4, concluded that the action of the inhibitor was cathodic. The essential features of this cathodic theory (23.24) were that organic inhibitors are capable of forming onium ions and so exist in the acid medium as cations. These are cathodically adsorbed by electrostatic attraction, and form a "blanket" on the cathodic areas. The adsorption takes place in such a way that the nitrogen atom is directly attached to the metal surface. The resulting inhibitor film prevents hydrogen ions from reaching the surface without actually changing the metal surface. Various degrees of inhibition are obtained depending on the extent of adsorption, the closeness of packing of the adsorbed film, and the cross-sectional area of the molecule. Evans (12) supporting the cathodic theory, considered the protective action of colloid inhibitors to depend on the screening of cathodic sites by positively charged inhibitor particles. Many colloidal particles become positively charged in acid solution but negatively charged in alkaline solutions.

Hence inhibition occurs predominantly in acid solutions. However, they did not find that the increase in hydrogen overvoltage, increase in potential of the metal, and retardation of the metal dissolution were proportional to each other.

However, Mann (25) stated that organic inhibitors operated simply by imposing a large ohmic resistance at the metal interface. Results on the measuring of film resistances are very conflicting. Machu (26) found a direct relation between film resistance and inhibition, maintaining that when the film resistance reaches a value of 3 ohms, maximum efficiency was obtained regardless of inhibitor concentration. Rhodes and Kuhn (27) also postulated that the formation of a film at the cathodic sites increased cell resistance and so provided protection. Bockris and Conway (28) found negligible film resistance and concluded that Machu's explanation of inhibition was highly improbable.

There are several objections to the simple cathodic theory. Hoar (29) and Mears (30) stated that the polarization measurements, on which the cathodic theory was based, involved quite high current densities and were, therefore, not relevant to the conditions found in corrosion. In 1914 Mazzuchelli (31) found that compounds of the quinine and quinoline type increased both the anodic and cathodic polarizations. Cavallaro (32) stated that at low current densities a number of inhibitors affected both the anodic and cathodic reactions. Putilova et al (9) said that all organic inhibitors without exception act as polarizers of the anodic process to a

greater extent than the cathodic one, and that no direct relationship between effectiveness of inhibitors and the rise in hydrogen overpotential had been found. Makrides and Hackerman (33) showed that inhibitors operated under strongly oxidising conditions and so the mechanism of inhibition could not be connected with the "poisoning" of the hydrogen deposition reaction. The addition of most inhibitors causes the rest potential to move more noble (34). Hoar and Hackerman explained this on the basis of predominantly anodic polarization, stating that it is very difficult to explain on the cathodic theory of inhibition. Also the cathodic theory does not explain why certain inhibitors are specific in their use - eg. potassium thiocyanate inhibits the corrosion of aluminium and iron, but stimulates the corrosion of cadmium and zinc. By modifying the original cathodic theory, Bockris (35) and Fischer (36) were able to explain the specificity of inhibitors, but they were still unable to explain the ennoblement of the rest potential. Most supporters of the cathodic theory gradually came over to an adsorption theory.

The adsorption theory, proposed by Kuznetsov and Iofa (36), is based on the addition of positively charged ions to a corrosive media leads to a retardation of the cathodic and anodic processes when adsorped: but the introduction of negatively charged particles accelerates them. There are a large number of exceptions to that statement - eg. anions of many organic acids are inhibitors

in neutral solutions. Putilova et al (9) stated that the protection of metals was due to the formation of a layer of products of the inhibitor, the metals, and the ions of the corrosive medium.

Hackerman et al (13,38 - 42) and Hoar (43) have tended to support the theory of Rhodes, Kuhn, and Machu that the adsorption was general over the metal surface. Whereas Rhodes, Kuhn, and Machu regarded it to be mainly chemisorption in nature, quoting the relatively high heats of adsorption and specificity of adsorption to support this (38). The chemisorption (and therefore anodic polarization) was assumed to be far greater than the physical adsorption (and hence cathodic polarization). The mechanism of bonding is that a link is formed by the donation of electrons by the "bonding atom" of the inhibitor molecule to the d-shell of the electronic orbit of the metal. The chief evidence of this comes from the effect of structure on inhibitor efficiency (44).

Frumkin (45), Antropov (46), Brasher (47), and De (48) have all suggested that adsorption, and hence inhibition, is influenced by the potential of the metal in its environment. This theory involves the charge of the metal surface rather than the potentials of the half cells.

When a metal is in equilibrium in a solution there is a potential difference between the metal and the solution. Helmholtz suggested that this is due to two parallel layers of charged particles, acting as a condenser. The potential/ distance relationship is shown in Fig.6. As the capacitance

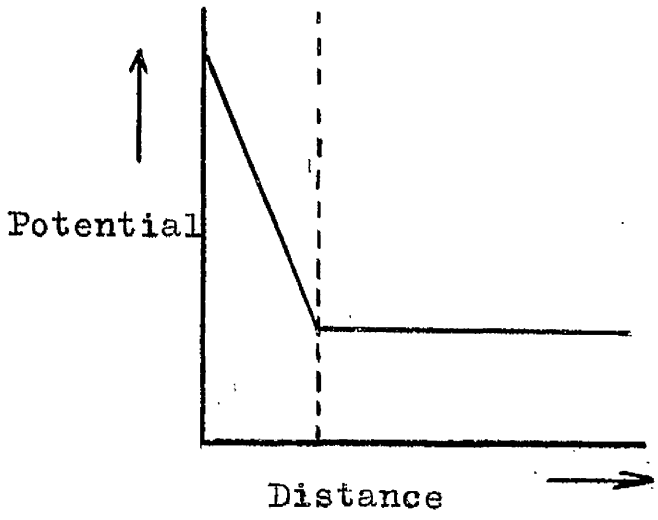

Helmholtz

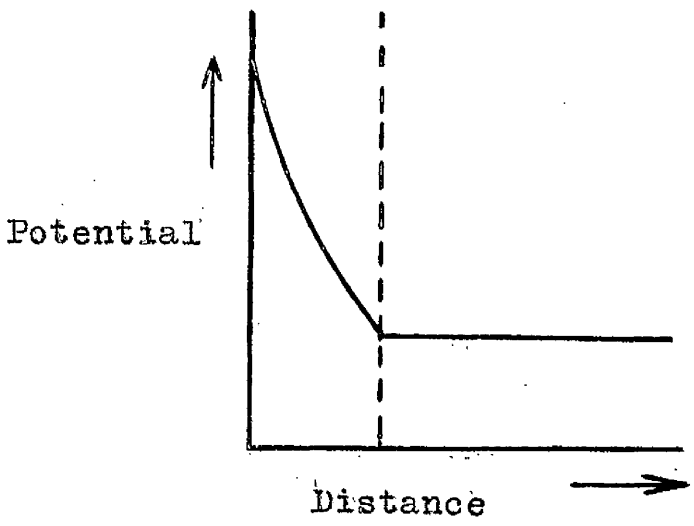

Gouy-Chapman

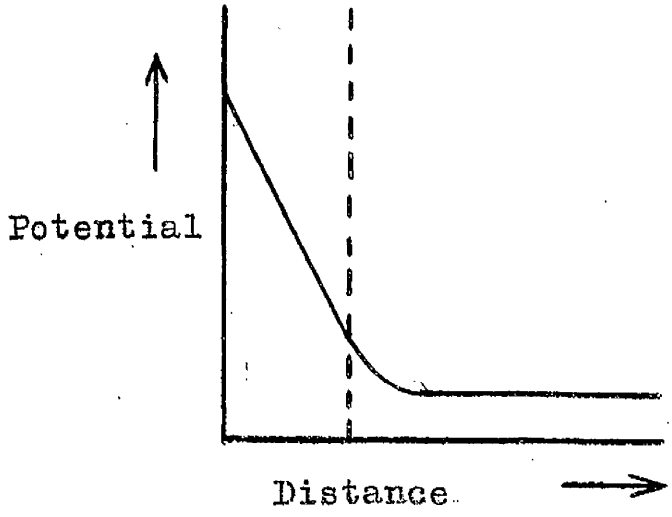

Stern

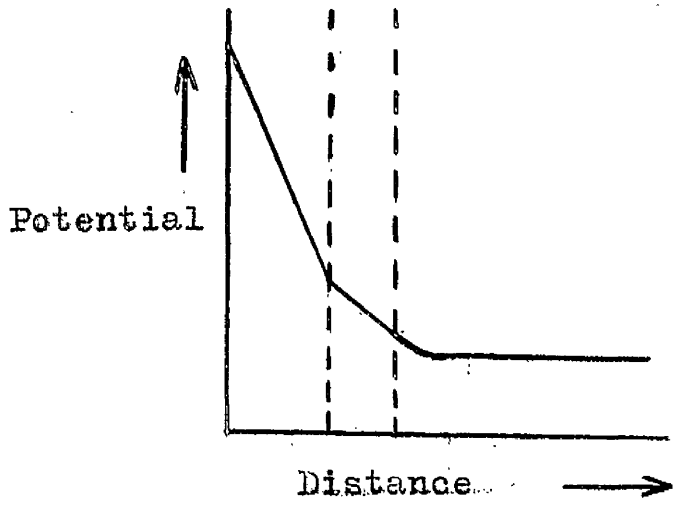

Grahame

Fig.6 Potential/Distance Relationship of the Various Double Layer Models.

varied with electrolyte and potential difference, this theory was not wholly satisfactory.

Gouy and Chapman proposed that every ion in solution attracted an ion of opposite charge, and so the resultant diffuse layer was an equilibrium between the electric field of the electrode and the thermal kinetic forces of the solution. This theory, however, did not agree with practical observations of potential and capacitance.

Stern then postulated that the interface could be treated as two series capacitors - the Helmholtz double layer and a diffuse layer.

As the Stern model is not wholly satisfactory, Grahame (49) proposed an extension of the Stern model Although both anions and cations can be adsorbed by forces other than electrical (eg. Van der Waals or chemical) anions are less strongly hydrated. He claimed that the non-electrical forces are chiefly operative for anions which become adsorbed with loss of their hydration shells. The Stern layer is then composed of two parts - a relatively thin surface layer of strongly adsorbed anions whose centres of charge lie in a plane (inner Helmholtz layer), and a Stern layer (outer Helmholtz layer) of hydrated counterions whose centres of charge lie in a plane and whose charge is given by the Stern theory. Electro-chemical reactions at the metal interface are affected by the distribution of charge, potential, and capacity of interface.

Frumkin (45), introducing his concept of zero-charge potential, supposed that the ionic adsorption depended on the sign and magnitude of the surface charge at the metal/solution interface. Under corrosion conditions if the metal surface is negatively charged, the adsorption of cations is most probable and vice versa. Adsorption of both anions and cations is possible when the charge on the metal is zero or very small. The sign of the surface charge is given by -

$$\phi = E_o - Eq=o \ .$$

where E_o = potential under corrosion conditions.

$Eq=o$ = potential under the absence of any charge. $Eq=o$ is the zero-charge potential of the metal. Both potentials must be measured on the same relative scale.

Charges of similar polarity in the Helmholtz double layer tend to oppose the attractive forces, causing surface tension. A change in potential at the metal/solution interface causes a change of surface tension, and when there is no charge on the Helmholtz double layer, the surface tension is a maximum. The zero-charge potential is the potential at which this occurs.

Antropov (46), saying that all metals behave in the same manner at the same ϕ-potential, claimed that if the electro-capillary properties of a substance are found for one metal (for convenience, mercury) it is possible to estimate the adsorption of the same substance on another metal provided the potential of that metal on the ϕ-scale is known. Fig. 7. shows the electrocapillary properties of

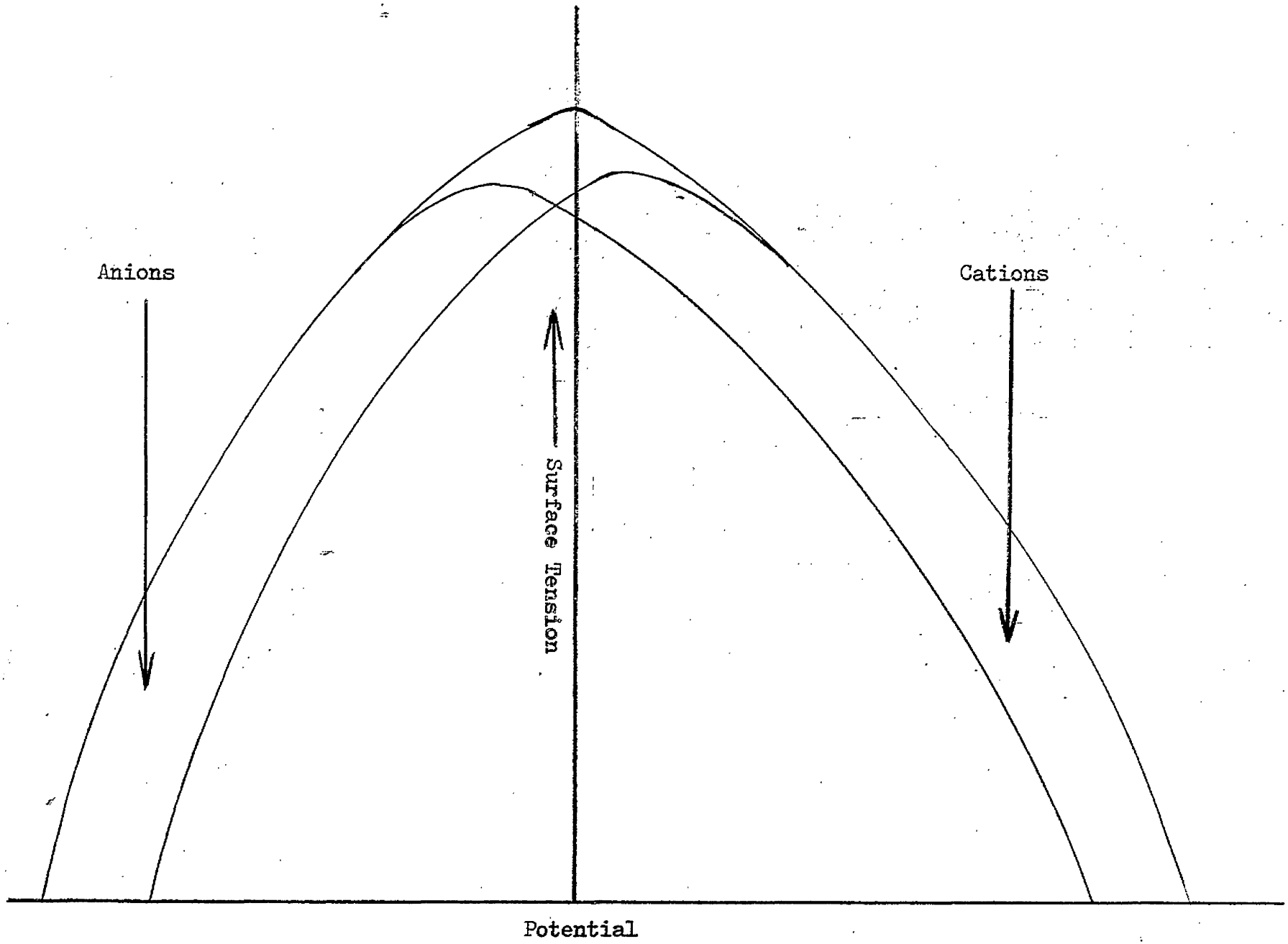

Fig. 7 The Electro capillary Properties of Mercury.

mercury. Strongly adsorped anions depress the positive branch of the curve while strongly adsorped cations depress the negative branch.

Antropov (50) said that, in corrosion protection, the change in structure of the electrical double layer due to the inhibitor is as important as the effect of a purely mechanical coverage of the metal surface by the inhibitor particles.

The electrocapillary curves for solid metals are more difficult to obtain. The usual methods are to study the contact angles of gas bubbles on the metal surface and also differential capacitance measurements. Brasher (47), using these techniques said that inhibition both in acid and neutral solutions was initiated by adsorption and that the potential of the metal on the ϕ-scale was the criterion as to whether adsorption is possible.

This theory is not without its opponents. Pandey and Sanyal (51) do not consider it useful for inhibition evaluation, although Zierzykowska (52) believes the theory a useful one.

Gatos (53) introduced a polarographic method for evaluating inhibitor efficiency. He determined the current/potential relationship for the metal anode and a dropping mercury cathode. As the potential increased, the current increased, reached a maximum, and then dropped to a limiting current value. Gatos said that inhibitor efficiency was related to the peak obtained - the greater the depression of the peak the more efficient the inhibitor.

More recently, Ariz and Din (54) used the reaction number (R.N.) to determine inhibitor efficiency. A metal of specific area is dropped into a definite volume of HCl and the variation of temperature with time noted. Then,

$$R.N. = \frac{T_{max} - T_{ini}}{t}$$

where Tmax and Tini = maximum and initial temperatures of the solution.

t = time taken to reach Tmax.

A high R.N. value constitutes an easily corroding metal. By adding inhibitor to the acid, its efficiency as an inhibitor may be worked out. They said that weakly adsorbed inhibitors increased the time factor, while strongly adsorbed inhibitors progressively decreased Tmax.

Adsorption, whether it is electrostatic, specific or chemical, of the inhibitor on to the metal surface is the primary condition for metal protection (55), although various mechanisms depending on the metal conditions and the environmental conditions have been observed.

Foroulis (56) working with amines on the corrosion of iron, copper, nickel, and copper/nickel alloys, concluded that corrosion depended on the metal, acid anion and the nature of the anion in solution. He also postulated that the adsorption of the amine is in the cationic form as opposed to the free amine form. Balezin (57) stated that inhibition resulted from adsorption, and subsequent chemisorption, of the inhibitor on the metal surface, but the formation of the protective film depended on the concentrations of the inhibitor, oxygen, and oxide film.

Snyder (58), when working with substituted pyridines, anilines, and pyrroles, determined a small positive charge on the adsorbed nitrogen atom. This supported the n-complex theory of Klemm who postulated that the nitrogen atom acts as an anchoring group with the remainder of the adsorbate attached loosely to the metal surface. Interaction between the nitrogen atom and the metal resulted from a charge transfer complex formation involving the nitrogen's n-electrons. Yao (59) confirmed these findings and added that, on adsorption, a hydrophobic surface film was formed on the metal with the hydrocarbon chains randomly orientated. Roebuck and Britchett said that adsorption occurs at the cathodic sites via the nitrogen atom by a polar linkage (60).

Duwell, Todd, and Butzke (61), studying acetylenic alcohols as acid inhibitors, concluded that the initial adsorption step was through the electron-rich acetylenic linkage to form a π-bond.

Murakawa and Hackerman (62) studied the adsorption of organics in the acidic corrosion of iron. The efficiency of the inhibitors was greatly influenced by the anion previously adsorbed on the iron. Adsorption was not always directly onto the metal, but via an already adsorbed ion. Hackerman and Snavely (63) found that the synergistic effects of anions and organic cations is greater than could be expected by a simple shift in potential by anion adsorption. This was attributed to the stabilization of the adsorbed anion layer by organic cations, possibly by co-valent bonding.

Molecular structure of the organic compounds play a dominant role in the degree of enhancement of the inhibitor by the foreign anion with the greatest enhancement coming when the anion and organic cation show a tendency to electron-pair bonding. Iofa (64), studying the influence of anions, found that organic cations were poorly adsorbed on to cobalt and were therefore ineffective inhibitors. In the presence of foreign anions their adsorption increased. A similar effect was found with iron (65). These observations were attributed to the formation of a metal-anion dipole, the negative sign of which acted as an adsorption site for the organic cationic inhibitor.

Fujii and Kobayashi (66), studying mercaptans, said that corrosion inhibition occurred in two steps - the dehydration of the metal surface by hydrogen bridging and then the adsorption on the metal surface. The filming properties of the mercaptans are improved when used in conjunction with strongly electron-donating substances (esters or alcohols).

Barratt (66), studying corrosion inhibition with radioactive amines, showed that inhibitor films are not static like protective coatings. The density of the film changes and "active" areas move, causing a redistribution of inhibitor. Over-treatment with inhibitor can result in the formation of a film capable of holding water in a tight emulsion. Such a film would offer little, or no, protection to the metal substrate.

I.4. Effect of Flow.

(a) Elementary Hydrodynamic Theory.

When a fluid flows through a tube or over a surface, the pattern of flow will vary with velocity, physical properties of the fluid, and the geometry of the surface. This flow was first examined by Reynolds (67). He studied the behaviour of an aniline dye injected into a glass tube through which he controlled the water flow. At low flow rates, the dye remained at the axis of the tube, indicating that flow consisted of independent parallel streams. As the flow increased, instabilities began to form in the dye stream and at high flow rates the dye stream broke up and mixed with the bulk of the water. The rate of this mixing increased with increasing the flow.

The point at which mixing commenced was dependant on the velocity of flow (V), the pipe diameter (d), the fluid density (ρ), and the fluid viscosity (μ). The critical velocity was predictable by the dimensionless group $\frac{vd\rho}{\mu}$, known as Reynold!s Number (Re). The lowest critical velocity where instability of the dye commenced corresponded to Re = 2,000 and the upper critical velocity where mixing was general corresponded to Re = 2,500. Below Re = 2,000, the water flow was said to be laminar or streamline (ie. there is no bulk motion of fluid perpendicular to the pipe axis) whereas above Re = 3,000, eddy currents were responsible for the transverse motion of the water and a state of turbulence existed. Reynolds defined turbulence as a random sinuous fluid motion, but Hinze (68) thought a more precise

definition was "an irregular condition of fluid in which the various quantities show a random variation with time and space coordinates, so that statistically distinct average values can be discerned".

Above the critical velocity Reynolds found that there were two types of flow:

(1) Water enters the tube smoothly and free from eddies.

(2) Water enters the tube in a state of violent motion.

In the first case, flow was smooth for some distance before turbulence set in. In the second case the violent motion died down to give either fully developed turbulent flow or laminar flow.

Hinze (68) explained this by the existence of two forms of turbulence:-

(i) Wall Turbulence - generated and continuously affected by the tube walls.

(ii) Free Turbulence - turbulence in the absence of walls.

A term "pseudo-turbulence is also used. This refers to the hypothetical case of flow with a regular pattern that shows a distinct constant periodicity in time and space.

Typical velocity profiles for laminar and turbulent flow are given by Fig. 8.

Boundary Layer.

When a fluid flows over a solid surface, a velocity profile is set up perpendicular to the direction of flow due to the viscous drag of the liquid. The fluid in contact with the surface will be at rest, otherwise the

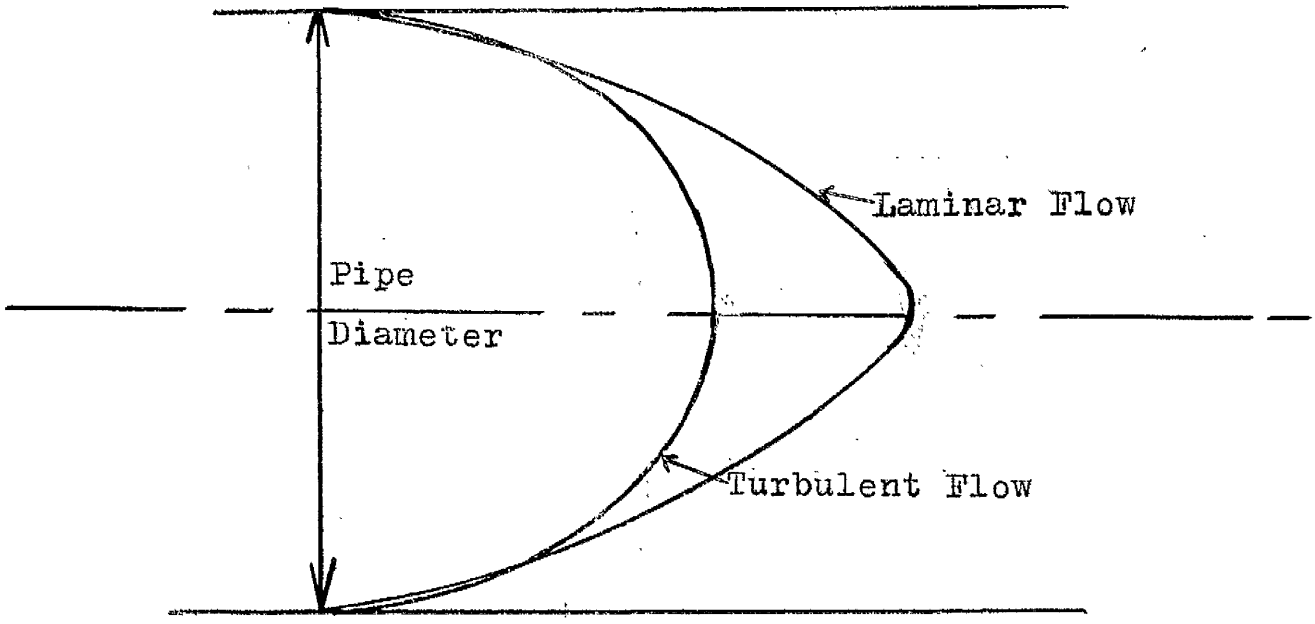

Fig.8 Velocity Profiles for Pipe Flow.

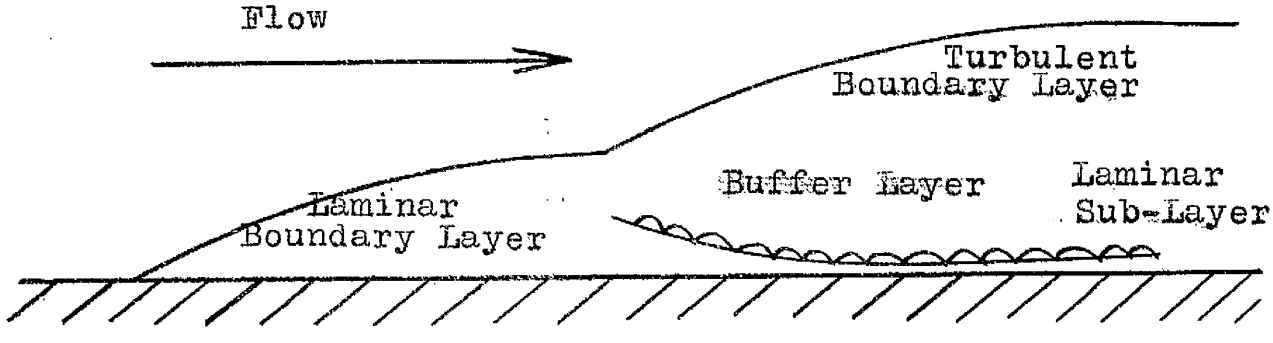

Fig.9 Development of the Boundary Layer.

velocity gradient and shear stress at the surface would be infinite. The thickness of the boundary layer will be a function of distance from the leading edge, being zero at the leading edge and increasing as distance from the leading edge increases.

At a certain critical boundary layer thickness the flow changes from laminar to turbulent. Prandtl (69) postulated that in fully developed turbulent flow, the velocity of the fluid adjacent to the wall be zero and laminar in nature. This layer will be extremely thin and termed the laminar sub-layer. Above this layer was a transition region beyond which the flow was fully turbulent. This transition region is termed the buffer layer (Fig.9.).

Flow in Non-Circular Tubes.

Nikuradse(I32) carried out experiments in non-circular tubes. The main difference between circular and non-circular tubes was that the isotachs (lines of equal velocity) did not become round when passing in from the boundary, but under the influence of the tube wall, had peaks extending into the corners. Prandtl explained these by introducing the idea of secondary motion at the corners in an inward direction along the bisector of the angle and outwards along the wall. This causes the flow to be three-dimensional and the secondary flow increases the speed at the corners.

In calculating the Reynolds Number for non-circular ducts, the diameter term is replaced by the hydraulic mean diameter (dm) which is defined as -

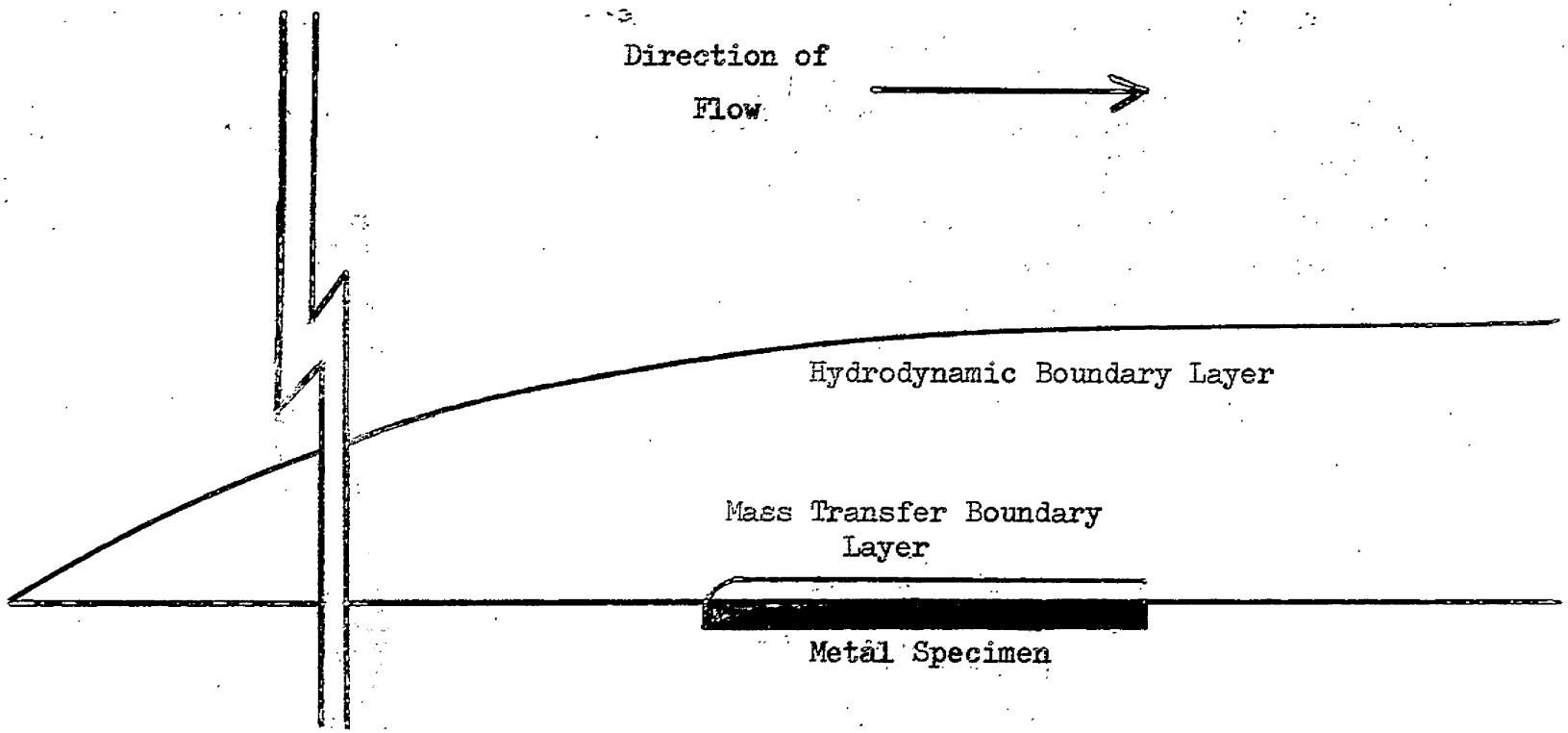

Fig.10 The Development of the Boundary Layers.

$$dm = 4 \times \frac{\text{crossectional area}}{\text{wetted perimeter}}.$$

For a square-sided duct, dm becomes equal to the length of side of the duct (70).

Mass Transfer Boundary Layer.

During electrolyte flow past a metal surface, which is dissolving, there exists near the surface a region in which the concentration of reacting species is different from that in the bulk of solution. This region is called the mass transfer boundary layer (Fig. 10). Within this boundary layer almost all the concentration changes from the surface to the bulk values takes place. With increase in distance from the leading edge of the metal surface, the thickness of the mass transfer boundary layer increases due to ions diffusing from the electrolyte adjacent to the surface. So the thickness increases from zero at the leading edge to some constant value some way down the metal surface.

(b) Effect of Flow on Corrosion.

It has been known for a long time that the relative motion of a fluid over a metal surface modifies the corrosion of that surface (71). A little motion could make attack more uniform by eliminating differential aeration and metal ion concentration cells. Generally, electrolyte motion increases the total weight loss by supplying the corrosives at a faster rate and also thinning the quiescent layers at the metal surface, making it easier for corrosives to reach the metal. Alternatively high velocities may change the characteristics of the corrosion products and greater

protection could be afforded. With certain alloys increased oxygen supply may induce passivity or increase the supply of inhibitor to a dead space. So the opposite effects can be seen with increased velocity.

When the velocities become very high, erosion can occur and break down any passive film on the metal.

However, although contradictions are known, corrosion is increased with increased velocity which primarily influences the diffusion phenomena, having little effect on the activation controlled processes. (72).

Heyn and Bauer (73), studying the corrosion of iron in water, found that the corrosion rate increased rapidly with increasing velocity, reaching a maximum at 0.0043 ft./sec. Subsequent increase in velocity caused a decrease in corrosion rate. As the tests were carried out by suspending iron in beakers and passing water over them, the actual velocities determined would be uncertain due to convection currents and turbulence set up. Friend (74) found similar results when he suspended iron foil in glass tubes, but he obtained a maximum at 0.15 ft./sec., a maximum at 2.5 ft./sec., and any increase after that caused a slight increase in corrosion rate. He also stated that in acid corrosion, the corrosion rate was always proportional to the velocity of the acid flowing over the surface.

Speller and Kendell (75), using the principle that corrosion is directly proportional to the dissolved oxygen concentration, studied the effect of velocity in steel pipes in the range 0.0043— 8.0 ft./sec.. In the

range 0.0043 – 0.10 ft./sec. corrosion falls within the very low velocity range of the pipe and shows a considerable increase with increase in velocity. Corrosion, in the range 0.10 — 8.0 ft./sec. increases rapidly through a critical velocity and then more gradually, finally reaching a maximum. Apart from the main cathodic reaction, they stated that oxygen was consumed at the metal surface in two ways - (a) By depolarising the film of hydrogen.

(b) By oxidising Fe^{++} to Fe^{+++}.

An increase in velocity brought oxygen into more intimate contact with the metal surface.

Russell, Chappell, and White (76) found that the corrosion of steel in water increased with increasing velocity over the range used (0 - 9 ft./sec.). By suitably altering the surface condition of the steel (eg. polished surface, rust-coated surface) they found it possible to reproduce the apparently conflicting results of Heyn and Bauer, and Friend.

Roetheli and Brown (77) using rotational velocities, studied the corrosion rates of steel in water. As the rotational speed was increased, the corrosion rate increased to a maximum, decreased to a low value, and increased to a somewhat higher value at higher velocities. This maximum was explained in terms of two opposing tendencies -

(a) The accelerated transfer of oxygen due to a reduction of liquid film thickness.

(b) The increased rate of formation of ferric hydroxide.

At higher velocities, the corrosion rate increases as, due to

erosion, the ferric hydroxide layer becomes non-uniform. They also concluded that turbulence, which is a function of velocity, vessel shape, and liquid properties, had a marked effect on the corrosion product and therefore on the corrosion rate. Wilson (78) thought that velocity was important in determining the thickness of the film through which oxygen must diffuse in the corrosion process.

Wormwell (79, 80) studied the effect of rotating cylindrical steel specimens on the corrosion rates in sea-water and other saline solutions. Results showed that, at high rotational speeds, protection of the steel was due to a film formed on the metal surface by an increased supply of oxygen. Hatch and Rice (81) also showed that the effect of increasing velocity was to change the oxygen concentration gradient near to the metal surface.

Romeo et al (82) studied the effect of metal corrosion from the hydrodynamical aspect and concluded that:
(a) Velocity alone was not a basis for corrosion, testing results under hydraulically different conditions.
(b) The nature of the corrosive medium could produce different effects on changing velocities - this was attributed to the changing solubilities of metallic salts at different levels.
(c) When a corrosion product layer was formed, the reactions leading to continued corrosion would take place within the layer where conditions would be very different from those in the bulk flow. The transfer of chemicals would be accomplished mainly by diffusion.

(32)

(d) Velocity and pipe size affected the corrosion rate by altering the supply of oxygen and other chemicals in the water.

(e) Four phases existed in the corrosion process -

(i) Anodic and cathodic areas would form. As there was not yet any corrosion product formed increased velocity would generally increase corrosion rate.

(ii) Anodic and cathodic sites increase in size and number and protective layers would form. Corrosion would follow some complex law, involving pH and velocity.

(iii) Corrosion product layer was extended uniformly over the metal surface.

(iv) Corrosion proceeds at an almost uniform slow rate as long as there is no change in environmental conditions.

(f) By assuming that an increased supply of oxygen increases the corrosion rate and that corrosion products on the metal are not impermeable, the following could be deduced -

(i) In turbulent flow in rough pipes, Reynolds Number was not a criterion of similarity in corrosion processes.

(ii) In laminar flow in rough pipes, corrosion would increase with turbulence.

(iii) In turbulent flow in smooth pipes and the same Re, the corrosion rate would be proportional to the first power of the velocity; with the same velocity, the corrosion would by inversely proportional to the diameter raised to the 0.125 power, and with the same diameter the corrosion rate would be proportional to the velocity raised to the 0.875 power.

Putilova et al (9) claimed that the suggestion made by Whitman (83), regarding the influence of the rate

of access of oxygen to the metal surface, was unacceptable, since the minimum, showing corrosion as a function of rotational speed, is also observed in experiments carried out in solutions containing no oxygen.

They also claimed that data obtained from experiments with cylindrical samples rotating in the corrosive media cannot be considered as modelling the influence of flow rate on the corrosion process. Ross and Hitchen (84) and Ross and Jones (85) have also stressed this point. When a sample rotates, the rate of corrosion is influenced, not only by the motion of the liquid, but also by the properties which are specifically associated with rotary motion. Rotating the samples causes depolarization of the anodic process and conversely an increase in polarization of the cathodic process.

Makrides and Stern (86) used rotating iron cylinders to study the effect of speed on the diffusion rate of Fe^{+++} to the cathodic areas on the specimens. They claimed that the diffusion of Fe^{+++} could be related to velocity and that the rest potential of the specimen was unaffected by the speed of rotation in hydrogen saturated solutions.

Ross and Hitchen (84) investigated the effect of flow of water on the electrochemical behaviour of tubular couples of iron/copper, carbon/copper, and copper tubes of different diameter. With water flowing through the cell continuously the polarization curves were constructed for various flow rates and oxygen concentrations.

With the iron/copper couple, the iron was unaffected by flow-rate, but the copper cathode was made more noble and less polarised by increased flow. At $Re_{..}$ = 4000, the oxygen content of the circulating water was allowed to become gradually exhausted. The corrosion rate dropped with decreasing oxygen content, but the distinction between iron anode and copper cathode persisted.

In the carbon/copper couple, the anodic processes on the copper surface were increased by increasing the water flow in the laminar region. Under laminar flow the copper anode potential becomes less positive and less polarized but in turbulent flow the anode becomes ennobled although depolarization continued.

Experiments with copper tubes of different diameters showed that anodic control was exerted whenever the flow pattern was the same in both tubes. When laminar flow existed in the larger tube and turbulent flow in the smaller tube, the smaller one becomes cathodic to the larger one. This is due to the change in polarization characteristics of the copper anode in changing from laminar to turbulent flow.

The results show the importance of fluid velocity in its effect on the cathodic processes. It is fairly clear that this is due to the degree of availability of oxygen at the metal surface. This is given by -

(a) Laminar Flow.

$$N_L = \frac{D.\Delta C}{\delta_L}$$

where N_L = the number of molecules of oxygen across a boundary layer of unit area in unit time.

D = diffusivity of oxygen.

ΔC = mean difference in oxygen concentration between the bulk solution and cathodic equilibrium.

δ_L = mean thickness of boundary layer.

(b) Turbulent Flow.

The diffusional transfer, under these conditions, is helped by eddy diffusion (E) of the bulk solution, so the total diffusivity is written as (D + E). The above equation becomes - $N_T = \frac{(D + E).\Delta C}{\delta_T}$

This represents the transfer of oxygen to the cathode surface in the turbulent region.

If it is assumed that oxygen is consumed at the cathode by a rapid and irreversible reaction, ΔC approaches the bulk concentration unless the boundary layer is very thin. With this exception, the cathodic depolarization rate is inversely proportional to boundary layer thickness which itself is dependent on Re. Under laminar flow δ_L is large (ideally it approaches the tube radius) and the cathodic depolarization is flow dependent. Under turbulent flow, as δ_T is very much less than δ_L, the boundary layer is a less important barrier and the concentration difference, ΔC, may be less than the bulk concentration. Both δ_T and ΔC decrease with increasing Re and cathodic depolarization may be relatively insensitive to Re.

The stability of the iron anode was explained by the rate of formation of Fe^{++} at the iron surface always equalling, or exceeding, the rate of transportation by diffusion, or turbulence, away from the surface. As copper

provided ions at a lower rate, the copper anode is sensitive to flow rate. The ennobling effect of the copper under turbulent conditions was said to be due to a passivating effect of oxygen, transferred to the surface at an increased rate.

Ross and Jones (85) concluded that, in the case of corrosion of steel in H_2SO_4, the effect of increased velocity was to depolarize both the anodic and cathodic reactions, the latter to a greater extent. Oxygen diffusion largely causes the cathodic depolarization. They also found a certain velocity when the corrosion rate was the same as in static conditions.

Donat (9) investigated the corrosion of steel tubes in conc. H_2SO_4 and found that corrosion rate and velocity were related by -

$$\rho = 0.0026\ Re^{0.8}$$

where ρ = corrosion rate in $g/m^2 hr$.

Balezin and Orlova (9), working with mild steel in H_2SO_4, concluded that the concentration of the acid has no effect on the corrosion rate at high velocities. For normal H_2SO_4 the relation between corrosion rate and velocity was -

$$C = a + bV^{0.8}$$

where C = corrosion rate

V = velocity.

a and b are constants.

Venzcel, Knutsson, and Wranglen (87) measured the corrosion rate of copper in flowing salt solution. At very high Re, the corrosion of copper was virtually independent of

flow velocity - the mass transfer processes being so rapid that the rate-determining step is the ionization of the metal. At low velocities, the corrosion rate is limited by the rate of removal of corrosion products from the metal surface, provided that the supply of oxygen is large and not rate determining.

Butler and Stroud (88) also worked with salt solution and mild steel tubes and found that corrosion rate followed - $k = K_c . V^{n}$

where k = corrosion rate

V = velocity.

For laminar flow, $n = 0.33$ and for turbulent flow $n = 0.9 - 1.0$.

Foroulis and Uhlig (89) studied the corrosion rate of steel in 0.35 N. H_2SO_4 at speeds up to 4000 rpm. (3.5m/sec.). Their results, similar to the earlier corresponding ones, were explained by an initial inhibiting effect of oxygen on the corrosion rate. Polarization measurements confirmed that small amounts of oxygen increased the anodic polarization, probably by adsorption on to the anodic sites. Higher concentrations of oxygen caused a depolarization of the cathodic areas, accompanied by an increase in corrosion rate. In the absence of oxygen, velocity is without effect because the reaction is controlled by activation polarization accompanying hydrogen evolution and this is unaffected by velocity.

(c) Effect of Flow on Inhibition.

Balezin (90) stated that the effect of flow on inhibitors is to remove, or vastly reduce, their protective powers. This has been found to be the case in practice. Chufarov (91) reported that when solutions are stirred the ability of inhibitors to function is sharply reduced. Beck and Hessert (92) also found that the protective power of colloidal inhibitors fell when the solutions are stirred. This was simply explained by the removal of the coagulated inhibitor from the metal surface in the stream of acid.

Hatch and Rice (81) studied the effect of sodium hexametaphosphate (Calgon) as an inhibitor in the corrosion of steel in flowing water. With untreated water, the corrosion rate first increases very rapidly as velocity increases, and then levels off. With inhibitor present, at the lowest velocity, the corrosion rate is greater than with untreated water. Then as the velocity increases inhibitor efficiency improves, but still the corrosion rate increases. At higher velocities the corrosion rate drops gradually. Increasing the concentration of inhibitor has the effect of causing the maximum corrosion rate to decrease and occur at a lower velocity.

The corrosion rate was therefore dependent on the rate of supply of both oxygen and inhibitor to the surface. Hitchen (84) attributed this increased inhibitor efficiency at higher velocities to the constant replacement of inhibitor, at the metal surface, by eddy diffusion transfer.

Putilova et al (9) repeated their corrosion experiments, in flowing acid media, in the presence of hexamine and triethanolamine. In the case of hexamine, at the velocities employed (0.12m/sec. and 0.80m/sec.), hexamine acted as an inhibitor at all concentrations. At the lower velocity triethanolamine acted as an inhibitor at all concentrations of acid, but at the higher one, it acted as a stimulator at normalities between 2 and 4. Potassium iodide showed the same tendencies as triethanolamine when tested in flowing conditions.

Jones (85) showed that at all but the lowest concentrations of inhibitor, the inhibitor efficiency of thiourea in sulphuric acid was significantly reduced. This was attributed to the increased depolarization of the cathode reaction by the increased diffusion of inhibitor to the metal surface. At low concentrations of thiourea (2×10^{-6} M) the dissolution process is one where the anodic reaction is depolarised in a fashion which is only slightly velocity sensitive.

At medium concentrations (2×10^{-3} M) the efficiency is similar to those under stagnant conditions.

At high concentrations (5×10^{-3} M) at high flow rates, further depolarization occurs, but at low flow rates initial inhibitive effects are maintained. This suggested that there were mixed reactions occuring at the anode sites, not all of which are diffusionally controlled. The result of this change in anodic behaviour is that the initial inhibition obtained at high concentrations is progressively

lost as the flow rate increases.

I.5. Effect of Molecular Structure on Corrosion Inhibition.

If it is true that the best inhibitors require chemisorption and a lowering of metal reactivity, it should be possible to correlate certain measurable adsorption properties, and hence inhibition possibilities with known chemical properties associated with the various molecular structures (93). Physical properties (eg. molecular weight and molecular area) have a small effect on inhibitor efficiency and even when a strong dependance is noticeable, it can usually be traced to solubility limitations or micelle formation.

Stromberg (94) studied amino-acid as inhibitors in the corrosion of mild steel in copper sulphate solution. He found that slight differences in the carbon chain between functional groups altered the inhibitor efficiency appreciably. Amino-acids have the structure -

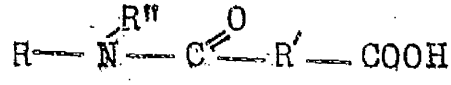

His results can be summarised as follows:-

(i) Optimum length of R was C_8 to C_{12}.

(ii) Optimum length of R' was C_2.

(iii) Optimum form of R'' was H.

(iv) Branching is undesirable.

(v) Aromatic rings in the R' chain were undesirable.

(vi) Unsaturation adjacent to the polar groups was also undesirable.

Although Stromberg found addition of methylene groups in a long alkyl chain did not affect the efficiency a great deal, Hackerman (93) showed that the addition of a methylene group to a heterocyclic imine ring increased efficiency 20% each additional CH_2 group and 5% in the case of aliphatic amines. He also found that low molecular weight amines were more efficient than high molecular weight aliphatic amines. As this cannot be explained by increased barrier resistance due to chain length or increased surface coverage, the explanation must lie in a more fundamental property - viz. the bonding characteristics. This was explained (95) by the steady change in bond angle between ring atoms, even though the rings are not planar. X-ray measurements confirmed this (96). Ayers and Hackerman (97), working with pyridine and seven of its methyl derivatives, concluded that molecular area was not of first order importance and, besides efficiency increasing with the number of substituted methylene groups, it also increased with the electron density of the nitrogen atom. The electron density of the nitrogen atom may increase efficiency by -

(i) an increase in the number of chemisorbed molecules.

(ii) an increase in the availability of the chemisorbed molecules.

Hackerman, Hurd, Annand (98) showed that inhibitor efficiency increased markedly at the 9 - 10 membered rings - a position where certain properties of an homologuous series are frequently at a maximum or minimum (95.96). More

striking, however, was the effect of ring closure on inhibitor efficiency - ring compounds (a) were decidedly more effective than secondary amines.

(b)

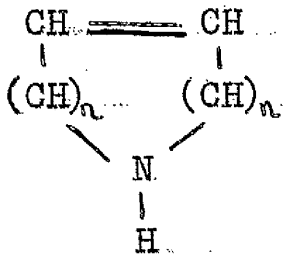

(a)

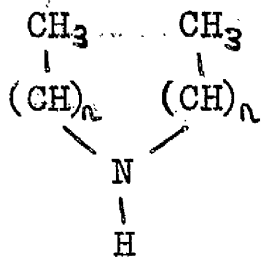

(b)

In another series of experiments Hackerman (99) made a comparison between cyclic amines and para-substituted nitrogen-methyl anilines under identical conditions. The results showed no dependance on base strength, molecular weight or area.

Interpretation took into account the Π-orbital nature of the free electrons on the nitrogen bond - the more Π-orbital character present in the bond at the metal/inhibitor interface, the more efficient the inhibitor, other factors being constant.

Hackerman, Hurd, and Annand (100) examined three types of low polymer amines (poly(4-vinylpyridine), 4-vinylpiperdine, and polyethyleneamine) to determine their efficiency in HCl. The results showed that soluble molecules containing multiple repeating units (identical in functionality) are more efficient inhibitors than their corresponding monomers. This was explained by the polymers being adsorbed to the metal surface at more than one point and the increased stability of the net total adsorption bonding in the polymer (ie. a high tendency, once adsorbed,

to remain adsorbed), to form a strong metal-inhibitor bond.

By using nuclear resonance Cox (101) studied the electronic structure of substituted anilines as corrosion inhibitors. He concluded that the ability of the molecule to inhibit corrosion was determined by the electron density of the amine nitrogen atom. Szlarska-Smialowska and Dus (102) stated that the process of adsorption was influenced by -

(i) the adsorping strength

(ii) the resistance hindering the diffusion of inhibitor molecules.

The inhibitor efficiency of compounds containing the same aliphatic substitute is higher if selenium is the bonding atom. This agrees with Makrides and Hackerman (34) as selenium is far more electronegative than either nitrogen or sulphur.

Aramaka and Fujii (103) studied the influence of self-association of high molecular weight amine-type inhibitors and found that efficiency decreased when another proton donor or acceptor was present.

Foster, Oakes, and Kucera (104) systematically altered propargyl alcohol (itself a corrosion inhibitor) and studied the resulting structures for inhibitor efficiency. The inductive effect of the substituent groups tend to influence the availability of the π-electrons and so modify the efficiency. Only one substituted compound was an effective corrosion inhibitor and they found that steric factors played no part in efficiency.

Blomgren, Bockris, and Jesch (105) found that for a given conjugate linkage, CN^-, SH^-, and S^- substituents tend to improve inhibitor efficiency whereas OH^-, NH_3^+, and SO_3^- reduce it; Balezin (106) also found this to be true.

Although a lot of work has been done on the effect of molecular structure on inhibitor efficiency, no outstanding success has been reached. This probably results from attempting to stretch a little knowledge too far. Most of the conclusions reached point to the amount of the Π-orbital character of the free electrons, and the electron density, of the "anchoring" atom as determining the inhibitor effectiveness.

I.6. Benzotriazole as a Corrosion Inhibitor.

Benzotriazole (Mol. Wt. = 119.1) is a heterocyclic compound with the following structure -

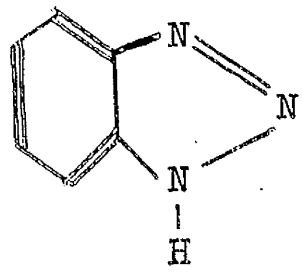

This was established by Jensen and Friediger (107) after studying the dipole moments of benzotriazole dissolved in benzene and diozane.

Heathfield and Hunter (108) studied benzotriazole and its derivatives and found that association could take place - the degree of association increasing with increasing concentration - but that compounds with no imino-hydrogen remained unimolecular. Results showed that association occurred through N - H - N bonds and they suggested that association occurred principally through the 1 and 3 nitrogen

atoms of separate molecules via the hydrogen atom (1.3 association) and to a lesser extent by 1.2 association. Scholes and Cotton (109) also studied benzotriazole and its derivatives and their corresponding inhibitor efficiencies. It appeared to them that the N - H group and one of the other nitrogen atoms were necessary to corrosion inhibition, the inhibitors forming a polymeric complex on the metal surface. These complexes were modified by various anions in the solution, and, in some cases, contained water of crystallisation.

By treating copper with benzotriazole, the chemical resistance of the surface is greatly improved. Results (110) show that the film remains bright after 5 days in 3% salt mist which would normally cause staining in 16 hours: in 100% humidity with 0.1% v/v SO_2, the copper is unaffected for 6 weeks compared to 16 hours; the film lasts up to 6 times as long in 10ppm H_2S than an untreated surface. However, the film will not withstand attack from NH_3 or NH_4^+ - compounds.

Cotton and Dugdale (111) retarded, or prevented the pitting corrosion of water systems, constructed of copper or copper alloys by treatment with benzotriazole. The surfaces were degreased, pickled, exposed to a solution of benzotriazole in isopropyl alcohol or water, or to benzotriazole vapour with condensation. Test specimens were contacted for 2 minutes with a 2% wt. solution of benzotriazole at 60° - 100° C and dried. These specimens showed no pitting after 3 months in water which caused pits in similar untreated specimens. Unsuccessful treatment resulted in the same results as untreated specimens.

Cotton (112) claimed that the action of benzotriazole was to act as a cathodic inhibitor to the oxygen reduction reaction, aided to a lesser extent by the surface layer effects. Barannik (113) postulated that the presence of sulphur or nitrogen with free pairs of electrons in the molecule of a 5-membered heterocyclic compound of the azole group (benzotriazole is a member of this class) suggest that these compounds may have an inhibiting effect on the corrosion of metals, by the formation of insoluble chemisorbed films.

Other examples of the action of benzotriazole as an inhibitor concern the addition of benzotriazole to the corrosive media. Hatch and Hagan (114) stated that in recirculating water systems, benzotriazole (in concentrations of 1 - 5 ppm. with, or without, molecularly dehydrated phosphates) controls the corrosion of copper and its alloys in the presence of a more cathodic metal. The compound is also stable and effective in water, treated for lime and bacteria control.

Wall and Davis (115) showed that adding benzotriazole to closed water systems cut down the rate of dissolution of copper into the water. They carried out experiments over a period of 60 days and found that, to operate the system efficiently, the benzotriazole must be above a certain critical concentration and within an optimum concentration range. However, it is also known (116) that there exists in certain waters organisms which feed on benzotriazole forming an insoluble yeast-like substance.

Hence benzotriazole would be useless for the treatment of such waters.

Liddell and Birdeye (117) found that the efficiency of benzotriazole (concentration 5 mg/litre) was greatly increased in the presence of highly condensed polyphosphates. Schaeffer (118) reported that the discolouration of non-ferrous metals by aqueous solutions of detergents could be prevented by the presence of up to 0.1% of water soluble material, having the nucleus -

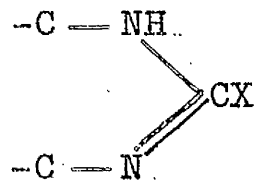

(1)

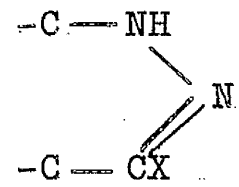

(2)

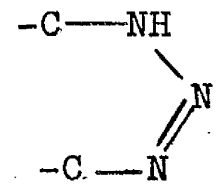

(3)

The structure of benzotriazole satisfies structure 3 and all three structures satisfy the findings of Cotton and Scholes (109) on corrosion inhibition by benzotriazole and its derivatives.

Benzotriazole is also used in engines and radiator cooling systems where copper in the presence of aluminium, iron, and steel can cause severe pitting. It reduces pitting and also has the added advantage that it can be used in conjunction with antifreeze (119).

Benzotriazole and its derivatives are used in greases (120), paints, lacquers, inks (121) and as vapour phase inhibitors (122). It also has a value as an impregnant of paper for transporting copper and its alloys (110). Chemical analysis of the copper/benzotriazole complex

formed by pretreatment has shown that the copper/benzotriazole ratio is

(i) 1:1 if produced from cuprous salts.

(ii) 1:2 if produced from cupric salts.

Potentiometric titrations have indicated that the complex formation takes place by the release of labile hydrogen attached to the nitrogen.

Unfortunately it has not been possible to produce a positive correlation between the very thin surface film formed on pretreatment and the above compounds produced by aqueous reaction. The film is so thin that it does not give a definite electron diffration pattern - so the film must be either amorphous or microcrystalline and less than 50^{o}A thick. It is reasonable to assume that the complex formed is similar to one, or other, or both of the complexes mentioned above. If the reaction occurs by removal of the labile hydrogen, it is possible to suggest that a long chain structure is produced for cuprous benzotriazole and a flat planar one for cupric benzotriazole. Whatever the adsorption mechanism, there is little doubt that pretreated copper and its alloys are significantly protected against corrosive attack in atmospheric and static corrosion.

CHAPTER 2

Preliminary Work in Static Media.

2.I. Introduction.

From the literature survey it will be noticed that much of the experimental work carried out on inhibitors is applicable to static media only and that very little work has been done on inhibitors in flowing media. However, the general finding of the work that has been carried out is that inhibitors lose their effectiveness in flowing media. It is also known that results obtained in a static environment cannot be applied to the same flowing environment with any certainty at all. As no explanation has been put forward as to why this happens, this course of study was undertaken to investigate this observed phenomenon and attempt an explanation.

Copper is capable of bonding with a wide variety of organic compounds varying from chain aliphatic sulphides to benzene derivatives containing nitrogen and sulphur. Ultimately the compound chosen for this investigation was benzotriazole. Benzotriazole has been used as an inhibitor for copper and its alloys in static and atmospheric environments and has proved very effective. Benzotriazole has the advantage, as an inhibitor, that it acts chemically with the copper forming a complex bonding compound which protects the copper from further attack. It seemed logical therefore, to study the reaction of the copper-benzotriazole complex on the surface when subjected to a flowing medium.

Using benzotriazole and copper has the added advantage that they can both be obtained in a chemically pure state, so that any anomalies found in the course of experiments cannot be caused by any impurities in the system.

As most of the work done on inhibition has been carried out in aqueous acid medium, it was decided to carry out these experiments in an acid media - sulphuric acid being selected for the purpose. This was made up by diluting concentrated Analar sulphuric acid (S.G. = 1.84) with distilled water to the desired concentration. This was 10%v/v sulphuric acid.

Tough pitch extruded copper sheet (gauge 20) was used in the experimental work and it had the following composition -

Copper	99.9%
Oxygen	0.04%

On arrival a number of segments (3.8 x 1.8 cms.) were cut from the copper sheet, polished on successive grades of wet/dry grinding papers (Struers papers, grades 220, 320, 400, 600) greased, and stored in a dessicator until required.

2.2. Experimental Work.

Prior to any work in flowing media, some preliminary experiments were carried out in static media. These were to have a basis for comparison with results in flowing media and also to establish which form of investigation would prove to be the most fruitful. The preliminary experiments carried out were - (a) Weight Loss Experiments.

(b) Potential Experiments.

(c) Capacitance Experiments.

(d) Potentiostatic Experiments.

These experiments were carried out under various controlled conditions.

There are two methods by which benzotriazole may be used as an inhibitor and both of these were employed experimentally. These are -

(a) Pretreating the copper with benzotriazole before the copper is placed in the corrosive medium.

(b) Placing benzotriazole in the corrosive medium before the copper is placed in it.

2. 3. Specimen Preparation.

In order that the experiments could be carried out successfully the copper segments had to be made up into electrodes.

Preparation of Electrodes.

Two types of electrode design were used in the static experiments: one for the potential and potentiostatic work (type A) and another for the capacitance work (type B).

Type A.

This type is shown diagrammatically in Fig .II A length of PVC-covered wire was soldered on to the back of the specimen. The specimen was placed in a perspex mounting (2.5 cms.x 5.0 cms.) which had had an area equal to that of the specimen machined out. The wire soldered on the back of the specimen passed through a hole drilled in the mounting. A thin layer of araldite was smeared over the

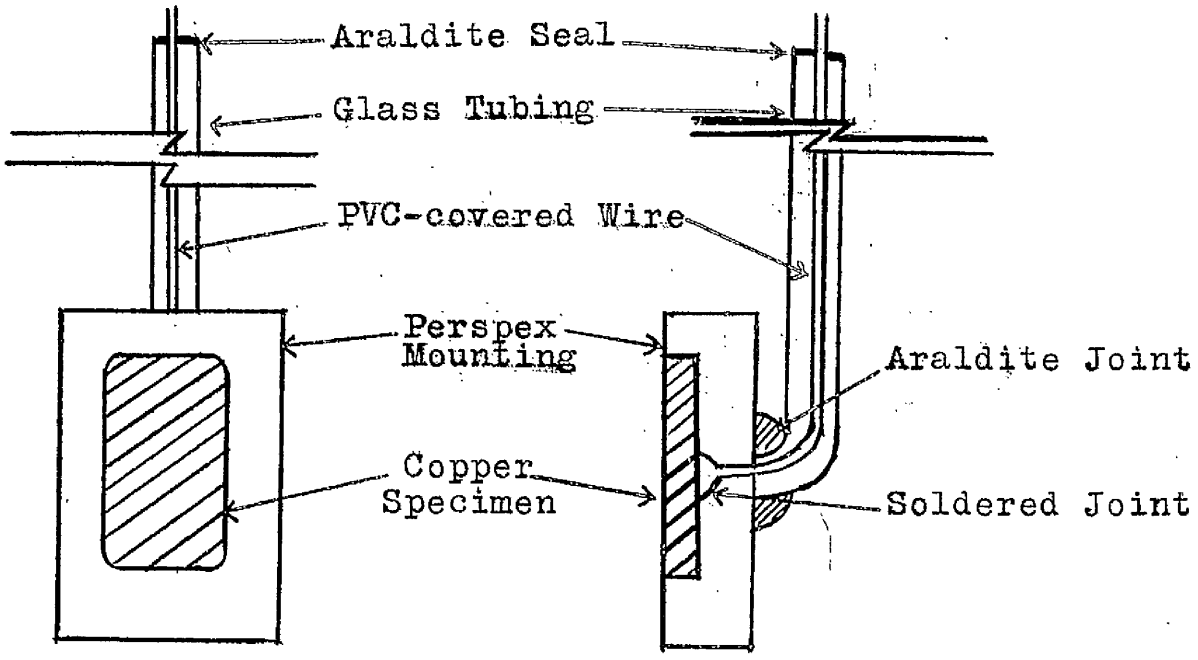

Fig.I1 Electrode used in Potential and Potentiostatic Experiments.

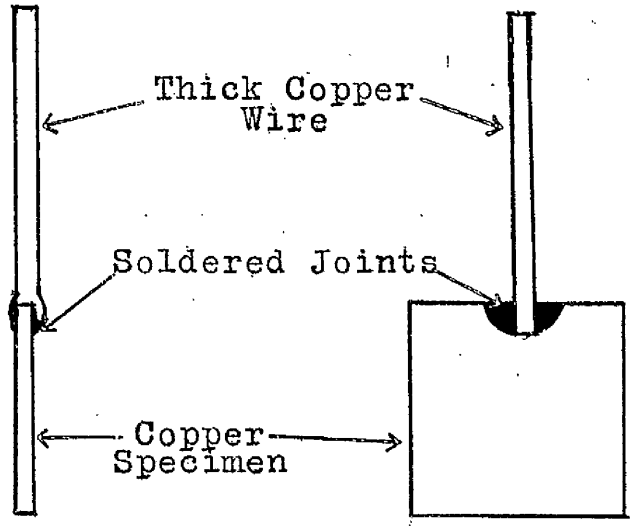

Fig.I2 Electrode used in Capacitance Measuring Experiments.

back of the specimen which was then pressed into the perspex. On partially drying the excess araldite around the edge of the specimen was cut away, so that only the front face of the copper would be exposed to the acid. A glass tube was bent and araldited to the back of the perspex mounting and the PVC-covered wire passed up through the glass.

These electrodes could be easily renovated after an experiment by grinding the front face of the electrode on grinding paper.

Type B.

This electrode design is shown in Fig. I2. A length of thick copper wire had a small notch sawn in one end. A copper segment (1.9 x 1.8 cms.) was inserted into the notch. The notch was then tightly closed and the copper wire soldered on to the segment.

Just prior to use, the electrode was masked off with tape which had a hole stamped out. The only area exposed to the acid was that exposed by the tight-fitting tape.

Pretreatment of the Copper Surface.

In order that benzotriazole forms a uniform coating on the copper surface, the surface must be absolutely free from grease and dust, and also be totally water-wet. To obtain such a surface two methods were tried -

(a) Bright-Dip Method.

The bright-dip solution was a mixture of concentrated sulphuric and nitric acids with a trace of concentrated hydrochloric acid.

The copper was de-greased, and washed in distilled water. Then it was placed in the bright-dip solution for a few seconds, removed and immediately washed in distilled water.

This method was unsuccessful as it left the copper surface blotchy and uneven, so much so that the benzotriazole only took on certain areas of copper (Fig. I3).

(b) "Duraglit" Method.

This method was suggested by The Geigy Company Ltd. which supplied the benzotriazole and deal also with industrial methods of pretreating copper with benzotriazole.

The copper was thoroughly de-greased as before, well rubbed with a small pad of duraglit (a metal polisher), and then polished with a clean, dry soft cloth. The resultant surface film was removed by rubbing with a paste of pure calcium carbonate and washed off with a wetting agent solution (10% EDTA and 20% sodium n-octyl sulphate). Finally the copper was thoroughly washed in the distilled water.

This procedure left the copper with an absolutely clean, water-wet surface onto which benzotriazole could be uniformly coated (Fig.I4).

Consequently, this latter procedure was preferred and used throughout the experimental work.

Both the figures show the effect of 10 ppm. H_2S on the specimens and this is a quick test to ensure that treatment has taken place (110).

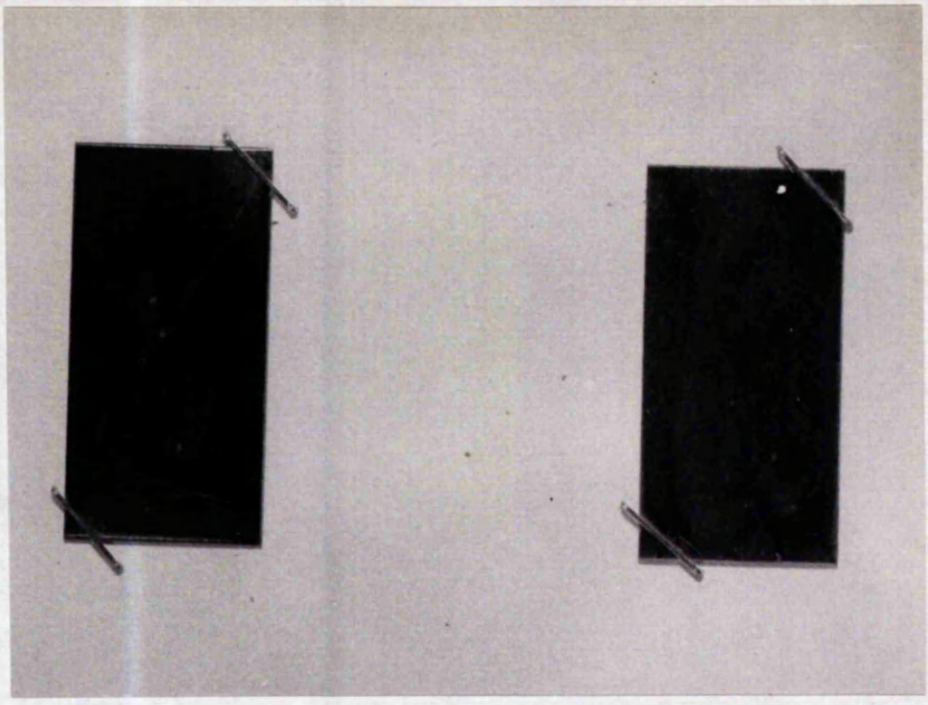

Blank Pretreated Specimen

Fig. I3 Pretreatment by the Bright-Dip Method.

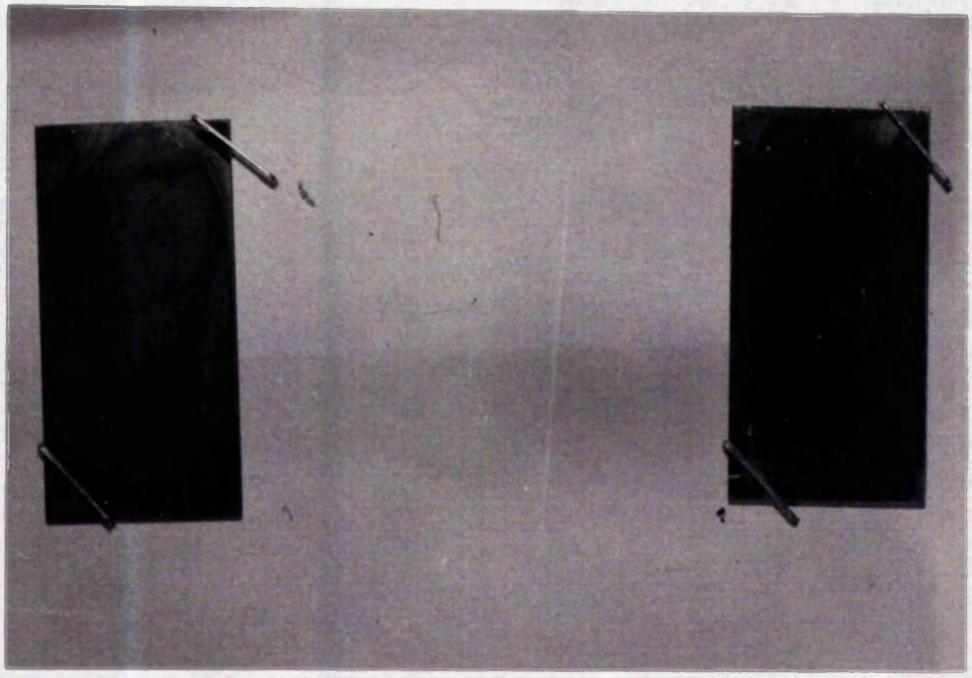

Blank Pretreated Specimen

Fig.I4 Pretreatment by the Duraglit Method.

Treatment of the Copper Surface.

The solution used in this treatment was a 0.5% wt/v solution of benzotriazole in distilled water. The temperature of this solution was maintained at between 60°C and 70°C by a Simmerstat - it was found that above this temperature bubbles were formed on the copper surface, causing a non-uniform coating of benzotriazole on the copper surface.

The copper electrode was prepared as described above and the water-wet specimen immersed in the treating solution. After two minutes it was removed, washed in distilled water, and dried between two filter papers. Care must be taken at the drying stage to avoid getting dust or grease on the surface as this would cause a weakening in the benzotriazole/copper film with subsequent loss in protection.

Treatment of the electrodes was carried out just prior to their use in an experiment.

2.4. Experimental Procedure.

Although these experiments were initially carried out as preliminary ones, the results will be mentioned later as those obtained at zero velocity.

(a) Weight Loss Experiment.

The copper segments were de-greased in acetone and dried. Then they were swilled in conc.HCl, distilled water, acetone, and dried. After weighing, the segments were placed in boiling tubes containing 40mls. of 10% sulphuric acid, with varying amounts of benzotriazole dissolved in.

After being left in a constant temperature bath (25°C) for a month, the specimens were removed and the scale removed

by immersion in de-aerated concentrated HCl, washed in distilled water, dried, and re-weighed. The difference in the two weighings gives the weight loss at that particular concentration of benzotriazole. Four separate experiments were carried out at each concentration and, as the results agreed within 10%, the average over the four runs was taken.

Graph 1. shows the relationship obtained for weight loss of copper (mdd x 100) and the concentration of benzotriazole in the acid (% mole.).

As the concentration of benzotriazole increases from 0%, the weight loss, and therefore the corrosion rate, decreases. A minimum value is obtained at 0.13%. Further increase in benzotriazole concentration results in an increase in weight loss. Above a concentration of 0.45%, benzotriazole acts as a stimulator to the corrosion of copper in sulphuric acid.

Pretreatment of the copper was even more efficient than the optimum concentration of benzotriazole.

These results are similar to the ones obtained by Makrides and Hackerman (34) and Jones (15) both working with thiourea and sulphuric acid.

(b) Potential Experiments.

The experiments were performed in the apparatus shown schematically in Fig. I5. The probe was made from glass tubing which had been heated, drawn out, and curved. The tip of the probe was ground on wet/dry grinding paper so that it could be placed almost touching the metal face (about 1mm from it).

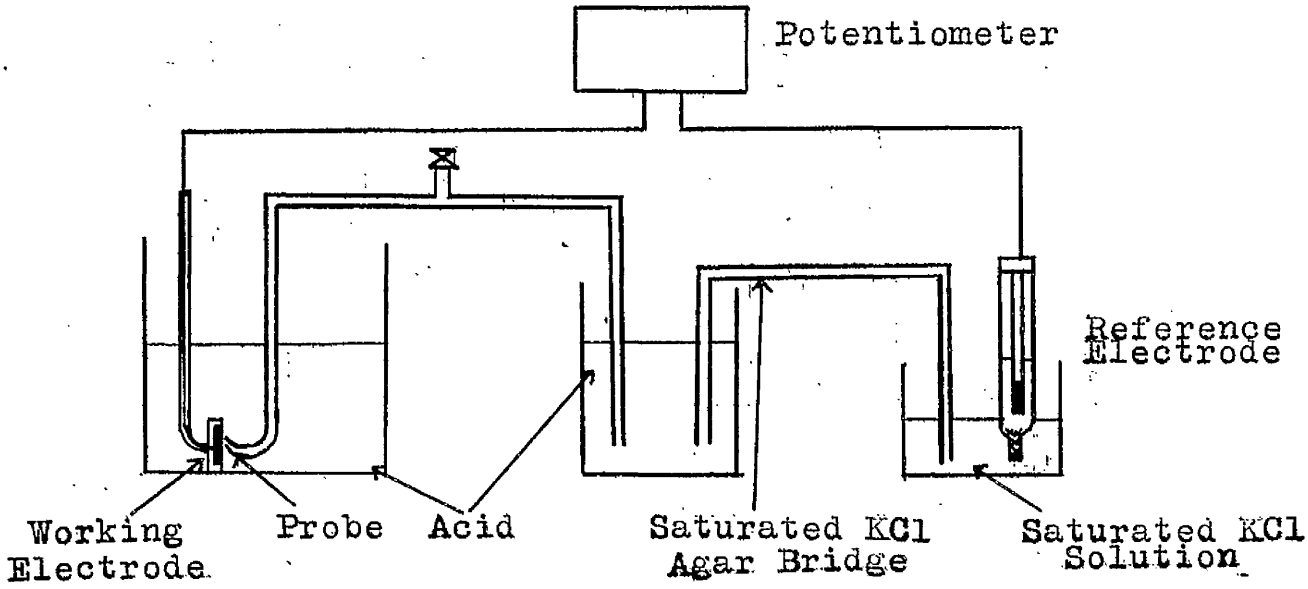

Fig.I5. Arrangement used for Potential Experiments

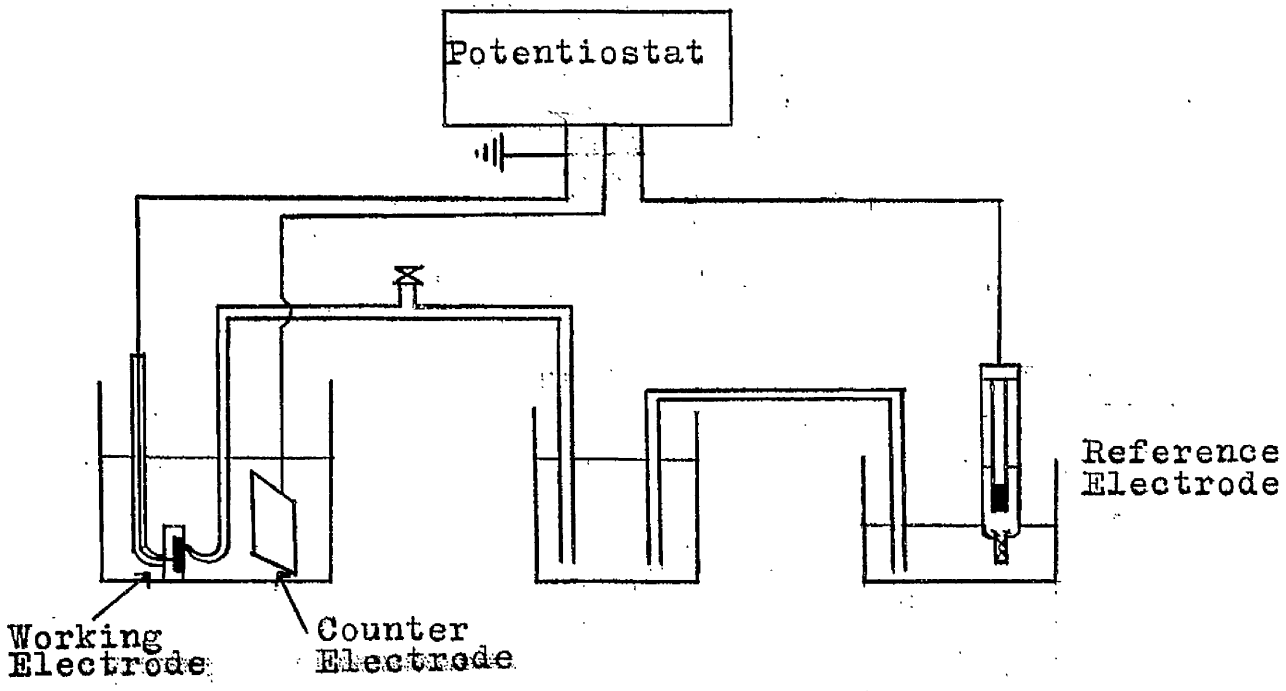

Fig.I6. Arrangement used for Potentiostatic Experiments.

400 mls. of acid were used and the benzotriazole added in successive amounts after each reading. On the addition of the benzotriazole, the copper was allowed to reach a new steady rest potential before a reading was taken.

Another experiment was carried out in which the benzotriazole was all added at one concentration, instead of a small amount at a time and progressing through the concentration range that way.

The results of these two types of experiment did not differ outside experimental error and are shown in Graph 2.

On increasing the concentration of benzotriazole in the acid, the potential of the copper specimen moves to a more noble potential than the rest potential. On increasing the concentration above 0.1%, the potential moves more active and above a concentration of 0.5% the specimen moves to a more active potential than its rest potential at 0% benzotriazole. The rest potentials at 0% and 0.5% benzotriazole are equal.

Below a concentration of 0.15% (maximum inhibitor efficiency as given by weight loss experiments) the rest potential of the copper changed very quickly on the addition of inhibitor. Whereas above this concentration, it changed more slowly.

Again Hackerman and Makrides (34) and Jones (15) found similar results, except that Jones found that at very low concentrations of inhibitor, the rest potential of mild steel moved more active before going more noble.

(c) Capacitance Experiments (performed at a frequency of I kc/s.)

The electrodes used in these experiments have already been described. They were washed, dried, and masked off with tape. A platinum spade was used as a counter electrode. Both were placed in a beaker containing 100 mls. of acid and connected to the terminals of an electrolytic conductivity bridge.

A balance was obtained by successively altering the resistance, capacitance, and finally resistance arms of the instrument until minimum sound was heard in the earphones.

A separate electrode was used for each reading at a particular benzotriazole concentration. This enabled both the capacitance and the resistance of the copper/acid interface to be obtained. A relationship is known (125) which relates the capacitance of the electrical double layer and the fraction of area of coverage by an inhibitor. This relation is -

$$\theta = \frac{Cu - Ci}{Cu - Cs}$$

where θ = fraction of area of surface coverage.

Cu = capacitance of untreated copper in uninhibited acid.

Ci = capacitance of untreated copper in inhibited acid.

Cs = capacitance of copper when saturated with inhibitor at that particular concentration.

In these experiments Cs was taken as the capacitance of pre-treated copper. A better representation of the fraction of surface coverage will then be obtained.

Graph 3 shows the relation between the fraction of area coverage (θ) and the concentration of benzotriazole.

The fraction of surface coverage increases as the benzotriazole concentration increases from zero, a very sharp increase occurring between 0.1% and 0.15%. After reaching a maximum at 0.15%, there is a steady fall in the fraction of coverage to an almost constant value above 0.75%.

Graph 4 shows the relation between the resistance of the copper/acid interface and the benzotriazole concentration.

As can be seen, it follows almost the same shape as Graph 3. The resistance increases to a maximum at 0.125% and falls to a constant value in the range 0.75% to 1.0%.

(d) Potentiostatic Experiments.

The potentiostatic experiments, under various conditions, were carried out using the apparatus shown in Fig. I6.

400 mls. of acid were used and the apparatus set up as shown. The electrode, having been made up as previously described, was polished on fine wet/dry grinding paper (Struers 600), washed with distilled water, and placed 1mm. from the probe. The potentiostat was set up at -1000mV with respect to the reference calomel electrode and the instrument switched on. The current to maintain this potential constant was noted after it had become steady. The potential was moved 50mV anodically and, after becoming steady, the current was again noted.

This procedure was carried out in a stepwise manner until +200mV with respect to the reference electrode was reached.

At this potential, the anodic current flowing was so large that at a higher value it may begin to effect the reference circuit. The reference circuit had been shown to be affected by passing too high a current in the cell (126).

In this way, the polarization curve (potential-current curve) for the specimen could be obtained. The various conditions for which polarization curves were obtained are given below:-

(i) Using uninhibited acid.

Polarization curves for both untreated and treated copper (Graphs 5 and 6) were obtained. In order to determine the effect of reversing the trace, the experiments were repeated, starting at + 200 mV. and going in a stepwise manner to -1000mV. (Graphs 7 and 8).

Graphs 5 and 6 were also used as a basis for comparing the effects of the various conditions imposed.

Experiments were also carried out using oxygenated (Graph 9) and de-oxygenated (Graph I0) acid. Gas-saturation of the acid was carried out in the packed tower of the flow system and is described in the next chapter.

(ii) Using inhibited acid.

In these experiments a known weight of benzotriazole was dissolved in the 400mls. of acid before the immersion of the electrode. The concentration range employed for these experiments was 0% to 1.0% benzotriazole in the solution. A separate solution was made up for each individual experiment. Graphs II & I2 show the polarization curves for these concentrations of benzotriazole.

By using the idea of polarization resistance (Rp), it is possible (127) to evaluate the weight loss (and therefore corrosion rate) from the above polarization data. The relationship is

$$Rp = \left(\frac{\partial E}{\partial i}\right)_{Ecorr.} \qquad (1)$$

where Rp = polarization resistance.

$\left(\frac{\partial E}{\partial i}\right)_{Ecorr}$ = rate of change of potential with current density at the corrosion potential.

Rp is also related to the corrosion rate -

$$K = \frac{C}{Rp} \qquad (2)$$

where K = corrosion rate.

C = constant of the system.

So combining the two expressions -

$$K = \frac{C}{\left(\frac{\partial E}{\partial i}\right)_{Ecorr.}}$$

By using this expression the corrosion rates may be estimated from polarization data.

The value $\left(\frac{\partial E}{\partial i}\right)_{Ecorr.}$ is read from the polarization graph within ± 15 mV of passing through the line i = 0 . The constant, C, can be evaluated by obtaining $\left(\frac{\partial E}{\partial i}\right)_{Ecorr.}$ at a concentration where the corrosion rate is known. This was done by taking a weight loss value in initial series of experiments. (see Appendix II for calculations.)

Graph 13 shows the relation between these theoretical weight losses from polarization data and the concentration of

benzotriazole. As can be seen by comparison with graph 1, there is very close agreement with the two sets of values.

All the results obtained in static media will be discussed in detail, and in comparison with those obtained in flowing media, in Chapter 4.

GRAPH I. Weight Loss of Untreated Copper in Inhibited Aerated Acid.

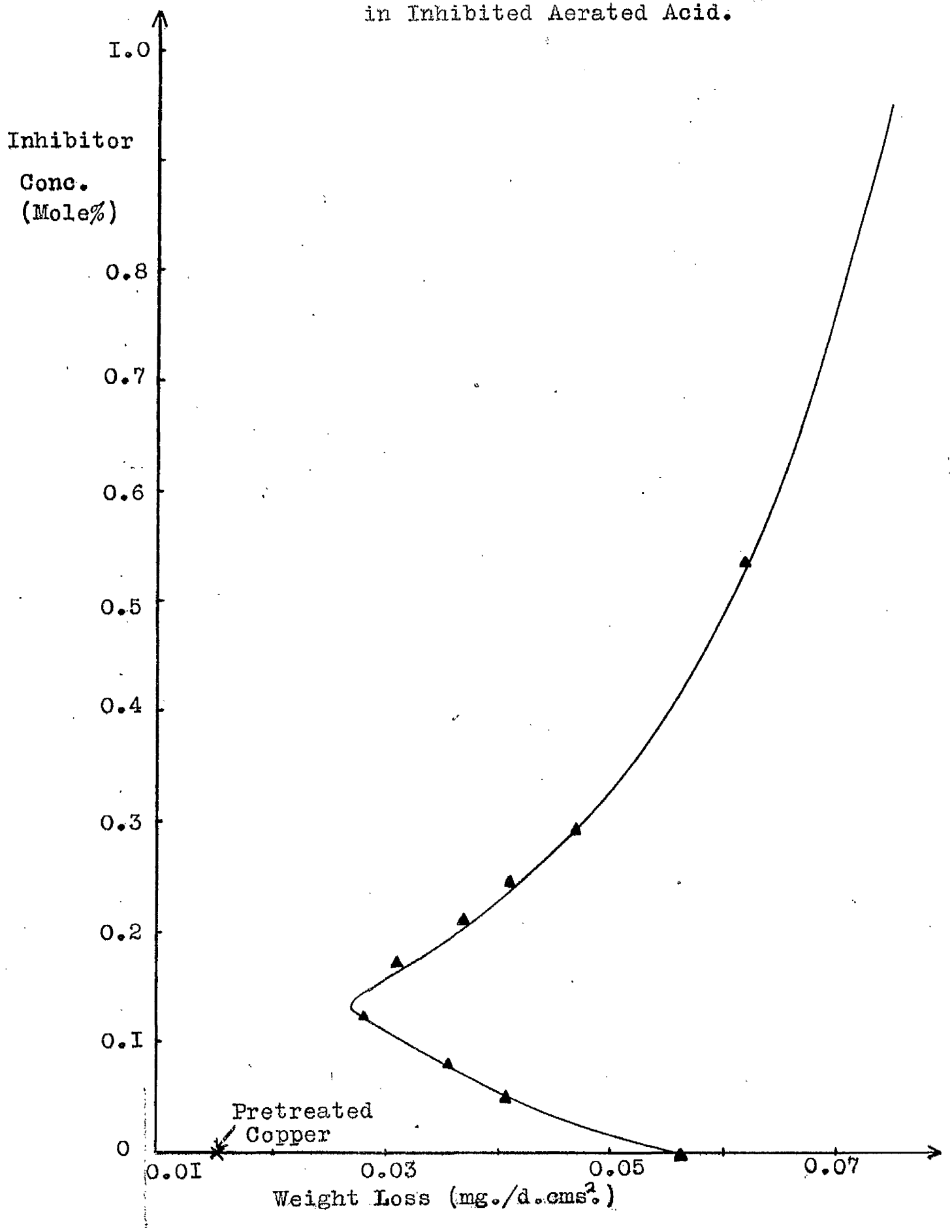

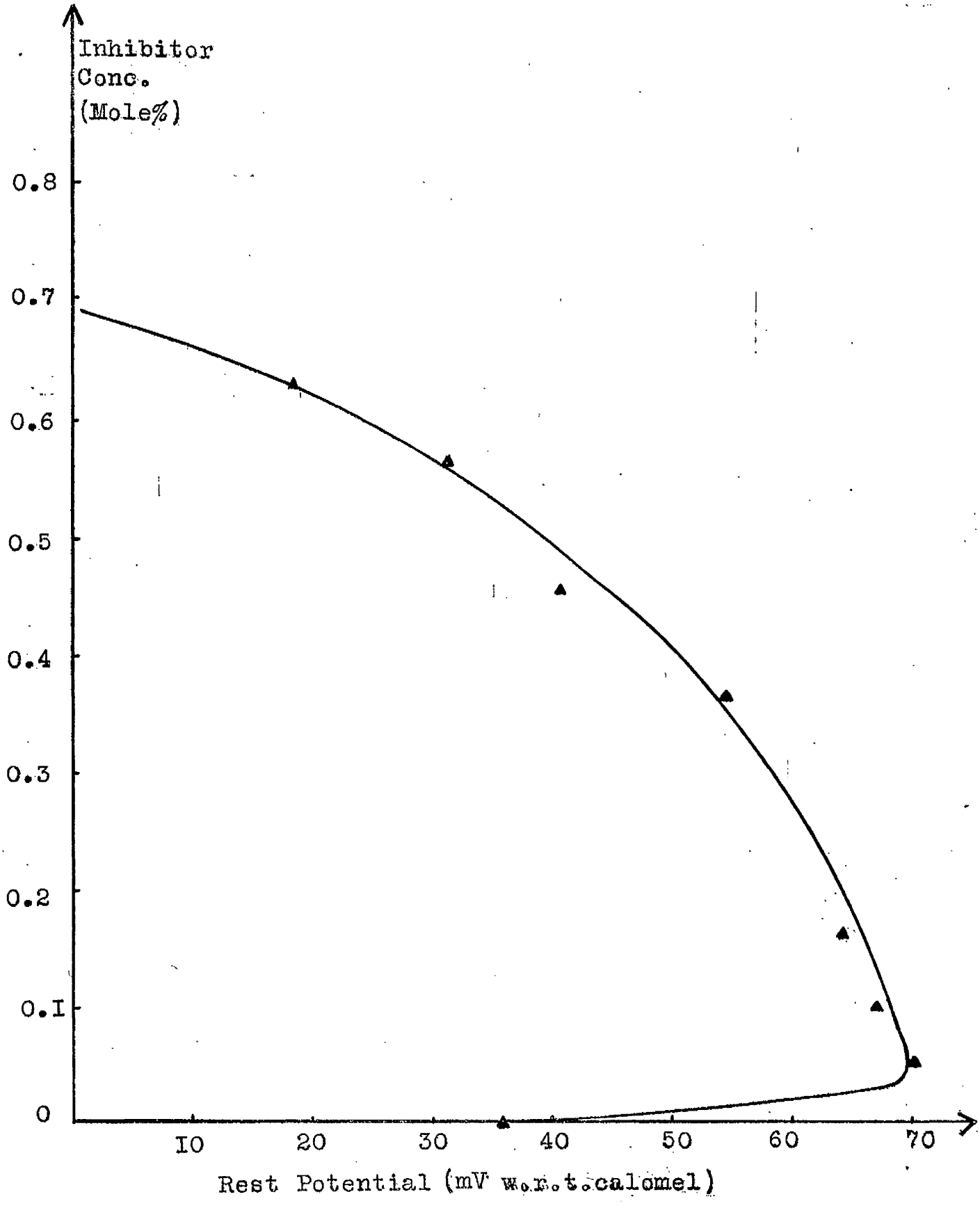

GRAPH 2. Variation of Rest Potential of Untreated Copper in Inhibited Aerated Acid.

GRAPH 3. Variation of Fraction of Surface Area of Coverage of Benzotriazole in Inhibited Aerated Acid.

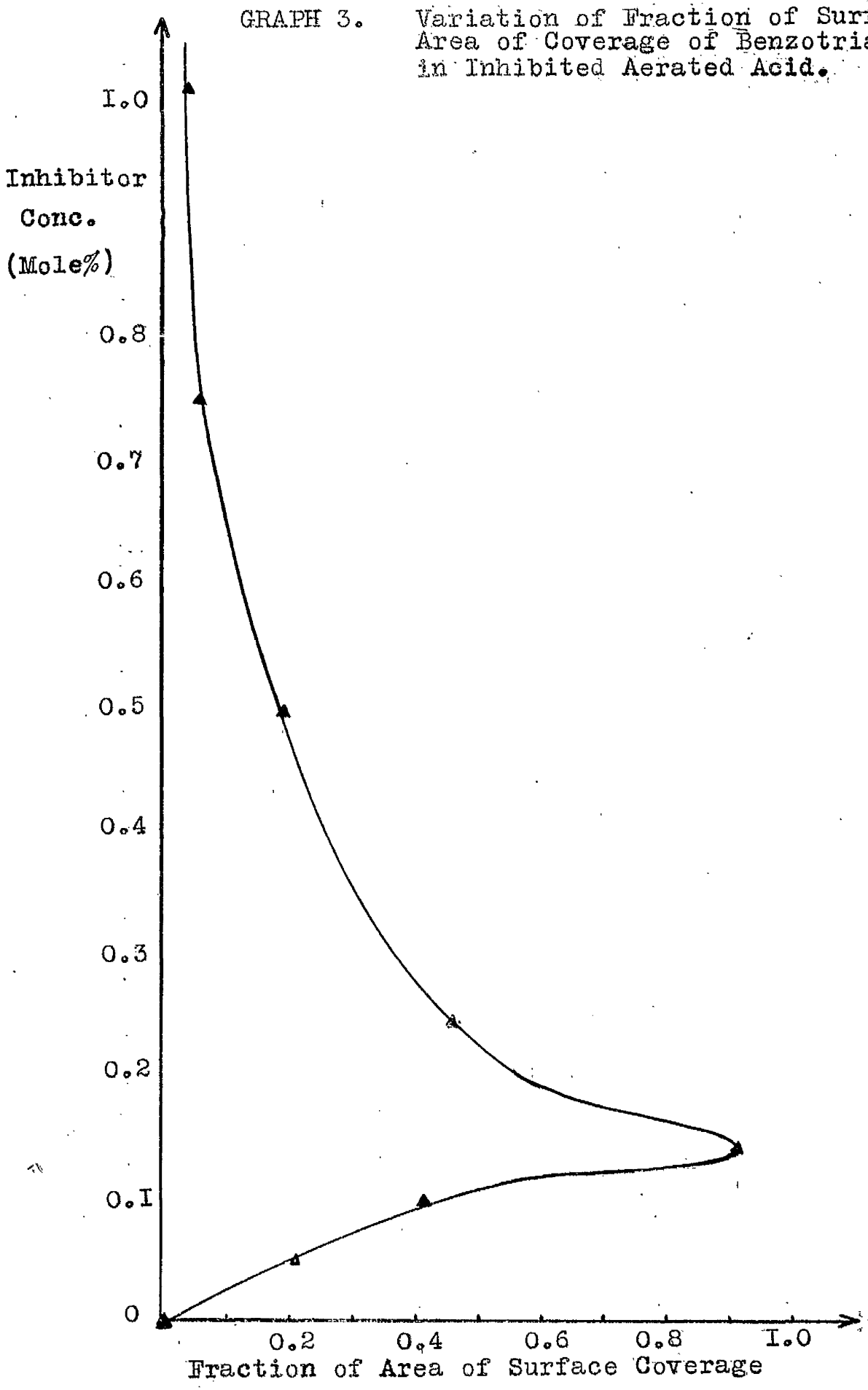

GRAPH 4 Variation in Resistance of the Electrical Double Layer of the Metal in Inhibited Acid.

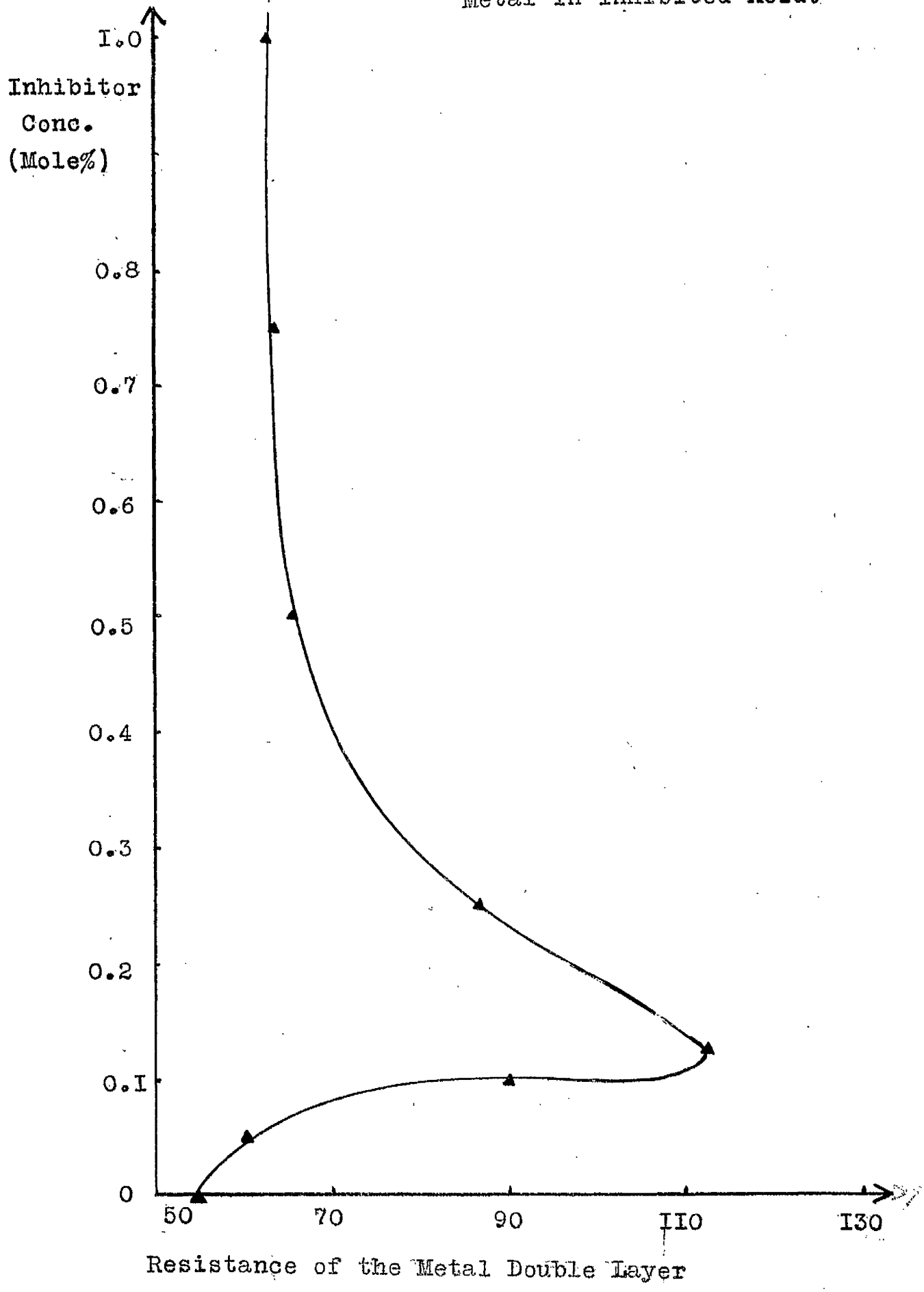

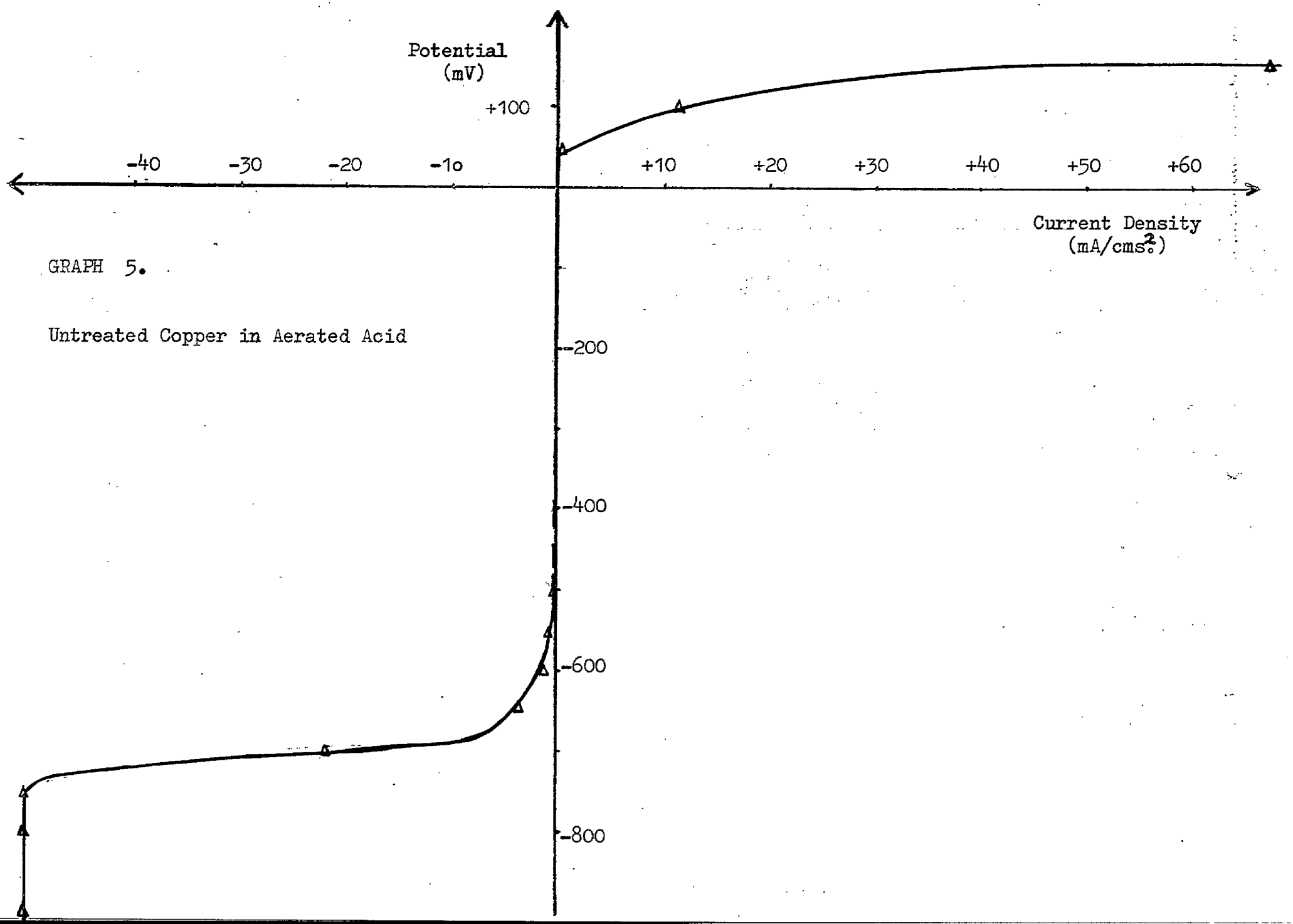

GRAPH 5.

Untreated Copper in Aerated Acid

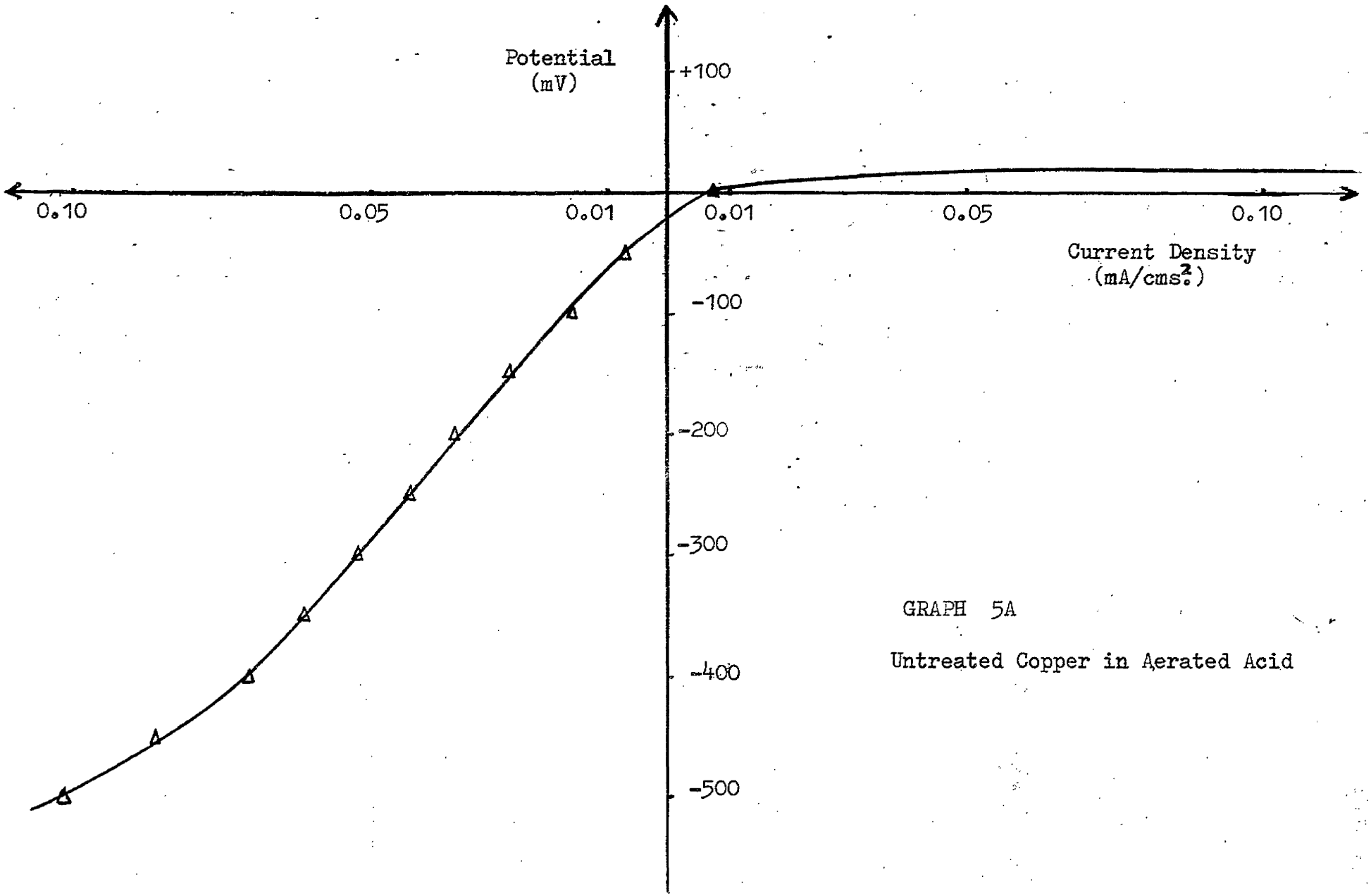

GRAPH 5A

Untreated Copper in Aerated Acid

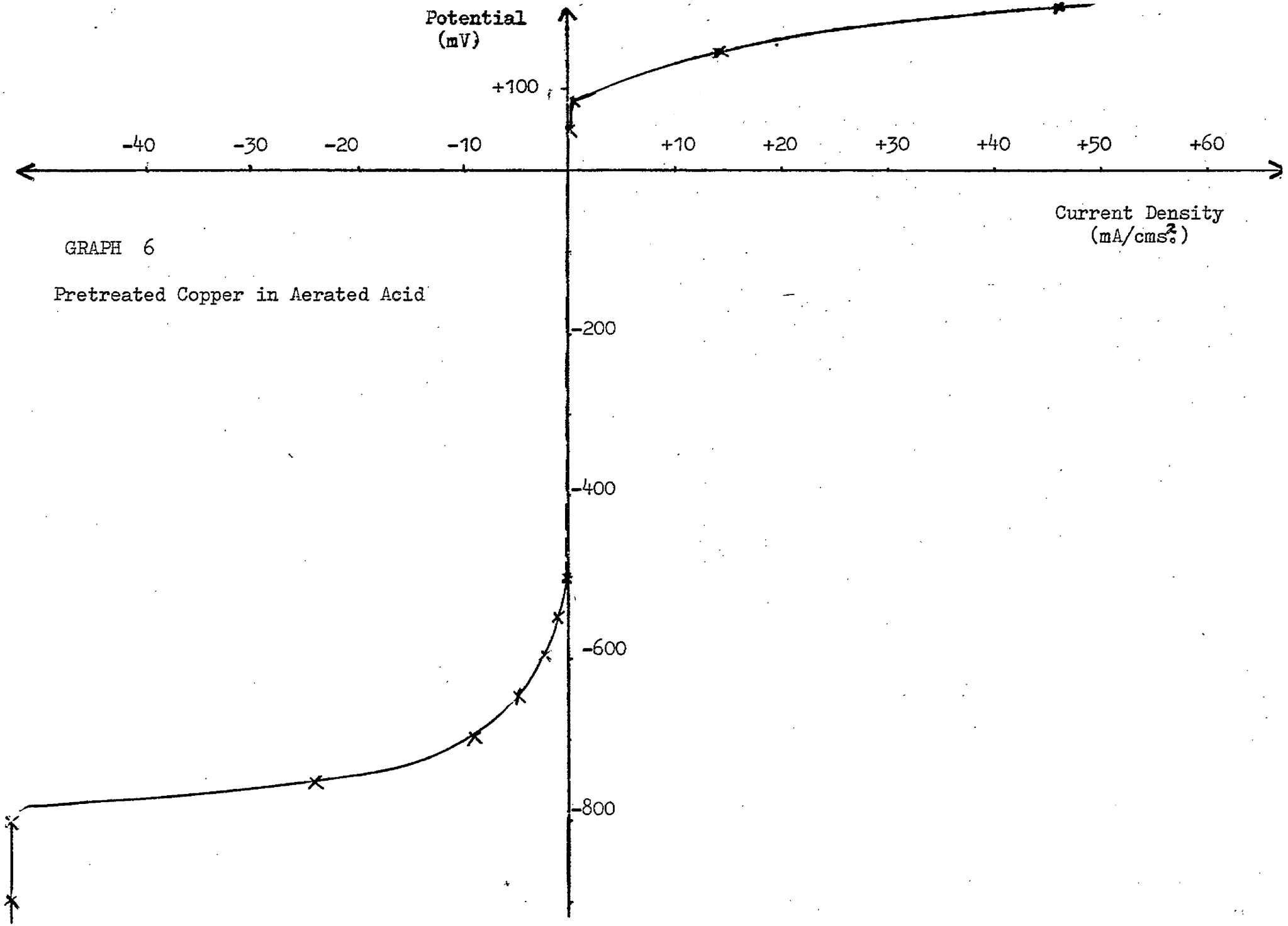

GRAPH 6

Pretreated Copper in Aerated Acid

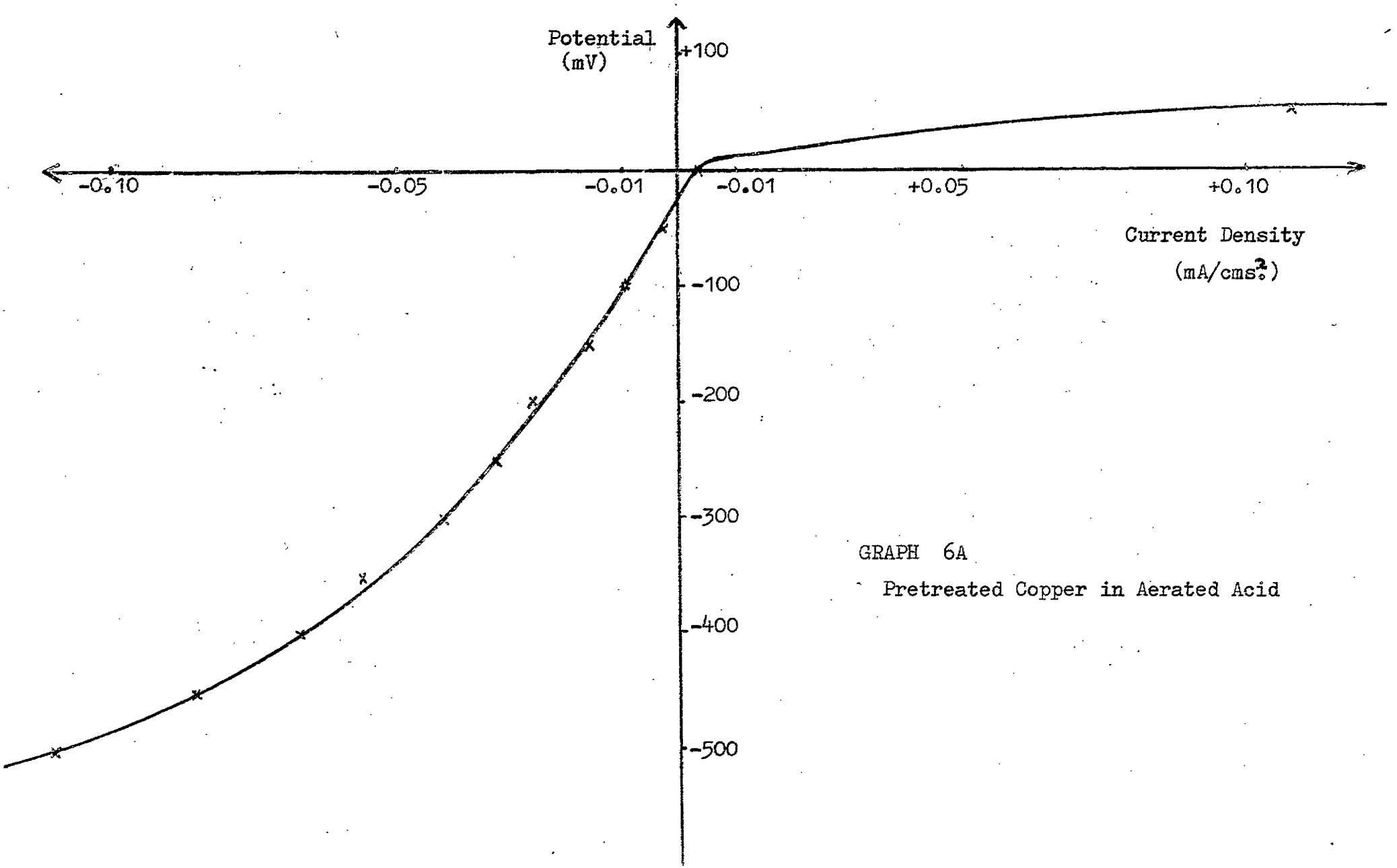

GRAPH 6A

Pretreated Copper in Aerated Acid

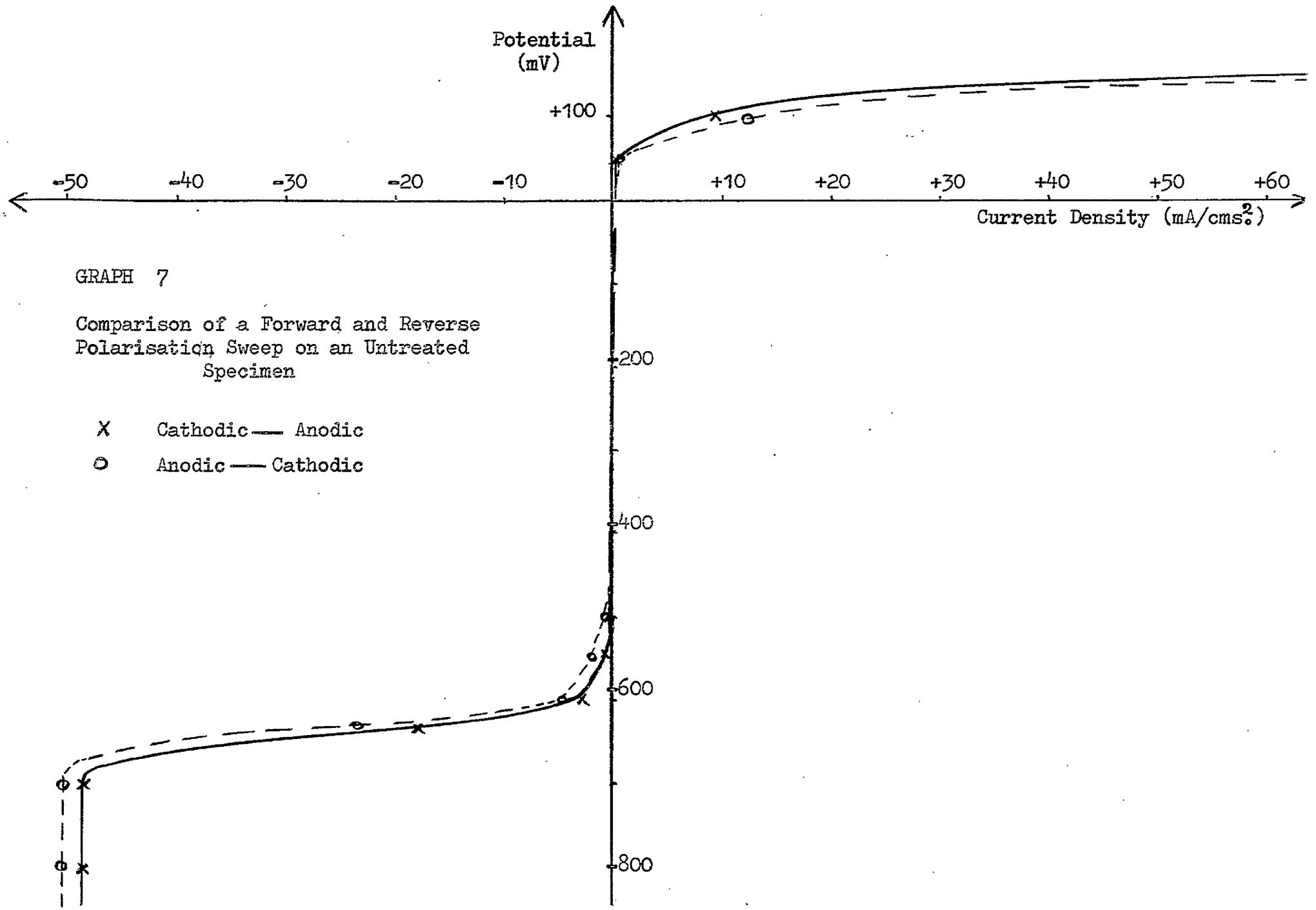

GRAPH 7

Comparison of a Forward and Reverse Polarisation Sweep on an Untreated Specimen

X Cathodic — Anodic

O Anodic — Cathodic

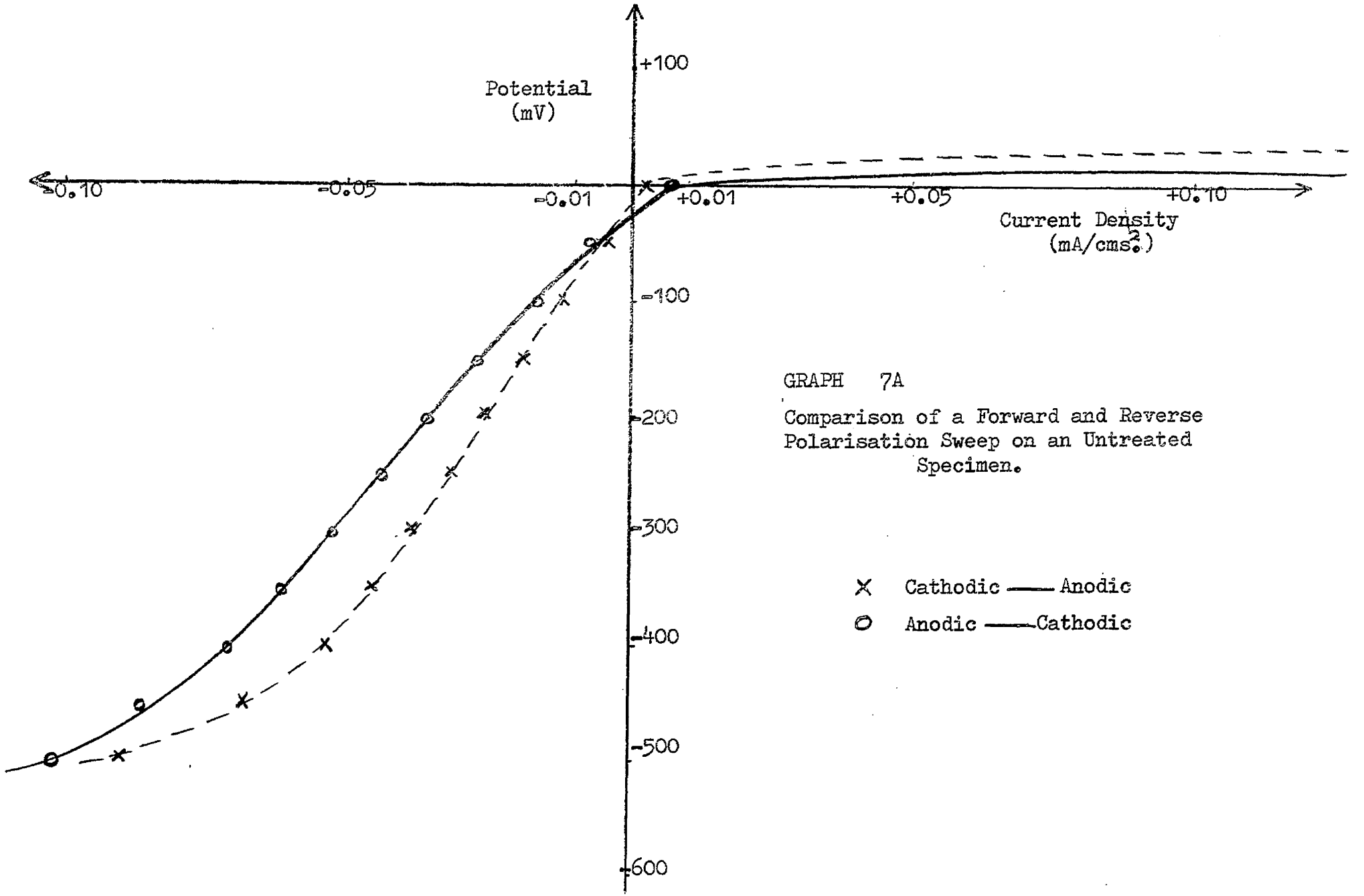

GRAPH 7A

Comparison of a Forward and Reverse Polarisation Sweep on an Untreated Specimen.

× Cathodic —— Anodic

○ Anodic —— Cathodic

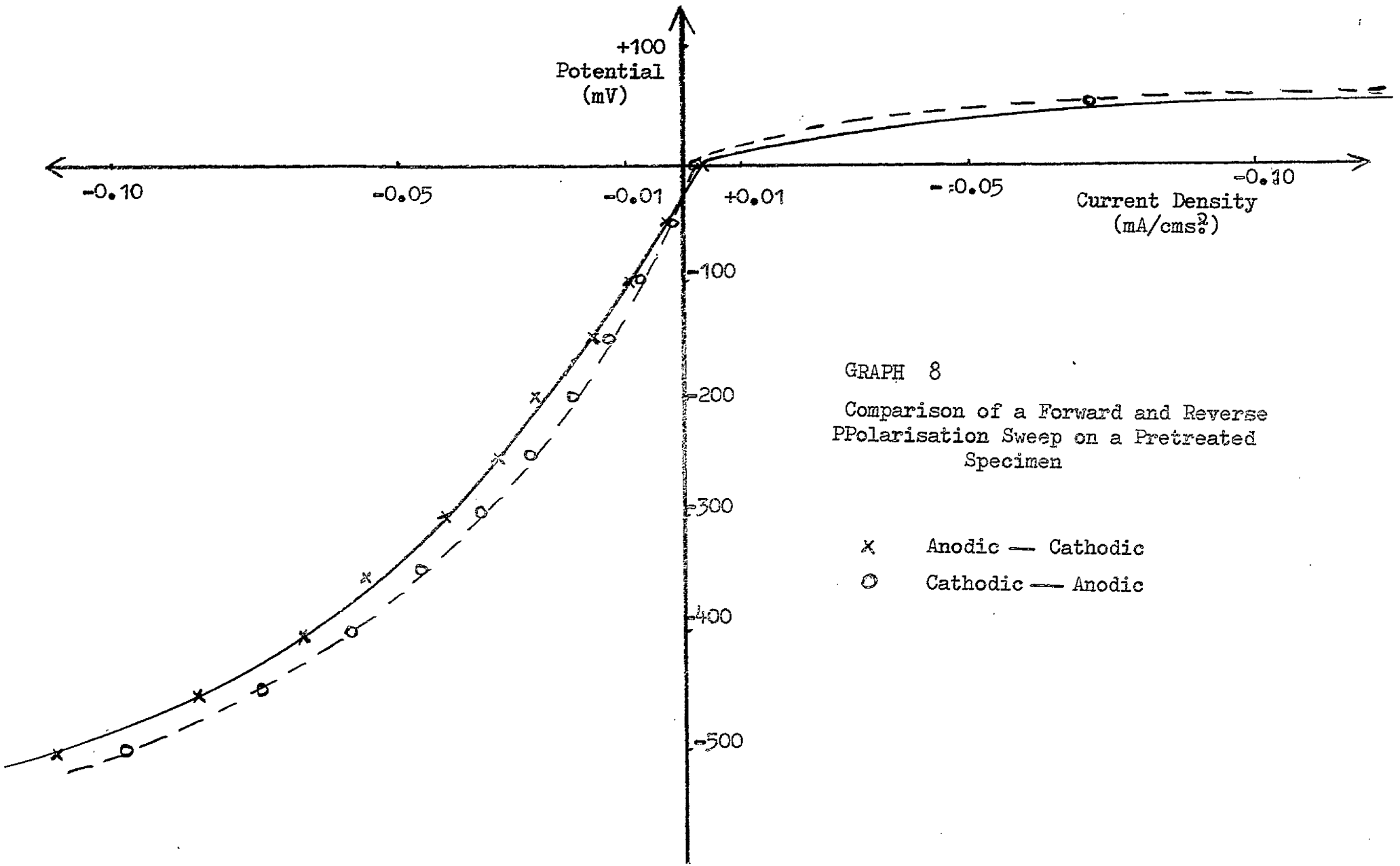

GRAPH 8

Comparison of a Forward and Reverse PPolarisation Sweep on a Pretreated Specimen

× Anodic — Cathodic

O Cathodic — Anodic

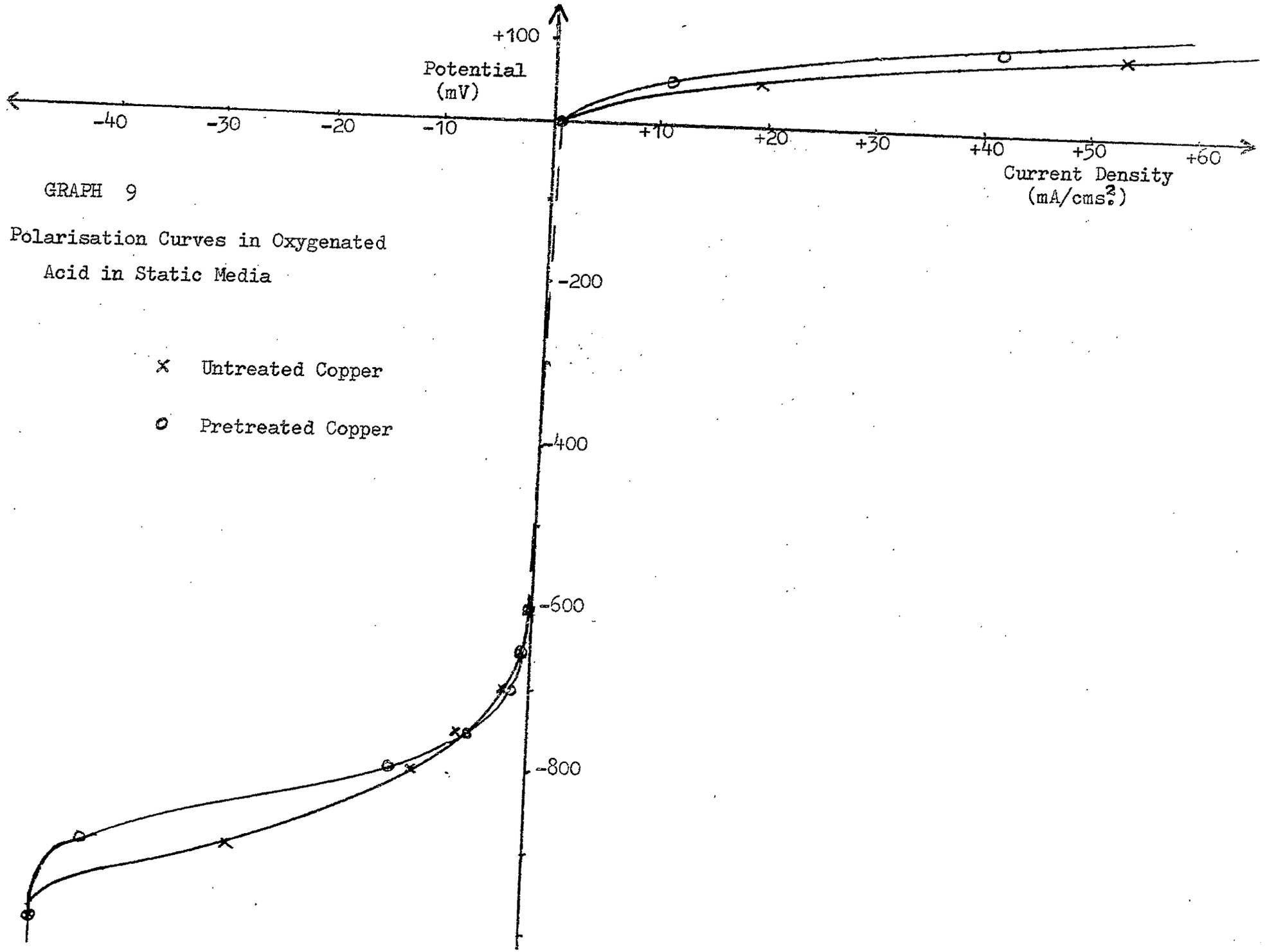

GRAPH 9

Polarisation Curves in Oxygenated Acid in Static Media

× Untreated Copper

o Pretreated Copper

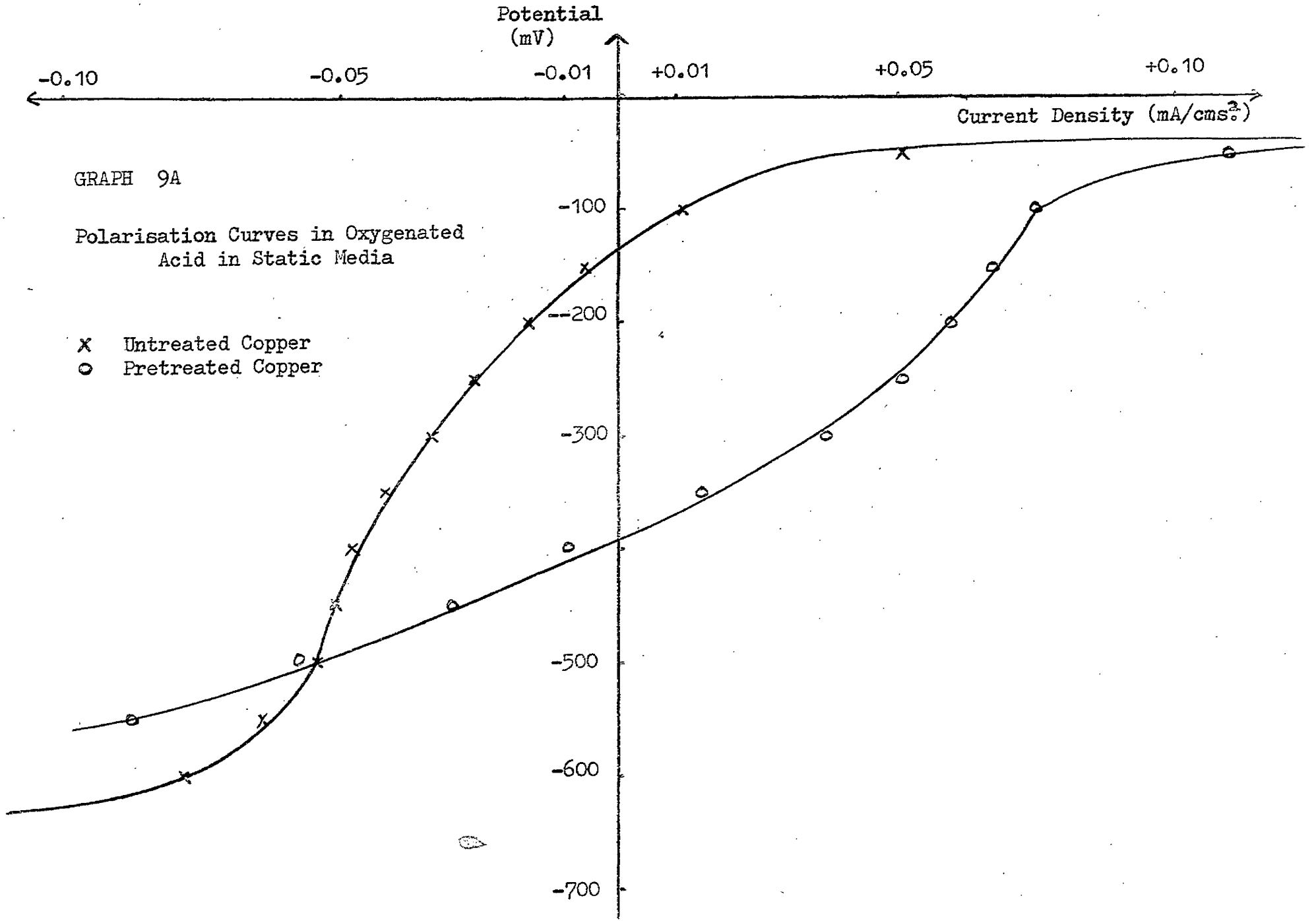

GRAPH 9A

Polarisation Curves in Oxygenated Acid in Static Media

X Untreated Copper
O Pretreated Copper

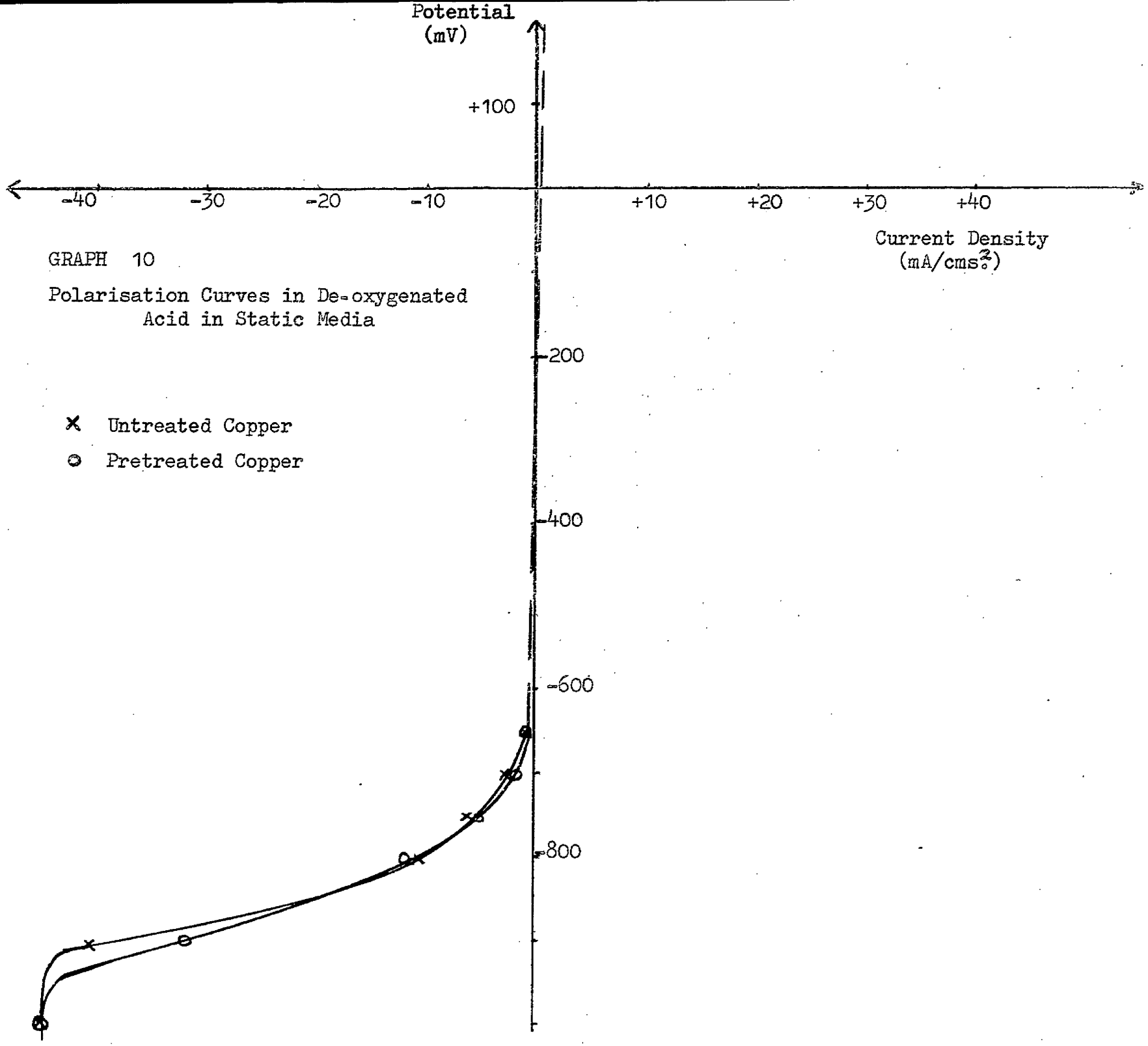

GRAPH 10

Polarisation Curves in De-oxygenated Acid in Static Media

× Untreated Copper

○ Pretreated Copper

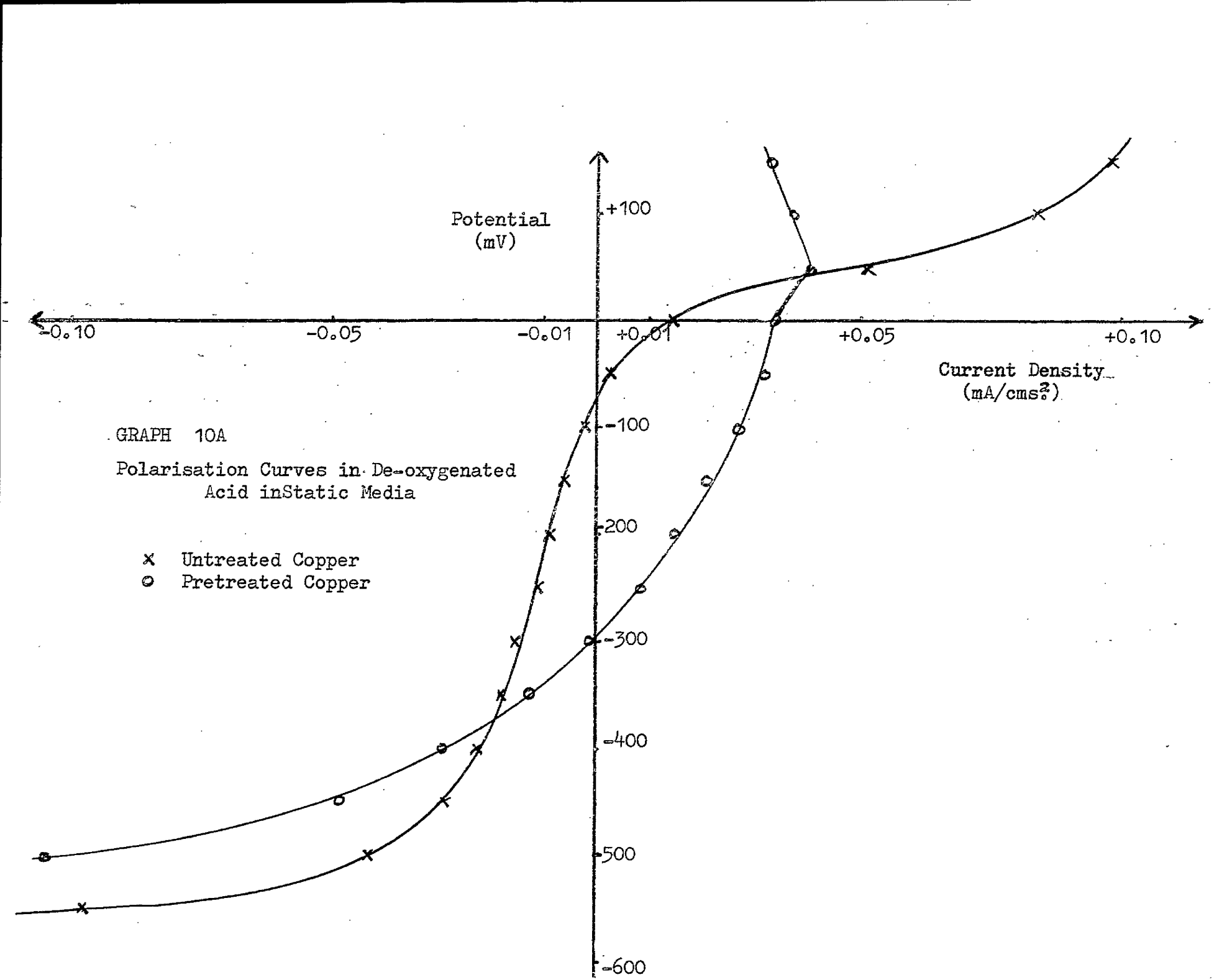

GRAPH 10A

Polarisation Curves in De-oxygenated Acid inStatic Media

× Untreated Copper
o Pretreated Copper

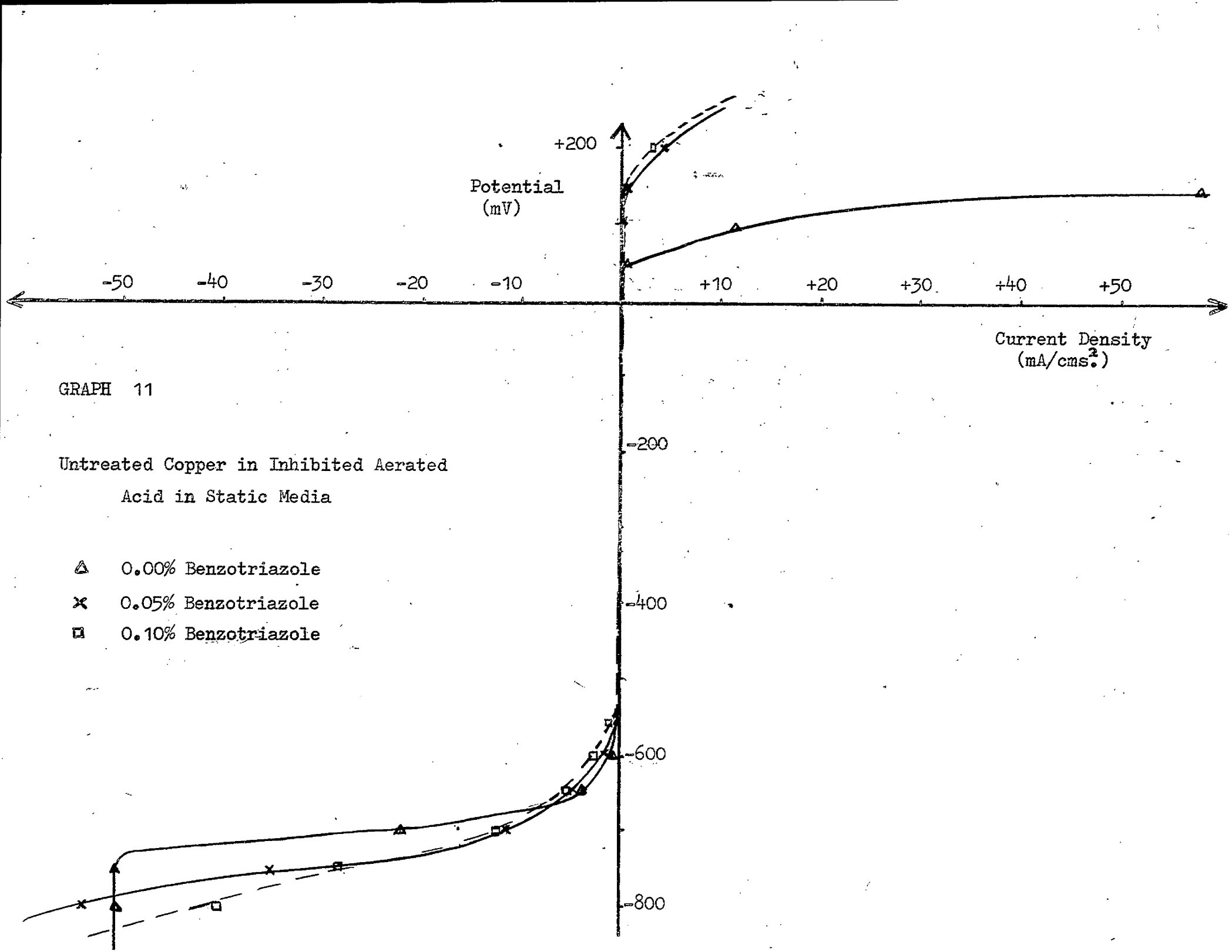

GRAPH 11

Untreated Copper in Inhibited Aerated Acid in Static Media

△ 0.00% Benzotriazole

× 0.05% Benzotriazole

□ 0.10% Benzotriazole

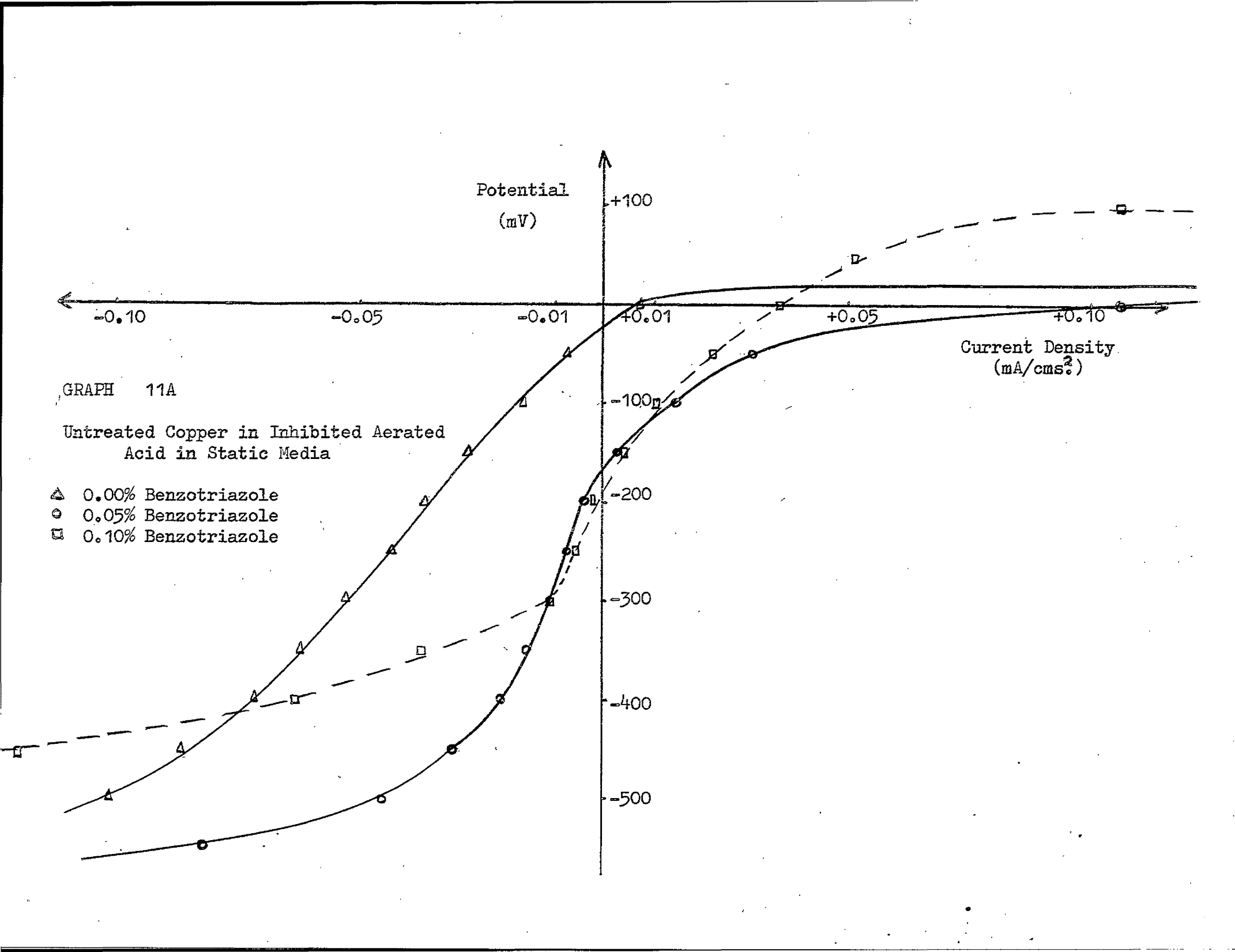
Potential
(mV)
+100
-100
-200
-300
-400
-500
-0.10
-0.05
-0.01
+0.01
+0.05
+0.10
Current Density
(mA/cms.²)
GRAPH 11A
Untreated Copper in Inhibited Aerated
Acid in Static Media
0.00% Benzotriazole
0.05% Benzotriazole
0.10% Benzotriazole

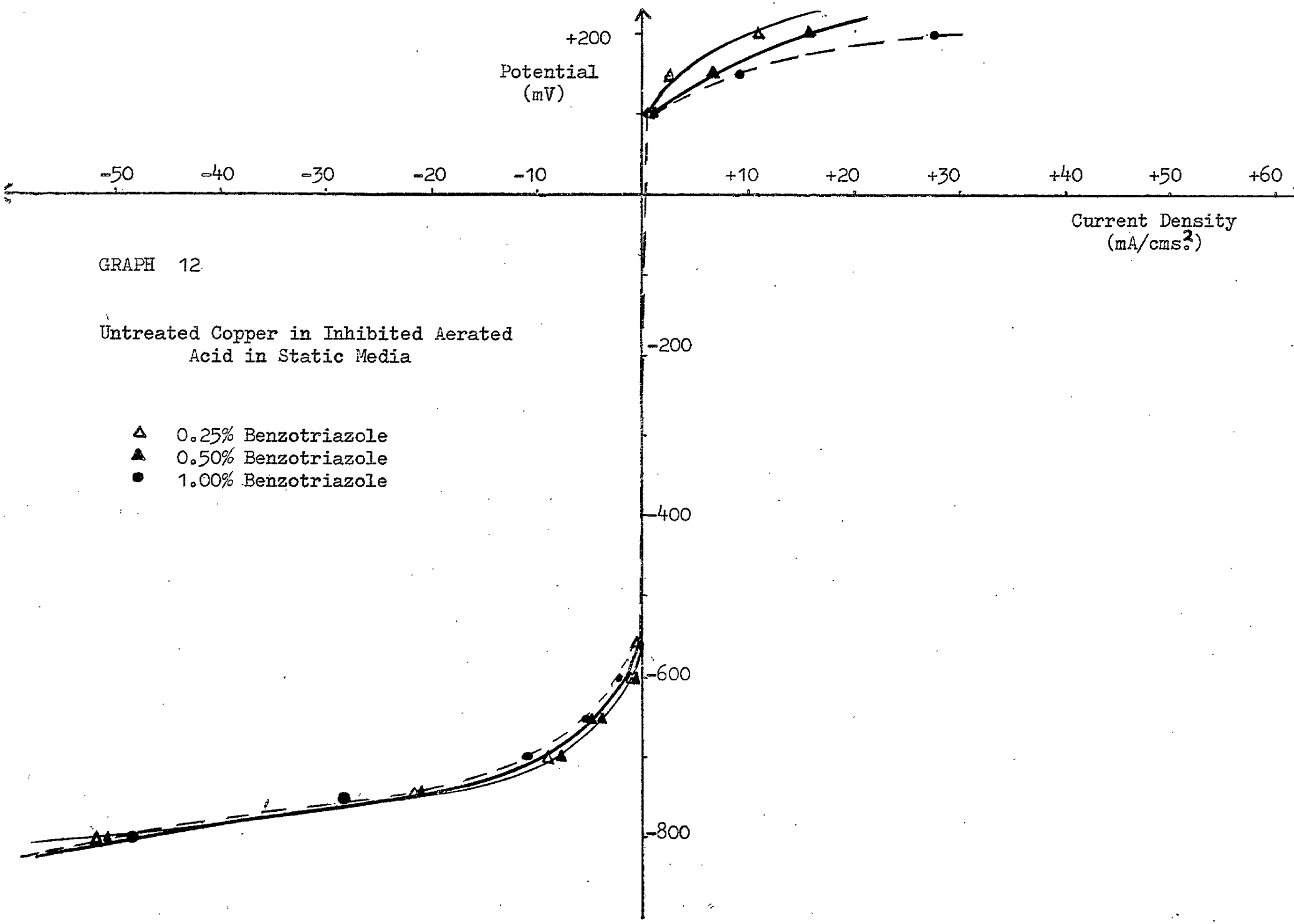

GRAPH 12

Untreated Copper in Inhibited Aerated Acid in Static Media

△ 0.25% Benzotriazole
▲ 0.50% Benzotriazole
● 1.00% Benzotriazole

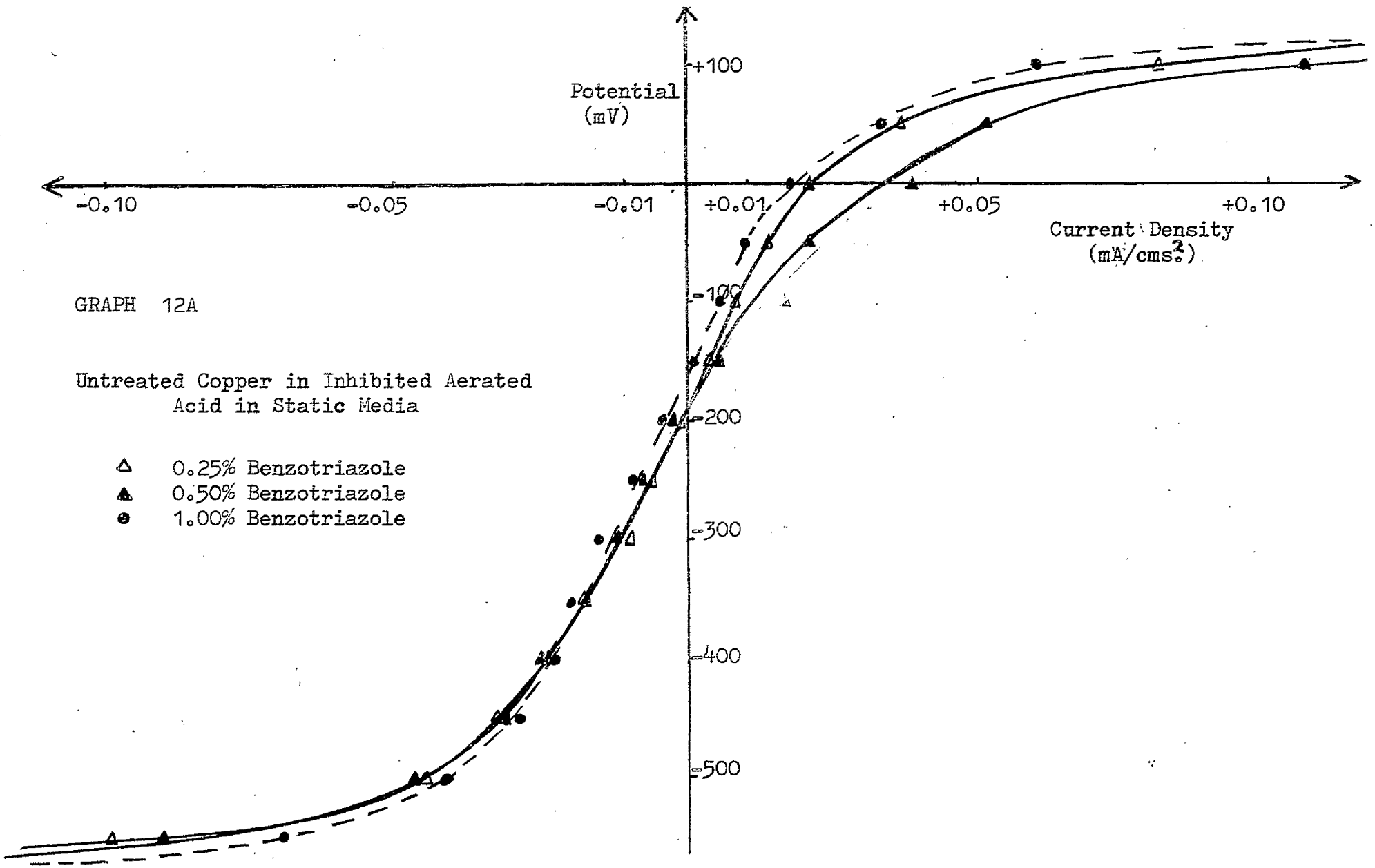

GRAPH 12A

Untreated Copper in Inhibited Aerated Acid in Static Media

- △ 0.25% Benzotriazole
- ▲ 0.50% Benzotriazole
- ● 1.00% Benzotriazole

GRAPH I3 Theoretical Weight Loss of Copper from Polarisation Data.

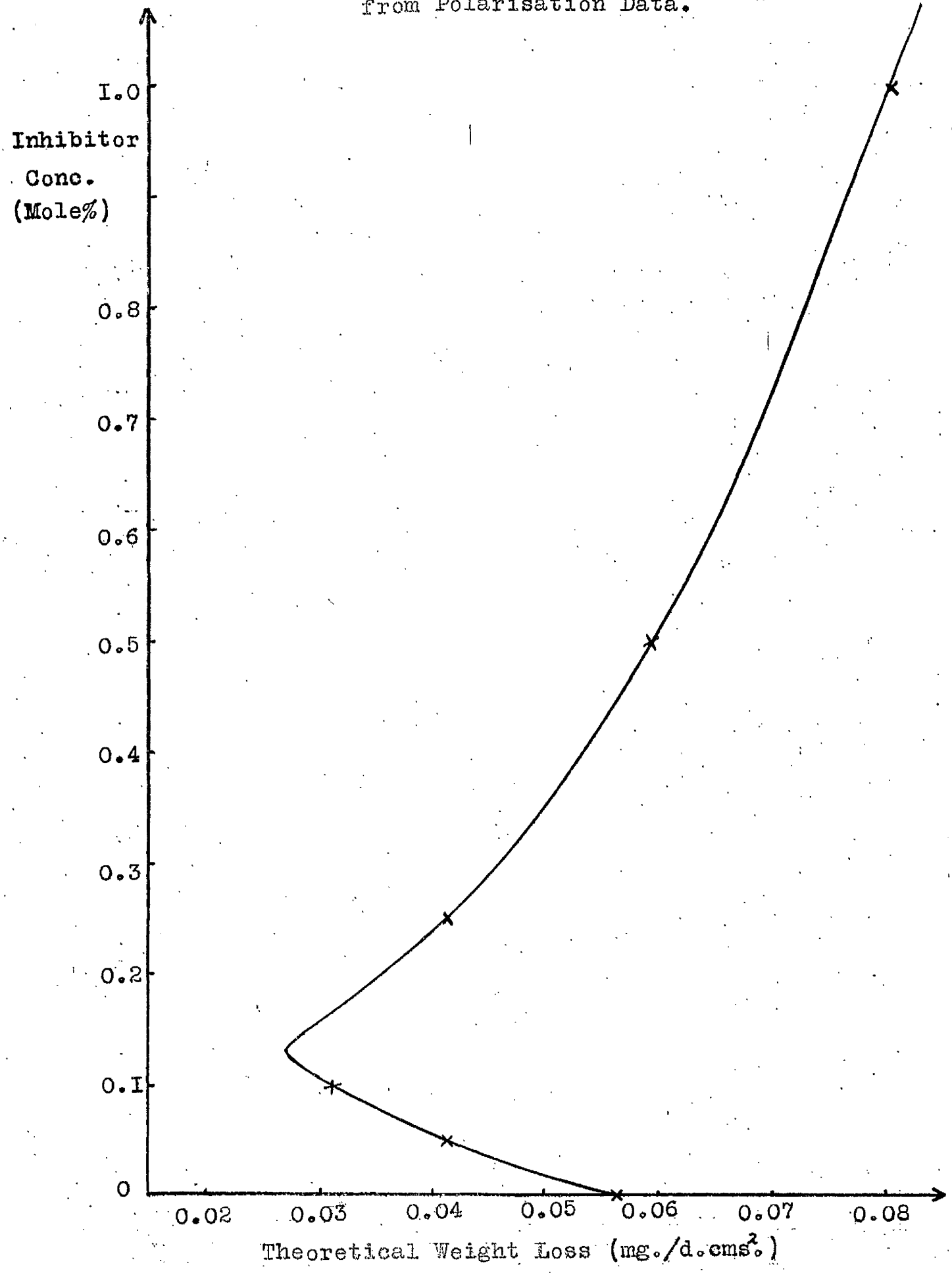

C H A P T E R 3.

Experimental Work in Flowing Media.

3.I. Introduction.

In electrochemical experiments where it is desired to observe the influence of varying flow rates on the metal surface, it is essential to have a system in which fully developed flow exists. Rotating cylinders and discs have been used for this purpose. It has been claimed that with rotating cylinders a uniform mass transfer rate over the entire surface is obtained - no complications over entry length exist. With small cylinders very high linear velocities are obtained at high revolutions, but this introduces centrifugal forces which may force the corrosion products to separate from the surface. The use of thin discs has indicated that the dissolution rate is higher at the edges than at the inner portions due to a thinner diffusion layer at the outer edge. The use of metal specimens inserted in large plastic cylinders suffers from the drawback that the specimens may have to be distorted in order to make them flush with the walls of the system.

An important factor to be taken into account is that the flow should be a representation of practical conditions - ie. flow in ducts. The rotating methods described above hardly fall into the category of hydrodynamics present in most cases of corrosion under dynamic conditions. In the present work the copper was obtained in sheet form, so that the use of a square duct made it possible for the specimens to be inserted

into the system without any distortion.

For a square duct no relationships between flow characteristics and entry length have been given in the literature. In this entry region, two pipe lengths are important; one for the velocity profile to form and one for the shear stress at the wall to reach its fully developed value. The entrance of the pipe involves either a sudden expansion or contraction in cross-sectional area and the configuration of the pipe entrance is important in determining the flow further downstream. However, the maximum entry length for fully developed boundary layers has been found to be approximately 70 pipe diameters for circular ducts over a large range of Reynolds Numbers. In this work an entry length of 96 pipe diameters was provided to allow smooth flow and a fully developed hydrodynamic boundary layer to develop.

3.2. Flow Apparatus.

(a) Flow System.

A schematic representation of the flow system (excluding the packed tower) is shown in Fig. I7; the flow system was constructed from $\frac{5}{8}$" q.v.f. glass tubing. An all-plastic centrifugal pump was used to circulate the liquid through the system. As shown, the acid was pumped from the reservoir (of capacity 20 litres) up to the surge tank (of capacity 15 litres). From there it flowed through the rotameters and the flow cell back to the reservoir tank. By-pass B enabled the acid to circulate, avoiding the flow cell so that the necessary fittings and adjustments could be made to the test section.

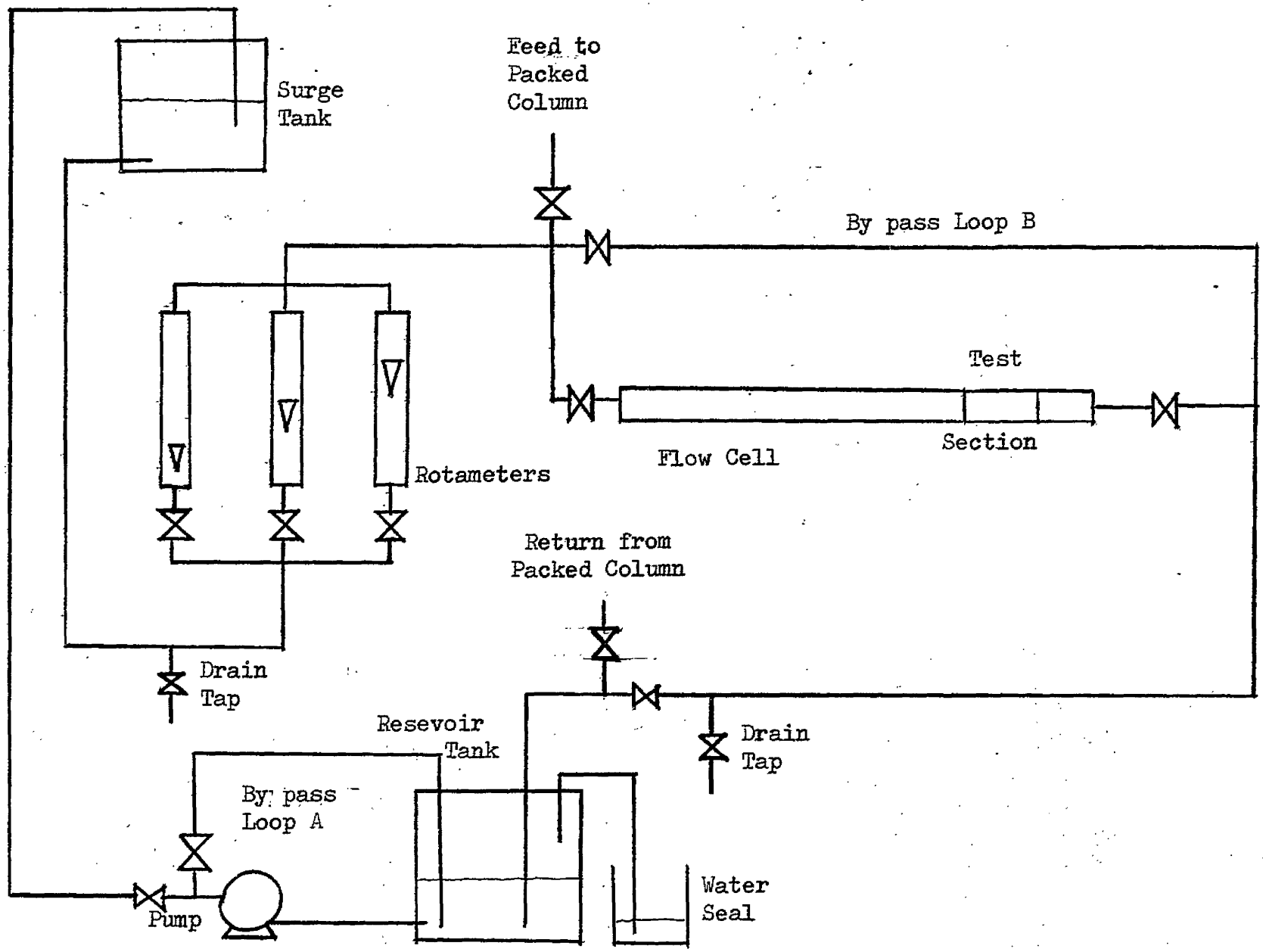

Fig. 17 Schematic Diagram of the Flow System.

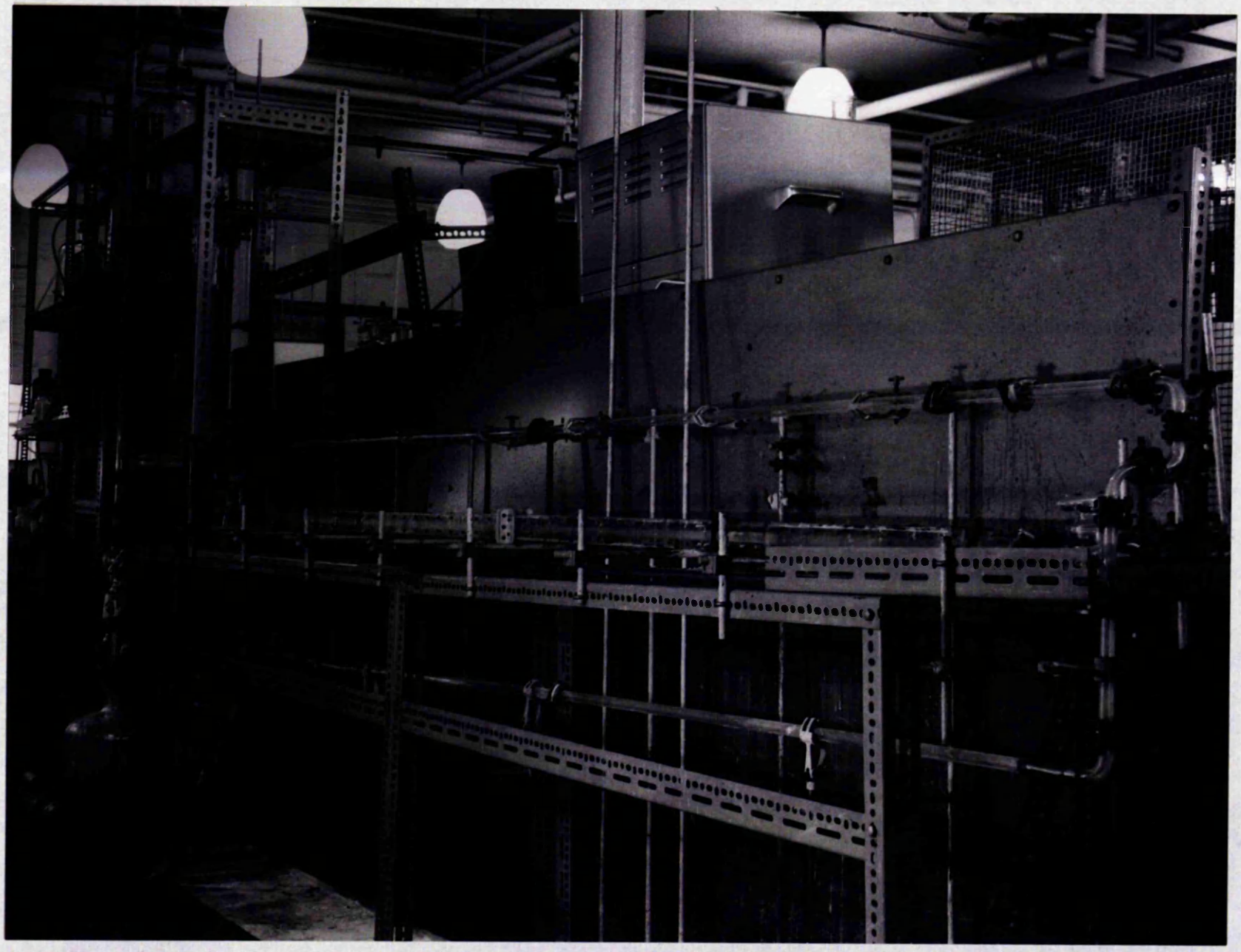

Plate Photograph of the Flow System.

The flow was measured by a set of three rotameters: 0 - 1.5 litres/min., 0 - 10 litres/min., and 0 - 35 litres/min. The flow was coarsely regulated by by-pass loop A and the fine adjustment made by the stop cock after the flow cell.

The surge tank served two purposes -

(i) It maintained the entire system under a positive head, so that no air could leak in.

(ii) It smoothed out any irregularities in the flow, caused by the pump.

(b) Flow Cell.

The flow cell was constructed from 0.9 cm. perspex and was of 1.8 cm. × 1.8cm. internal cross-section. A thin layer of polystyrene coating was applied in the shallow depression of the groove in order to make the joint leak-proof. The sides were then bolted together. As shown in Fig.I8, the perspex sides of the flow cell were continuous except for the test section where provision was made for the insertion and removal of the specimen decks. The total length of the flow cell was 9 ft. of which 6 ft. preceded the test section, thus ensuring that there were no disturbances due to the transformation from circular to square section flow, and also that flow had developed hydrodynamically. There was 18" after the test section to avoid any disturbances in reverting back to circular flow.

In order to make the changeover from circular to square section more gradual, a perspex block was placed at either end. A hole $\frac{5}{8}$" was drilled in one face and a 1.8×1.8 cms. square cut in the opposite one. The surfaces were

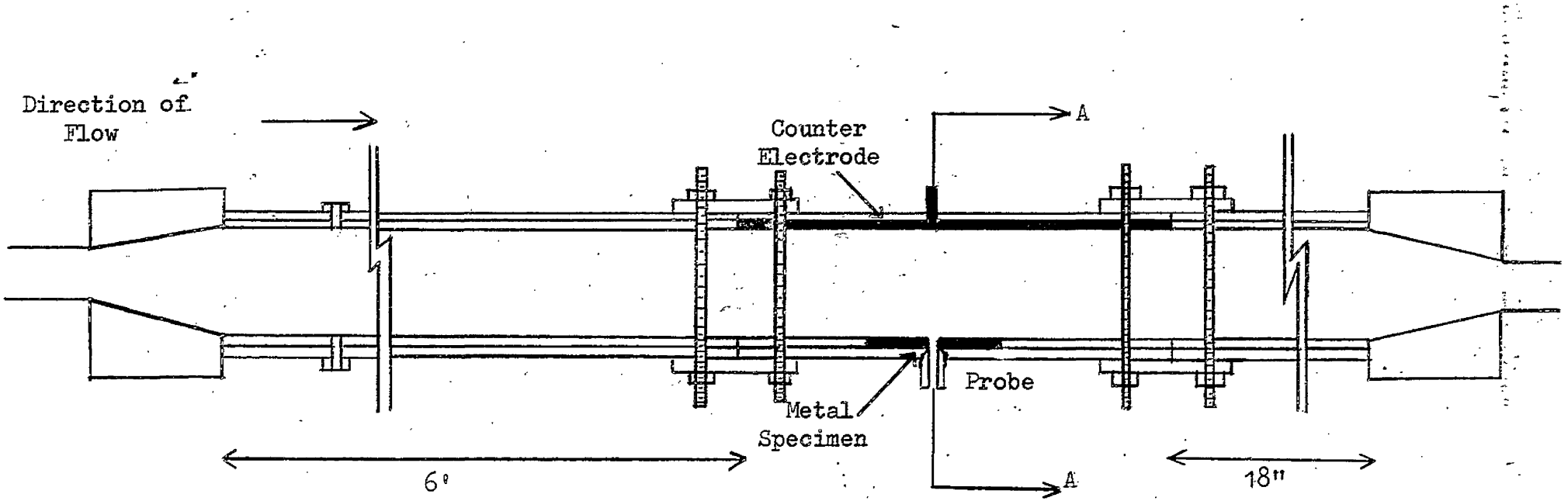

NOT TO SCALE

Section through A-A

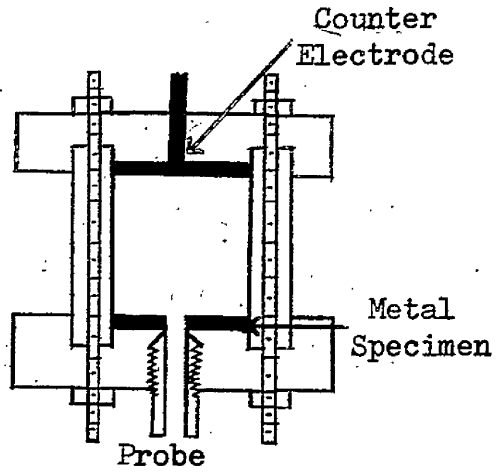

Fig. 18 Diagram of the Flow Cell.

carefully filed before joining, so that a smooth, gradual changeover was effected. These blocks were then glued to both ends of the flow cell.

(c) Specimen Decks. (Fig. I9)

These decks, which held the specimens, were made of perspex and were of the same cross-section as the flow cell. They could be inserted into the test section of the flow cell and bolted tightly. A thin layer of Sira adhesive was applied round the decks after insertion to ensure that the joints were leak-proof.

To prepare a deck for use, a shallow depression (just less than the thickness of the metal specimen, but equal to its length) was machined into the perspex. Two holds were drilled into the back of the perspex, one for the probe and the other for the electrical connection. A wire was soldered to the metal for the electrical connection and the metal araldited in the perspex. When the araldite had set, excess araldite was cut away and the metal made flush with the perspex by rubbing with various grades of wet/dry grinding paper (Struers papers 220, 320, 400, 600) - if the metal face were not flush with the perspex deck face, irregularities in the acid flow would occur. A small hole was drilled in the centre of the specimen so that the backside probe could be inserted and contact made with the face of the specimen.

A similar method was used to construct the counter electrode (platinised titanium), except for the electrical connections. The electrode was araldited to a perspex deck,

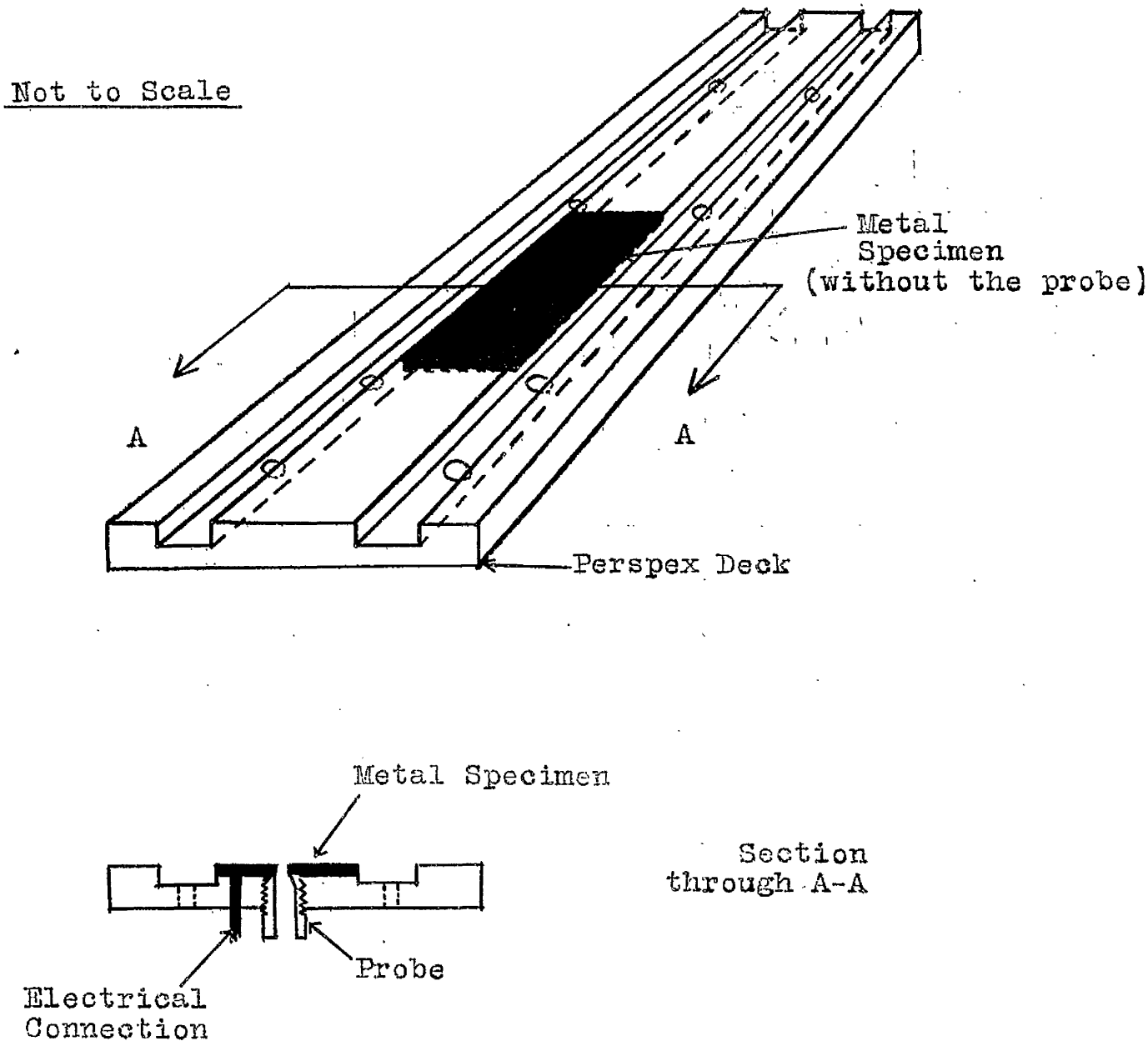

Fig.I9 Diagram of the Decks used in Flowing Media.

which had a hold drilled through it. Silver araldite resin was packed into this hole and a small copper rod inserted. Electrical connection to an instrument was then made by attaching the instrument lead to the copper rod by a crocodile clip.

Fig.20 shows the assembly of the electrodes in the test section.

(d) Electrode Probes.

In selecting a probe for measuring the potential at the metal surface, two factors must be considered:-

(i) the smooth flow of the liquid through the cell must not be disturbed, and

(ii) the iR drop between the metal and the probe must be reduced to a minimum.

A "back-side" probe fulfills these requirements and was selected in these experiments. However, Piontelli (123) showed that certain distortions were caused by this type of probe. (Fig.21). If the relative areas of the specimen and probe are large, the effects of these distortions are almost negligible. The probe (shown in Fig.20) was made from PTFE rods. The ends of the rods were drilled to form capillaries which fitted tightly into the holes drilled in the metal specimen. The whole body of the probe was actually screwed into the perspex backing of the specimen. The capillary of the probe was long enough, so that when it was screwed into the specimen deck, if protruded from the metal surface. The excess length of the capillary was then

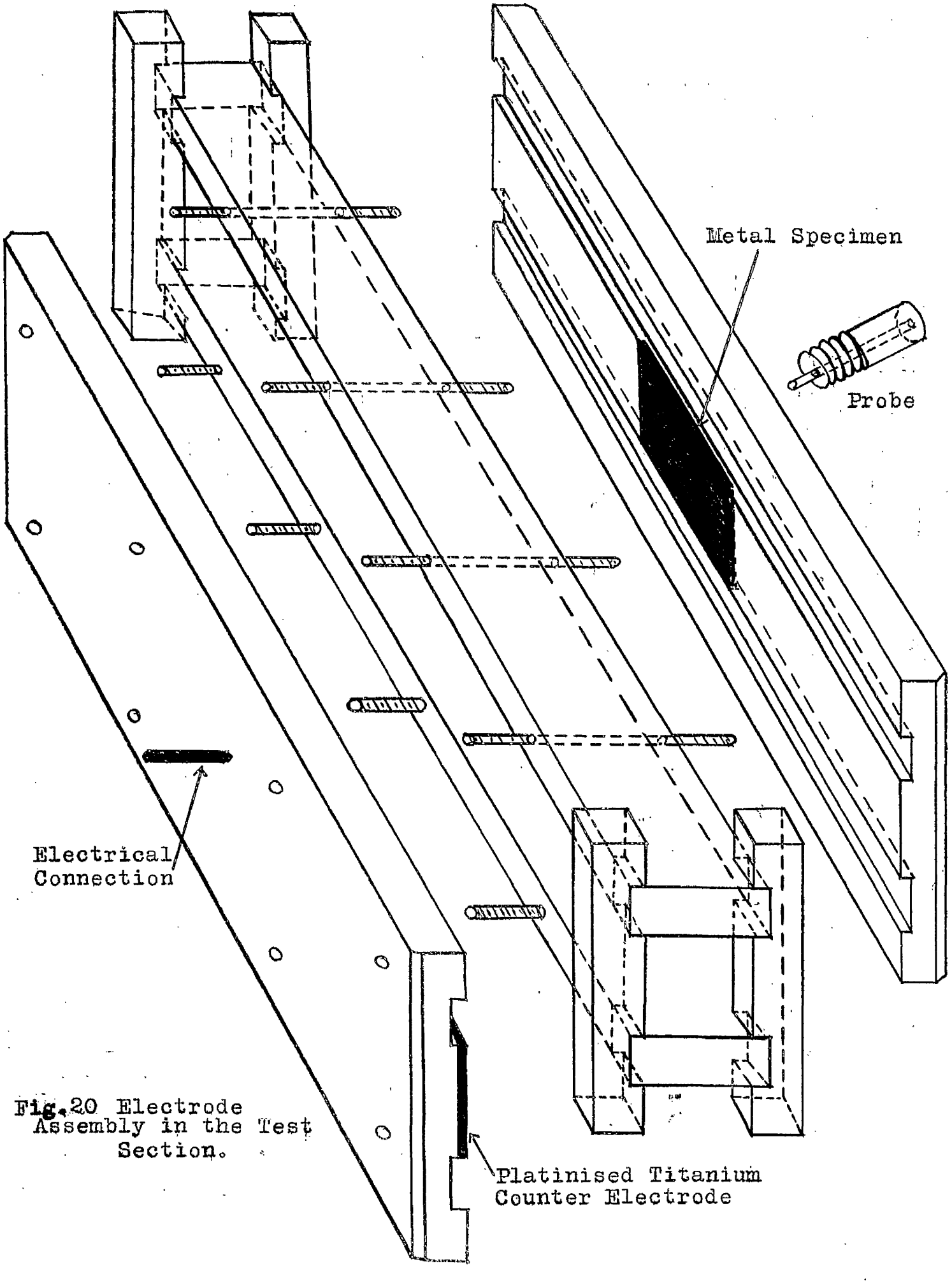

Fig. 20 Electrode Assembly in the Test Section.

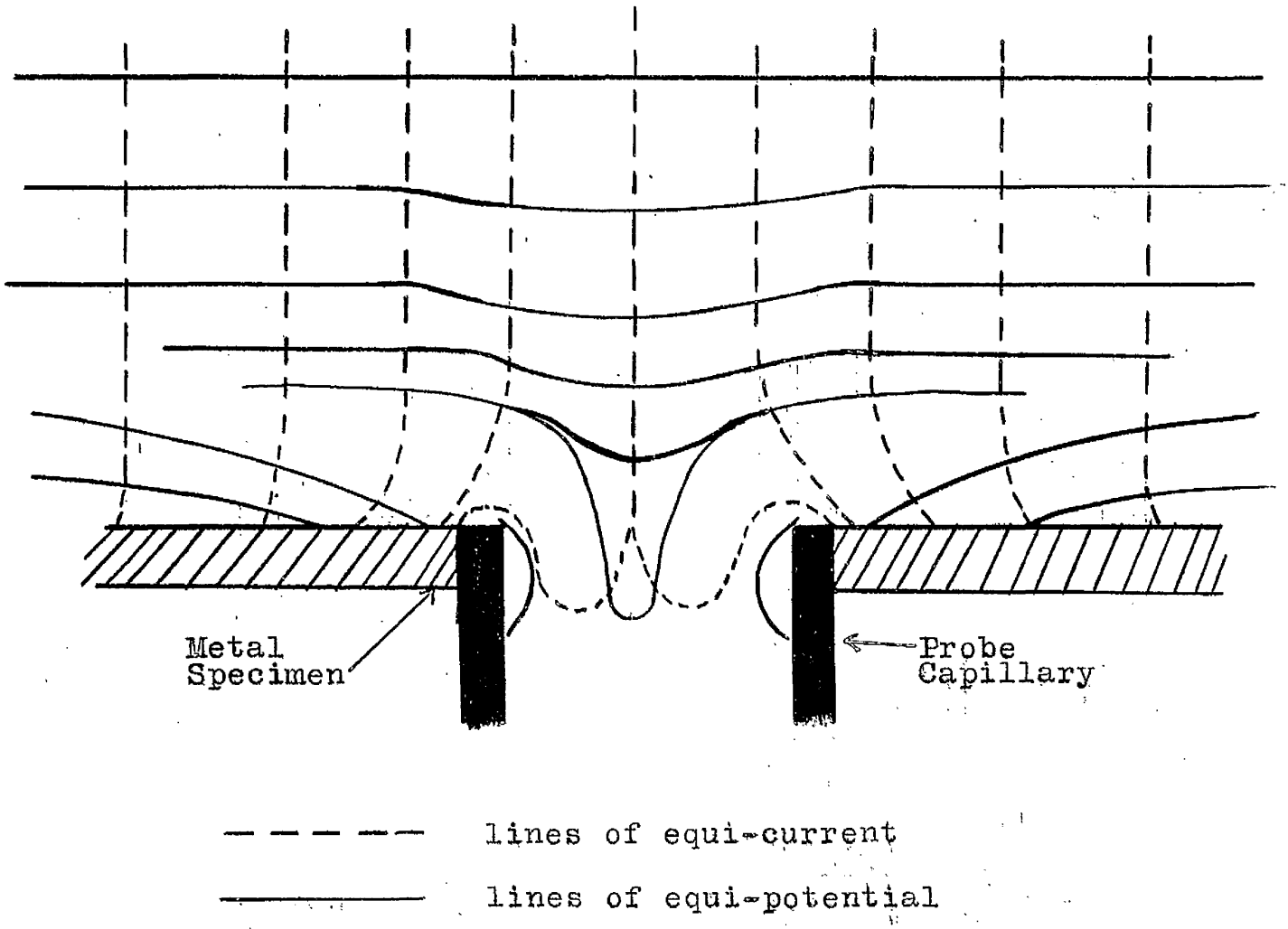

Fig.2I Diagram showing the Distortion of Potential and Current in the immediate vicinity of the Probe.

trimmed with a razor, so that no protrusion occurred on the metal surface.

N. Ibl (124), when studying the diffusion layer, found that, if flow of electrolyte occurred in a "back-side" probe, the concentration of the diffusion layer was found to vary with time. To prevent any flow of this nature, the arrangement used in Fig.22 was used. The test-tube (and the PVC tubing from the side-arm) was filled with electrolyte. Bung A, containing a very thick Agar-Agar potassium chloride bridge with its ends almost closed, was then very tightly fitted. Any movement in the probe is then solely due to the compressibility of the electrolyte and will be very small.

(e) Packed Tower.

The flow system, containing the packed column, is shown in Fig. 23 and a more detailed diagram of the tower is given on Fig.24. Like the flow system, it is constructed with q.v.f. glassware.

As before, the acid was pumped from the reservoir tank into the surge tank and then through the rotameters. After flowing through the rotameters, the acid was diverted up to the top of the tower. On passing through the tower and out at the bottom, the acid flowed back into the reservoir tank.

The gas (oxygen or nitrogen) flowed through two rotameters and into the bottom of the tower via a piece of glass tubing with a series of slits cut in it. On passing out at the top of the tower, the gas passed through a water seal and into the atmosphere.

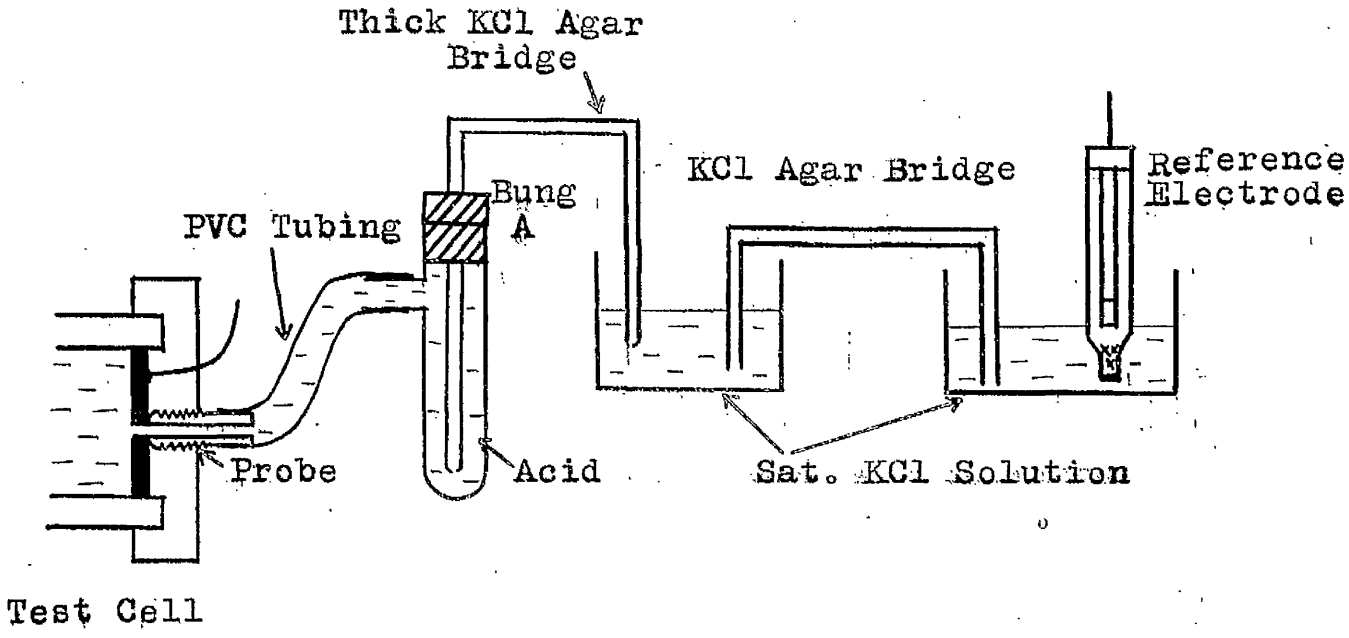

Fig.22 Arrangement used to prevent any flow of acid in the Backside Probe.

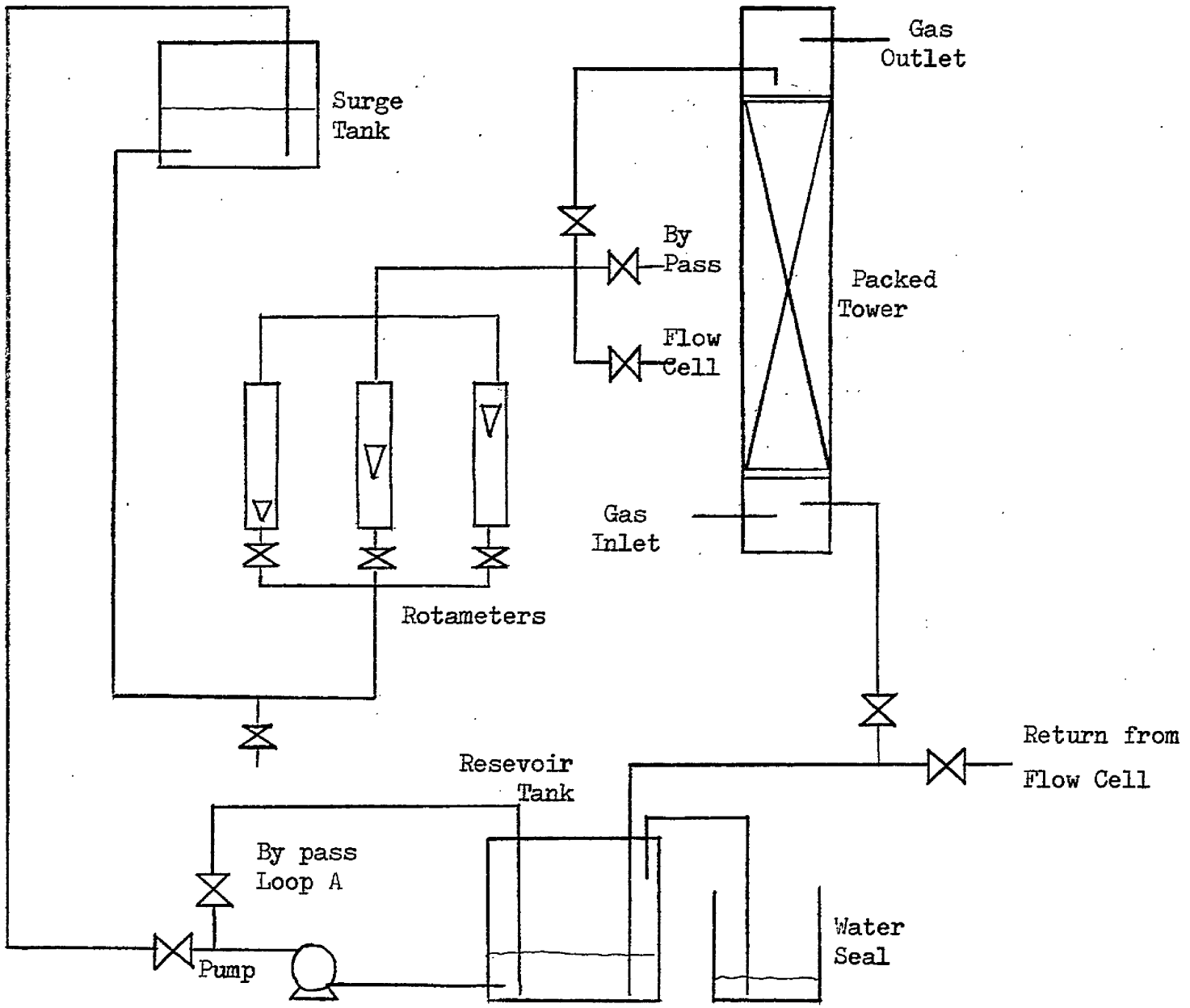

Fig.23 Schematic Diagram of the Packed Tower System.

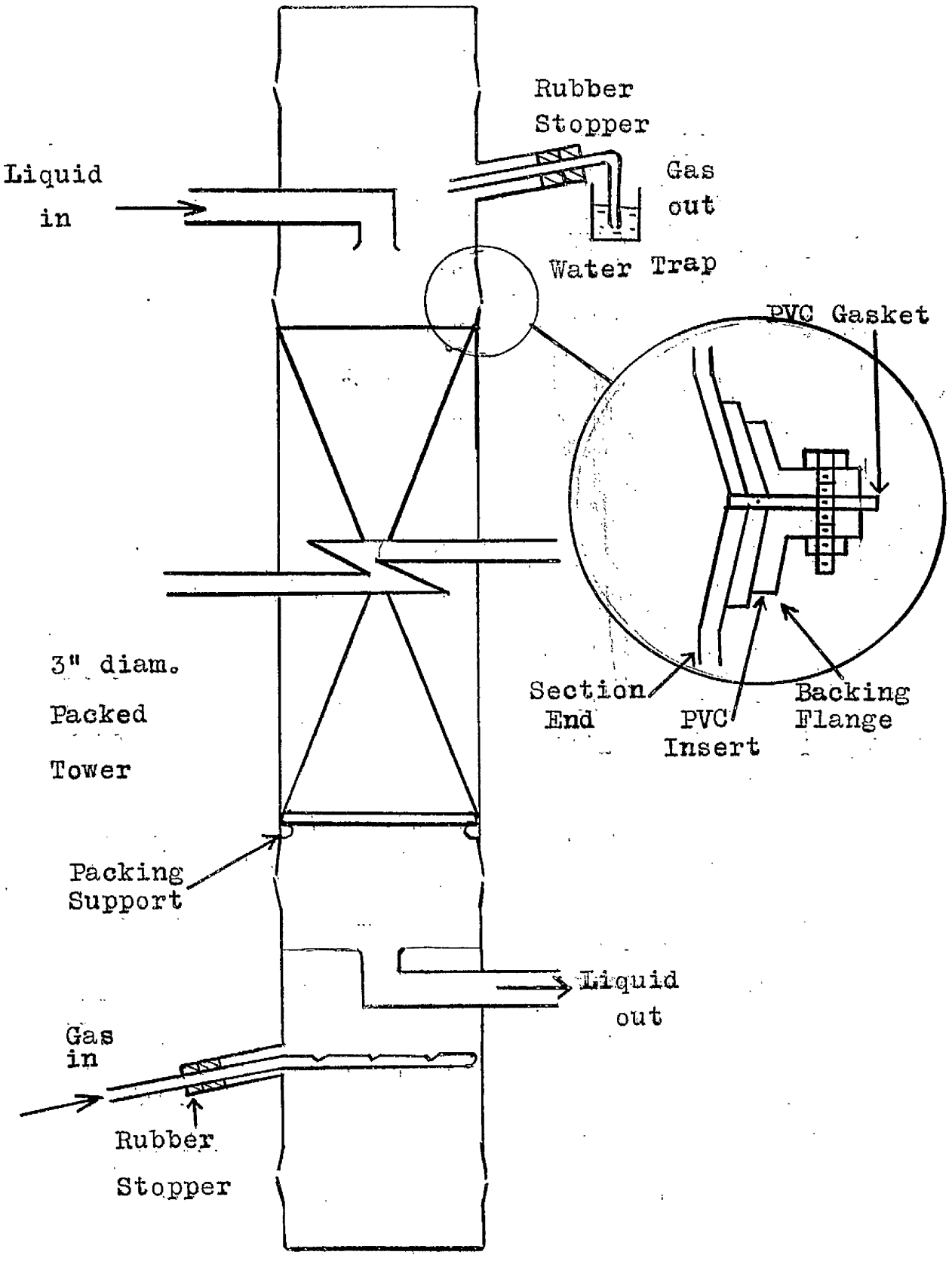

Fig. 24 Diagram of the Packed Tower.

The sensor of the Beckman Oxygen Analyser was fixed in the packed tower inlet line. This was to ensure a flow greater than 1.8 ft. / sec with no bubbles entrained in the acid. As in the outlet line from the tower, the acid had bubbles of gas entrained in it, the oxygen analyser would give an incorrect reading if placed there.

The packing used in the tower was single turn helices. As these were rather small for the packing support, just above the support to a depth of 1" - 1½" were placed larger diameter raschig rings. The total height of the packing was 24".

Measurement of Flow.

The flow of the acid through the system was measured by a series of three rotameters. These had been previously calibrated and the calibration charts are given in Appendix 2.

The height of acid in the surge tank was initially maintained at a high constant level by by-pass loop A. Coarse adjustments were made by the rotameters and the final fine adjustment of flow made by the stop-cock placed at the end of the flow cell. The graduation given on the rotameters could then be read off the calibration charts in mls./min.

Temperature.

The temperature of the acid was measured by means of a thermometer placed just prior to the flow cell. As the temperature was found to vary only between 23°C. and 28°C. during a run, no provision was made to maintain the temperature at a constant value.

Gas Adsorption.

To oxygenate or de-oxygenate the acid, the system was normally left operating overnight. This was for convenience only. As it was found that the desired oxygen concentrations (as given by the Beckman Oxygen Analyser) were obtained in 2 - 3 hours operation. The oxygen concentrations for the various conditions were -

(a) De-oxygenated Acid - 0.01 ppm. oxygen.

(b) Aerated Acid - 7.5 ppm. oxygen.

(c) Oxygenated Acid - 33.6 ppm. oxygen.

During an experimental run these values were maintained by bubbling the particular gas through the reservoir tank and checking the oxygen concentration of the acid at the end of the run.

3.3 Experimental Procedure.

The results from the work in static medium indicate that benzotriazole is an effective inhibitor within the concentration range 0 — 0.5%. The same concentration range (0 — 1.0% benzotriazole) will be used in the flowing system as was used in the static media. Although it would have been desirable to repeat the static experiments under flowing conditions, but the flow cell and the assembly of a specimen deck, it would not be possible to carry out any weight loss experiments. At first it was thought that these could be carried out by measuring the copper ion concentration in the acid, as this can be measured very accurately. However, this would only give the amount of copper in solution, neglecting the copper remaining on the surface as corrosion

product. Also, as it would be impossible to dismantle the specimen deck satisfactorily after a run, no direct weighing method could be employed.

Therefore, the experiments carried out in the flowing system were (a) Capacitance. (b) Potential (c) Potentiostatic. The volume of acid, which was made up beforehand, used in each case was 17 litres.

(a) Capacitance Experiments.

In order to bring the capacitance of the cell within the working range of the instrument used, a standard capacitance was placed in series with the cell (Fig. 25).

The specimens used had no hole drilled for a probe as there was no requirement for a reference circuit. Apart from that the decks were made up as described previously, ground down on wet/dry grinding paper so as to be flush with the front surface of the deck, washed and dried.

A thin layer of Sira adhesive was put in the groove of the deck and the deck screwed in to the test section. The counter electrode was assembled to the test-section in a similar way. A smear of adhesive was also put along the joints in the grooves of the test section to ensure that all joints were leak-proof.

While the decks were being assembled, the acid was flowing round the flow-cell by-pass at maximum velocity. After connecting the electrode terminals to the capacitance measuring device, the by-pass was closed as the flow-cell opened. The high velocity initially is to ensure that all the pockets of air are swept out of the flow cell.

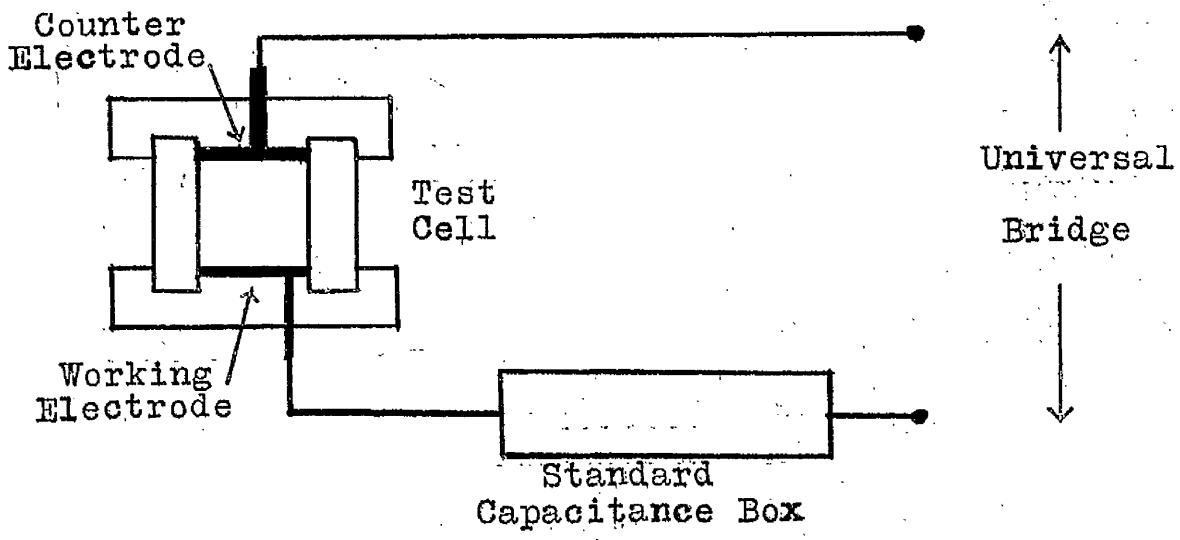

Fig.25 Arrangement for Capacitance Measurements in Flowing Media.

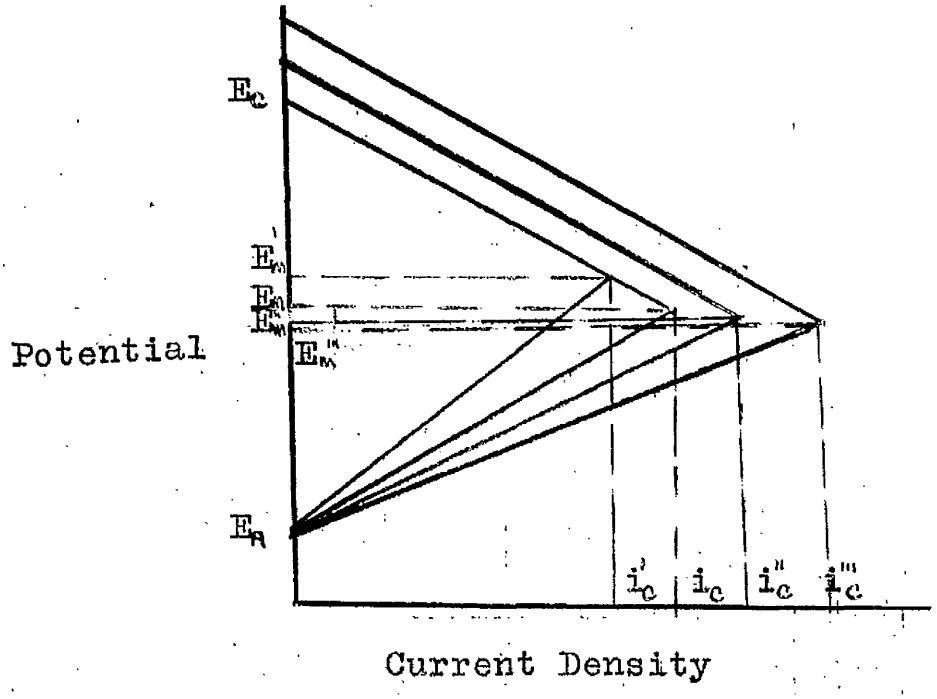

Fig.26 Explanation of the Potential Behaviour of Untreated Copper.

The experimental velocity was selected and maintained until the capacitance reading became steady. This usually took between 8 - 10 minutes. The steady capacitance value was noted and the velocity increased. This procedure was maintained throughout the velocity range.

On completion of the velocity range, the specimen was removed. A known weight of benzotriazole was added to the reservoir tank and dissolved by pumping the acid round the by-pass loop A. When all the inhibitor had dissolved, the above procedure was carried out with a new copper specimen.

This was continued throughout the concentration range and also carried out with a pretreated specimen. Pretreatment took place as before, but after the deck had been assembled. After treatment care had to be taken on smearing the adhesive on the perspex deck, as no adhesive had to get on the copper surface under any circumstances for reasons already mentioned.

By using the relation between capacitance and fraction of area of surface coverage, the fraction of area of surface coverage was worked out as a function of inhibitor concentration. Graph I4 shows this relation. It follows the same trend as in static mediumand is not velocity dependent. This would be expected as the mass boundary layer, which would be affected by the adsorption of benzotriazole, is far smaller than the hydrodynamic boundary layer and not affected by it.

(b) Potential Experiments.

The assembly of the specimen deck is as above except that a hole is drilled into the copper to accommodate the probe.

The probe is attached via PVC tubing to the reference system, shown in Fig. 22. The necessary connections are made to the potential measuring instrument (Pye Dynacap) except that the PVC tubing is not yet connected to the probe.

On diverting the acid from the by-pass loop through the flow cell, bung A in the reference system was loosened and the PVC tubing attached to the probe when the first sign of acid coming out of it occurs. Bung A is then made tight-fitting. In this way all the air is removed from the capillary of the probe.

The required velocity was then selected and the potential of the copper allowed to attain a steady value.

The same procedure as before was then adopted to proceed through the various velocity and concentration ranges, and varying degrees of oxygen concentration of the acid. These results are shown graphically in Graphs I5 to I8.

(c) Potentiostatic Experiments.

A specimen deck was assembled and fitted into the test-section of the flow cell as above. The counter electrode, the specimen, and the reference electrode were connected to the potentiostat which was set at the required potential (at the start of a run this was -1000mV with respect to the calomel electrode). The acid was diverted into the flow cell and the air removed from the capillary of the probe in the manner described above. The required flow rate was selected and the instrument switched on. The current required to maintain this set potential was taken after it had become steady. This usually happened very quickly, but 5 minutes

were allowed between changing the potential and noting the current. The potential was then changed anodically 50mV and the procedure repeated.

In this way the polarization diagram could be obtained for that particular specimen under those particular environmental conditions.

The same procedure was repeated with a new specimen at a different velocity. Benzotriazole was added and dissolved as described previously before a run was started. The oxygen concentration of the acid was also altered as described previously.

In this way, the polarization diagrams for various conditions could be obtained. The conditions used are listed below -

(a) Pretreated Copper in Aerated Acid.

As can be seen from graph I9, the behaviour of the treated specimens changes drastically within the ranges Re = 7400 and Re = 9830. So it was decided to concentrate the investigation on the range Re = 5000 to Re = 10,000 for this reason.

(b) Untreated Copper in Aerated Acid.

Graph 20 indicates that no drastic changes occur with untreated copper with the range Re = 7,400 and Re = 10,000.

So these experiments decided on the velocity range to be used ($5{,}000 < Re < 10{,}000$) and the preliminary experiments in static media indicated the benzotriazole concentration to be employed ($0 <$ benzotriazole $\% < 1.0$).

(c) Untreated Copper in Inhibited Aerated Acid.

Graphs 2I to 26 show the behaviour of untreated copper in flowing media at various inhibitor concentrations.

(d) Treated Copper in De-oxygenated Acid.

Graph 27 shows the specimen's behaviour.

(e) Untreated Copper in De-oxygenated Acid.

Graph 28 indicates the specimen's behaviour.

(f) Untreated Copper in Oxygenated Acid.

Graph 29 shows the specimen's behaviour.

(g) Treated Copper in Oxygenated Acid.

Graph 30 indicates the specimen's behaviour.

(h) Untreated Copper in De-oxygenated Inhibited Acid.

Graphs 3I to 34 show the behaviour of the specimen under inhibited acid concentrations.

These results seemed to indicate that oxygen plays a role in the breakdown of the Copper/benzotriazole film. An experiment was therefore carried out with treated copper in oxygenated acid with various concentrations of benzotriazole.

(i) Treated Copper in Oxygenated Inhibited Acid.

Graphs 35 to 40 show these results. This was to determine whether or not the copper/benzotriazole film could be renewed on breakdown or not.

All these results will be discussed in detail in Chapter 4.

The graphs designated with an A are graphs of the corresponding number, but of a larger scale around the zero current point.

GRAPH I4 Variation in Fraction of Surface Area of Coverage of Benzotriazole in Flowing Media.

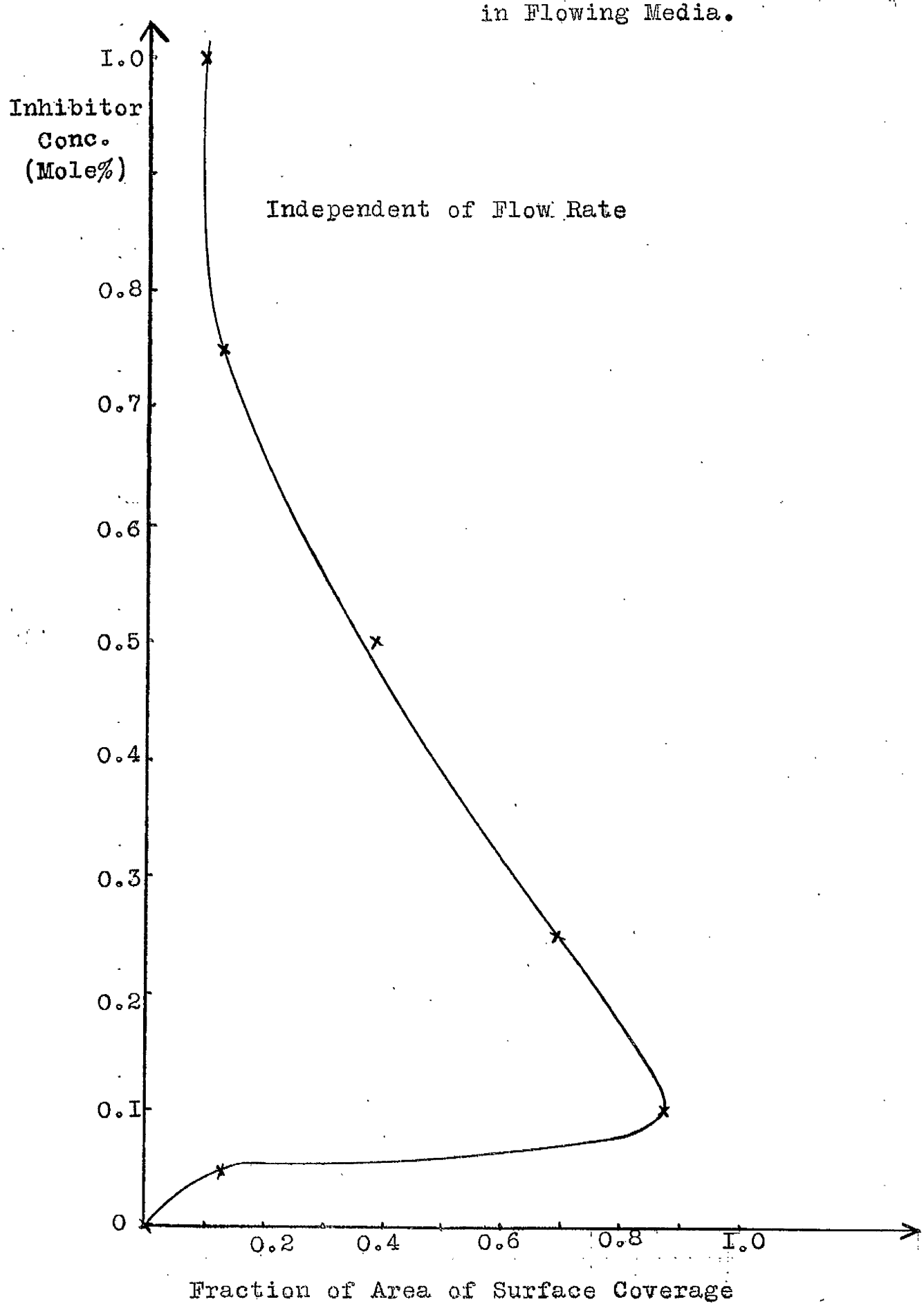

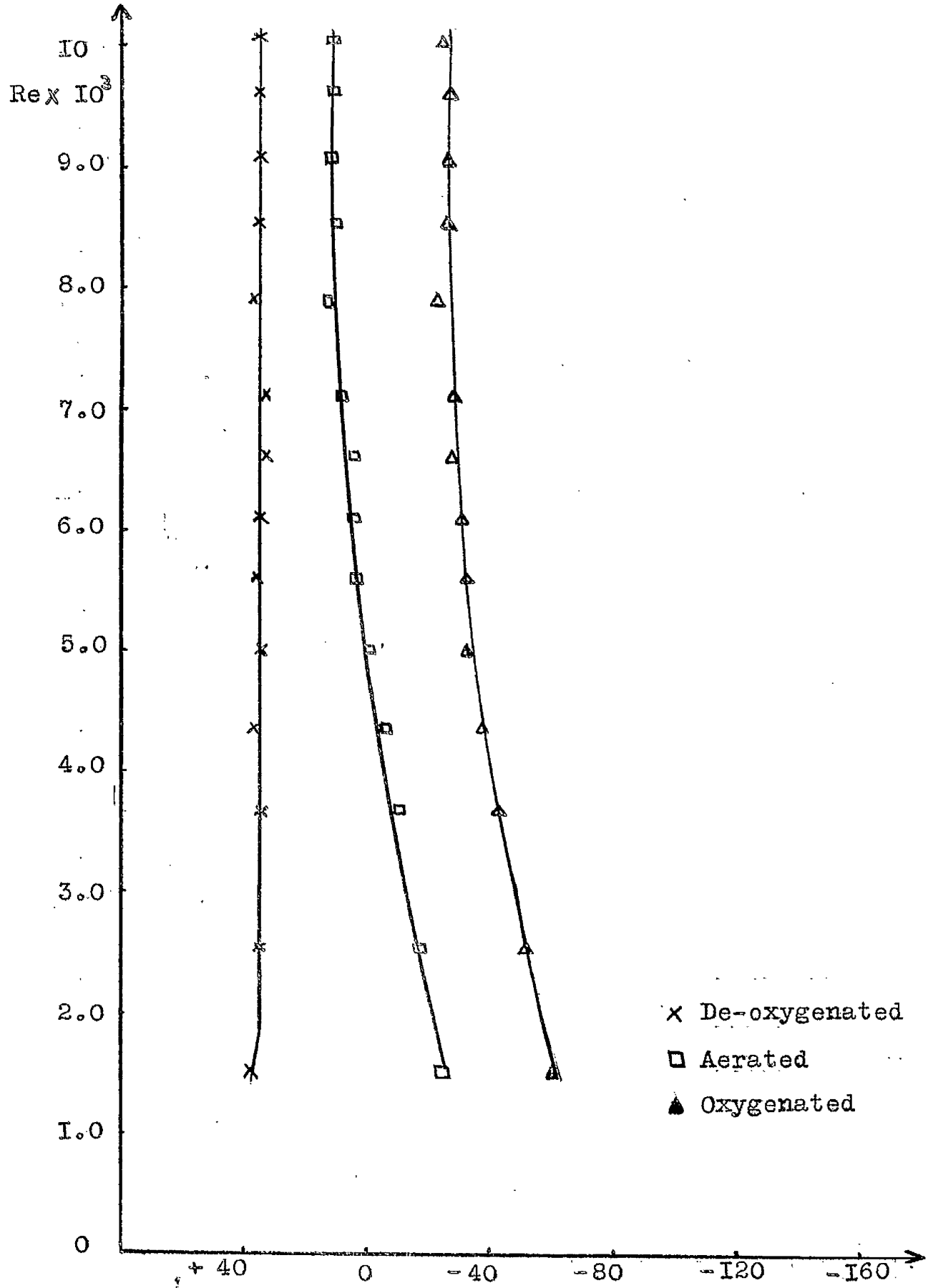

GRAPH 15 Potential Variation of Pretreated Copper in Flowing Media.

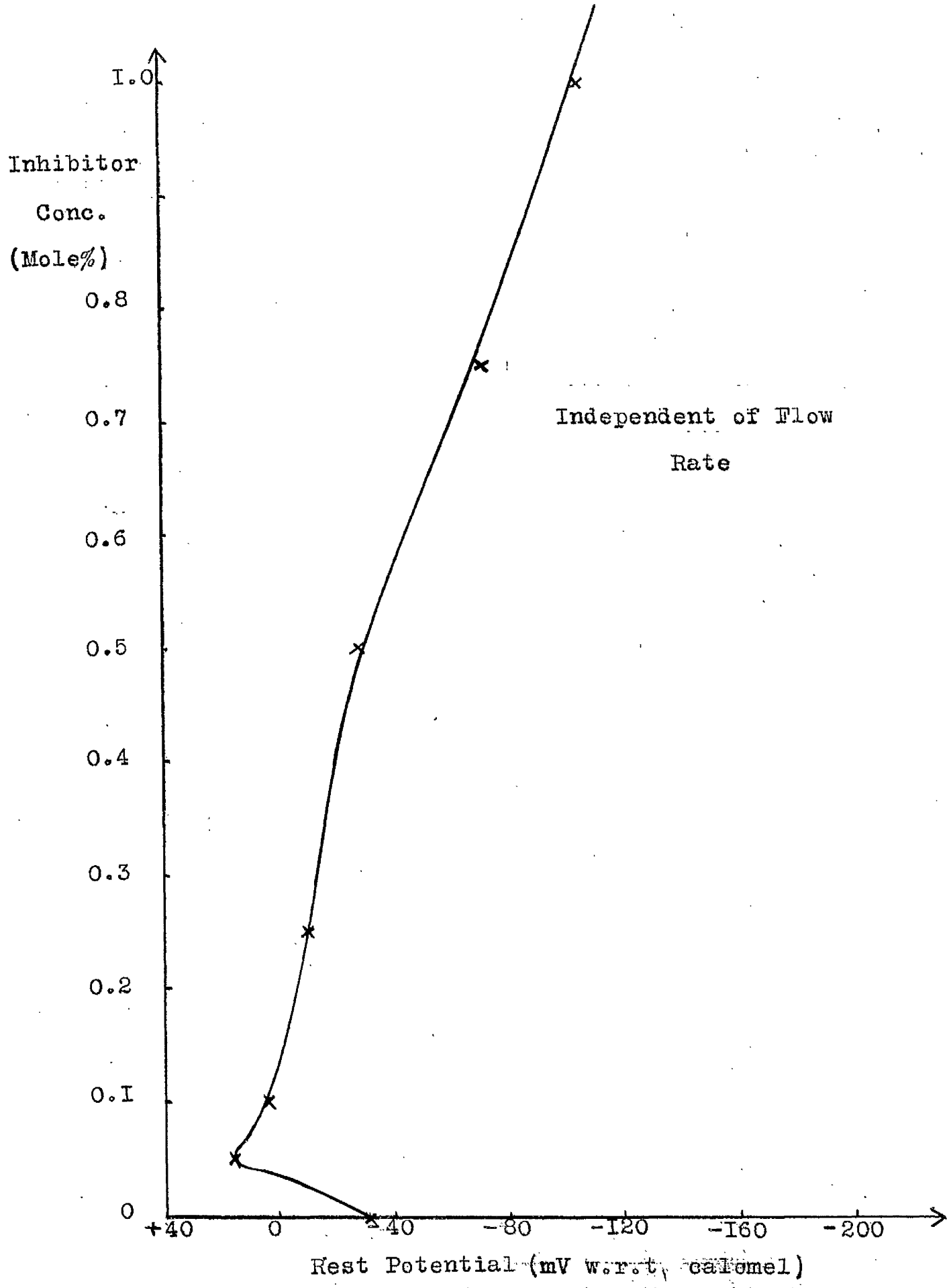

GRAPH I6 Variation in Rest Potential of Untreated Copper in De-oxygenated Acid containing Benzotriazole.

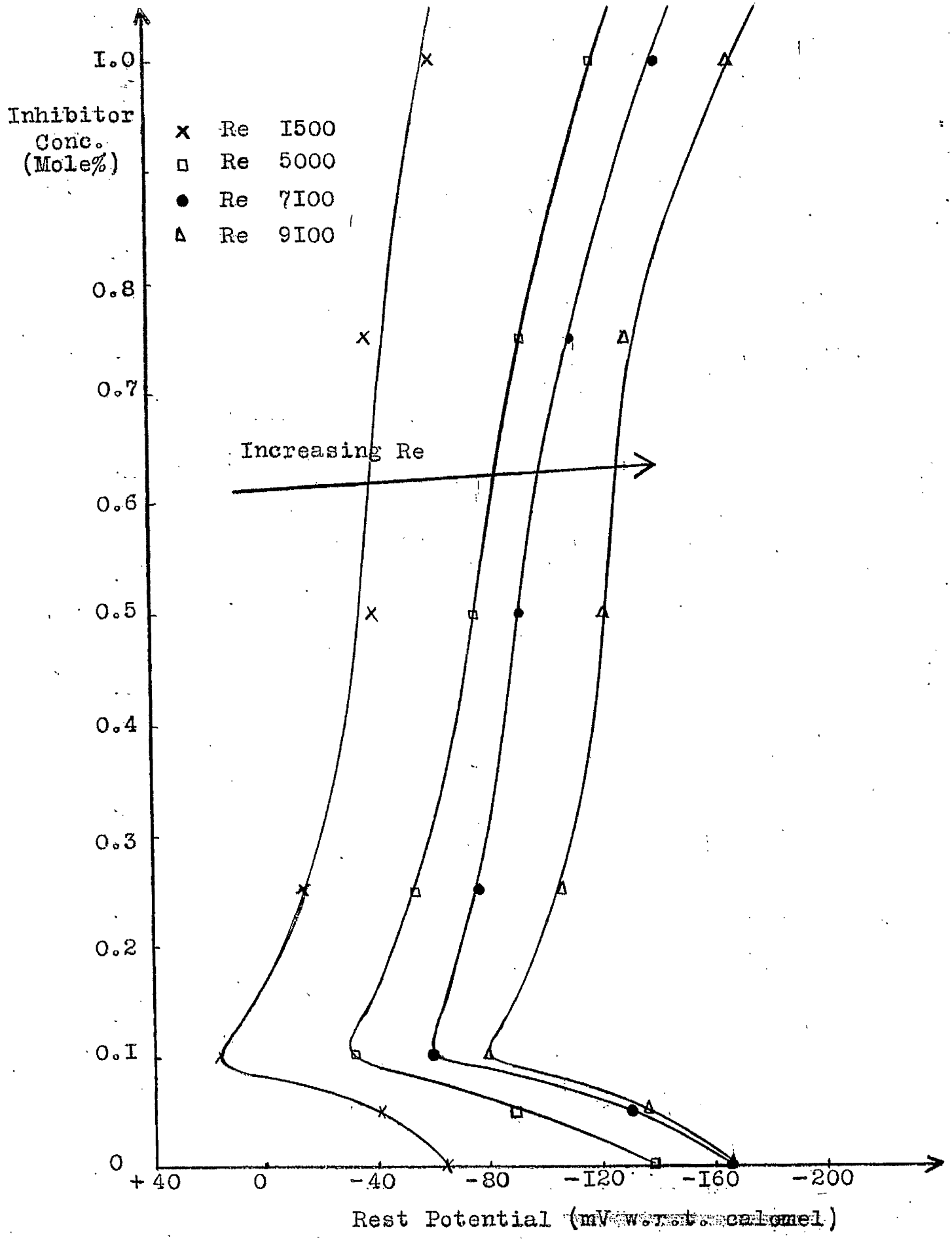

GRAPH 17 Variation in Rest Potential of Untreated Copper in Aerated Acid Containing Benzotriazole.

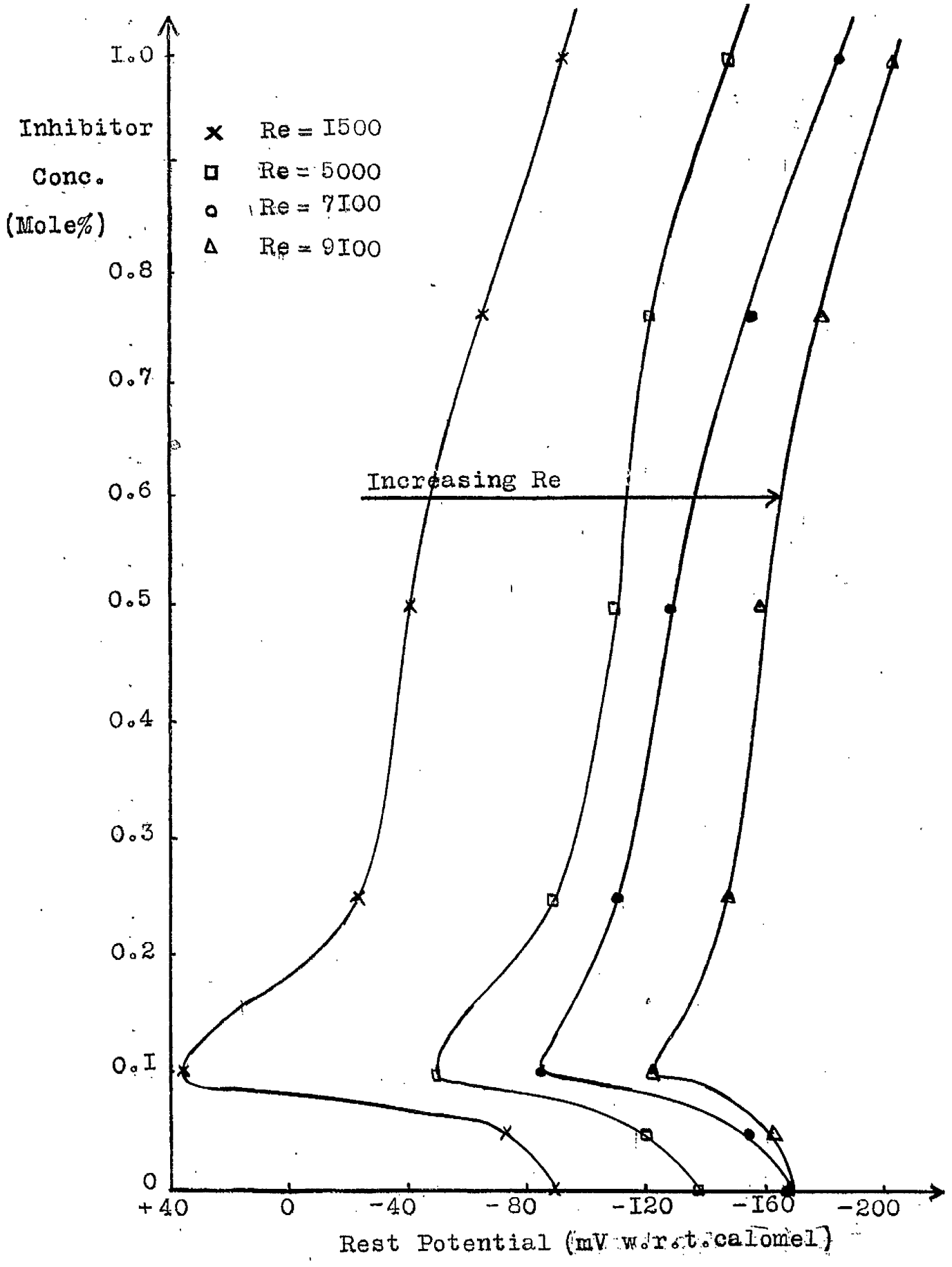

GRAPH 18 Variation in Rest Potential of Untreated Copper in Oxygenated Acid containing Benzotriazole.

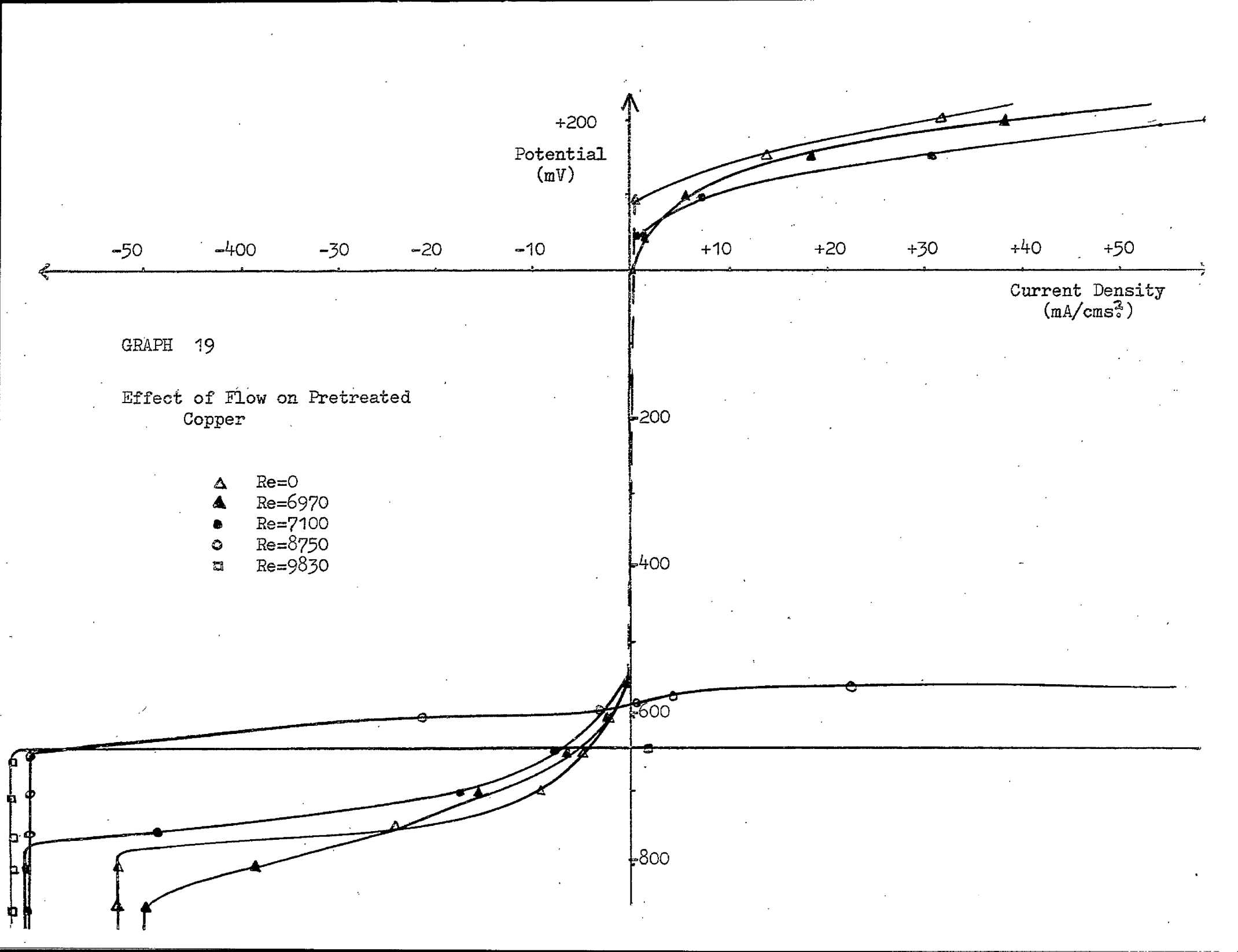
+200
Potential
(mV)
-50
-400
-30
-20
-10
+10
+20
+30
+40
+50
Current Density
(mA/cms²)
GRAPH 19
Effect of Flow on Pretreated
Copper
Re=0
Re=6970
Re=7100
Re=8750
Re=9830
200
400
600
800

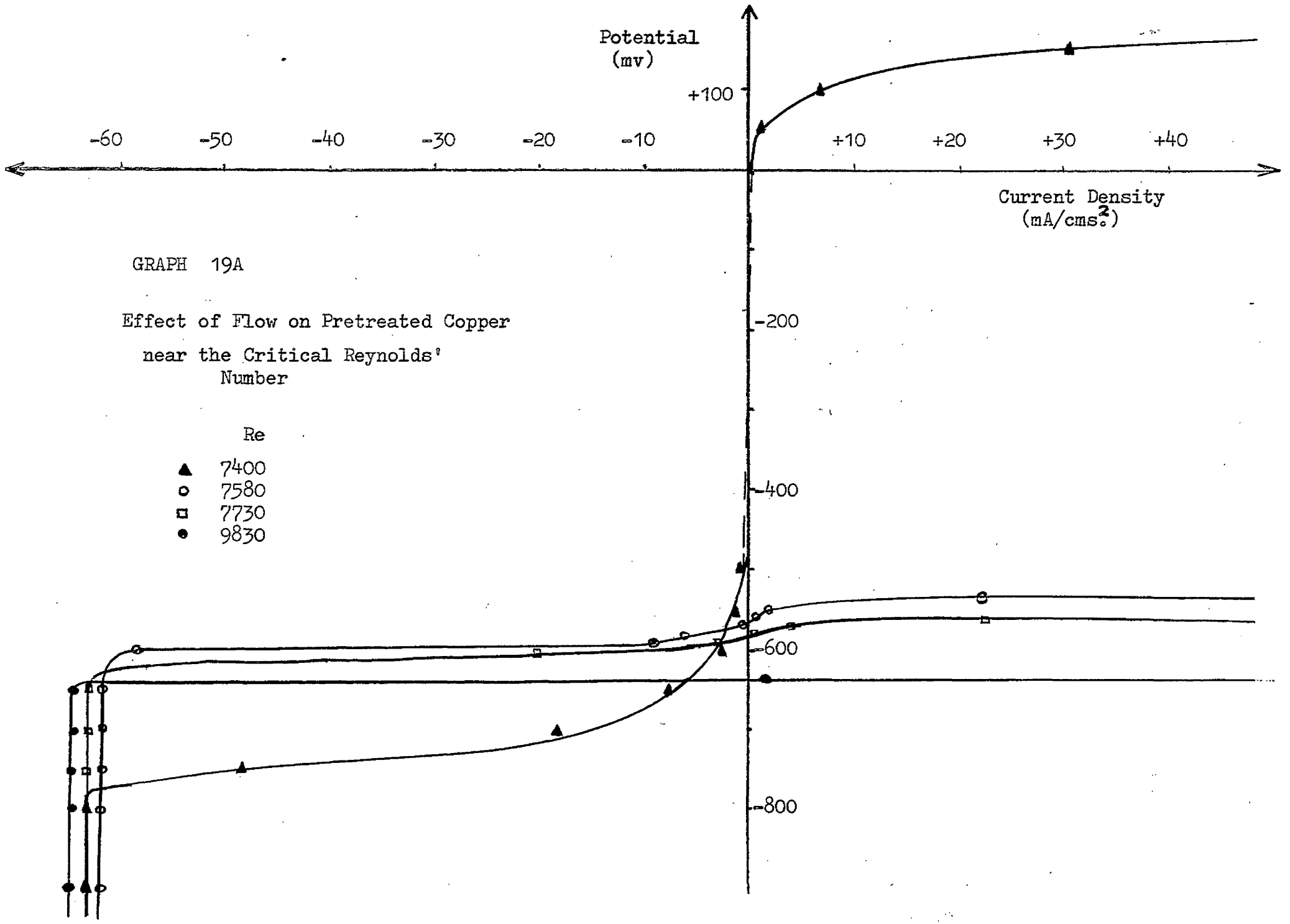

GRAPH 19A

Effect of Flow on Pretreated Copper near the Critical Reynolds' Number

Re

- ▲ 7400
- ○ 7580
- □ 7730
- ● 9830

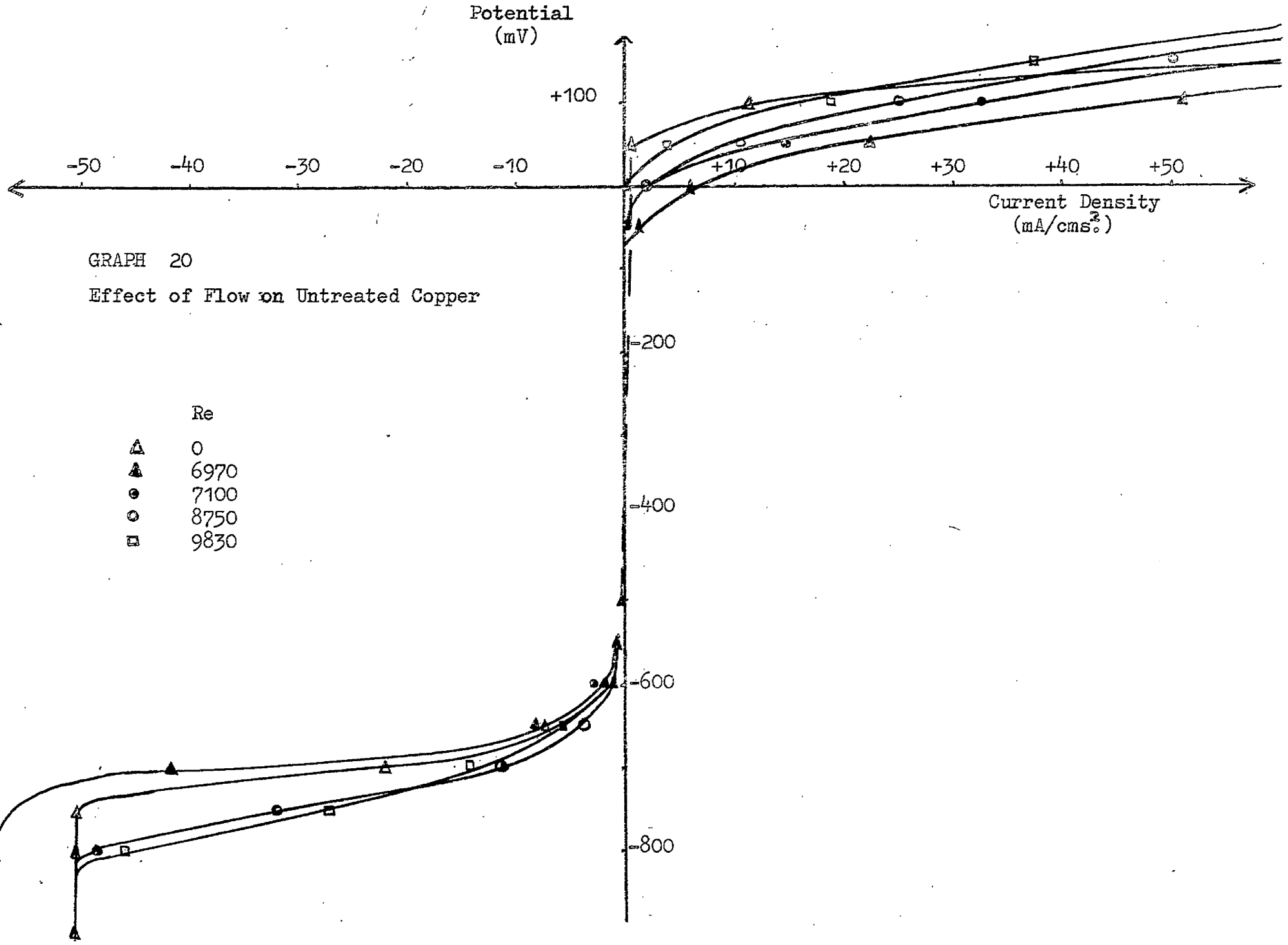

GRAPH 20

Effect of Flow on Untreated Copper

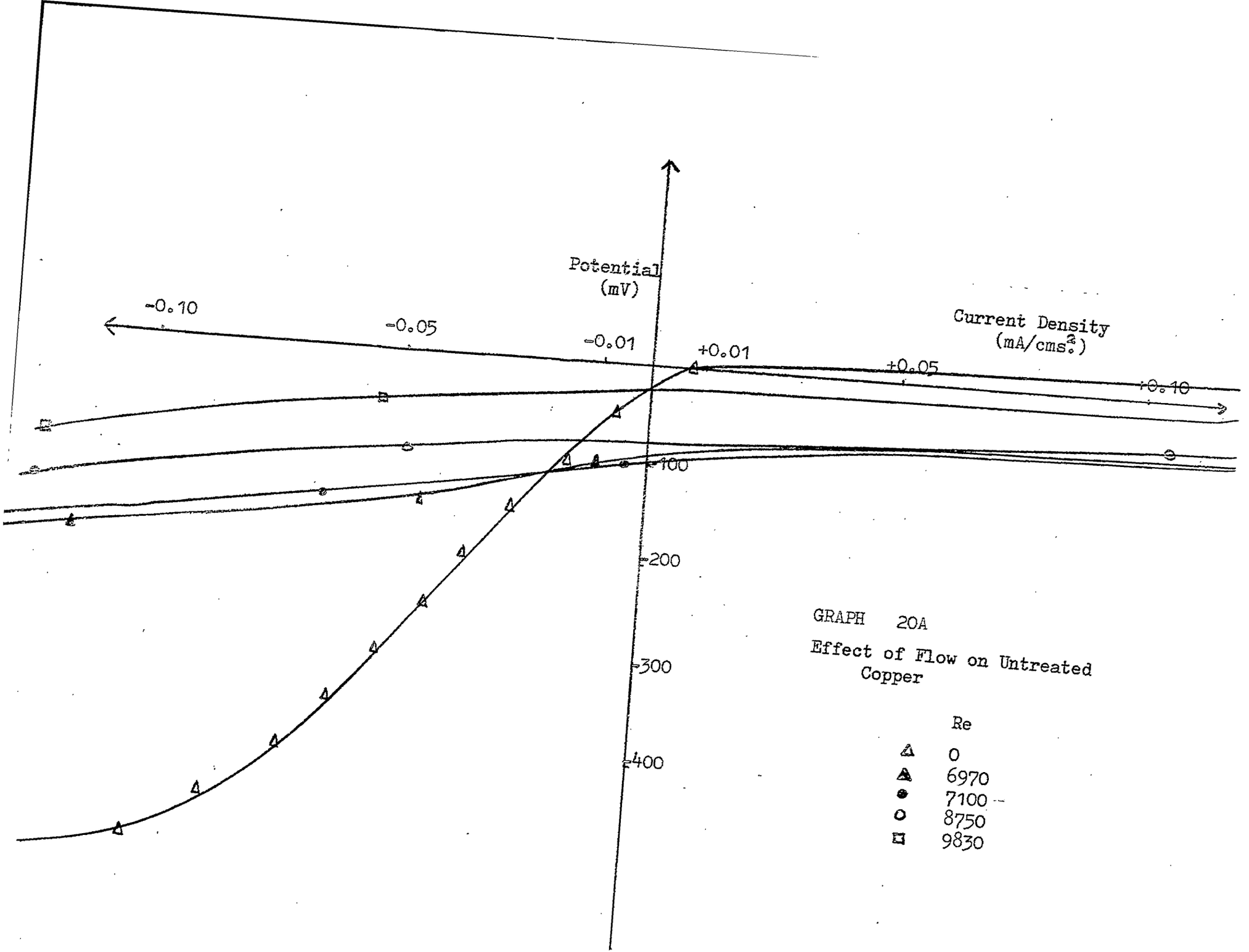

GRAPH 20A

Effect of Flow on Untreated Copper

	Re
△	0
▲	6970
●	7100
○	8750
□	9830

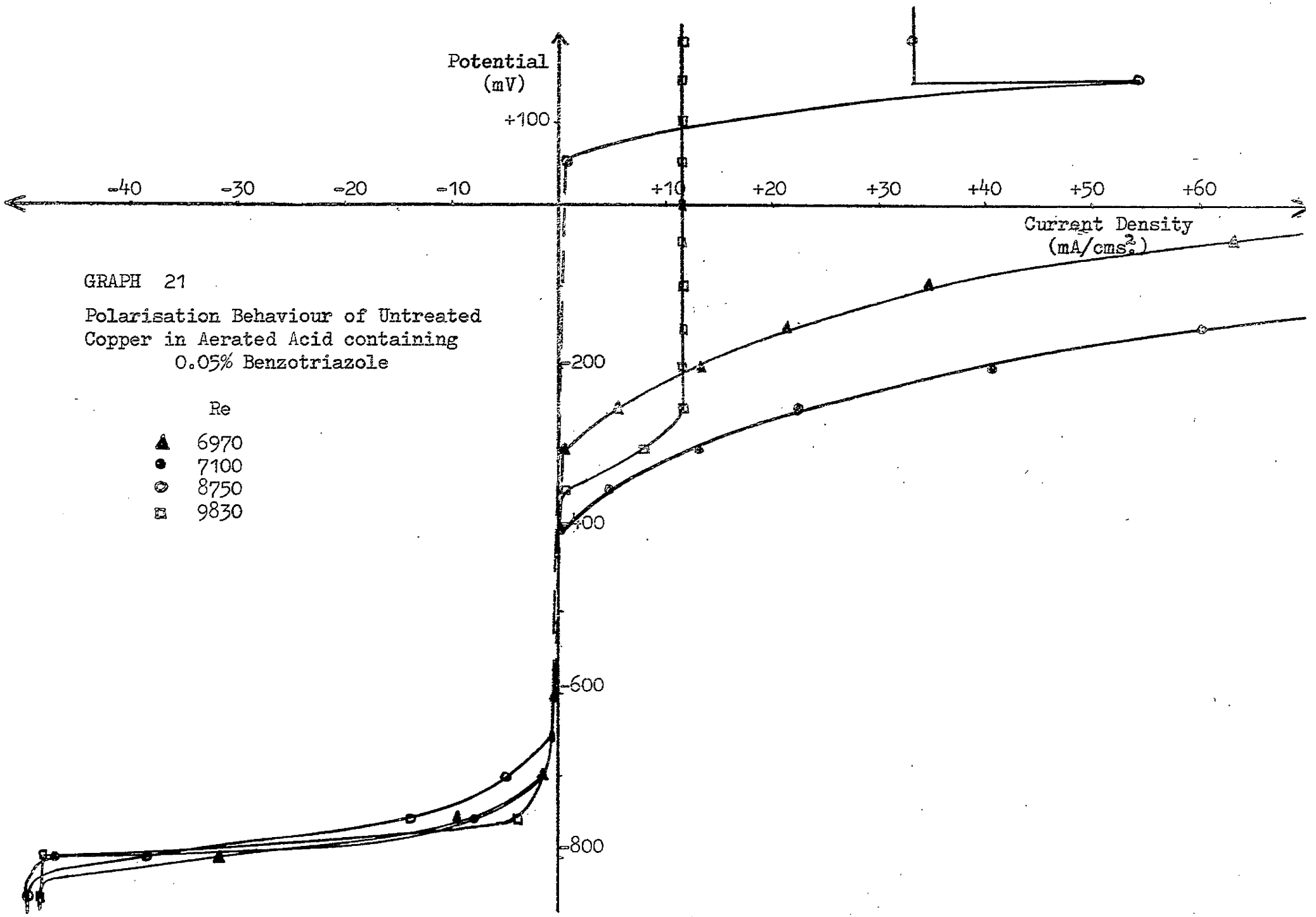

GRAPH 21

Polarisation Behaviour of Untreated Copper in Aerated Acid containing 0.05% Benzotriazole

Re

- ▲ 6970
- ● 7100
- ⊙ 8750
- ⊡ 9830

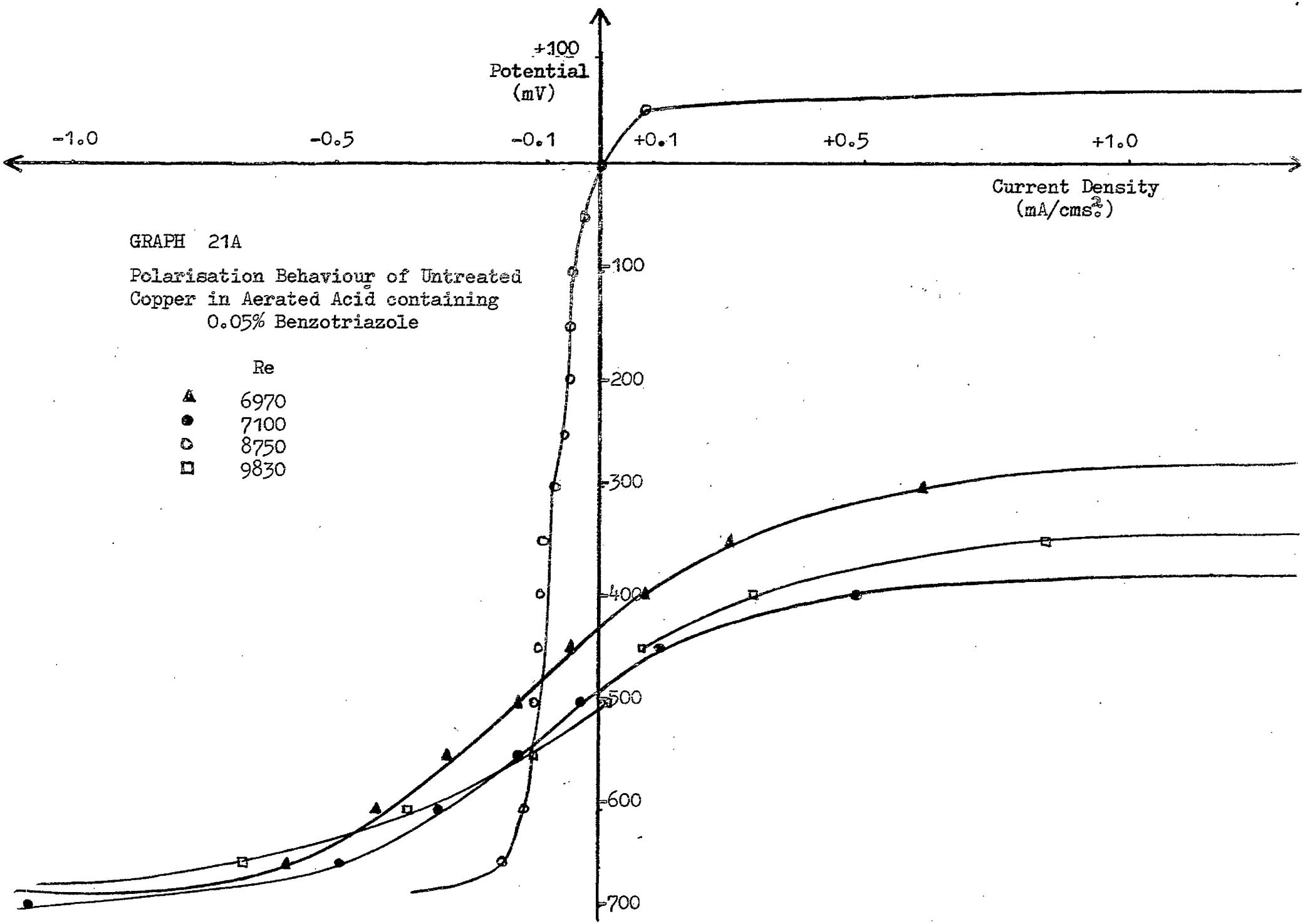

GRAPH 21A

Polarisation Behaviour of Untreated Copper in Aerated Acid containing 0.05% Benzotriazole

Re
6970
7100
8750
9830

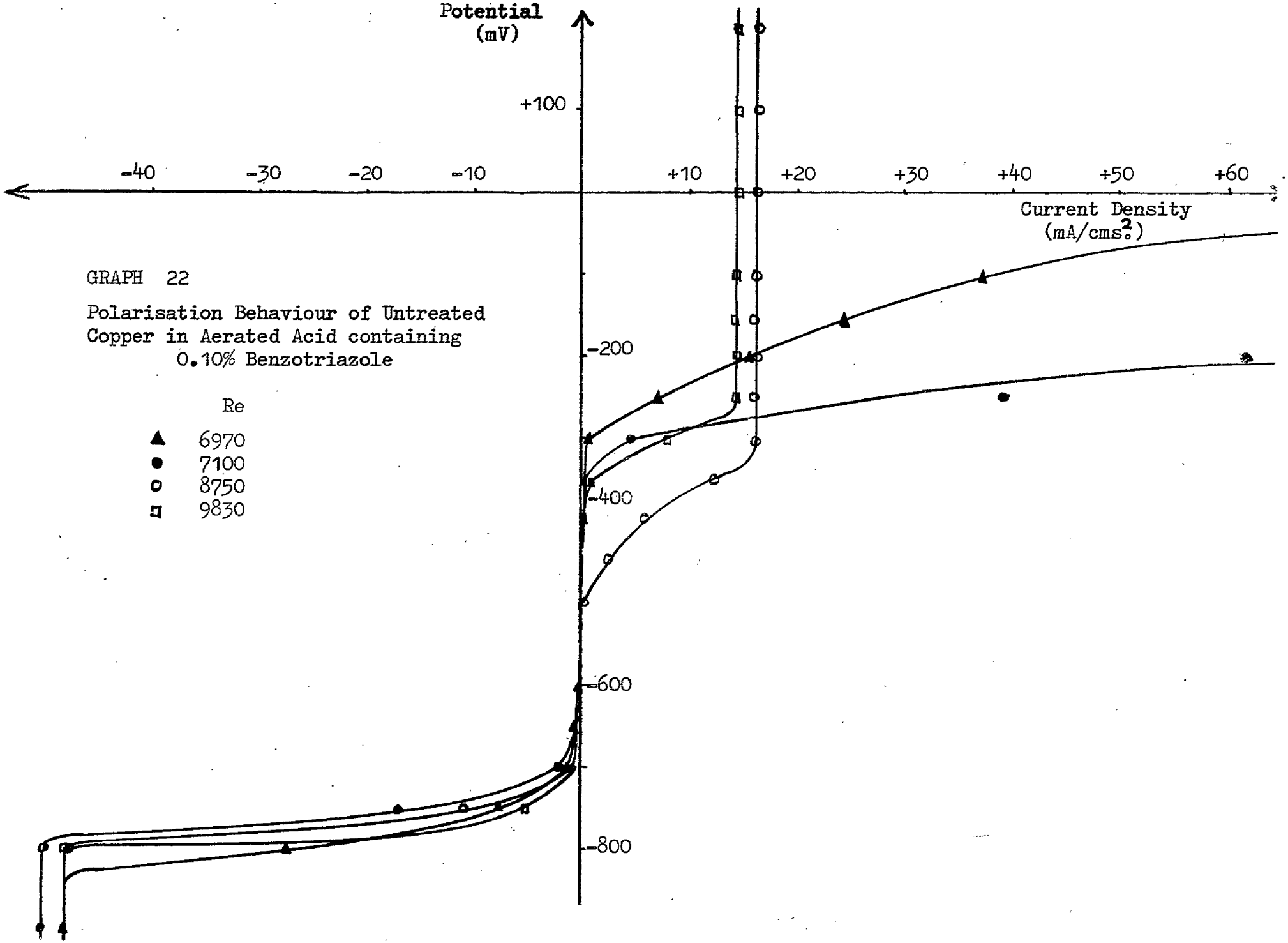

GRAPH 22

Polarisation Behaviour of Untreated Copper in Aerated Acid containing 0.10% Benzotriazole

Re
▲ 6970
● 7100
o 8750
□ 9830

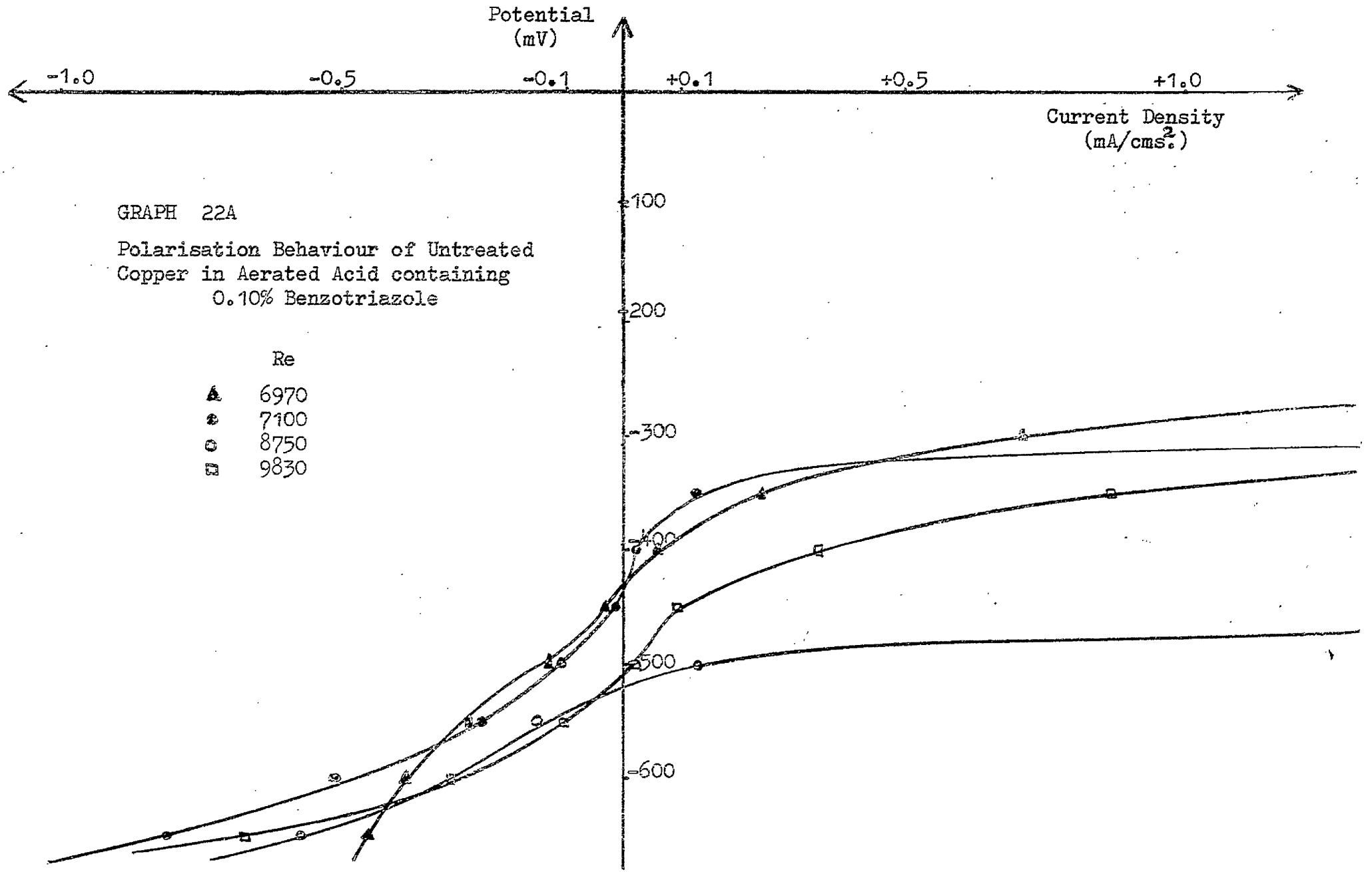
Potential
(mV)
-1.0
-0.5
-0.1
+0.1
+0.5
+1.0
Current Density
(mA/cms.²)
100
200
300
400
500
600
GRAPH 22A
Polarisation Behaviour of Untreated
Copper in Aerated Acid containing
0.10% Benzotriazole
Re
6970
7100
8750
9830

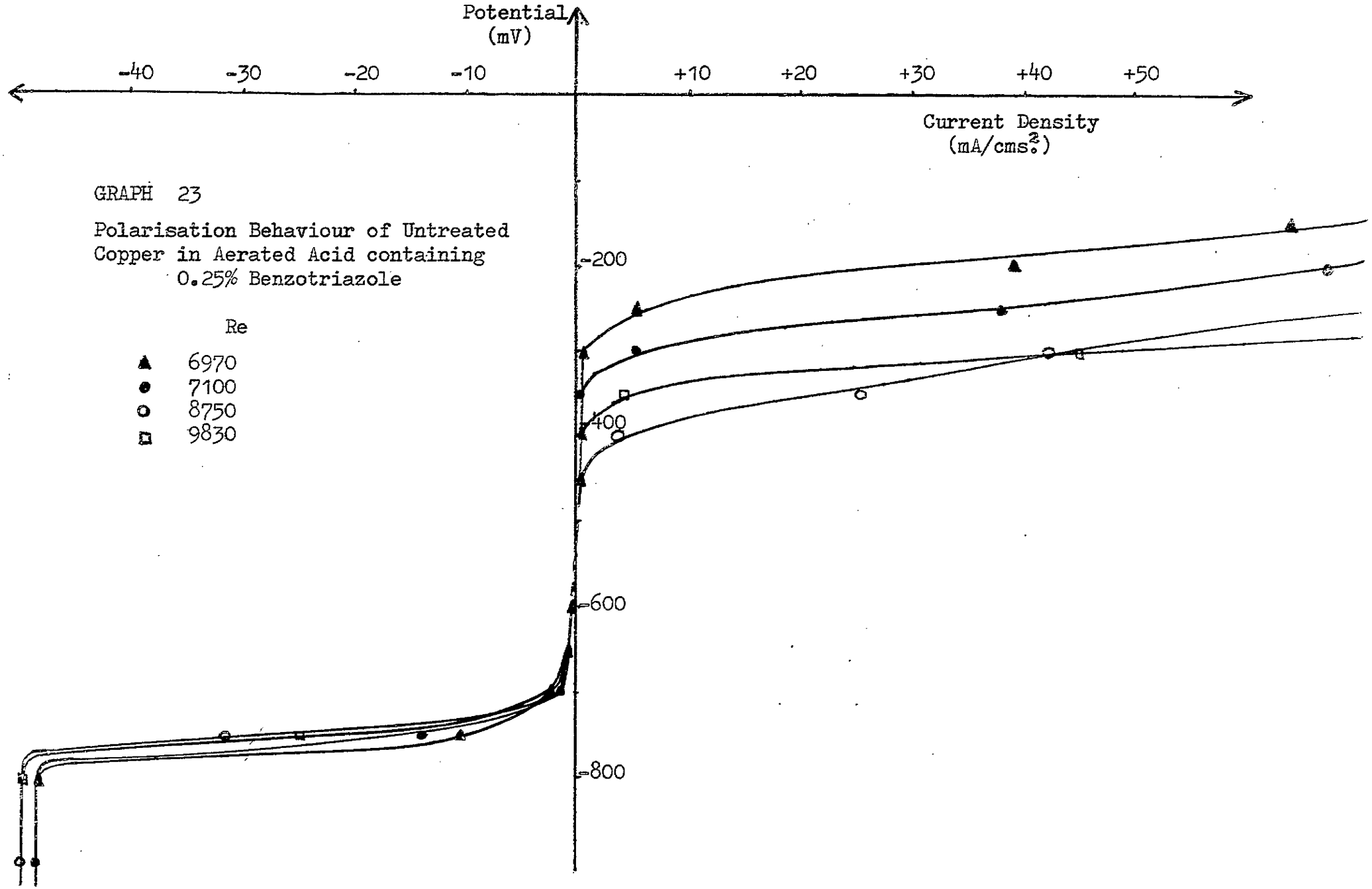

GRAPH 23

Polarisation Behaviour of Untreated Copper in Aerated Acid containing 0.25% Benzotriazole

Re

- ▲ 6970
- ● 7100
- ○ 8750
- □ 9830

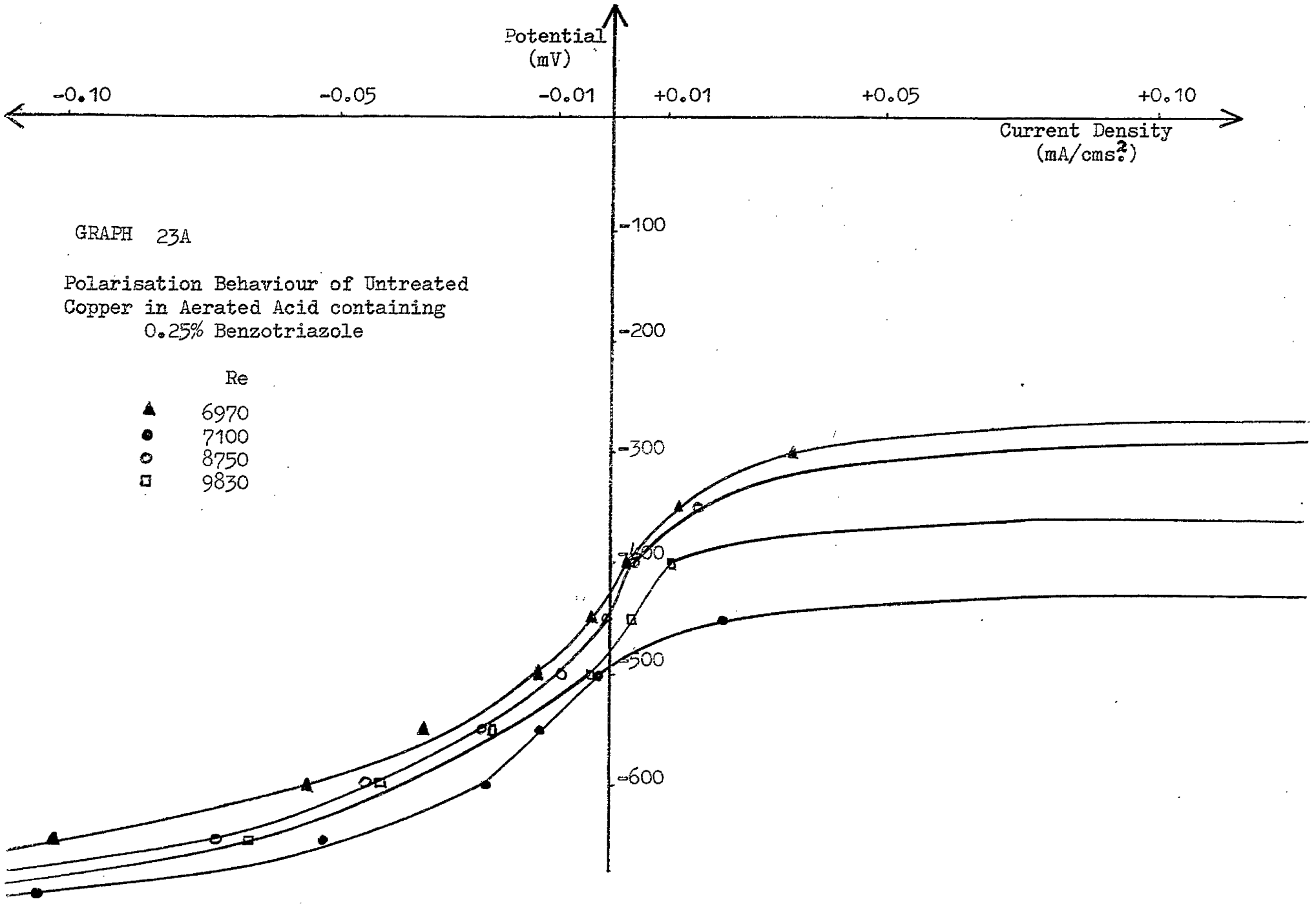

GRAPH 23A

Polarisation Behaviour of Untreated Copper in Aerated Acid containing 0.25% Benzotriazole

	Re
▲	6970
●	7100
○	8750
□	9830

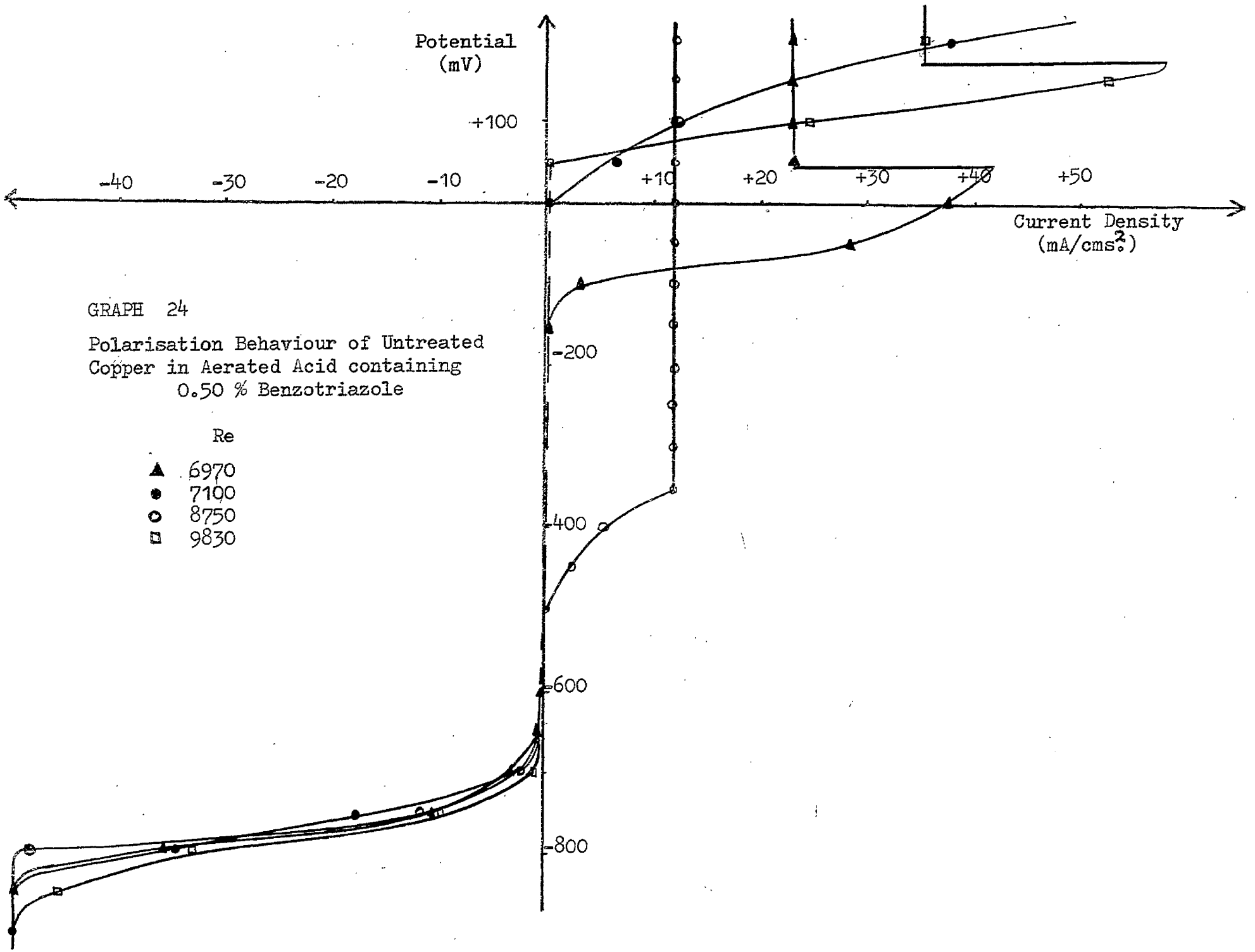

GRAPH 24

Polarisation Behaviour of Untreated Copper in Aerated Acid containing 0.50 % Benzotriazole

Re

- ▲ 6970
- ● 7100
- ○ 8750
- □ 9830

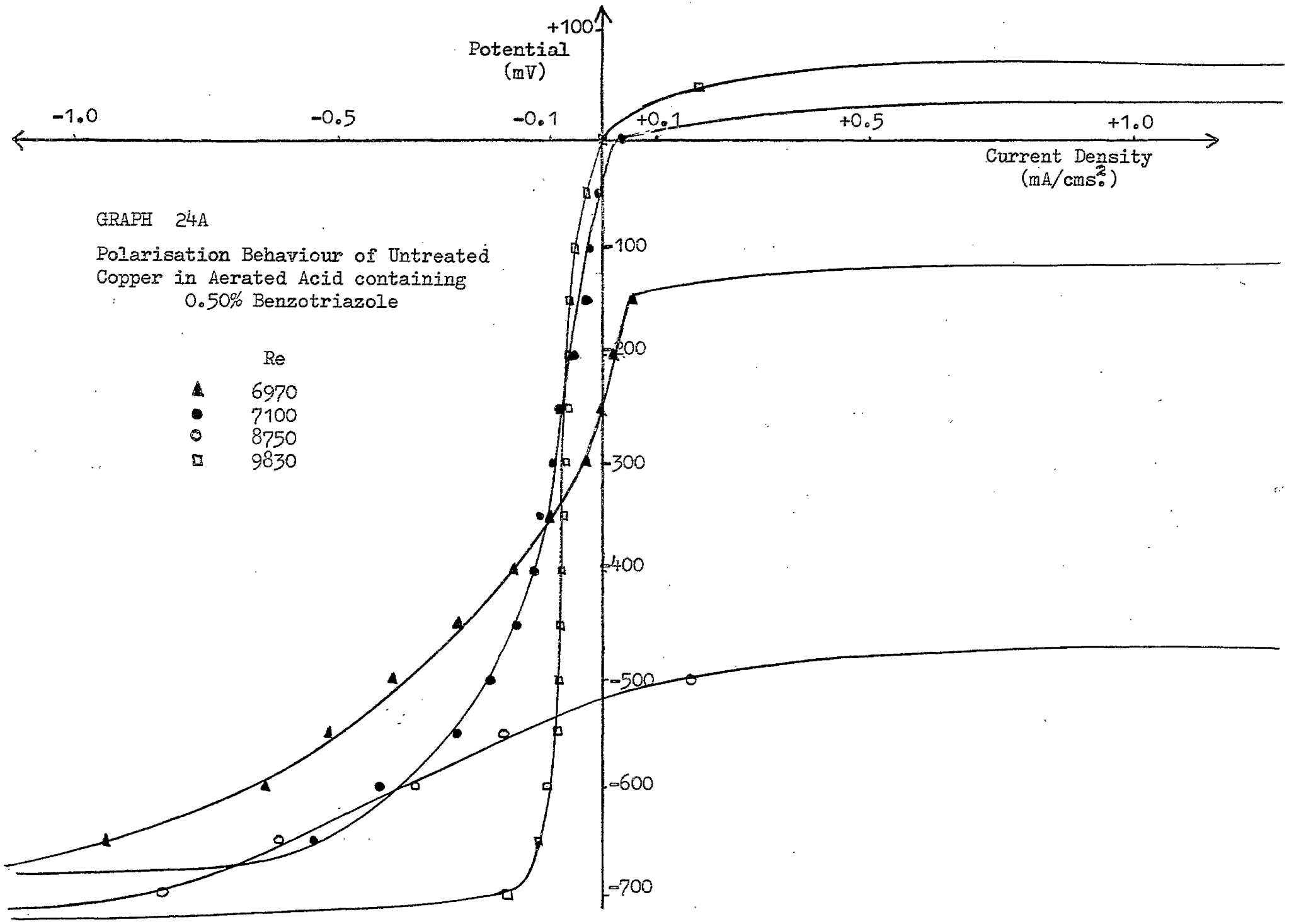
+100
Potential
(mV)
-1.0
-0.5
-0.1
+0.1
+0.5
+1.0
Current Density
(mA/cms.²)
-100
-200
-300
-400
-500
-600
-700
GRAPH 24A
Polarisation Behaviour of Untreated
Copper in Aerated Acid containing
0.50% Benzotriazole
Re
6970
7100
8750
9830

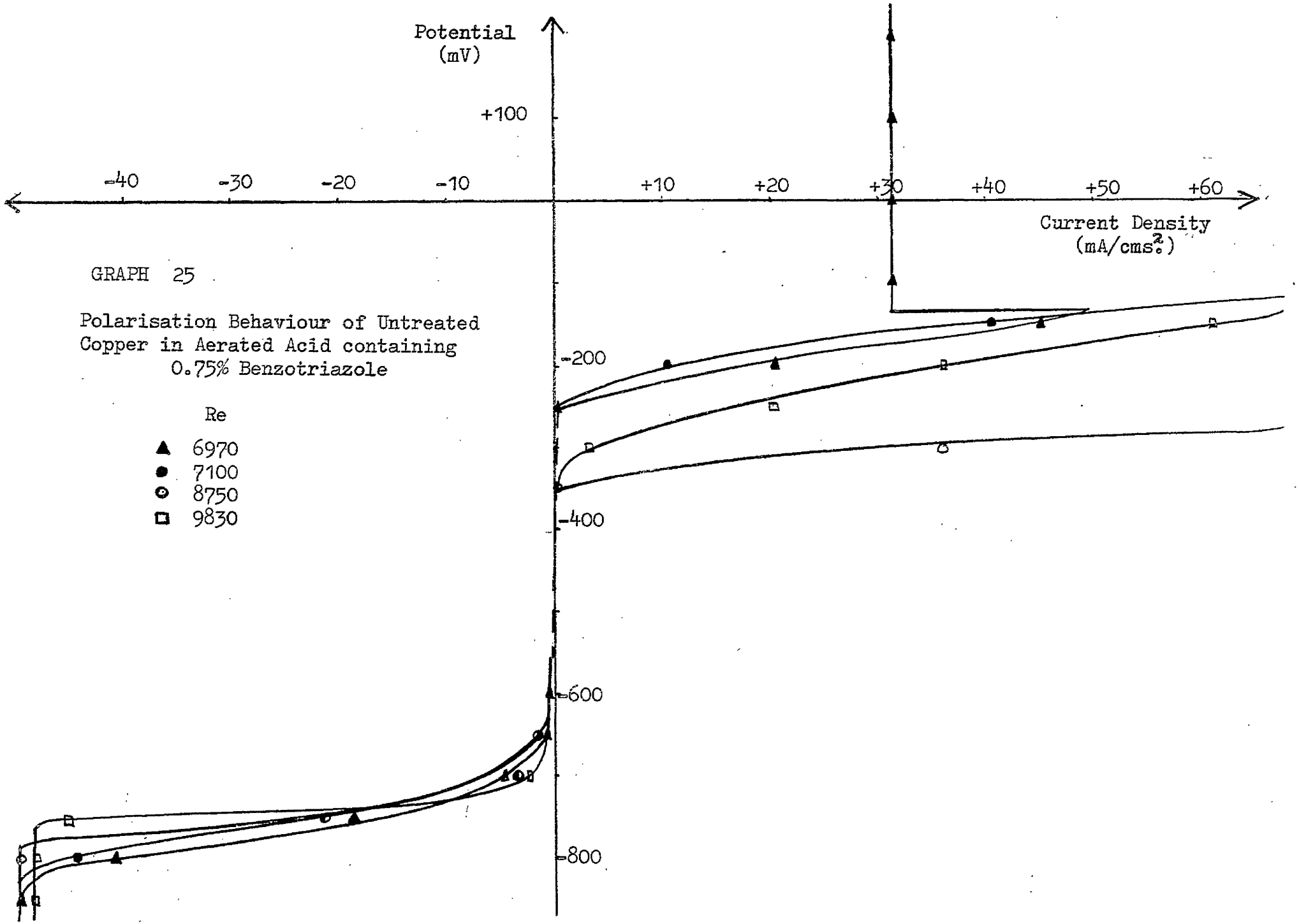

GRAPH 25

Polarisation Behaviour of Untreated Copper in Aerated Acid containing 0.75% Benzotriazole

Re

- ▲ 6970
- ● 7100
- ⊙ 8750
- □ 9830

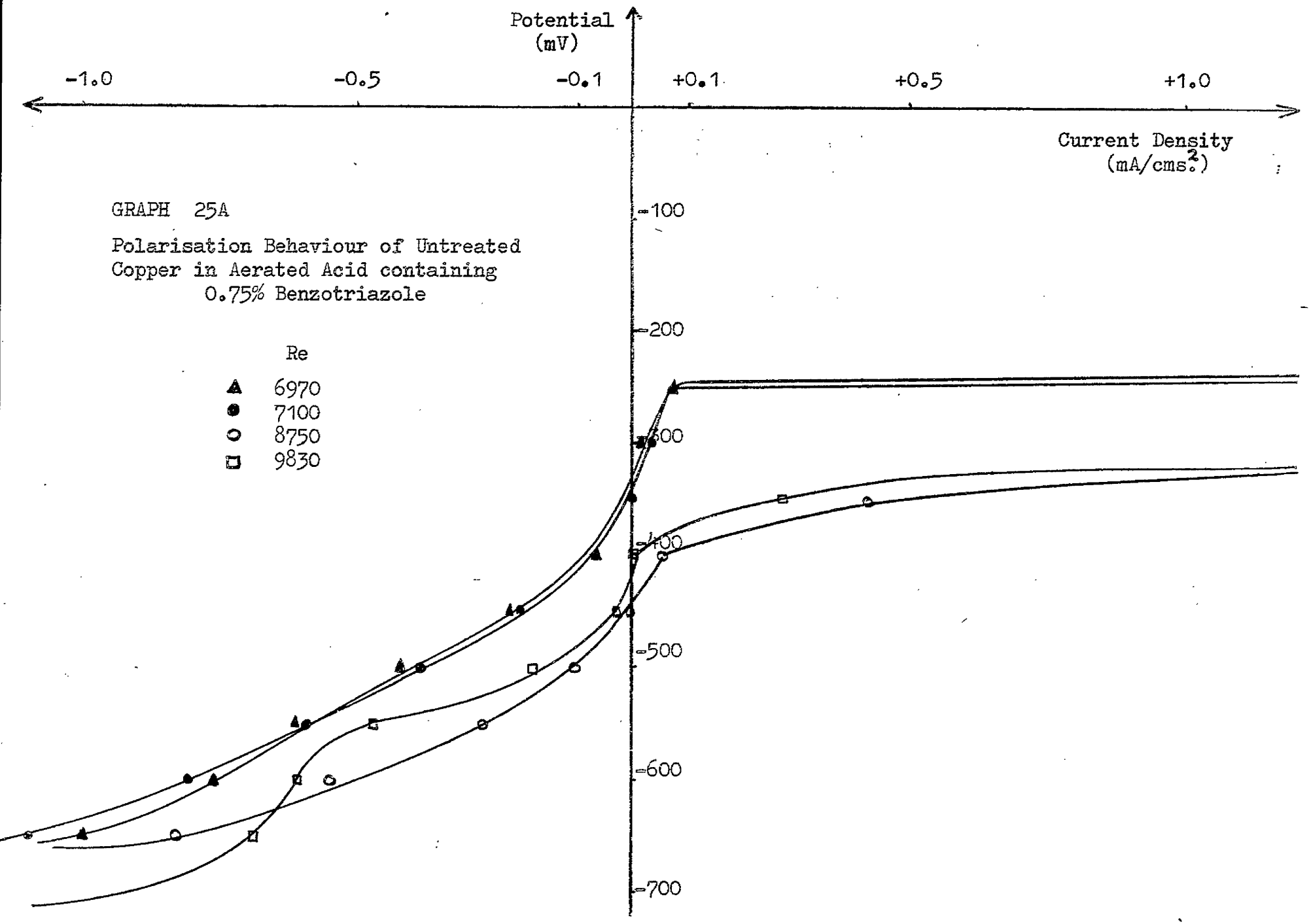

GRAPH 25A

Polarisation Behaviour of Untreated Copper in Aerated Acid containing 0.75% Benzotriazole

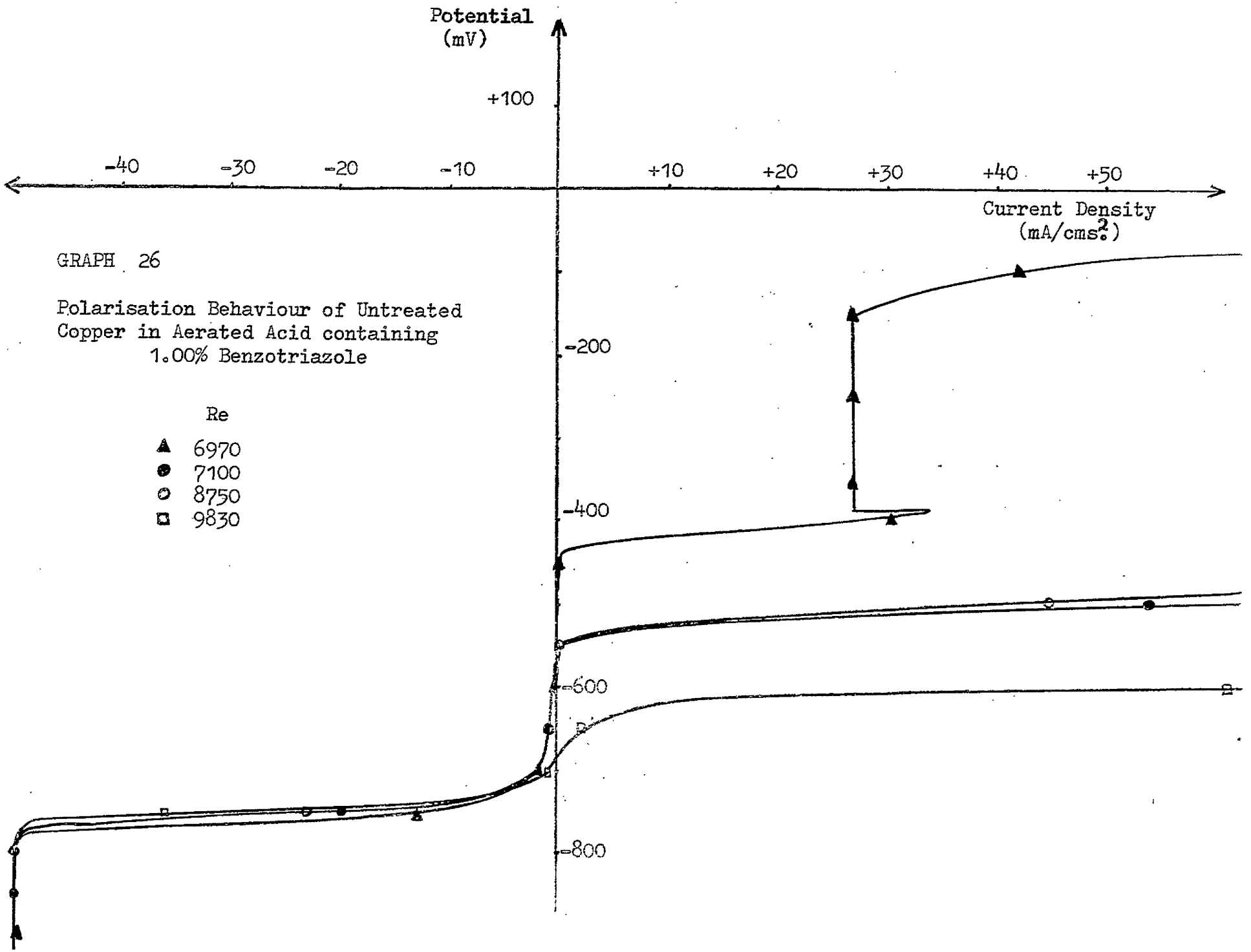

GRAPH 26

Polarisation Behaviour of Untreated Copper in Aerated Acid containing 1.00% Benzotriazole

Re

- ▲ 6970
- ● 7100
- ○ 8750
- □ 9830

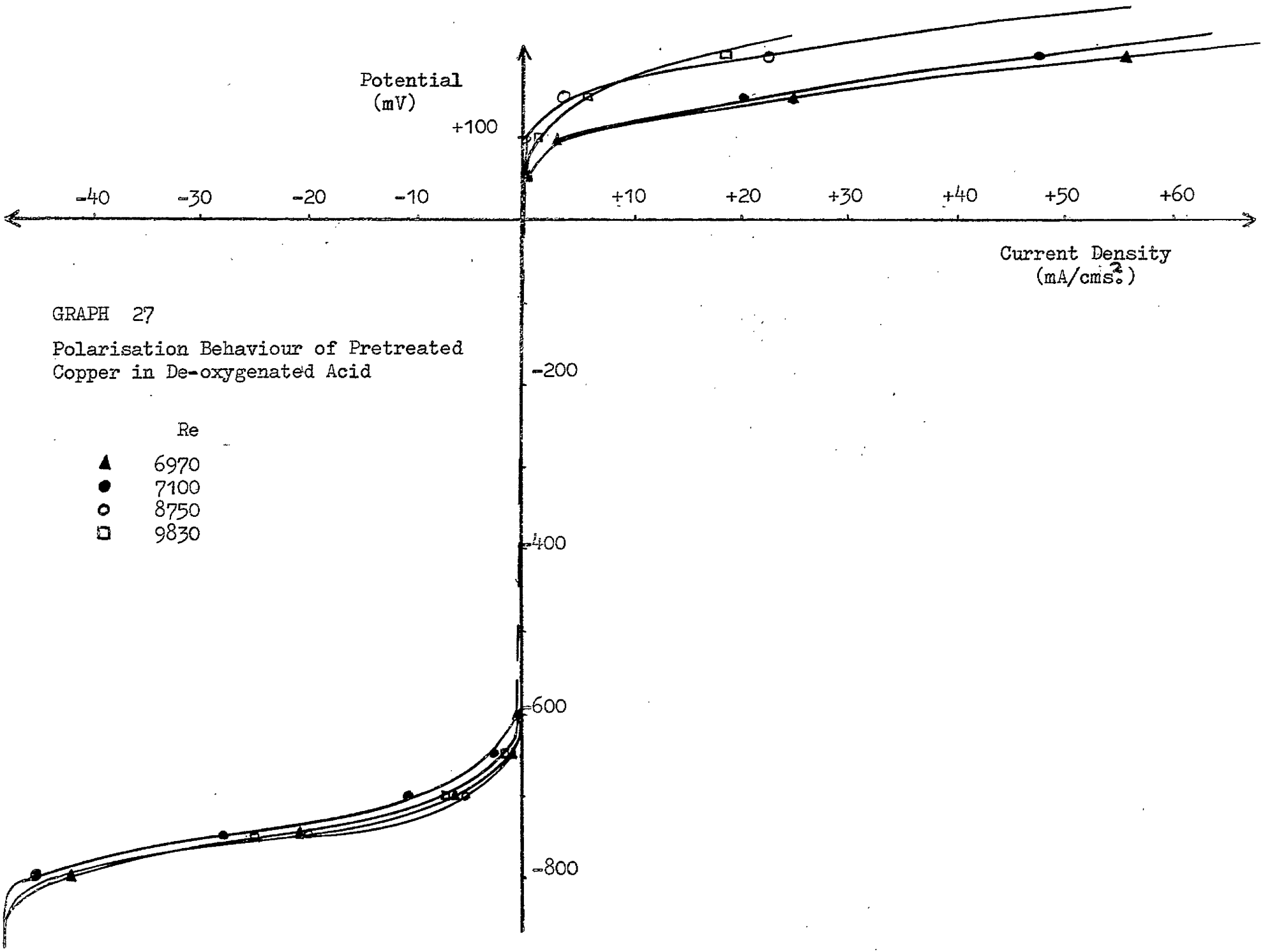

GRAPH 27

Polarisation Behaviour of Pretreated Copper in De-oxygenated Acid

Re
▲ 6970
● 7100
○ 8750
□ 9830

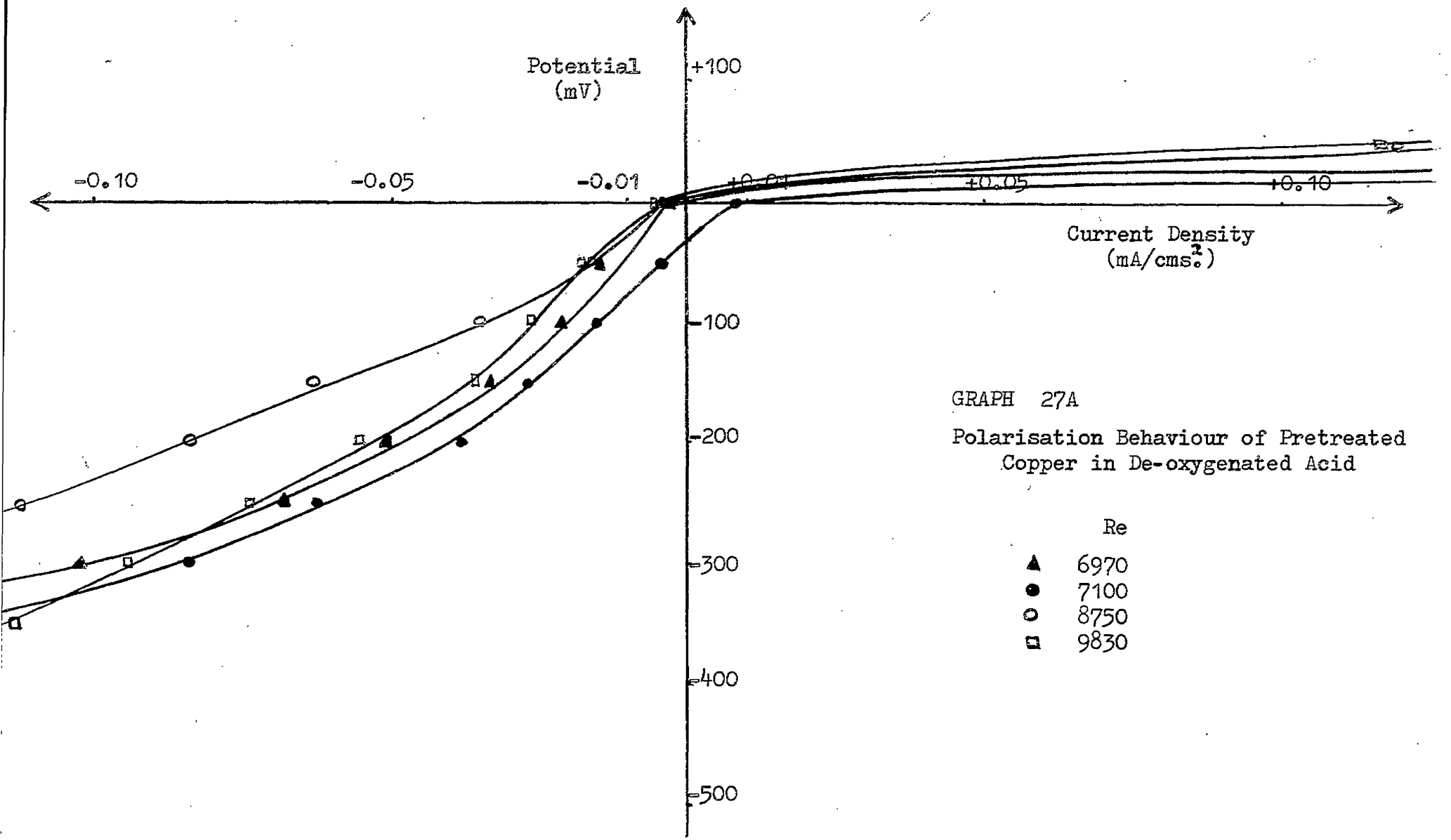

GRAPH 27A

Polarisation Behaviour of Pretreated Copper in De-oxygenated Acid

	Re
▲	6970
●	7100
○	8750
□	9830

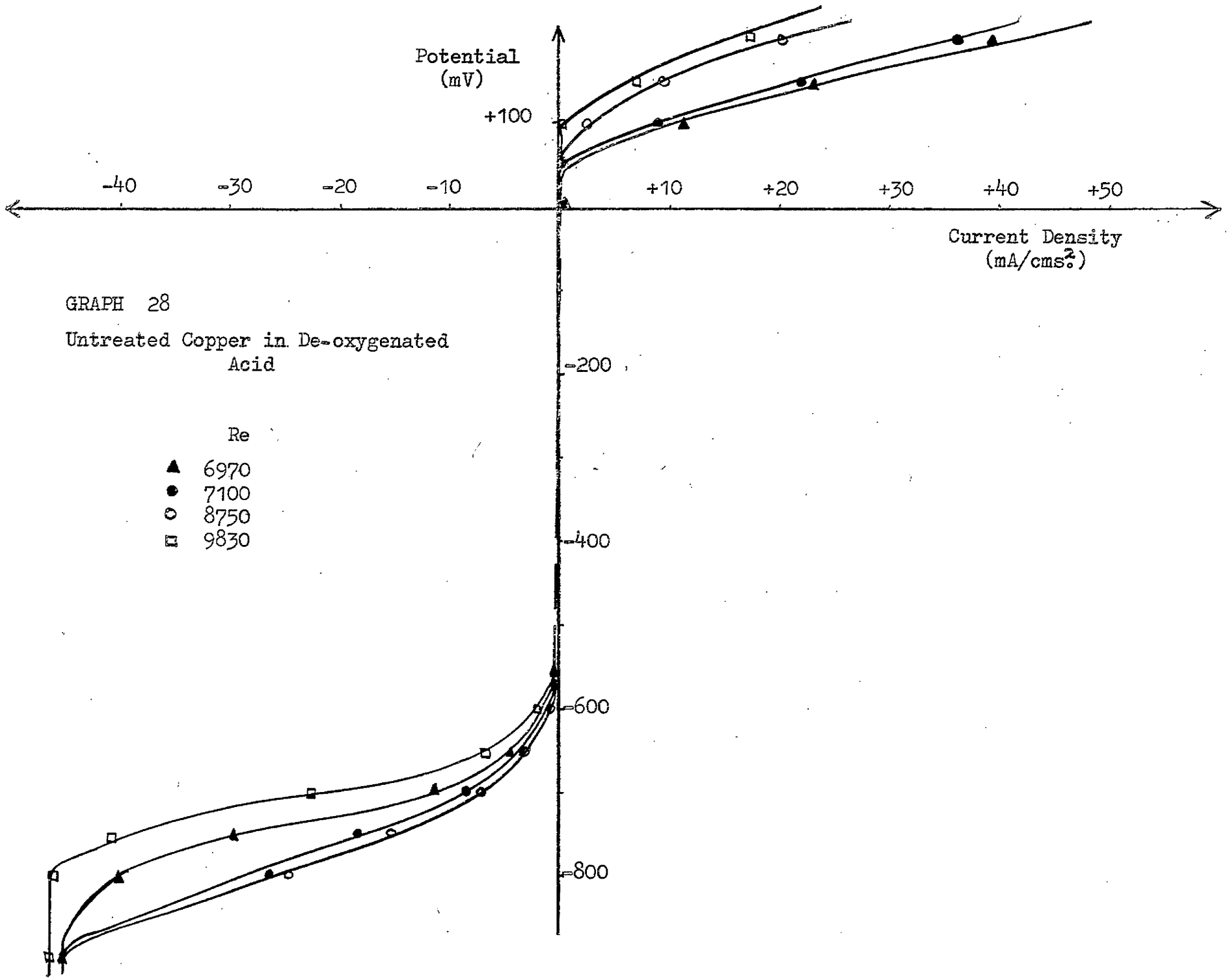

GRAPH 28

Untreated Copper in De-oxygenated Acid

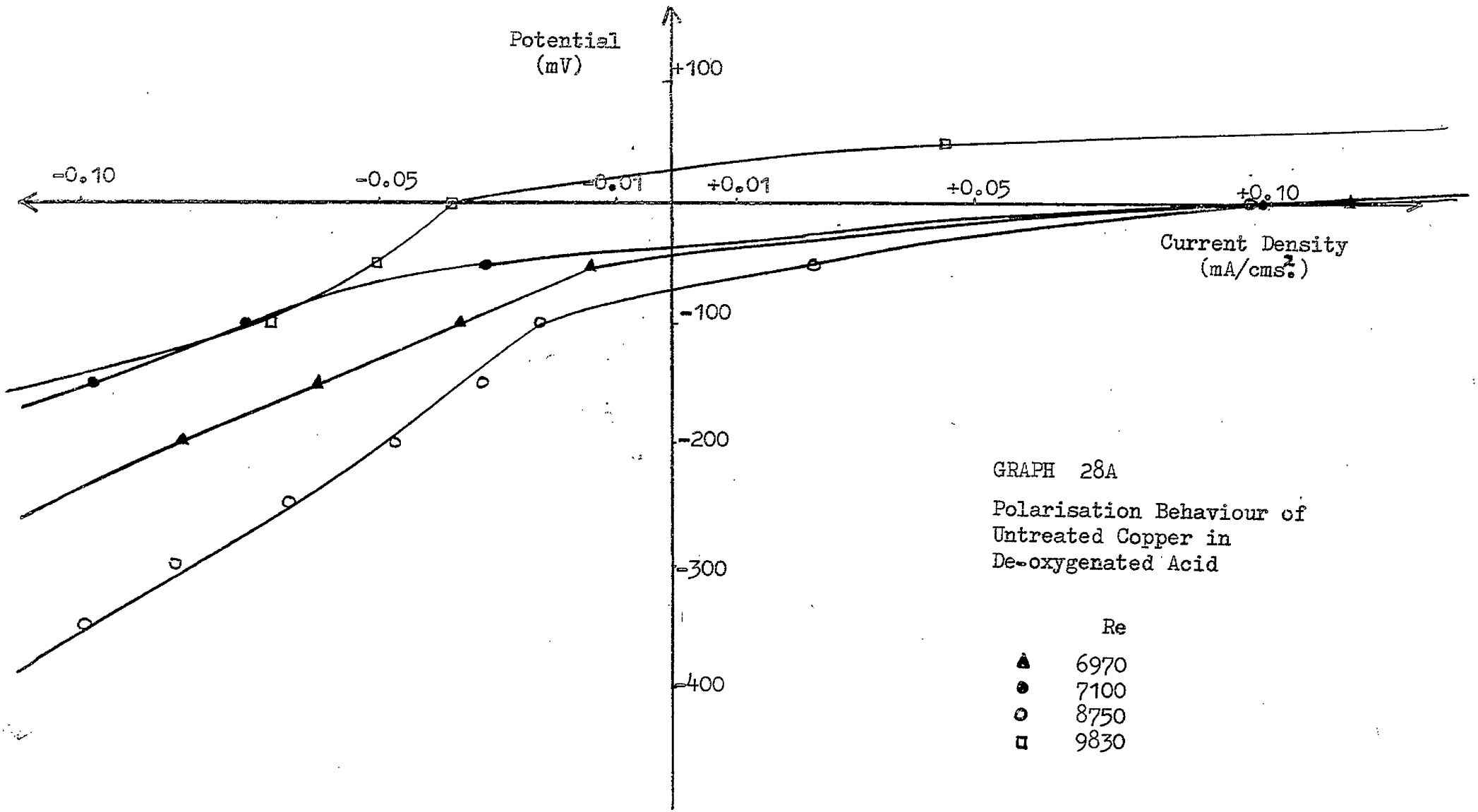

GRAPH 28A

Polarisation Behaviour of Untreated Copper in De-oxygenated Acid

	Re
▲	6970
●	7100
o	8750
□	9830

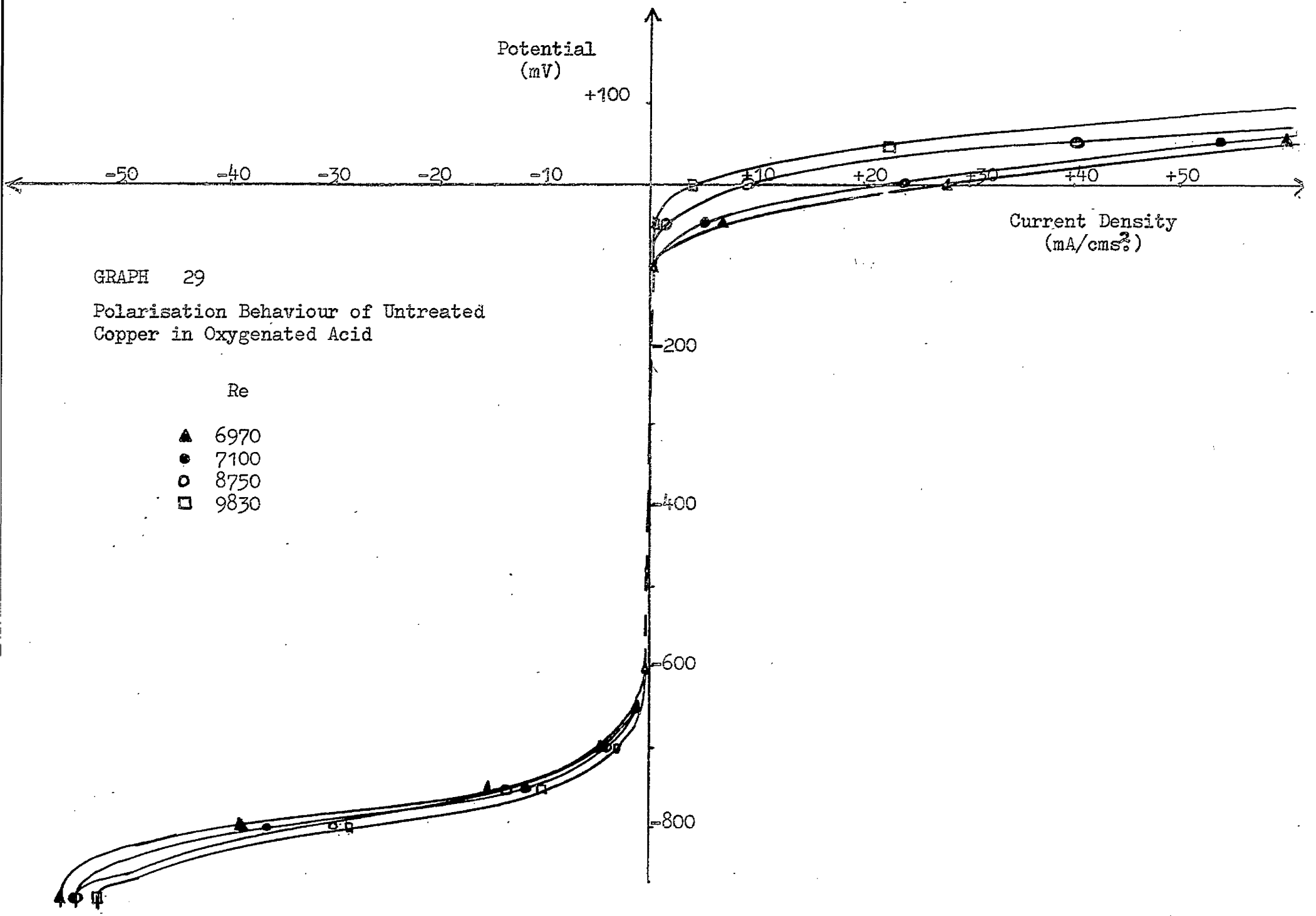

GRAPH 29

Polarisation Behaviour of Untreated Copper in Oxygenated Acid

Re

- ▲ 6970
- ● 7100
- ○ 8750
- □ 9830

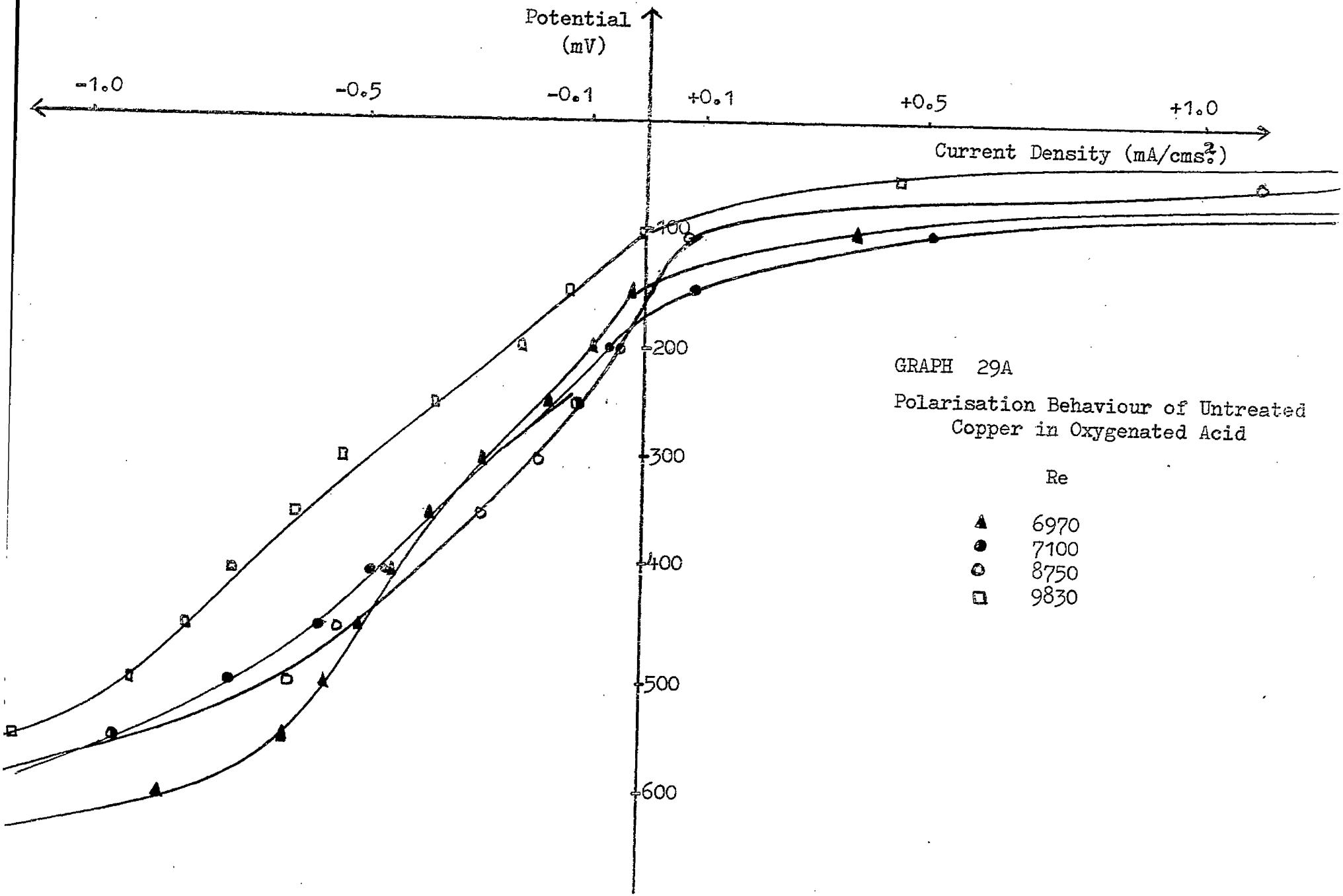

GRAPH 29A

Polarisation Behaviour of Untreated Copper in Oxygenated Acid

Re
6970
7100
8750
9830

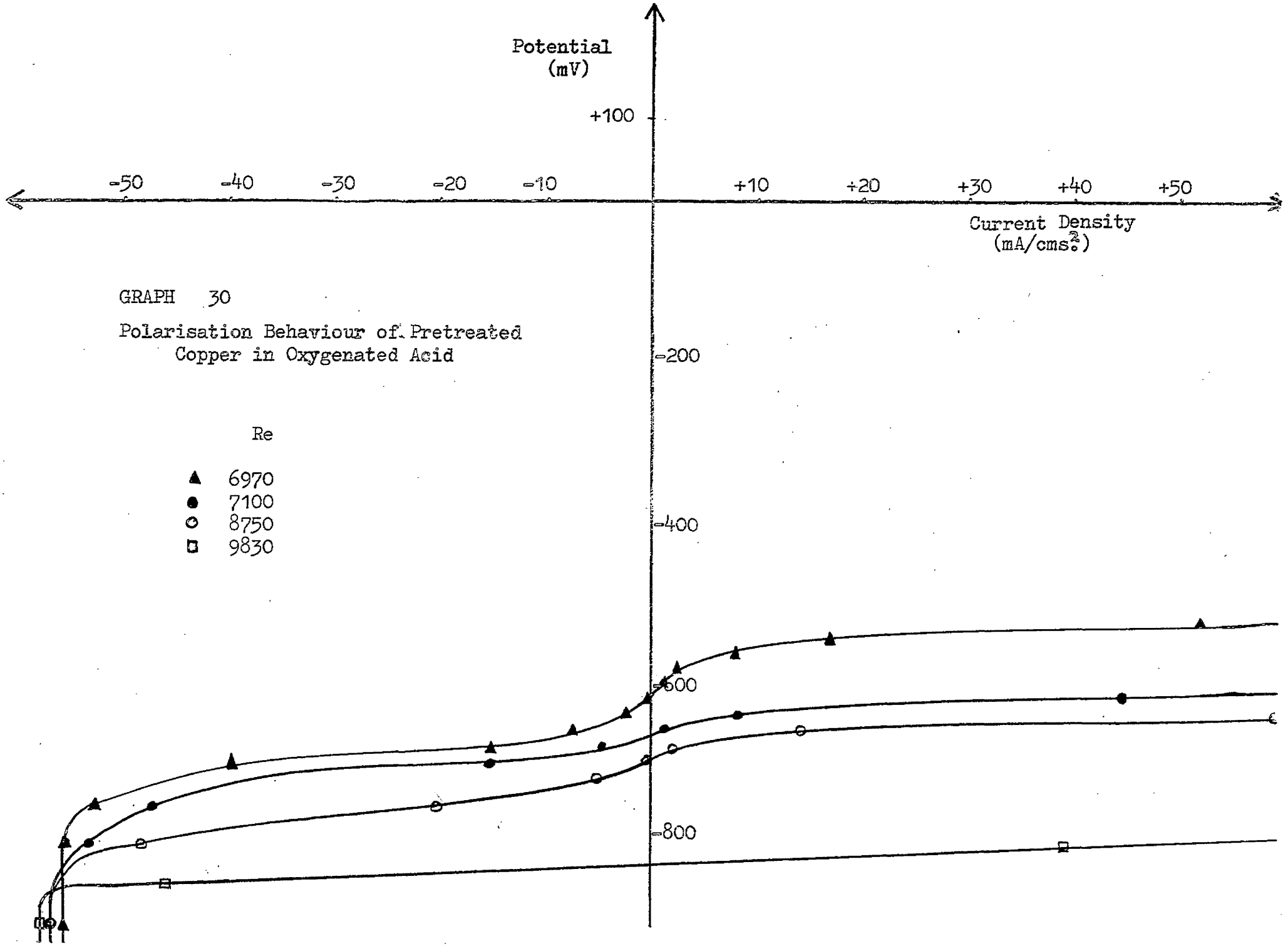

GRAPH 30

Polarisation Behaviour of Pretreated Copper in Oxygenated Acid

Re

- ▲ 6970
- ● 7100
- ○ 8750
- □ 9830

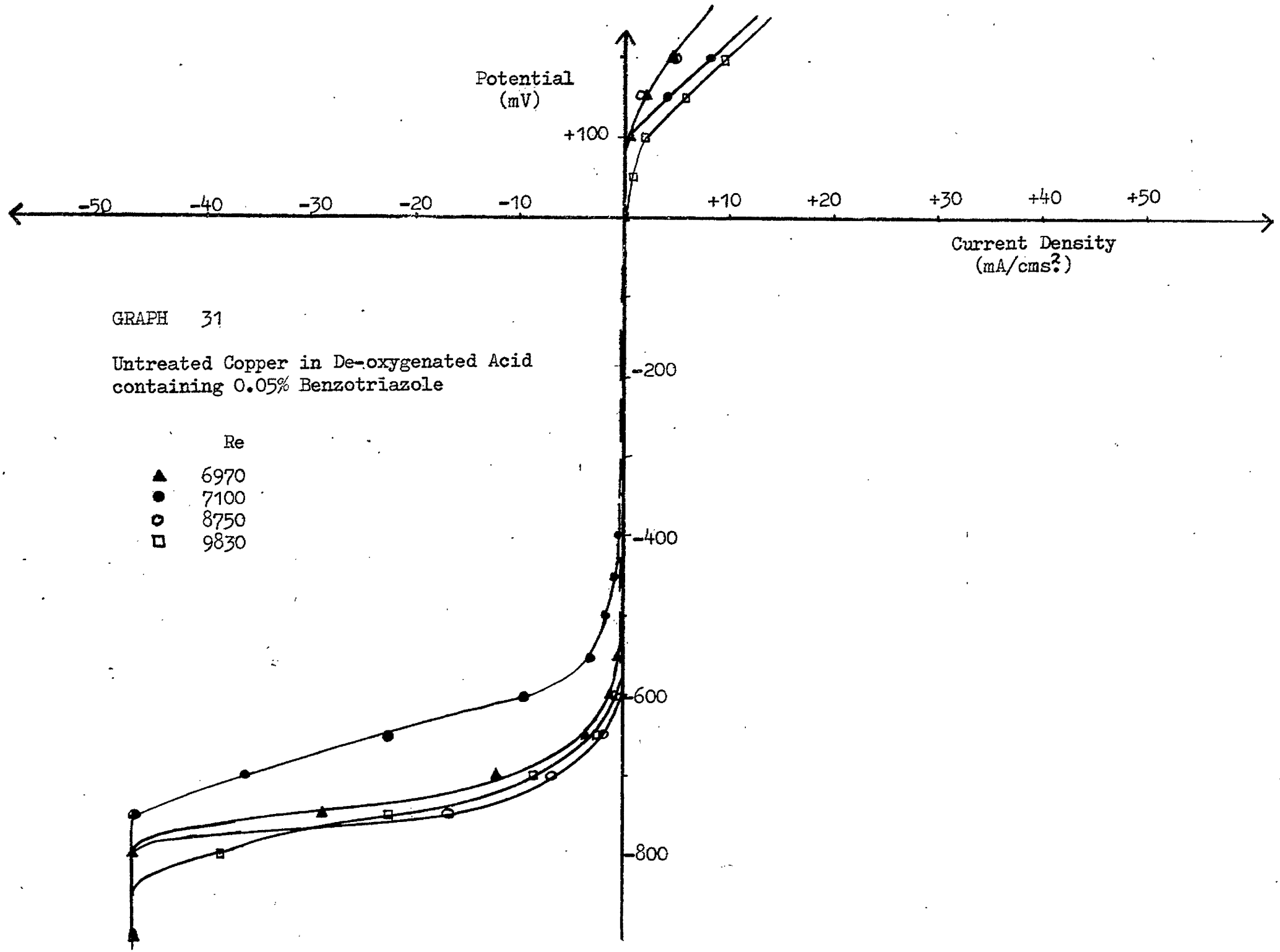

GRAPH 31

Untreated Copper in De-oxygenated Acid containing 0.05% Benzotriazole

Re

▲ 6970
● 7100
○ 8750
□ 9830

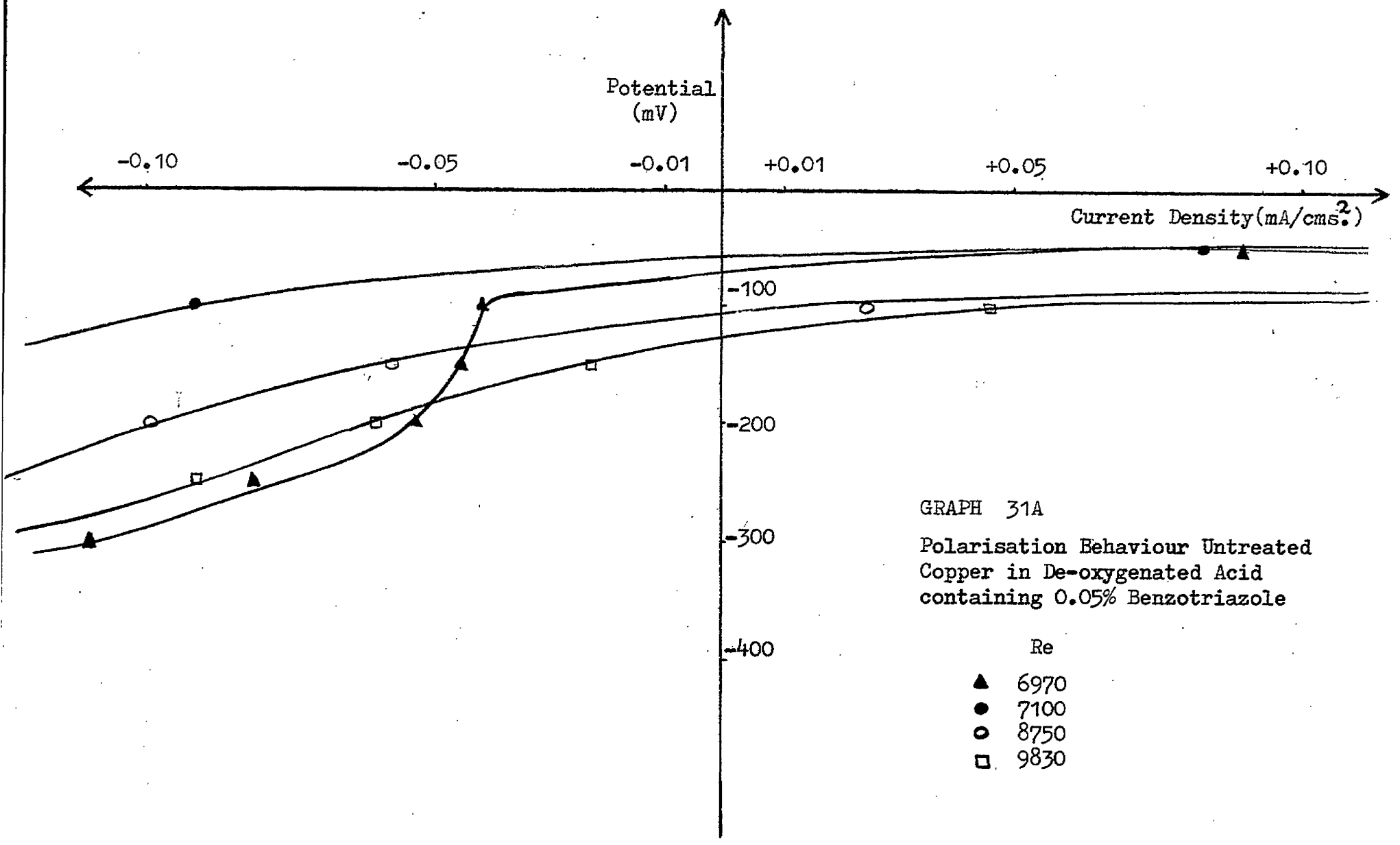

GRAPH 31A

Polarisation Behaviour Untreated Copper in De-oxygenated Acid containing 0.05% Benzotriazole

Re

- ▲ 6970
- ● 7100
- ○ 8750
- □ 9830

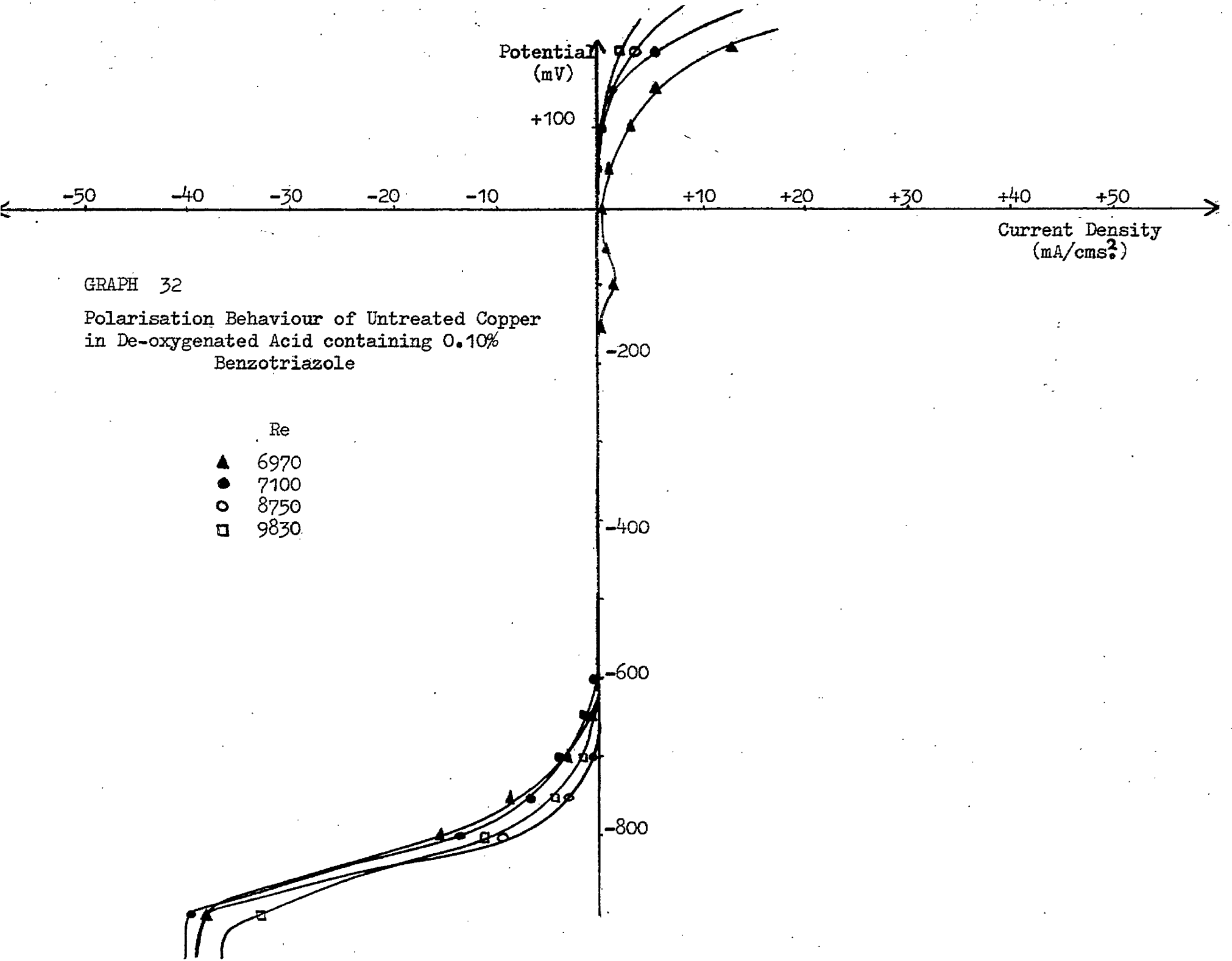

GRAPH 32

Polarisation Behaviour of Untreated Copper in De-oxygenated Acid containing 0.10% Benzotriazole

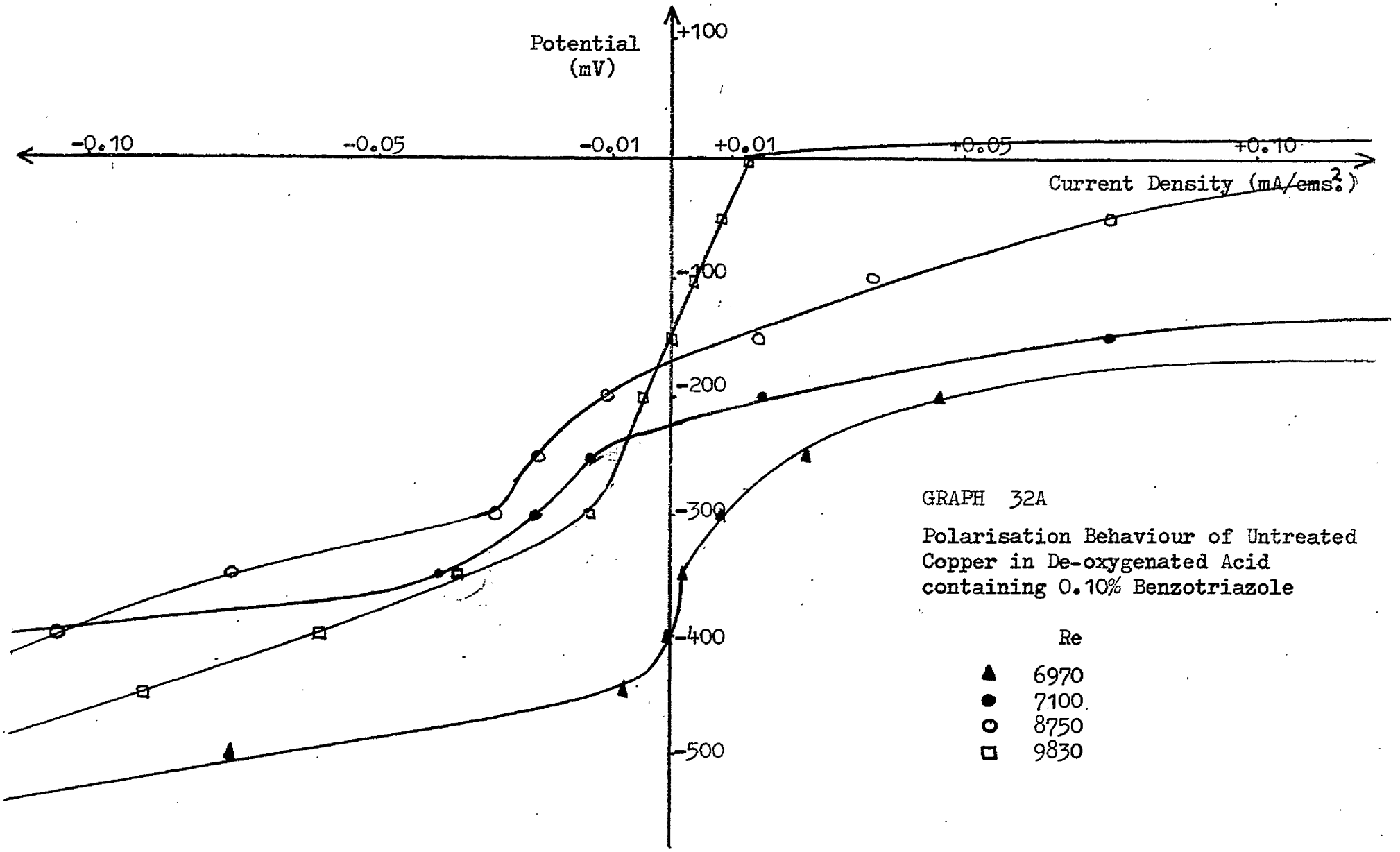

GRAPH 32A

Polarisation Behaviour of Untreated Copper in De-oxygenated Acid containing 0.10% Benzotriazole

Re
▲ 6970
● 7100
○ 8750
□ 9830

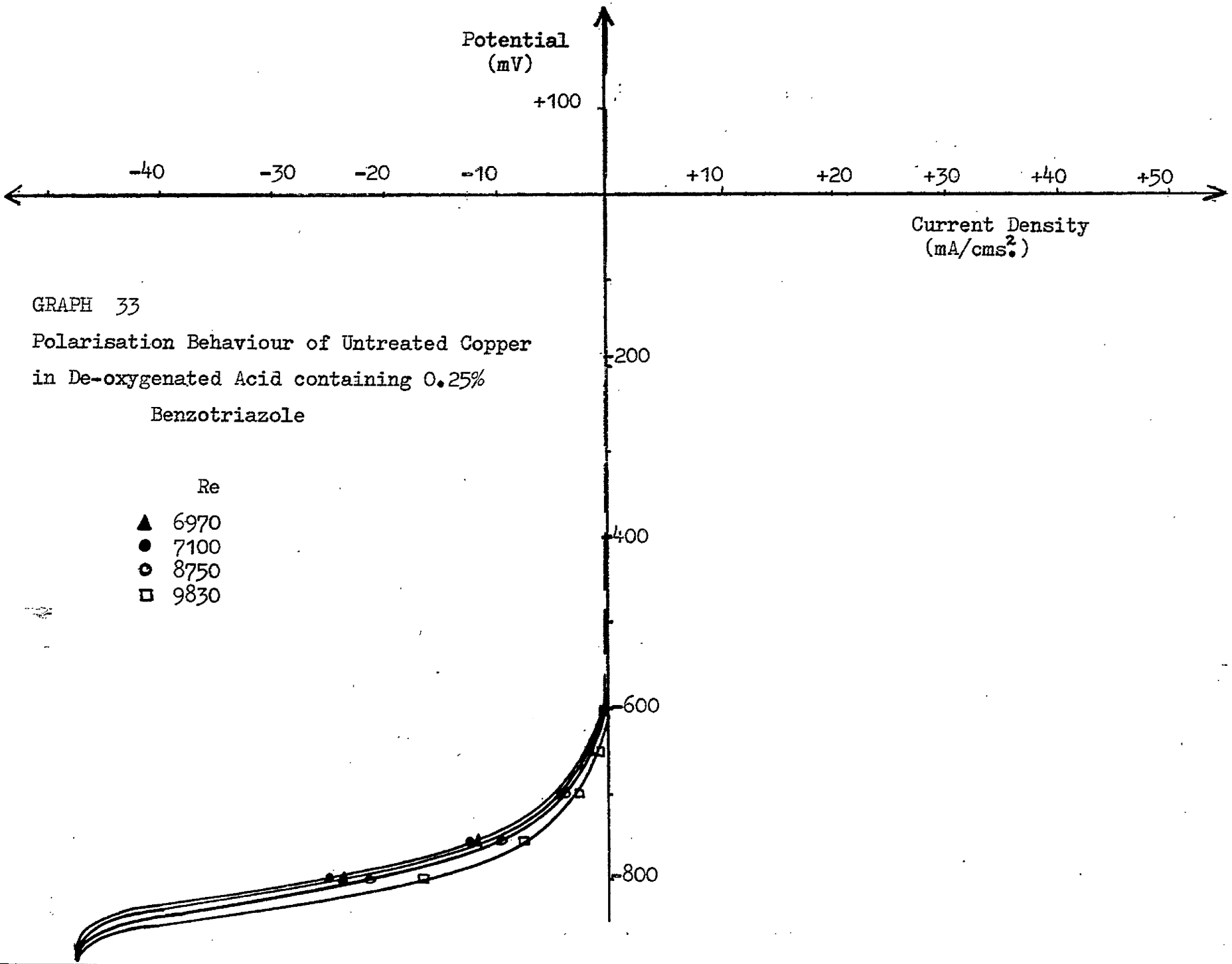

GRAPH 33

Polarisation Behaviour of Untreated Copper in De-oxygenated Acid containing 0.25% Benzotriazole

Re

- ▲ 6970
- ● 7100
- ○ 8750
- □ 9830

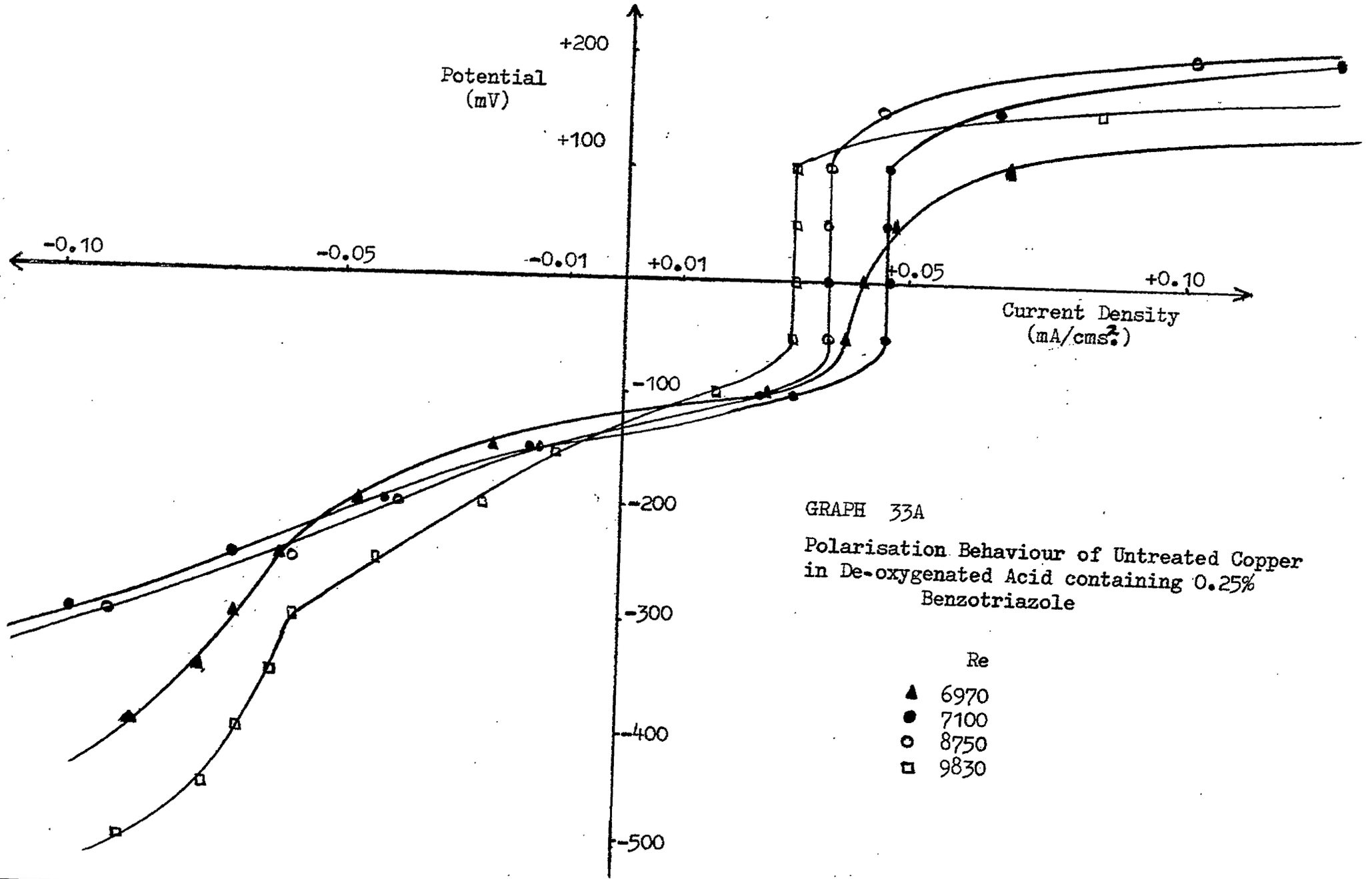

GRAPH 33A

Polarisation Behaviour of Untreated Copper in De-oxygenated Acid containing 0.25% Benzotriazole

Re

- ▲ 6970
- ● 7100
- ○ 8750
- □ 9830

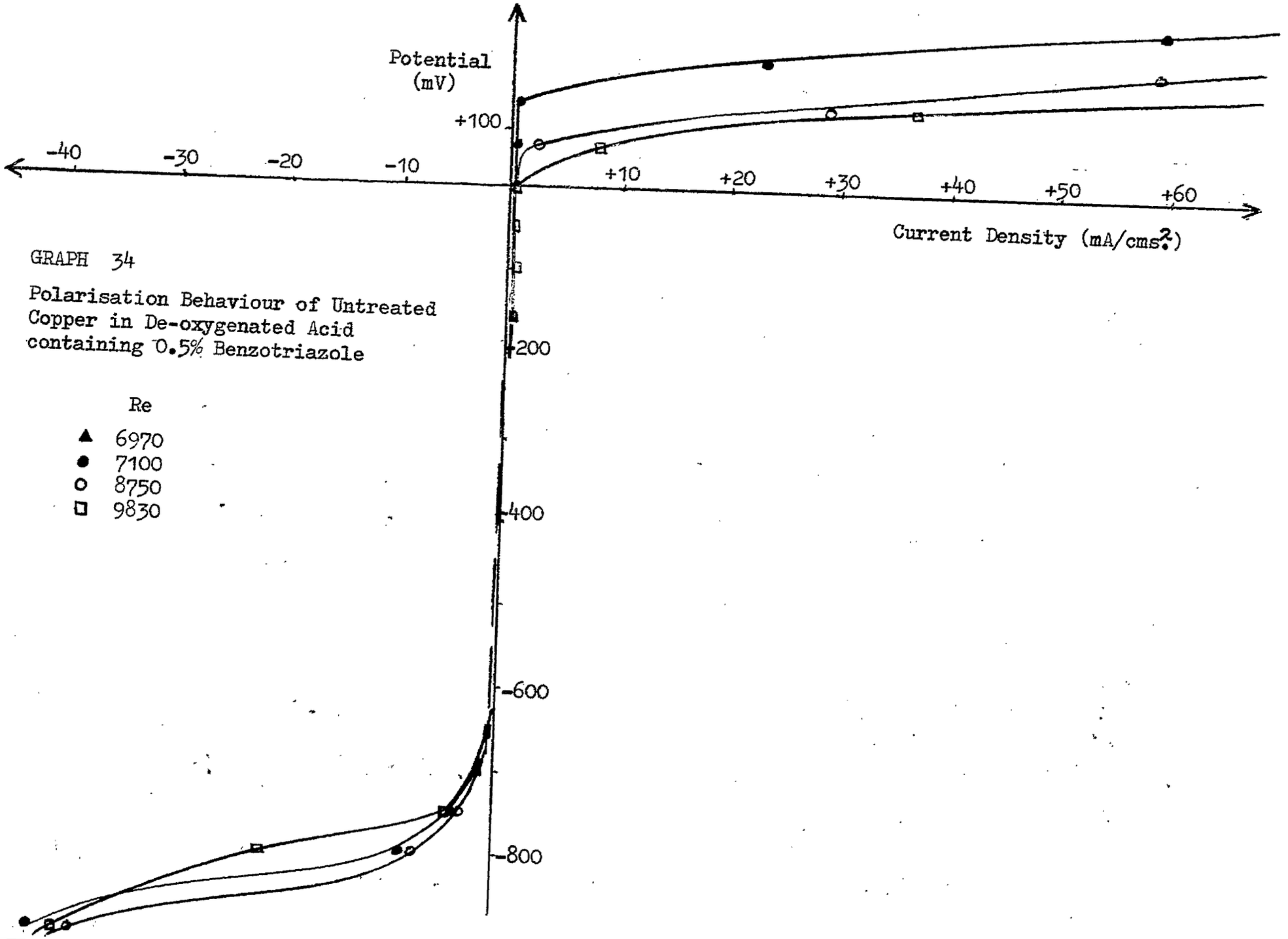

GRAPH 34

Polarisation Behaviour of Untreated Copper in De-oxygenated Acid containing 0.5% Benzotriazole

Re

- ▲ 6970
- ● 7100
- ○ 8750
- □ 9830

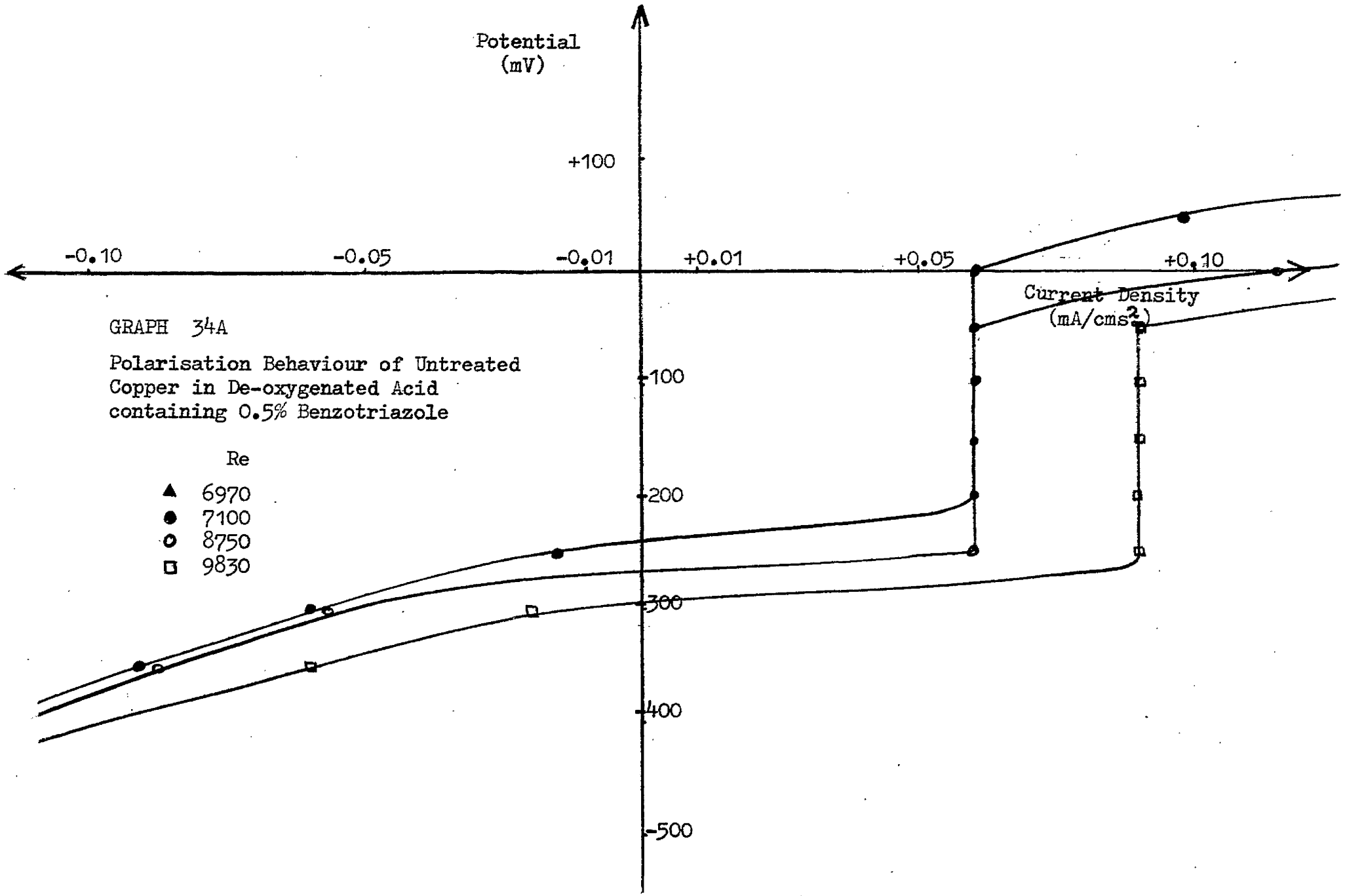

GRAPH 34A

Polarisation Behaviour of Untreated Copper in De-oxygenated Acid containing 0.5% Benzotriazole

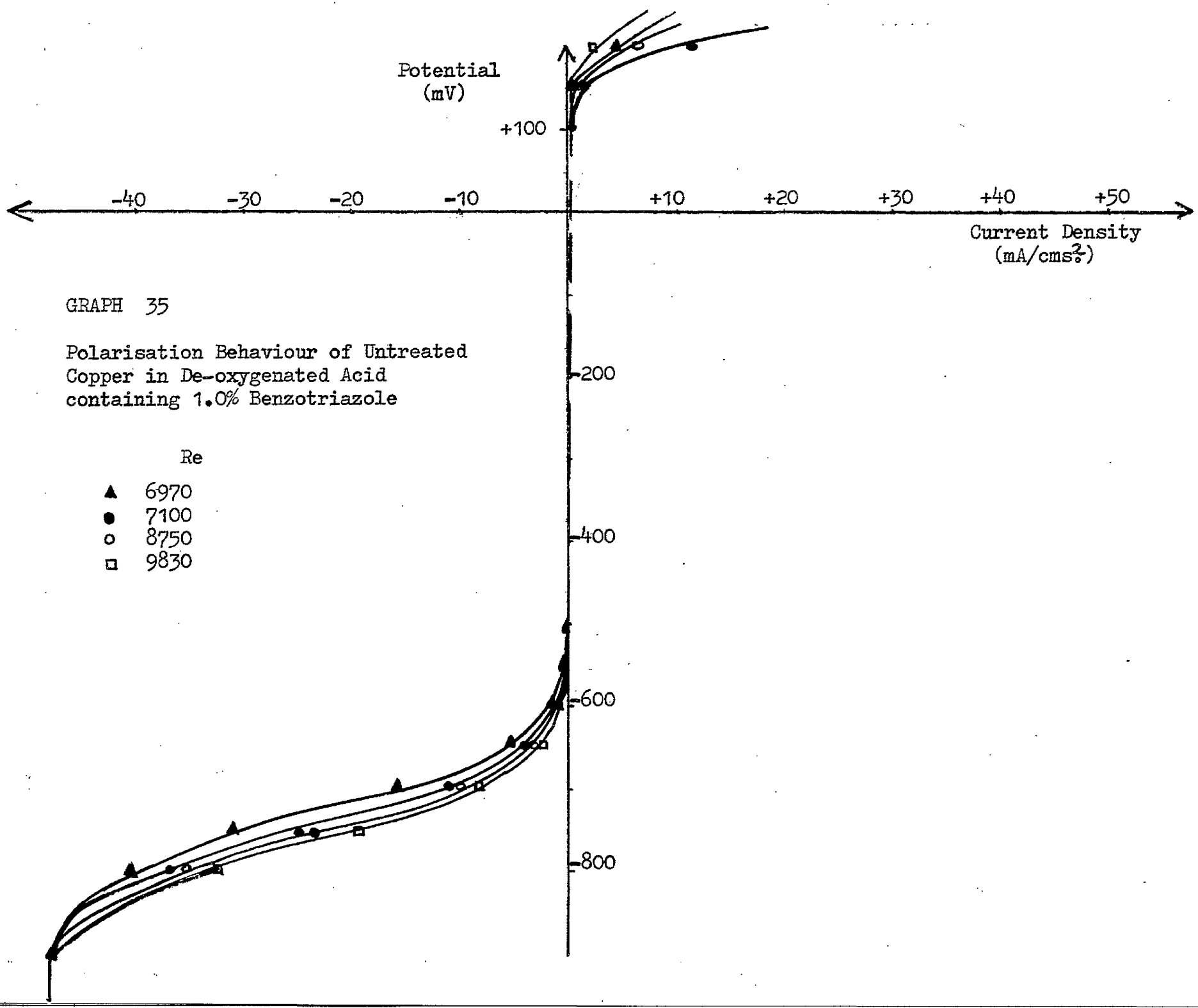

GRAPH 35

Polarisation Behaviour of Untreated Copper in De-oxygenated Acid containing 1.0% Benzotriazole

Re

- ▲ 6970
- ● 7100
- o 8750
- □ 9830

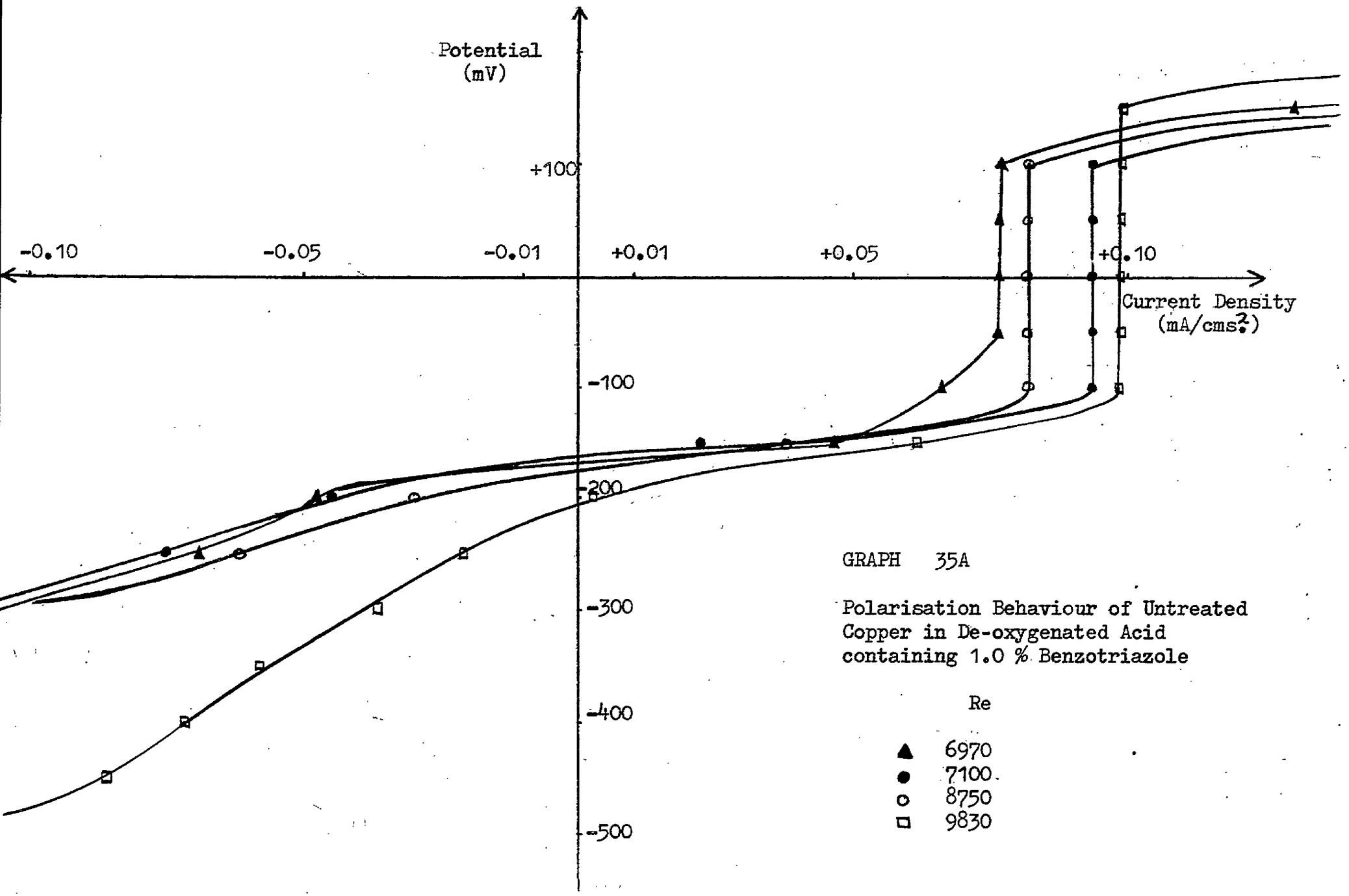

GRAPH 35A

Polarisation Behaviour of Untreated Copper in De-oxygenated Acid containing 1.0 % Benzotriazole

Re

- ▲ 6970
- ● 7100
- ○ 8750
- □ 9830

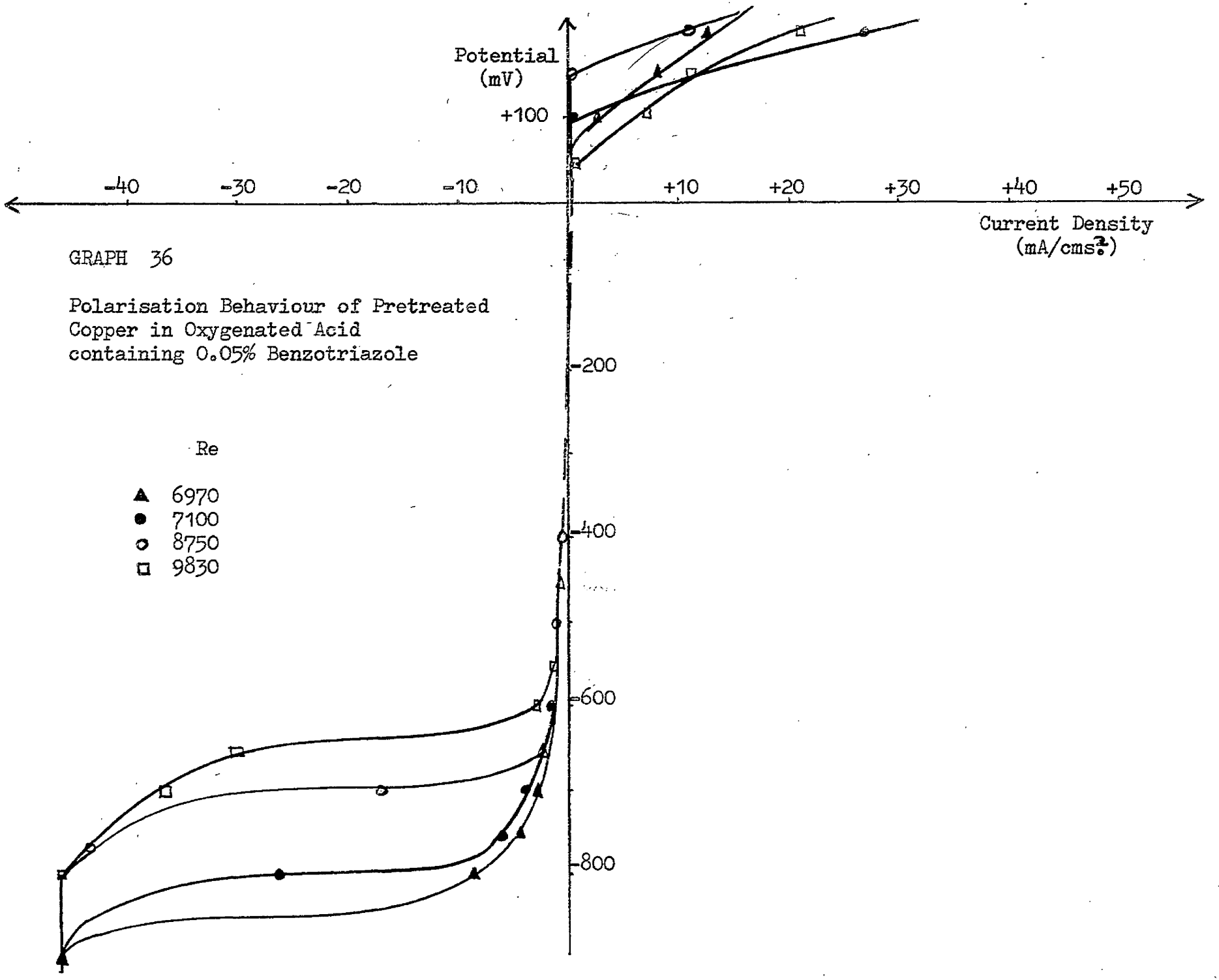

GRAPH 36

Polarisation Behaviour of Pretreated Copper in Oxygenated Acid containing 0.05% Benzotriazole

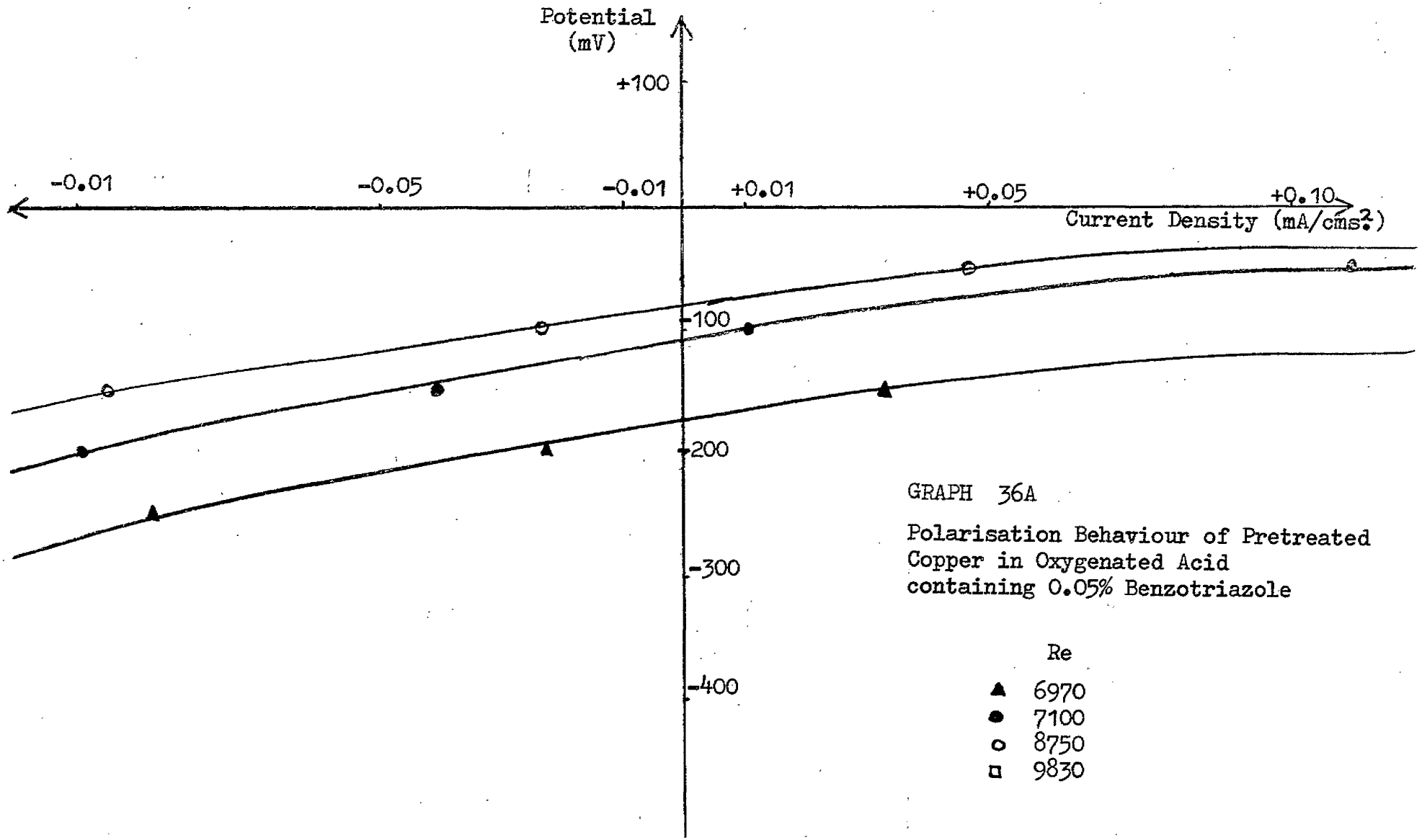

GRAPH 36A

Polarisation Behaviour of Pretreated Copper in Oxygenated Acid containing 0.05% Benzotriazole

Re

- ▲ 6970
- ● 7100
- ○ 8750
- □ 9830

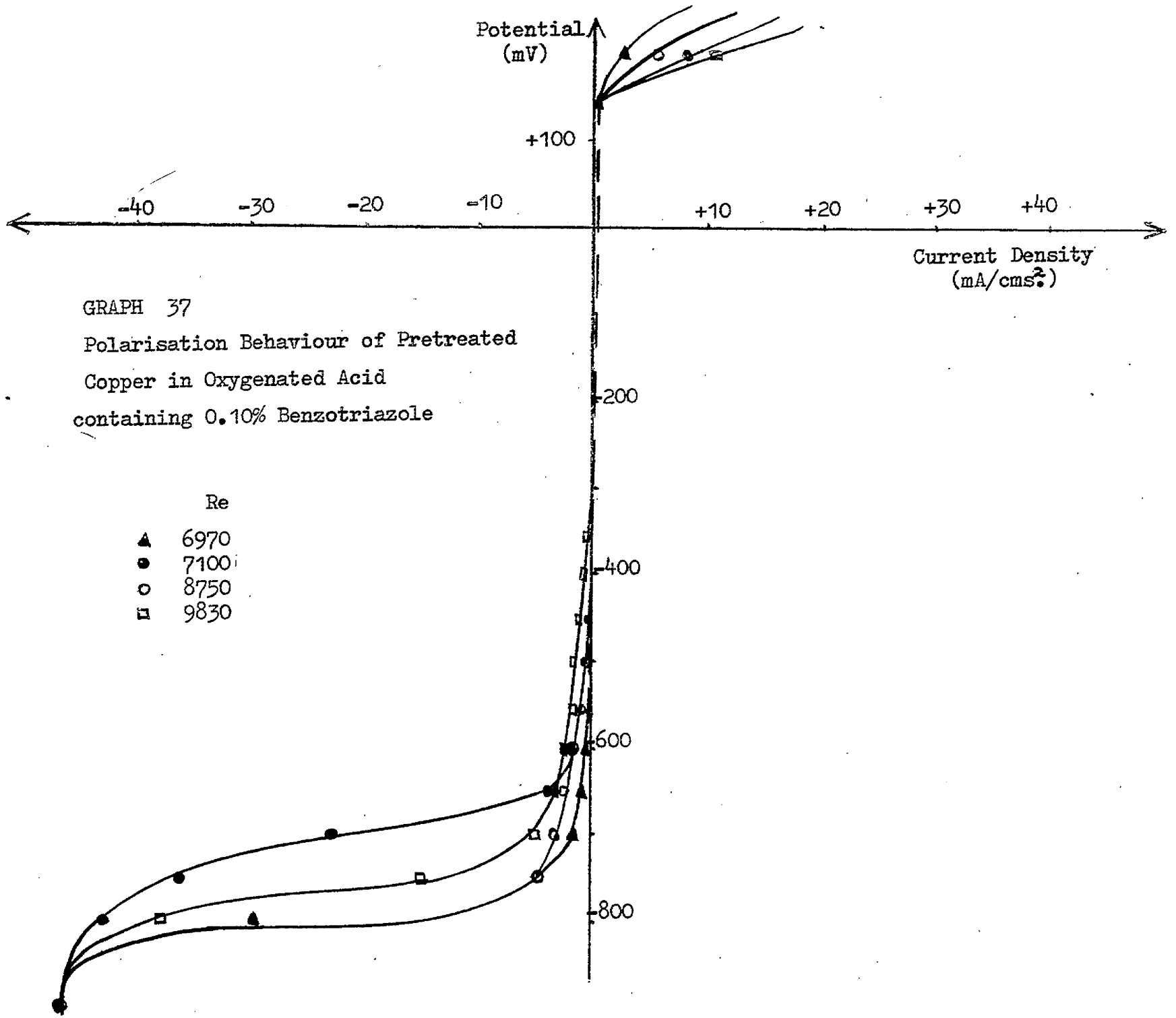

GRAPH 37

Polarisation Behaviour of Pretreated Copper in Oxygenated Acid containing 0.10% Benzotriazole

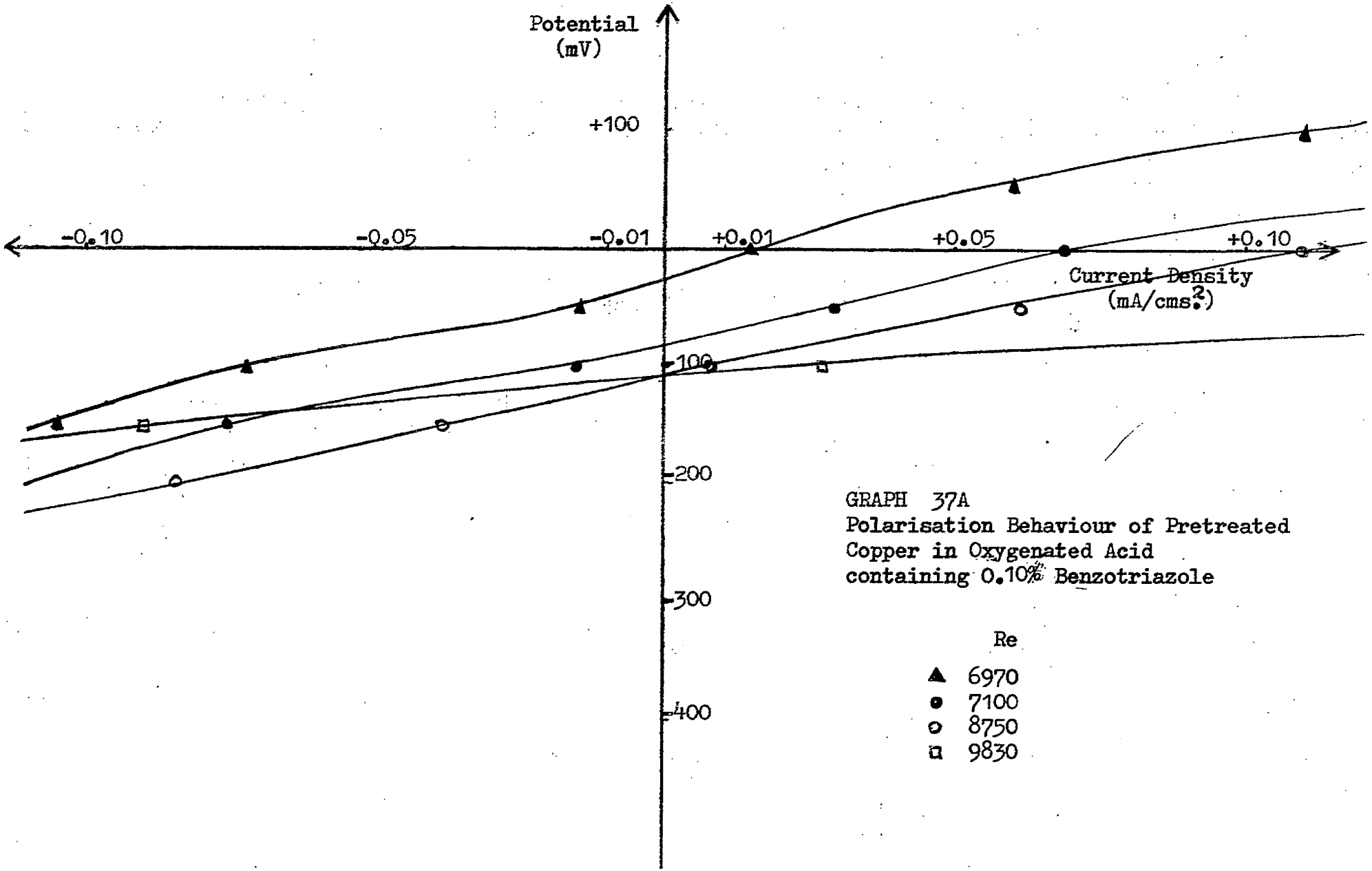

GRAPH 37A
Polarisation Behaviour of Pretreated Copper in Oxygenated Acid containing 0.10% Benzotriazole

Re
▲ 6970
● 7100
○ 8750
□ 9830

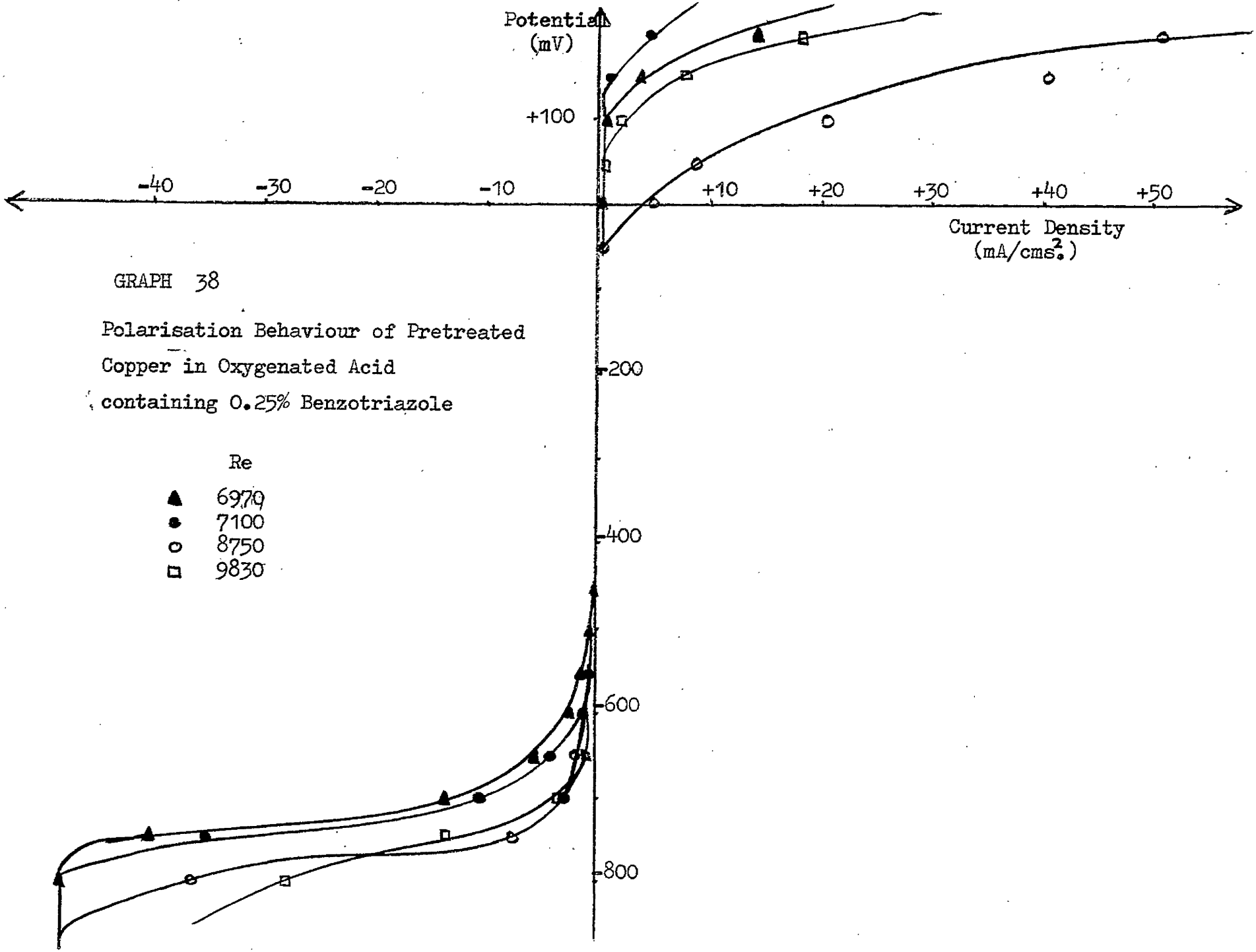

GRAPH 38

Polarisation Behaviour of Pretreated Copper in Oxygenated Acid containing 0.25% Benzotriazole

Re

- ▲ 6970
- ● 7100
- o 8750
- □ 9830

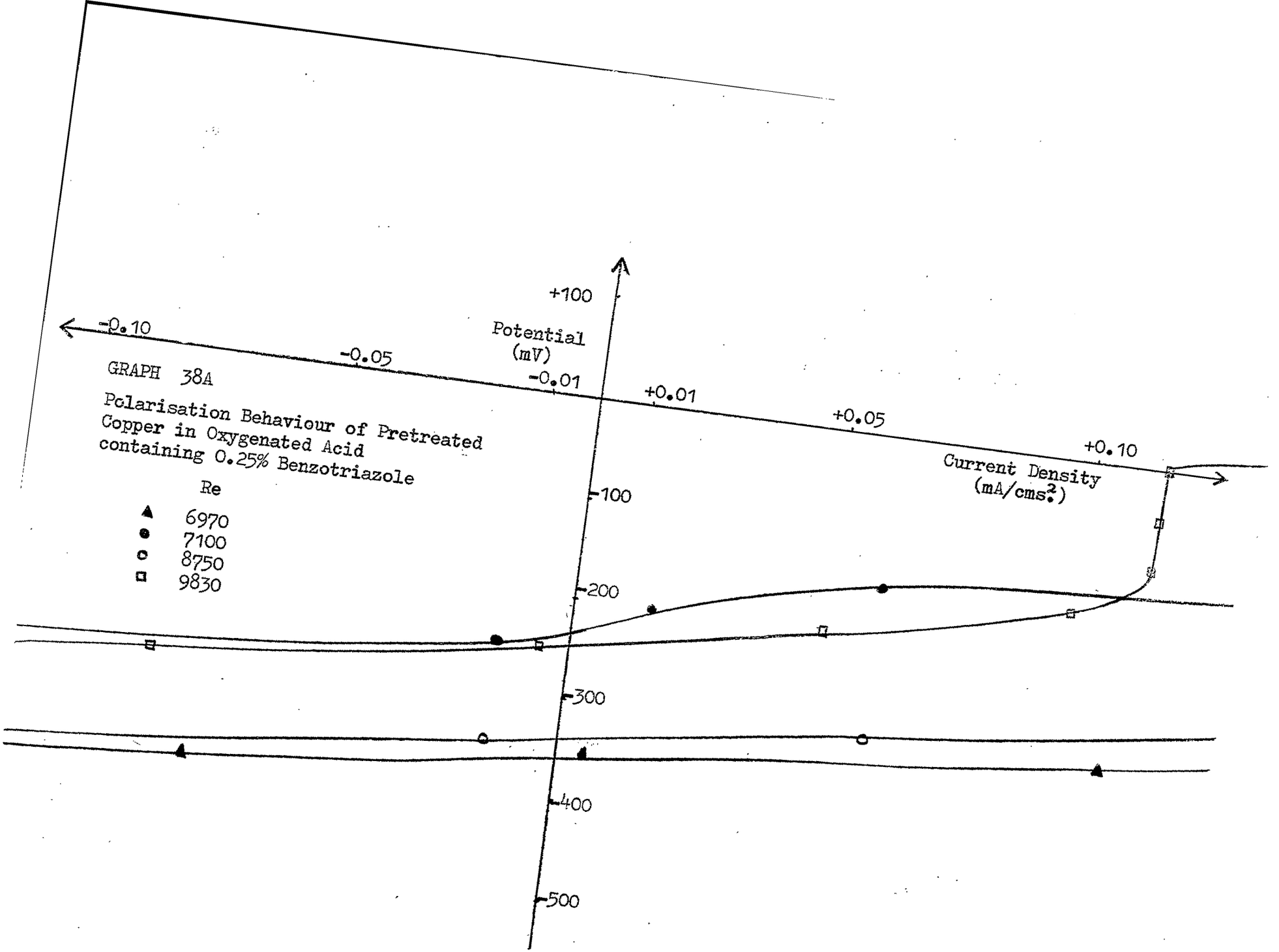

GRAPH 38A

Polarisation Behaviour of Pretreated Copper in Oxygenated Acid containing 0.25% Benzotriazole

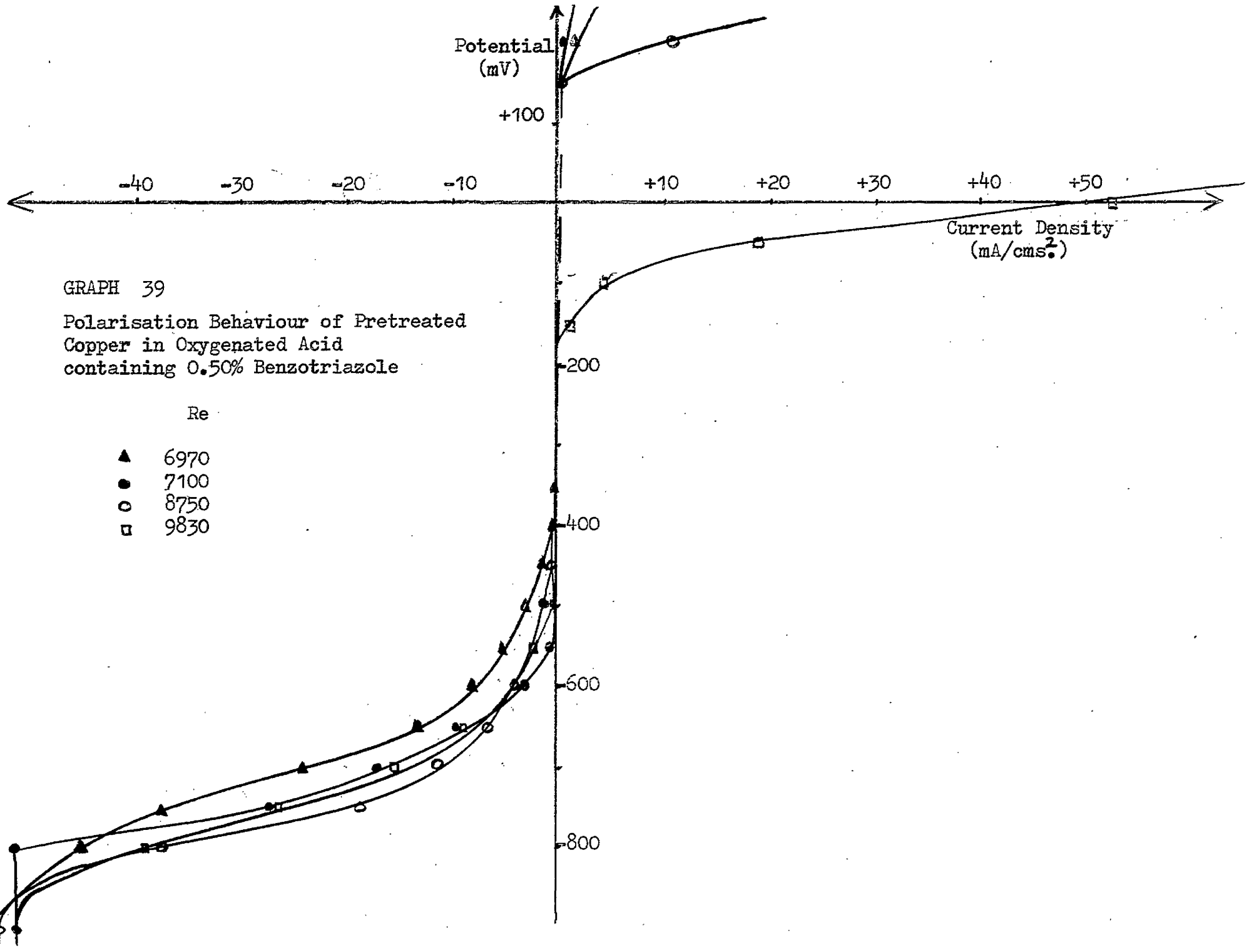

GRAPH 39

Polarisation Behaviour of Pretreated Copper in Oxygenated Acid containing 0.50% Benzotriazole

Re

- ▲ 6970
- ● 7100
- ○ 8750
- □ 9830

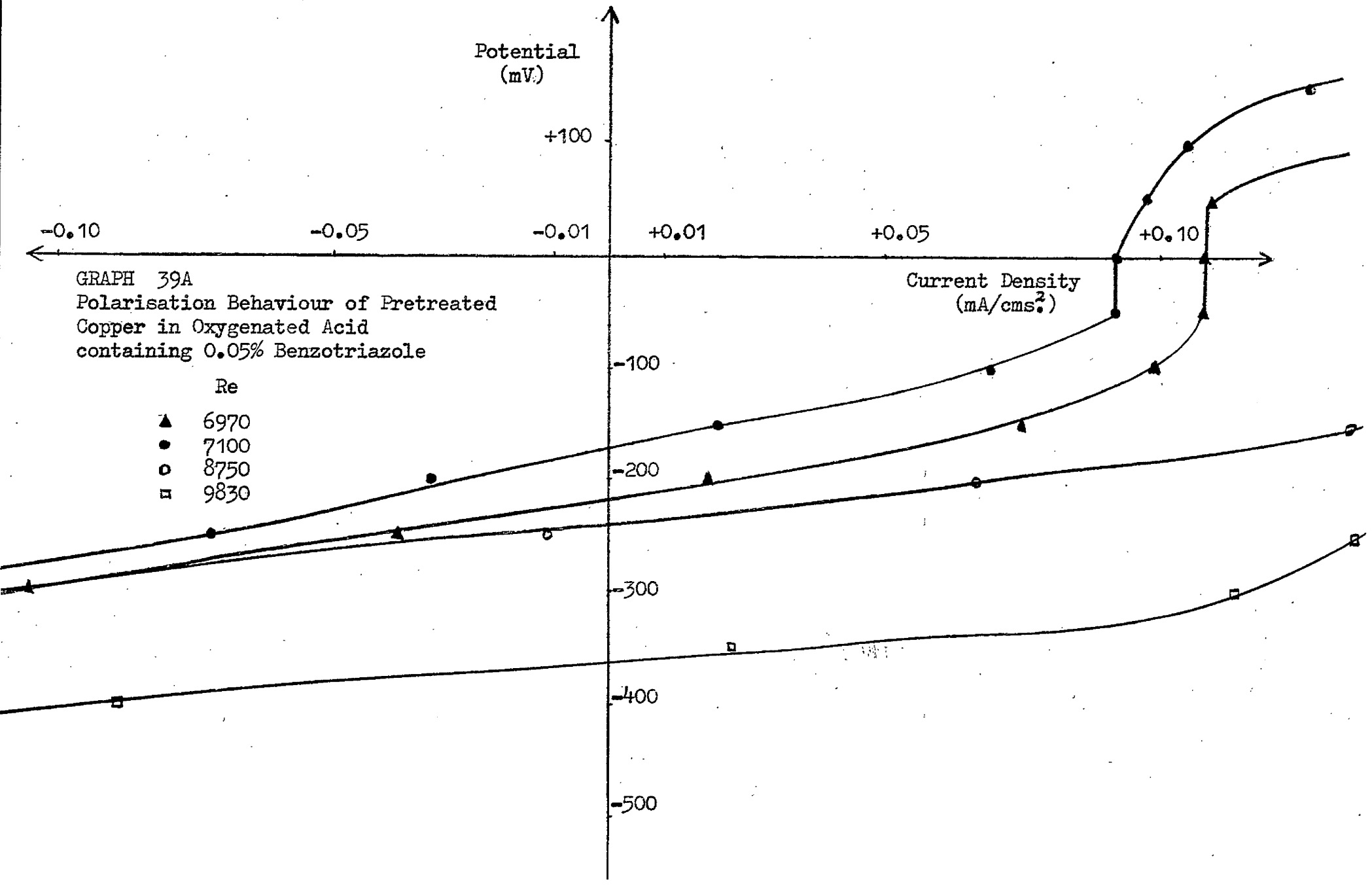

GRAPH 39A
Polarisation Behaviour of Pretreated Copper in Oxygenated Acid containing 0.05% Benzotriazole

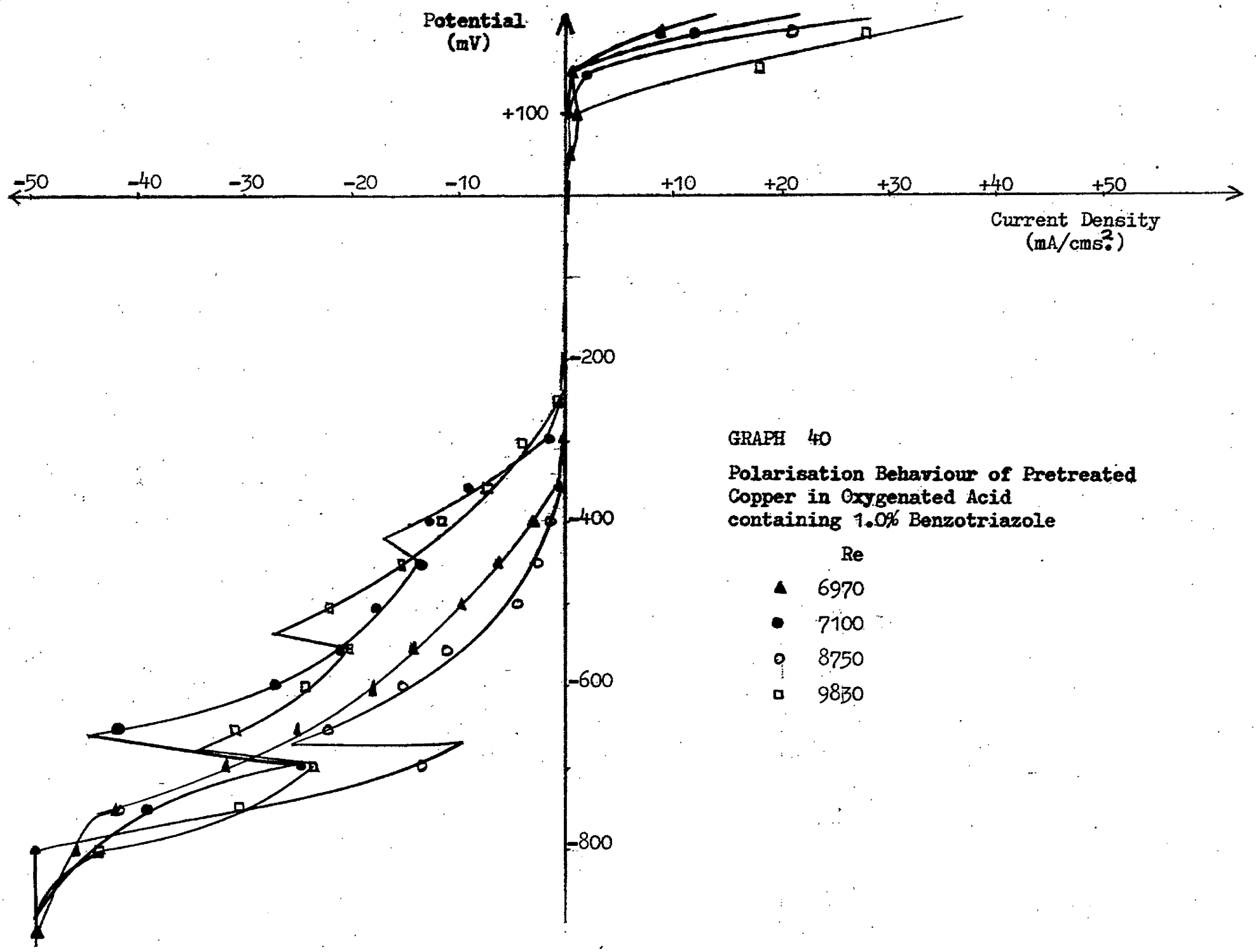

GRAPH 40

Polarisation Behaviour of Pretreated Copper in Oxygenated Acid containing 1.0% Benzotriazole

Re
▲ 6970
● 7100
○ 8750
□ 9830

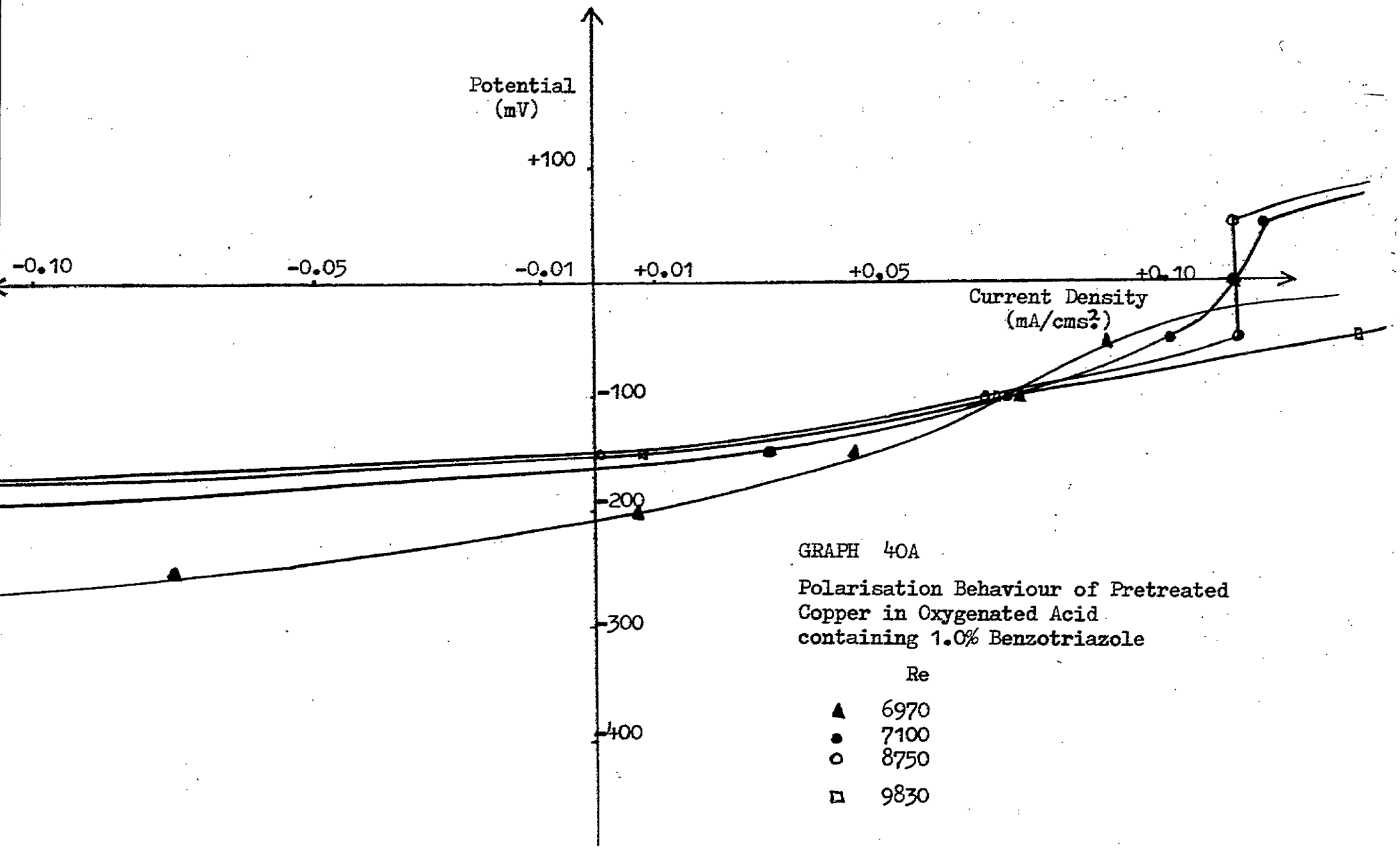

GRAPH 40A

Polarisation Behaviour of Pretreated Copper in Oxygenated Acid containing 1.0% Benzotriazole

	Re
▲	6970
●	7100
○	8750
□	9830

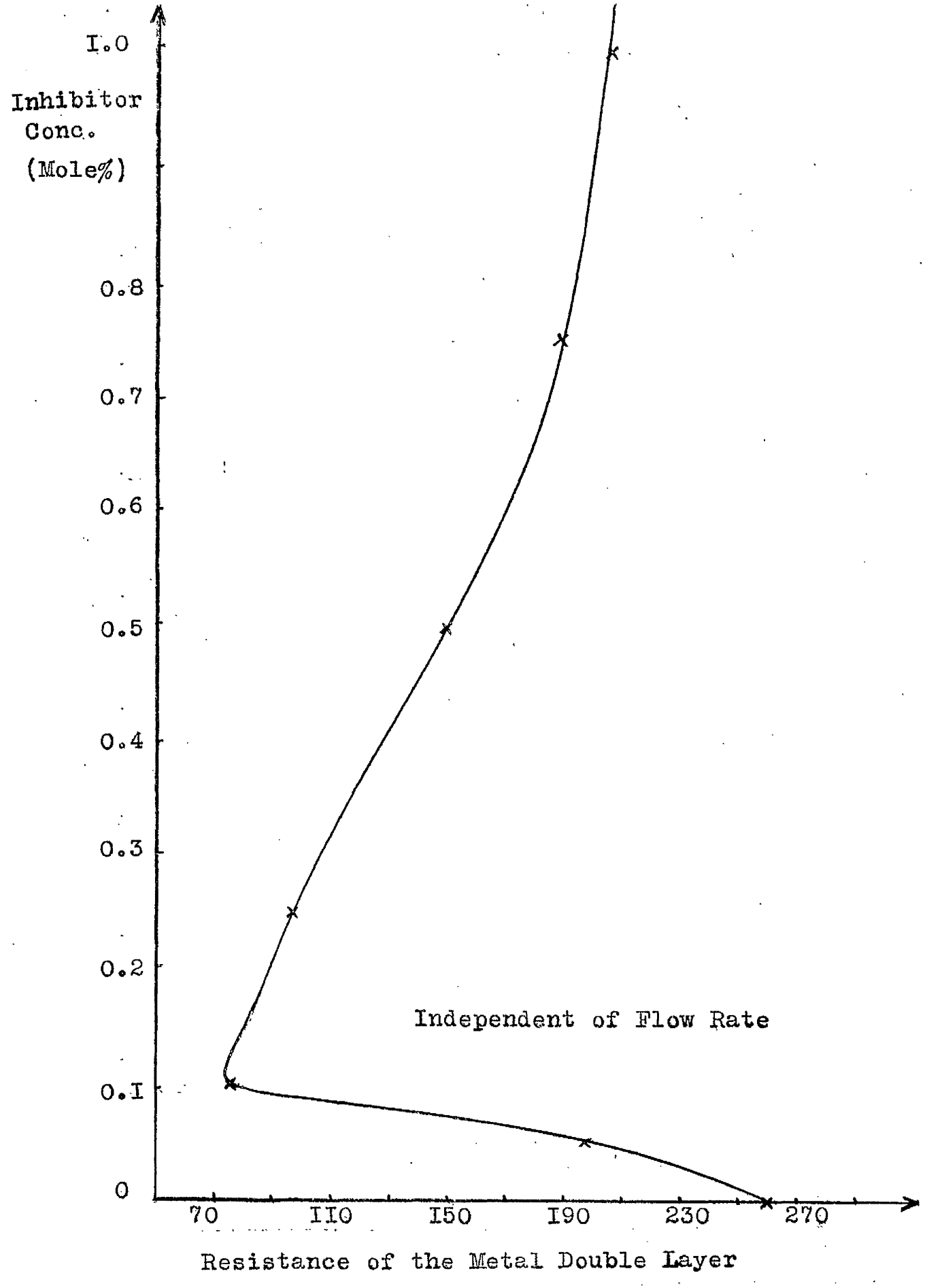

GRAPH 4I · Variation of Resistance of the Metal Double Layer in Flowing Inhibited Acid.

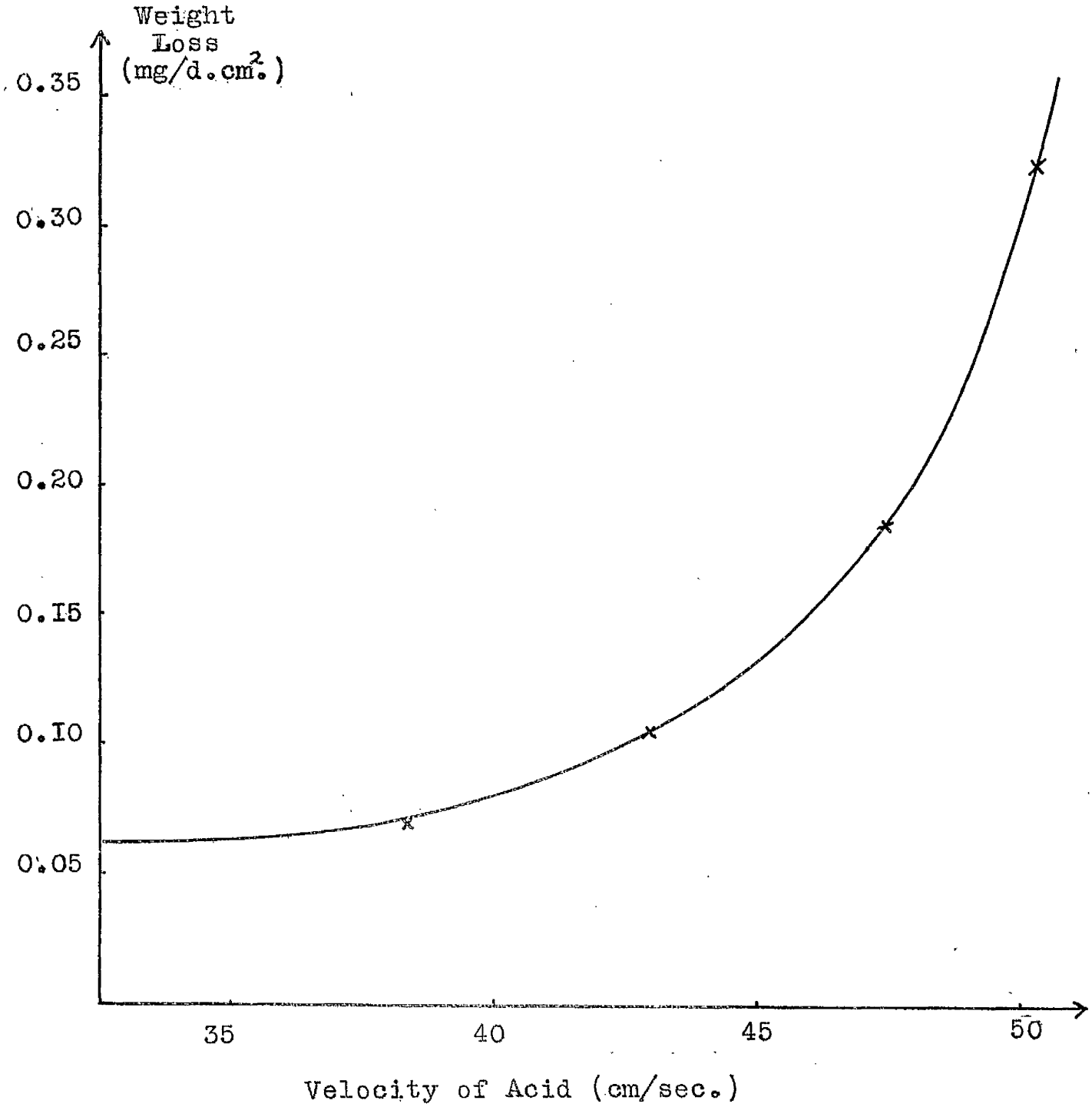

GRAPH 42 Theoretical Weight Loss of Untreated Copper in Flowing Aerated Acid.

CHAPTER 4

Results and Discussion.

4.I. Benzotriazole as an Inhibitor in a Static Medium.

The results of the weight loss (Graph 1) and rest potential (Graph 2) experiments do not differ significantly from the findings of Hackerman and Makrides, and Jones, both working with thiourea as an inhibitor in the corrosion of mild steel in acid aqueous media. The corrosion rate is reduced by the action of benzotriazole in concentrations less than 0.5% with maximum inhibitor efficiency occuring at a concentration of 0.125% (the critical concentration). Any further addition of benzotriazole causes the corrosion rate to increase and above a concentration of 0.5% benzotriazole acts as a stimulator to corrosion. The value of the critical concentration is approximately equivalent to the optimum benzotriazole concentration for pretreating copper and the concentration range for which benzotriazole acts as an inhibitor agrees with that recommended industrially. The change in rest potential caused by the addition of benzotriazole follows the same general trend as the corrosion rate. The rest potential becomes more noble (less active) below a concentration of 0.5% benzotriazole and more active above it. Below the critical concentration it was noticed that the potential changed to its new value more quickly than above it. The above workers noticed this phenomenon and suggested that two entirely different processes were involved. Hackerman and Makrides suggested that above the critical concentration the

behaviour might be explained by the depolarization of the anodic reaction.

When copper is placed in inhibited acid, adsorption of benzotriazole onto the copper surface takes place (Graph 3). Adsorption increases with increasing concentration of benzotriazole until a concentration of 0.125% is reached, and then on further increase in concentration it decreases to any almost constant value. It is known that two different complexes of copper and benzotriazole are possible; cuprous and cupric benzotriazoles. This adsorption and desorption phenomenon could be due to the formation of the copper-benzotriazole complexes at different benzotriazole concentrations and could also be responsible for the two different processes mentioned above.

Initially copper is dissolving from the surface, but on addition of low concentrations of benzotriazole, the formation of cuprous benzotriazole on the copper surface stabilises the copper, reducing the copper dissolution. As the concentration increases, more adsorption of benzotriazole as cuprous benzotriazole occurs and the metal dissolution continues to be reduced. At the critical concentration the formation of cupric benzotriazole in the bulk solution becomes possible. As the concentration of benzotriazole increases, the reaction forming cupric benzotriazole becomes more and more predominant and the cuprous benzotriazole complex is desorbed on breakdown. Above the concentration of 0.5% although some residual adsorption of benzotriazole remains on the metal surface, the copper is dissolving

at a faster rate than if no inhibitor were present due to the preferential formation of cupric benzotriazole in the bulk solution.

Reeve (128), studying the overall reaction

$$Cu \longrightarrow Cu^{++} + 2e$$

stated that the observed kinetics of the dissolution of copper in H_2SO_4 indicate a reaction

$$Cu \longrightarrow Cu^{++} + 2e \qquad (1)$$

at the surface.

$$Cu^{++} \longrightarrow Cu^{++}$$

at surface in bulk solution (2)

Reaction (1) was found to be the rate of determining step and could also consist of the intermediate reactions.

$$2Cu \longrightarrow 2Cu^{+} + 2e \longrightarrow Cu + Cu^{++} + 2e.$$

This gives the same overall reaction

$$Cu \longrightarrow Cu^{++} + 2e.$$

So that reaction (1) could be hindered by the formation of the cuprous benzotriazole complex in the manner mentioned above.

Hoar has stated that where the addition of inhibitor causes the rest potential of the metal to move more noble, the anodic reaction may be considered to be affected more than the cathodic reaction. This was noticed in a series of "galvanostatic" experiments. In these experiments two copper electrodes were connected together via an avometer, a variable resistance and a 12V battery and the current kept constant by operating the variable resistance. The potential of each electrode was measured against a standard saturated calomel reference electrode. At low current densities

(approximately 7$\mu A/cm^2$), both the anodic and cathodic reactions were polarized, the anodic reaction more so than the cathodic one. At higher current densities (above 15$\mu A/cm^2$) the anodic reaction became even more polarized whereas the cathodic reaction remained relatively unaffected. This trend continued throughout the concentration range employed.

Graph 4 shows how the resistance of the copper in the acid varies with increasing benzotriazole concentration. The resistance follows the same trend as the fraction of area of surface coverage by the inhibitor. As the conductivity of the acid remains unchanged throughout the concentration range any changes in the resistance of the cell must occur in the electrical double layer of the copper and the acid has not been "de-activated" by the inhibitor in any way. The conductivity of the acid was determined by measuring the solution resistance in a conductivity cell by a conductivity bridge.

With pretreated copper specimens where the metal surface is totally covered by a polymeric complex of cuprous and cupric benzotriazoles, the rest potential is more noble, the weight loss is less, and the resistance of the electrical double layer is greater. From Graphs 5 & 6 it can be seen that at most potentials the current passed is less with a pretreated specimen than an untreated specimen and that the oxygen evolution has been supressed. Graphs 9 & 10 show the behaviour of pretreated and untreated specimens in oxygenated and de-oxygenated acid. In oxygenated solutions the evolution of oxygen occurs at a lower potential whereas in de-oxygenated

oxygen evolution is supressed.

With pretreated specimens on the evolution of oxygen a black layer is formed on the copper. This film comes away from the surface, revealing a bright copper surface. This black film consists of benzotriazole and copper oxide. It appears that on the evolution of oxygen this film is weakened and drifts off the copper. In de-oxygenated acid oxygen evolution on pretreated copper is completely supressed and the surface remains quite bright. On untreated copper oxygen is just beginning to form and the surface has dulled.

This seems to suggest that oxygen in some way causes the breakdown or removal of the inhibitor complex film on the surface.

From Graph II & I2 it will be seen that the cathodic section of the curve in the presence of the varying concentration of benzotriazole behaves very similarly to the pretreated specimen (Graph 6). The anodic portion of the curve indicates that less current is passed and the oxygen evolution reaction is supressed to a greater extent than the pretreated specimen. Therefore the action of benzotriazole is not totally blocking as less than 90% surface coverage by benzotriazole produces the same cathodic effect and supresses the oxygen by a greater extent than a pretreated specimen. Benzotriazole is adsorbed onto the copper surface by losing its labile hydrogen and thus obtains a slight negative charge around the nitrogen atom. This nitrogen atom will act as an anchoring group on adsorption. When a copper surface is anodic, this could cause a stronger bonding of the benzotriazole to the copper by

increasing the positive charge on the metal. A larger potential or inhibitor concentration is then required to form the cupric benzotriazole complex in solution. With pretreated copper, the film cannot be renewed on breakdown, so that anodic inhibition, although better than untreated copper, is not as effective as inhibited acid at anodic potentials.

The determination of the rate of weight loss of a specimen from polarization data (Graph I3) using

$$K = \frac{C}{(\partial E/\partial i)_{E_{corr.}}}$$

agrees very closely with experimental findings (Graph I) and therefore seems applicable to this metal/acid system.

These results seem to indicate the inhibition of the corrosion of copper in sulphuric acid by benzotriazole occurs by anodic control supplemented by a blocking action by anodic adsorption and that breakdown in inhibitor efficiency is caused by the action of oxygen.

4.2. Benzotriazole as an Inhibitor in Flowing Media.

Graph I4 shows the relationship of the fraction of surface area of coverage by adsorption of benzotriazole to the concentration of benzotriazole in the acid solution. The relationship follows the same trend as in static media with maximum area of coverage being afforded at a benzotriazole concentration of 0.1%. As the mass transfer boundary layer is far smaller than the hydrodynamic boundary layer, the area of coverage is independent of the flow rate and dependant on the concentration of benzotriazole in the acid. This is as expected.

However, the resistance being independant of the flow rate, is a complete reversal of that in static media(Graphs 4 & 4I). When the area of coverage of the metal surface is a maximum, the resistance of the electrical double layer of the metal is at a minimum. So any inhibitor efficiency of benzotriazole in flowing acidic media cannot be attributed to the imposition of a resistance at the metal/solution interface, as was possible in the case of static medium. Also pretreated copper has a lower resistance than that obtained in 0.1% inhibited acid.

Graph I5 shows the dependence of the rest potential of pretreated copper on the flow rate of the acid. As can be seen, the rest potential in de-aerated acid is almost insensitive to flow, whereas with both the aerated and oxygenated acid there is an increase in rest potential. The rate of increase in potential decreases as the flow rate increases This phenomenon can be explained as in Fig.27.. In static medium the copper in equilibrium with the acid may be represented by CBA and the potential and corrosion current are given by E_m and i_c. When the metal is pretreated with benzotriazole, the anodic reaction is affected (AB moves to AD) and the corrosion potential increases to E'_m and the corrosion current decreases to i'_c. The effect of flow on the system is to enhance the cathodic oxygen reduction reaction (ie. E_c to E'_c). So if the anodic dissolution of pretreated copper remains unaffected due to flow, the effect will be to increase the potential and the current accordingly.

Graphs I6-I8 show the variation of rest potential with increasing benzotriazole concentration in the acid at

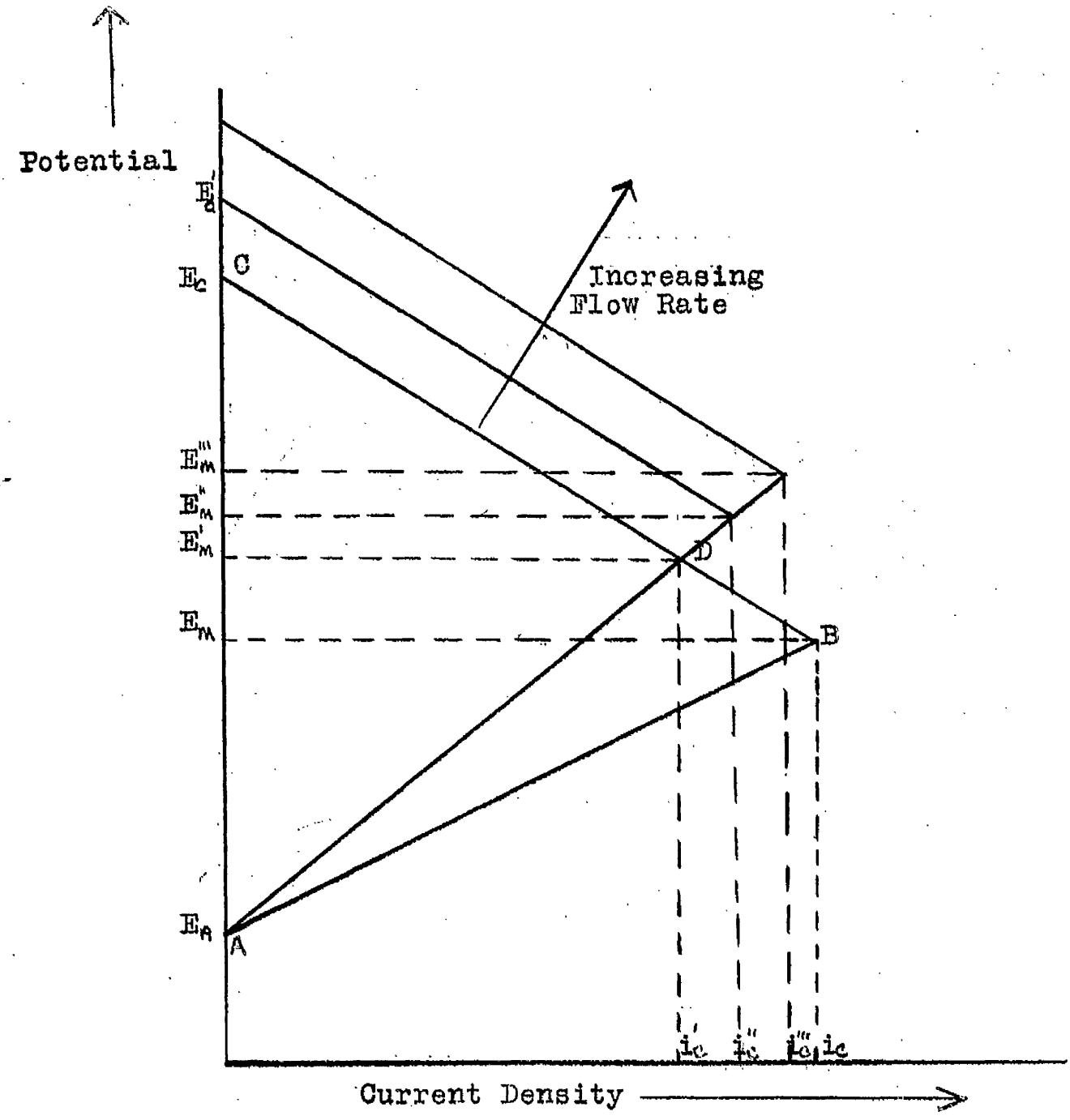

Fig.27 Explanation of the Potential Behaviour of Pretreated Copper in Flowing Media.

increasing flow rates; the acid being de-aerated (Graph I6), aerated (Graph I7), and de-aerated (Graph I8). As in static media, the general trend is to move the rest potential to a more noble potential on the addition of benzotriazole with a maximum occuring at a concentration of 0.1%. Further increase in concentration above this value causes the potential to move more active.

In de-aerated acid where the potential variation is independent of flow rate, the potential shift anodically (occuring between 0% and 0.1% inhibitor) and the concentration range where the potential is more noble than at 0% inhibitor, is smallest. In aerated acid, except at the highest flow rate, the rest potential is always more noble than the uninhibited acid and the potential shift has increased. With oxygenated acid the potential shift is larger than in aerated acid, but the concentration range over which the rest potential is more noble creases. This could be explained in a similar manner to the pretreated copper. Initially at low concentrations, adsorption of the benzotriazole onto the copper takes place, altering the anodic reaction and moving the rest potential more noble. Maximum rest potential corresponds to maximum surface coverage. Desorption causes the rest potential to move more active. As the flow rate increases, the effect on the anodic reaction decreases, although adsorption still takes place. Otherwise, as the flow rate increases the cathodic reduction of oxygen, the potential rise at higher flow rates would increase, in fact the reverse is true. (Fig. 26).

(a) Behaviour with Pretreated Copper.

As can be seen from Graph I9, the behaviour of pretreated copper is similar to that in static medium upto a Reynolds' Number of 7400. Above this Reynolds' Number, the copper/benzotriazole film has broken down in some way and metal dissolution is taking place at far lower potentials. The breakdown appears to be gradual as an increase in flow rate causes the breakdown to occur more sharply and at more cathodic potentials. The copper specimen has not reverted back to an untreated specimen as metal dissolution is occuring more vigourously after the breakdown on a pretreated specimen than on an untreated specimen. In fact at the highest flow rates metal dissolution and oxygen evolution occur simultaneously.

The surface of a pretreated specimen is a complex mixture of cuprous and cupric benzotriazoles and it has been shown (I29) that cuprous benzotriazole can be oxidised to cupric ions and benzotriazole purely by the action of the dissolved oxygen in solution. As the flow rate increases, the availability of dissolved oxygen at the metal surface increases correspondingly. This dissolved oxygen diffuses through the surface layer to the benzotriazole/copper film and oxidises the cuprous benzotriazole to cupric ions and benzotriazole. As the copper surface is still cathodic the slightly negatively charged benzotriazole will not be attracted back onto the surface, but attracted by the cupric ions in solution. The surface will now be partially protected by the remaining

cupric benzotriazole still chemisorbed on the copper surface, but corrosion can still occur from the anodic (unguarded) areas of the specimen. The corrosion over a pretreated copper specimen which had broken down, was not uniform but severely pitted and scarred; the type of corrosion caused by the type of galvanic action mentioned above.

If oxygen were the cause of breakdown of the pretreated complex film, as mentioned above, the film should remain intact in de-oxygenated acid. Graph (27) indicates that the film has not broken down in the manner it did when oxygen was available at the interface. The cathodic action appears to be entirely independant of flow rate. Comparison with graph (28) shows that the breakdown of the benzotriazole complex occurs at a higher potential than the untreated specimen and above the potential at which oxygen is evolved. As in static mediumthe oxygen is evolved at a lower rate than with untreated copper. This could be due to the fact on breakdown from cuprous benzotriazole to cupric ions and benzotriazole, there still exists a slight attraction between the benzotriazole and the specimen as breakdown has occurred when the specimen was anodic.

Graph (29) shows the behaviour of the untreated copper in oxygen-saturated acid. Although the cathodic portion of the curve is not flow dependent and the oxygen evolution occurs at a lower potential. The anodic reaction

is initially polarized, but at the higher flow rates it becomes slowly depolarized again. With pretreated copper in oxygenated acid(Graph 30) oxygen evolution and metal dissolution occur at a lower potential than in aerated acid and also breakdown occurs below a Reynold's Number of 5000 whereas in aerated acid, it occurs above 7400. The availability of oxygen in this case has increased and it seems highly likely that oxygen is the cause for the film breakdown and the benzotriazole loses its inhibitor effectiveness. Although if breakdown occurs when the specimen is anodic, the action is suppressed slightly. This is due to a slight attraction between the positively charged metal and the negatively charged benzotriazole.

If the film breaks down, perhaps it would be possible to repair the film. A series of experiments were undertaken with pretreated copper in inhibited oxygenated acid(Graphs 36-40) to see if this were possible. If breakdown occurs at a cathodic potential and there is no attraction between the copper and the free benzotriazole, the concentration gradient would drive the benzotriazole towards the copper as opposed to away from it. Then perhaps the film could be renewed or the inhibitor efficiency increased by adsorption or by a masking of the metal.

At low concentrations (Graph 36) the cathodic portion of the curve seems extremely flow sensitive. This would really be expected as it is within this region that the breakdown of the film takes place in oxygenated acid (Graph 30)and, if the film is to be renewed this is the region

where it would occur. Oxygen evolution is suppressed until positive (w.r.t. calomel) potentials are attained and even then gas evolution is less vigorous than with untreated copper in aerated acid.

As the concentration of benzotriazole is increased (Graphs 37-40) the cathodic portion of the curve becomes less flow sensitive whereas the anodic portion varies with the concentration of benzotriazole in the acid. The metal dissolution occurs at a lower potential initially. At a benzotriazole concentration of 0.I% the metal dissolution, although occuring at lower potentials than in static media, occurs at the highest potential in this concentration range. As the concentration of benzotriazole is increased, so the metal dissolution curve is depressed cathodically. The oxygen evolution is suppressed to a maximum at 0.I%, but all are suppressed to a greater extent than pretreated copper in oxygenated acid.

With the I.0% benzotriazole concentration the film seems to be undergoing breakdown and renewal successively in the cathodic region. The film breaks down momentarily, but with the high benzotriazole concentration in the solution, diffusion of the benzotriazole to the point of breakdown of the film occurs and either film renewal or a masking of the exposed area takes place. The metal dissolution occurs at potentials comparable to the lower inhibitor concentrations, but the oxygen evolution is suppressed as much as the 0.I% benzotriazole concentration.

From these experiments it appears that to employ pretreated copper in flowing aqueous acid media containing dissolved oxygen is extremely hazardous. If the film breaks down, severe corrosion of the copper will occur with the eventual failure of the component. With benzotriazole present in the medium, it seems that it is possible to have the film renewed or the system re-aquires its inhibitive action by diffusional control. This seems an expensive method to employ; using pretreated metal in a medium also containing the inhibitor.

It now seems logical to determine how the untreated copper reacts in inhibited acid.

(b) With Benzotriazole present in the Acid.

Graphs 21-26 show the polarisation behaviour of the untreated copper in aerated acid containing increasing concentrations of benzotriazole , increasing flow rates. These indicate that at the higher flow rates, the lower concentrations of benzotriazole offer better protection whereas higher concentrations are needed at the lower velocities. This is due to the relative amounts and solubilities of the cuprous and cupric benzotriazoles which could be formed on adsorption.

At low velocities the benzotriazole forms cupric benzotriazole, but this is relatively unstable. As flow rate increases, the cuprous complex becomes more stable and affords protection. At higher concentrations, the cupric benzotriazole is formed, but this stabilises the copper in

solution. Protection will be reduced even though some residual adsorption of benzotriazole remains.

At higher velocities the pH of the boundary layer increases and permits the stability of both benzotriazole complexes. An equilibrium is set up between the attraction of the benzotriazole by the anodic copper surface and the stabilising of the copper in solution as cupric benzotriazole. At low inhibitor concentrations the cuprous complex is formed but as the inhibitor concentration increases, the cupric form is also formed and corrosion takes place. At higher inhibitor concentrations both the benzotriazole concentration gradient and the attraction of the anodic metal surface draw the inhibitor towards the metal. Protection is then afforded by a masking of the metal surface.

It was hoped to confirm these results by applying the relation

$$K = C \Big/ \left(\frac{\partial E}{\partial i}\right)_{E_{corr.}}$$

to the system. Unfortunately, in many cases there were not enough points near to zero current to obtain $\left(\partial E/\partial i\right)_{E_{corr}}$ with any certainty. $\left(\partial E/\partial i\right)_{E_{corr}}$ could be obtained over a range of IOOmV, but this would invalidate the above equation. Using untreated copper in uninhibited acid, valid use of the above equation was possible, but not in this case.

With untreated copper in inhibited de-oxygenated acid(Graphs 3I-35) except at very low concentrations, the cathodic reaction remains unaffected by flow changes whereas

the anodic reaction is polarised and the oxygen evolution is suppressed. At intermediate and high concentrations of inhibitor, the anodic reaction is polarised, as above, but a region of passivation occurs before the oxygen evolution takes place. In all cases oxygen evolution occurs less vigorously than in uninhibited acid. This is probably due to the benzotriazole hindering the diffusion of oxygen away from the metal surface.

The polarisation data obtained for untreated and pretreated copper in static media agrees with the findings of Cotton who worked in 3% sodium chloride solution. He, however, explained the results in terms of the inhibition of the oxygen reduction reaction.

The phenomenon that, when pretreated copper breaks down in flowing media, the copper surface has been activated in way is borne out in practice. When two specimens (one treated, the other pretreated) are placed together in a corrosive media, the pretreated one is protected while the other corrodes. However, on the breakdown of the protective benzotriazole film, it is noticed that after a time the pretreated and untreated specimens have both corroded to the same extent. Therefore after breakdown the pretreated specimen must be corroding quicker than the untreated one.

It is also known(I3I) that, in potentiostatic experiments although the instrument is maintaining the specimen either anodic or cathodic, it is possible to obtain "kicks" of current in the reverse direction. The corrosion

mentioned previously (i.e. corrosion due to the pretreated film breaking down to form guarded and unguarded areas and scarring corrosion resulting) could therefore take place even though the specimen was being held anodic or cathodic by the instrument.

(c) Effect of Flow on Corrosion.

Graph 1b shows the variation of the rest potential of an untreated copper specimen in uninhibited acid with increasing flow rate. It will be seen that with de-oxygenated acid there is no significant dependance of rest potential on flow rate within the range shown(Re=1500 and Re=10,000). Any slight fluctuations in potential would most certainly be due to the last traces of oxygen(0.01ppm.) remaining in the solution.

However,with aerated and oxygenated acids the rest potential decreases with increasing velocity until a velocity corresponding to Re=6500. Above this flow rate the potentials of the two cases become equal and independent of flow rate.

This can only be explained by both the anodic and cathodic reactions being affected by the flow rate,the anodic reaction more so than the cathodic reaction. This is unlike pretreated copper where only the cathodic reaction was affected.

By injecting dye into the system,it was found that laminar flow existed below Re=5500 and turbulent flow existed above Re=6000. This means that in the turbulent zone the potentials of untreated specimensare the same in aerated and oxygenated solutions. In both cases the rate of increase in

the cathodic direction was constant within the laminar region and zero within the turbulent region.

Graph 20 shows the effect of flow on the polarisation behaviour of an untreated copper specimen in aerated acid. The effect of flow is initially to polarise the anodic reaction cathodically and to evolve oxygen at a lower potential than at Re=0. Further increase in flow rate causes the anodic reaction to be depolarised and to suppress the evolution of oxygen. The rate of evolution of oxygen also increases with increasing flow rate.

By using the relation $K = C/\left(\frac{\partial E}{\partial i}\right)_{Ecorr.}$ the weight loss of untreated copper at various flow rates has been worked out. The relation is shown in Graph 42 as corrosion rate against velocity. Unfortunately, these results only apply to the turbulent region. This is because during preliminary experiments in flowing media, it was decided that the breakdown of the copper/benzotriazole complex occurred between Re 7530 and Re 7400 and the working range was decided at Re 6000 and Re 10,000.

Within the turbulent region, these weight loss values fit an equation of the form-

$$K = cV^n$$

where K = weight loss.

V = velocity of the acid.

c and n are both constants.

This is a similar expression to the one derived by Donat for the dissolution of steel tubes in concentrated sulphuric acid.

Extrapolation of this curve back to the

commencement of turbulent flow gives a weight loss value of 0.053 mg/d.cms^2. As the experimental value for the weight loss in static media was 0.0566 mg/d.cms^2., there appears to be a velocity at which the corrosion rate is the same as in static media. Several workers have reported a minimum corrosion rate when increasing the flow rate. In this case it is not known whether the corrosion rate decreases or remains constant within the laminar region.

Traces of oxygen in solutions have been known to have an inhibiting effect by adsorbing onto the anodic sites of the metal. Copper is known to be covered with a layer of oxide and in these experiments this layer of oxide could have been removed in the very thorough cleaning process. On immersion in the acid the corrosion rate would first fall due to the formation of this protective layer of oxide. As the concentration of oxygen at the copper interface increases, so too the corrosion rate increases.

Graphs 7 and 8 show the effect of a reverse trace (anodic to cathodic) on the polarisation sweep. With untreated copper (Graph 7) the reverse sweep passes more current than its forward counterpart. This would be expected as initially the high anodic current produces a larger rate of dissolution. Consequently the area of the specimen will be effectively larger in the reverse trace and therefore the current passed will be more. As the area of the specimen has increased, the instrument will pass more current to maintain the same current density at the same potential. But to obtain

the current density for the drawing of the graph the original area of the specimen was used and a higher current density was therefore obtained. In the case of the pretreated specimen the reverse trace had to be commenced before the evolution of oxygen, as this would cause the peeling off of the benzotriazole film. However, the current passed is again more than its forward counterpart, probably for the same reason.

CHAPTER 5.

Conclusions and Suggestions for Future Work.

5.I. Conclusions.

The following conclusions may be drawn from this investigation -

(a) Pretreated Copper.

(i) In static conditions the corrosion of copper is greatly reduced and benzotriazole acts as an effective inhibitor.

(ii) Inhibitor efficiency results from the ability of the copper/benzotriazole complex to inhibit the anodic reaction.

(iii) In flowing conditions the copper/benzotriazole film behaves as in static medium upto a velocity corresponding Re=7400.

(iv) Breakdown of this complex inhibiting film is caused by dissolved oxygen oxidising the cuprous benzotriazole in the complex film to cupric ions and benzotriazole. After the breakdown of this inhibiting film, very severe corrosion occurs due to the formation of large cathodic(guarded)areas and small anodic(unguarded)areas.

(v) It is possible to renew the copper/benzotriazole film by including benzotriazole in the flowing media.

(vi) Oxygen evolution takes place less vigorously when benzotriazole is present in solution. This is due to a slight adsorbing of the negatively charged benzotriazole onto the anodic copper surface and ahindering of the oxygen diffusing away from the metal surface.

(b) With benzotriazole present in the medium.

(i) In static conditions, benzotriazole acts as an inhibitor within a certain concentration range (0-0.5% benzotriazole).

(ii) Inhibitor efficiency results from the inhibiting of the metal dissolution reaction by adsorption onto the metal and/or anodic sites on the metal .

(iii) Inhibitor efficiency in flowing media depends on the relative amounts and solubilities of cupric and cuprous benzotriazoles formed on the metal surface.

(iv) The inhibitor efficiency of benzotriazole in flowing media is due to the inhibiting of the anodic reaction and loss of inhibitor efficiency is due to a depolarisation of both the anodic and cathodic reactions, the cathodic more so than the anodic.

Hackerman, in his work on the adsorption of organic inhibitors, intended to correlate inhibitor efficiency (as determined by weight loss experiments) to the fraction of area of surface coverage by the adsorped inhibitor (as determined by capacitance experiments). In this investigation it has been shown that, within the range in which the inhibitor is effective, inhibitor efficiency can be related to the fraction of area of coverage. Anomalies occur outside this concentration range, where adsorption still persists but corrosion has been stimulated.

However in flowing media the fraction of area of coverage was found to be independent of flow rate, but dependant on the benzotriazole concentration in the acid.

The corrosion of copper in inhibited acid was found to be dependent on the relative solubilities and concentrations of the copper/benzotriazole complexes which in turn, are dependent on the oxygen concentration at the surface. This increases with increasing flow rate. So the corrosion is flow dependant whereas the surface coverage is not and will therefore not be an indication as to the efficiency.

So although in this case the fraction of area of coverage could be correlated to the corrosion rate in static media, it seems unlikely that this would be a universal inhibitor evaluation test. In flowing media, too many variables are present to permit the fraction of the area of surface coverage to be the sole indication as to the inhibitor effectiveness.

These experimental results also emphasise the findings of other workers that static results cannot be relief upon when used in flowing systems.

5.2. Suggestions for Future Work.

In this investigation the experiments were carried out below 30 C.. However it would be interesting to study the effect of temperature on the inhibitor efficiency of benzotriazole. There is a very great improvement in the coating characteristics of benzotriazole above 50 C.. This could be accompanied by an increase in inhibitor effectiveness as adsorption would be chemical, as opposed to physical. This would make the destruction of the inhibitor film by oxygen more difficult and repair of the film more easy. If the coating characteristics were greatly improved, pretreatment of the copper would be unnecessary at the higher temperatures.

As the breakdown of the copper/benzotriazole film is caused by the oxidation of cuprous benzotriazole to cupric ions and benzotriazole, inhibitor effectiveness should be maintained if the complex film consisted entirely of cupric benzotriazole. A method by which this could be effected would, therefore, be useful. The Geigy Company are producing a new inhibitor which consists of two benzotriazole molecules joined via the nitogen atoms. Like benzotriazole, this inhibitor will enter into combination with copper and its alloys. Due to this molecule having two nitrogen atoms to act as anchoring atoms, a more closely packed inhibiting film would be formed on the metal surface and may be less sensitive to the action of oxygen than benzotriazole itself. The study of this inhibitor and related molecules would prove interesting.

The exact nature of the adsorption bond is not known. The speed with which the potential changed seems to suggest a physical, rather than a chemical, bond. Further adsorption, and desorption, experiments may throw more light onto the bonding mechanisms undergone between the metal and inhibitor at various stages of the corrosion process.

It would be a great help to construct a standard corrosion cell, which it would be possible to study potential, weight loss, capacitance, and polarisation behaviour both in static and flowing conditions. At present many workers are investigating corrosion processes in flowing media, but many different flow models are being

employed. As the flow characteristics of each model will be vastly different, their results will not be strictly comparable. Such a cell, or model, would help to standardise methods of evaluating inhibitor effectiveness and make the different workers results comparable.

APPENDIX I

The instruments used in the experiments were:-

(a) Pye Dynacap pH meter (cat. no. II072).

Ranges: 0 - I000 mV.

400 - I400 mV.

7 sub-ranges of 200 mV.

Linearity: 0.I% of the full scale on main ranges.

0.3% of the full scale on sub-ranges.

Effect of Supply changes: a mains voltage variation of ± I5% gives a resultant shift of less than ± 0.5 mV. on all ranges.

Sensitivity: in all cases I mA output for a full scale deflection is given:

I μA/mV on main ranges.

5 μA/mV on sub-ranges.

(b) Wenking Potentiostat (mod. 6I/TR)

Ranges: ± 2000 mV adjustable against any external standard electrode.

Output voltage: 20 V.

Output current: I000 mA.

Sensitivity:

(i) Voltage - (a) after 30 min. warm up - 2 mV/hr.drift.

(b) after 300 hrs. operation - 5 mV/hr.drift.

(ii) Current - I.5% of full scale deflection.

Effect of supply changes: a mains voltage variation of ± I0% gives a resultant shift of less than ± 0.5 mV.

(c) Beckman Laboratory Oxygen analyser (model 777)

Ranges: 0 - 2.5 p.p.m. of dissolved oxygen.

0 - IO p.p.m..

0 - 40 p.p.m..

Linearity: 0.5% full scale deflection.

Accuracy: I.0% full scale deflection.

The key to the instrument is the Beckman Oxygen Sensor, a polarographic electrode which quickly and accurately determines oxygen in gaseous samples or dissolved oxygen in liquid solutions. The Sensor is $2\frac{1}{2}$ ins. long and $\frac{1}{2}$ in. diam.. Signals from the sensor are amplified and read out Beckman Model 777 Laboratory Oxygen Analyser.

The Sensor (fig.AI)

The sensor is basically a polarographic oxygen electrode and contains a silver anode and a gold cathode, both of which are protected from the sample by a thin Teflon membrane. A cellulose - base KCl gel is held in place by the membrane and serves as an electrolytic agent.

In operation, the sensor is placed in the sample and a potential of 0.8 V. is applied between the gold cathode and silver anode. The oxygen in the sample diffuses through the membrane and is reduced at the cathode. This reduction of oxygen causes a current to flow which is proportional to the oxygen concentration in the sample. The reactions are:-

Cathode : $O_2 + H_2O + 4e \longrightarrow 4OH$

Anode : $4\,Ag + 4\,Cl \longrightarrow 4\,AgCl + 4e$

As the oxygen in the sample is slowly consumed, it must

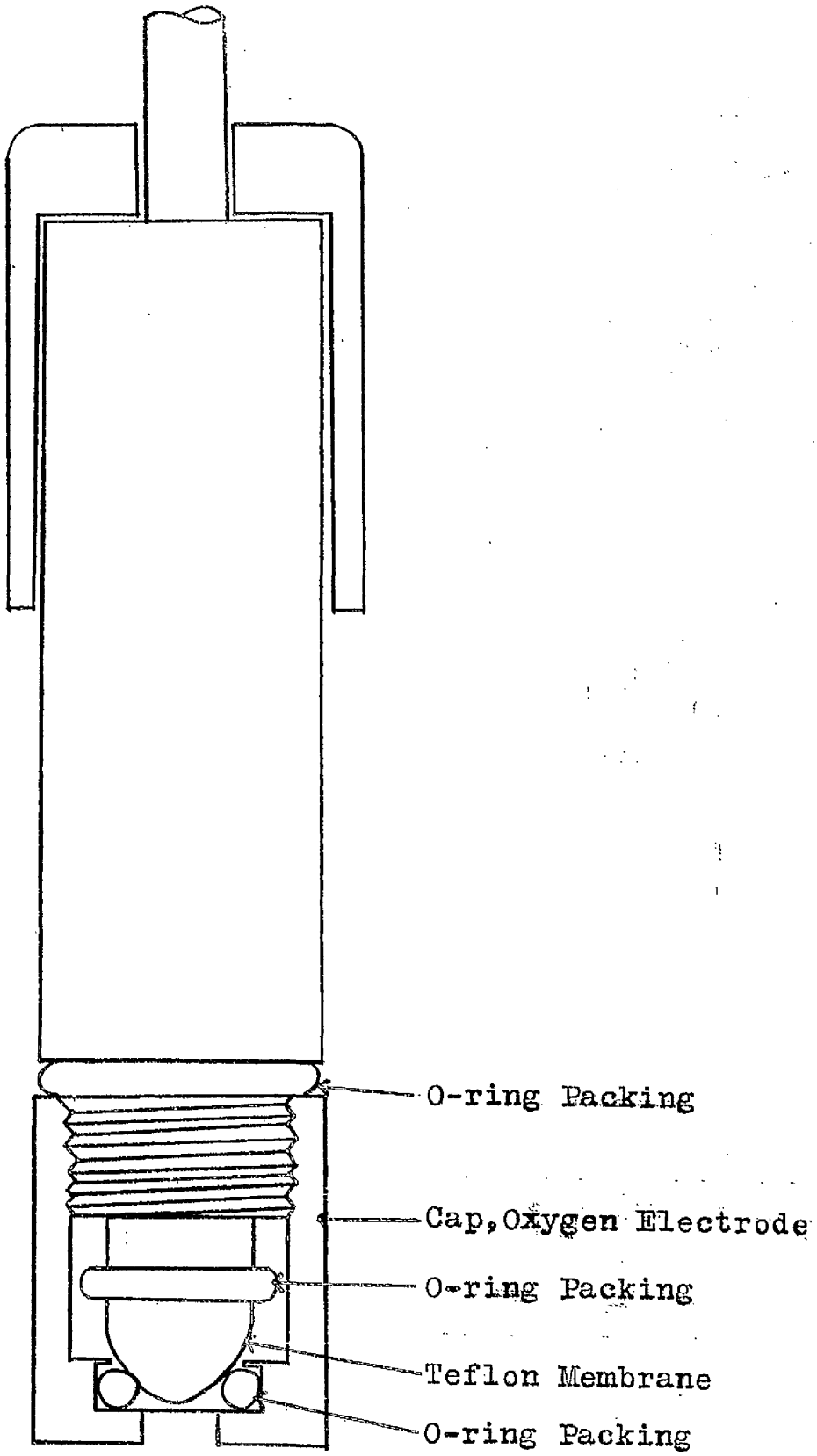

Fig.AI Diagram of the Sensor.

be replenished for the sensor to operate. The flow of the sample past the sensor must exceed I.8 ft./sec. for this purpose.

(d) Electrolytic Conductivity Bridge (Type 4896).

The instrument was used for capacitance measurements in static media.

Accuracy:-

Resistance - 0.5%

Capacitance - $\frac{1}{2}$ in I000 on the 0.0I μF decade.

2 in I000 on the 0.00I μF decade.

The balancing arm consists of a [illegible]-dial precision decade resistance in parallel with a mica variable capacitor consisting of decade dials plus an air capacitor. The Wagner earthing device, which enables a silent balance to be obtained consists of a fixed resistance and a variable resistance together with a variable air capacitor.

(e) Universal Bridge (Type D-897B)

This instrument was used for capacitance measurements in flowing media.

Ranges:- I$\mu\mu$F - I00 μF in three ranges.

Accuracy:-

I$\mu\mu$F - I00 $\mu\mu$F - ± 2% or ± I$\mu\mu$F (whichever is greater)

I00$\mu\mu$F - I0 μF - ± I% or ± 2$\mu\mu$F (whichever is greater)

I0μF - I00 μF - ± 0.5% falling to ± I% at I00 F.

The residual error of the instrument is less than 2.5$\mu\mu$F.

(f) Reference Electrode.

The electrode used in these experiments was a saturated calomel electrode, which nowadays is the most common one used.

This consists of a mercury electrode immersed in a saturated solution of mercurous chloride and electrical connection is made via a platinum wire and a solution of KCl. The value of the potential depends on the concentration of KCl.

	Potential Value.
0.I.N.KCl.	0.3338 - 0.00007 (t - 25) Volts.
I.O.N.KCl.	0.2800 - 0.00024 (t - 25)
Sat. KCl.	0.2415 - 0.00076 (t - 25)

Although the saturated calomel electrode is the most temperature sensitive one, it is the easiest to maintain and hence was used throughout this work. Several were made up and stored in a saturated solution of KCl. Periodically they were checked against each other before being used in an experiment.

APPENDIX 2

(I) Flow Relationship used in the Experiments.

The three rotameters were first calibrated in mls./min.. (Charts I,2,and3).

Reynolds' Number, $Re = \frac{\rho.d.v.}{\mu}$

where velocity, $v = \frac{Q}{3.24 \times 60}$ cms/sec. - Q is the flow-rate in mls/min..

density, ρ = I.III grms/ml.. } from 'International

viscosity, μ = I.0909 centipoise } Critical Tables.'

equi.diam., $d = \sqrt[2]{\text{Cross-sectional Area.}}$ (70).

$= I.8 \text{ cm}^2$.

Therefore $Re = \frac{I.III \times I.8 \times Q}{3.24 \times 60 \times I.0909 \times I0^{-2}}$

Therefore $Re = 0.94 \times Q$.

So, Reynolds' Number = 0.94 x Flow Rate (in mls/min.)

(2) Calculation of Specimen Areas.

(a) Weight Loss Experiments:-

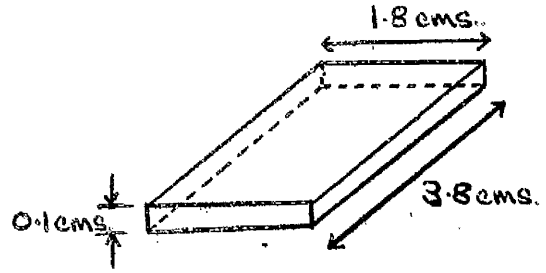

Area of specimen exposed,-

$= 2(3.8 \times I.8) + 2(0.I \times I.8) + 2(0.I \times 3.8)$

$= I4.78 \text{ cm}^2$/specimen.

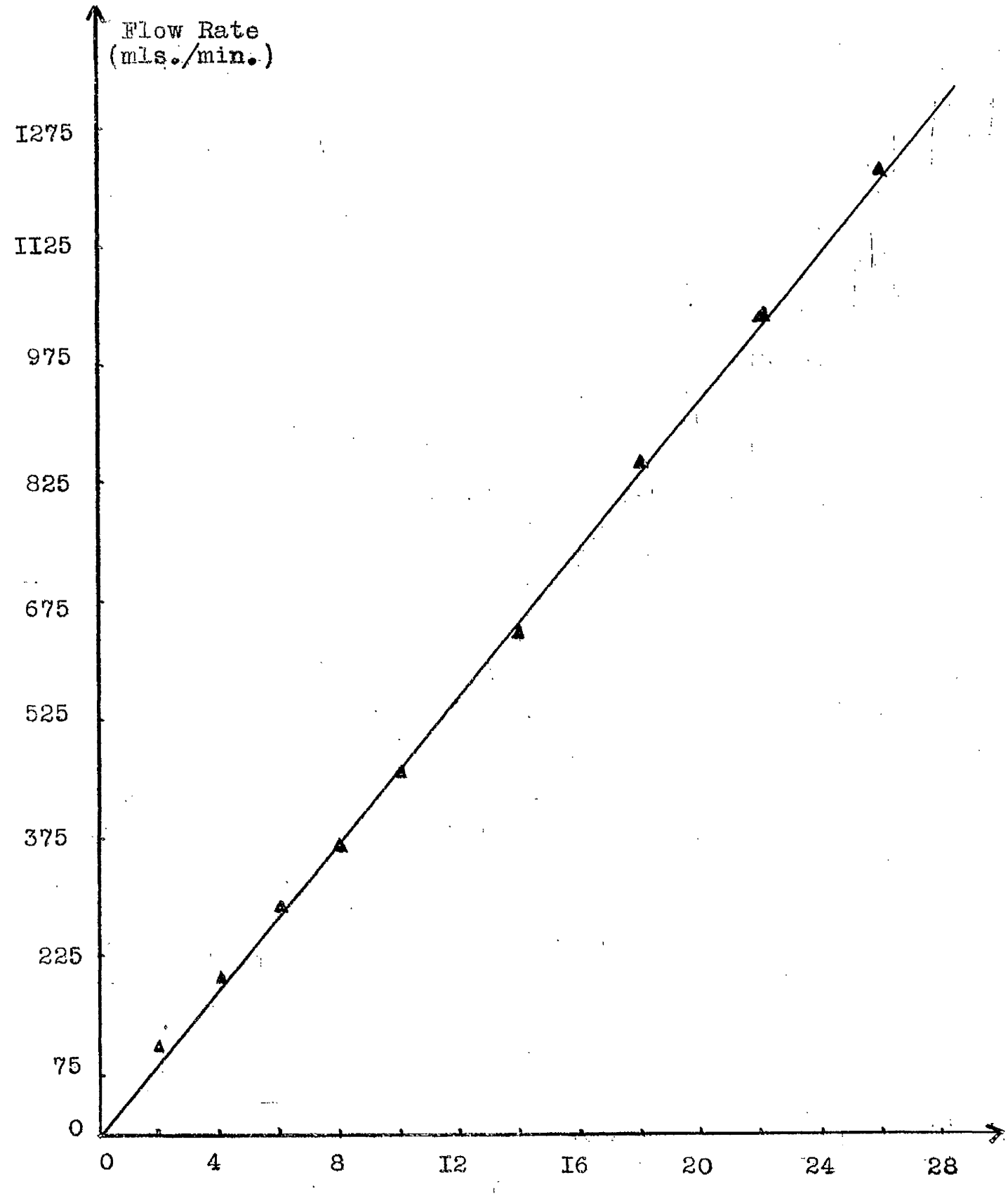

Callibration Chart I.

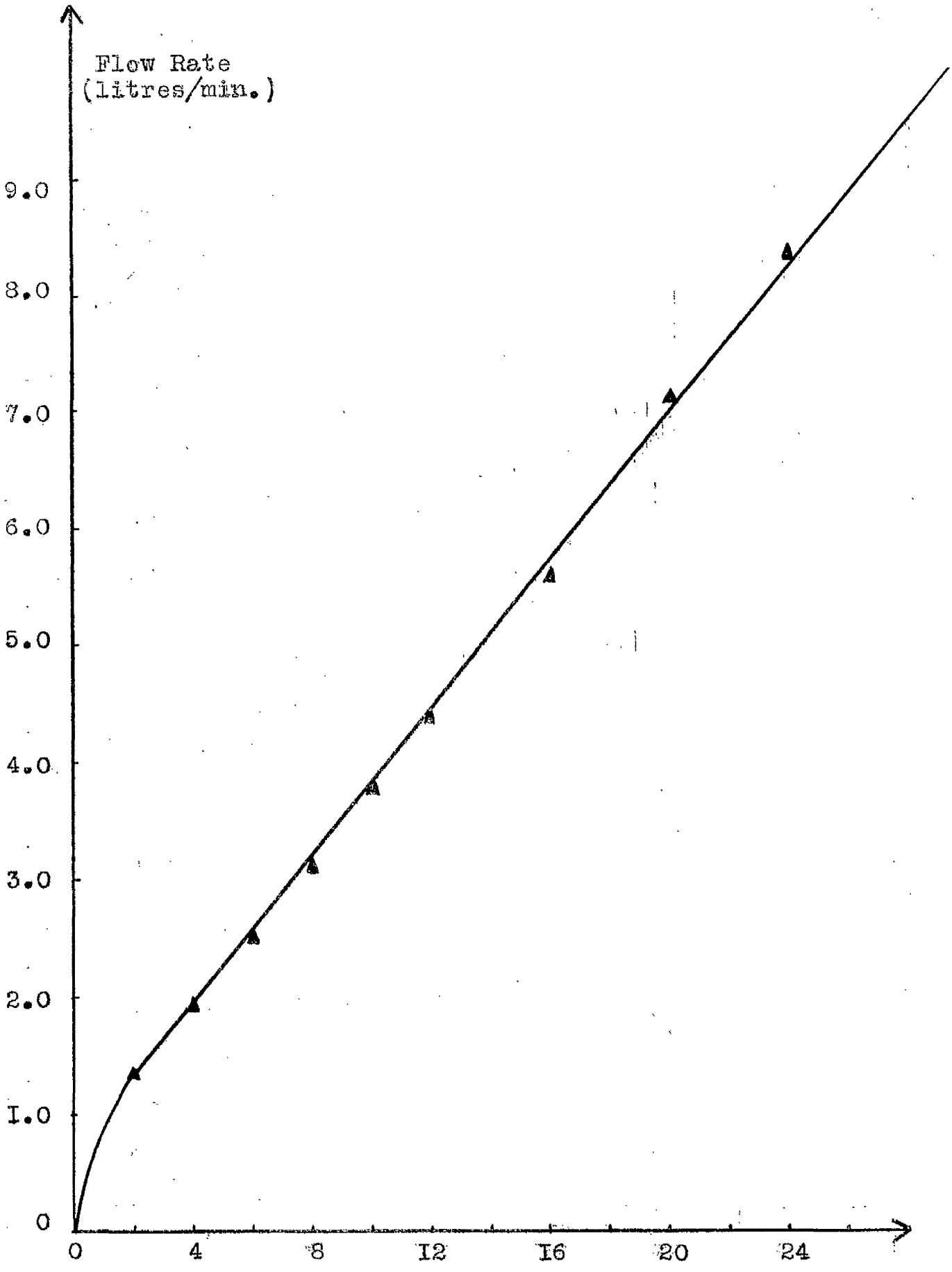

Graduation of the Rotameter

Callibration Chart 2.

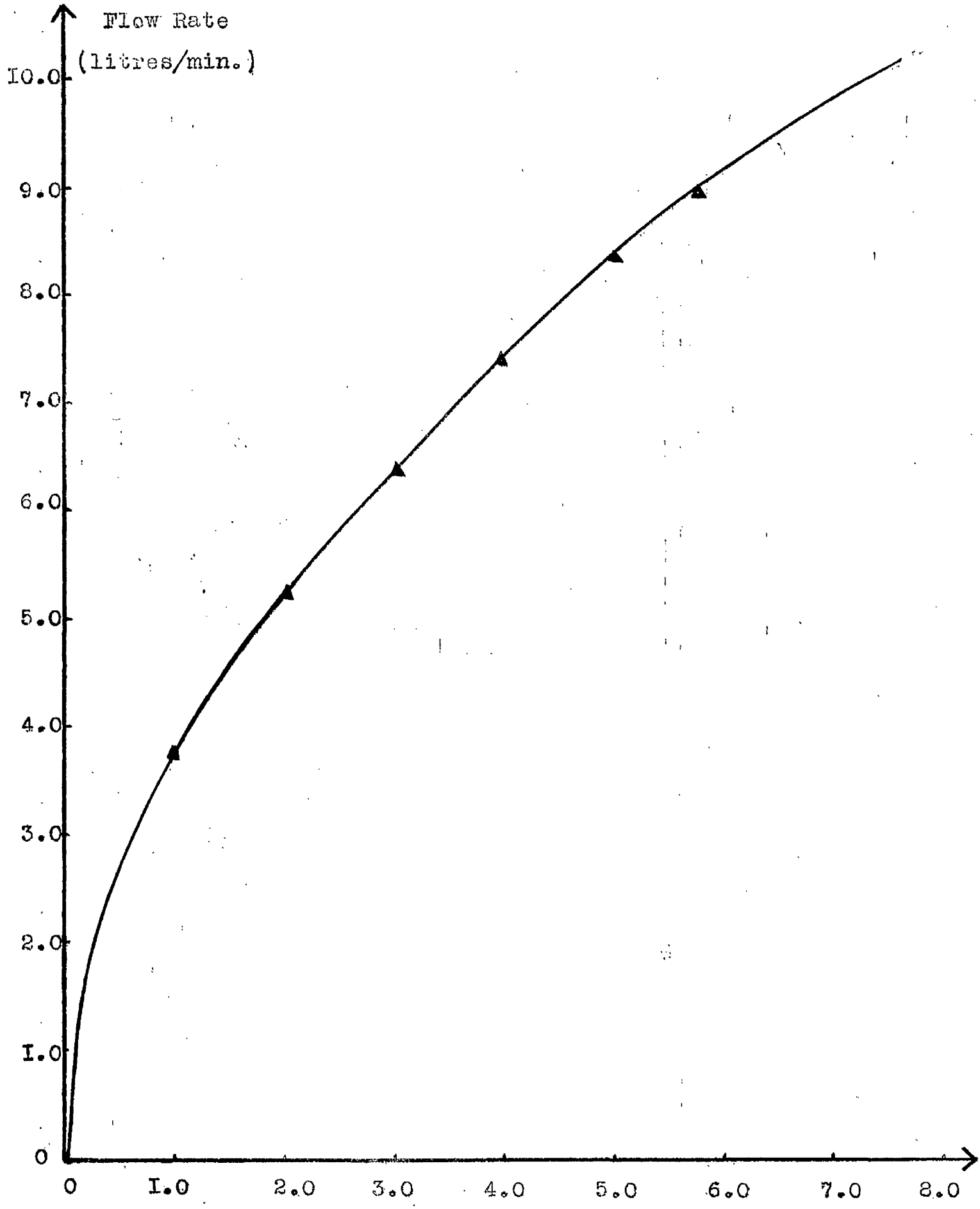

Graduation of the Rotameter

Callibration Chart 3.

Conversion factor for grms/specimen to mg/day.cm^2 .is given by:

$\frac{1000}{32 \times 14.78}$ as time for exposure was 32 days.

Therefore Conversion factor = 2.12.

(b) Potentiostatic work in Stationary Media:-

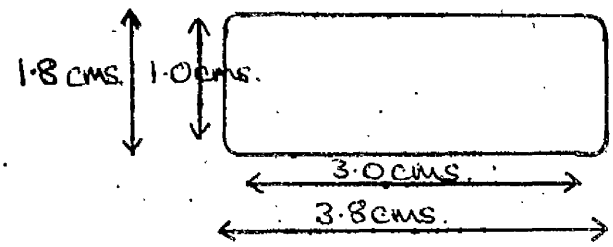

Assuming that the curved edges are of the form:-

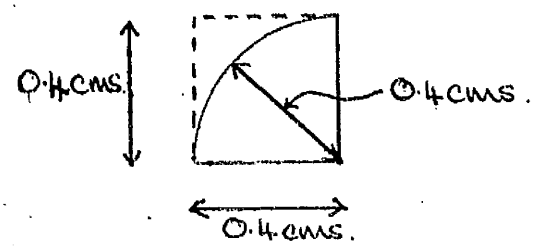

The area of the electrode exposed to the acid is given by:-

$$= (3.8 \times 1.8) - 4\left[(0.4 \times 0.4) - \tfrac{1}{4}(0.4 \times 0.4)\right]$$

$$= 6.84 - 0.14$$

$$= 6.70 \text{ cm}^2.$$

Area of the specimen = 6.70 cm^2.

(c) For Capacitance Measurements in Static Media:-

For this series of experiments, a hole (of area 0.083 cm) was punched in some masking tape which was then firmly placed completely over the copper surface.

Therefore the area of the specimen = 0.083 cm^2.

(d) In Flowing Media:-

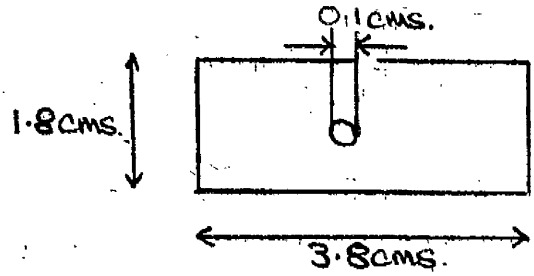

Area of the specimen = $(3.8 \times 1.8) - \frac{1}{4}(0.1 \times 0.1)$

$= 6.84 - 0.01$

$= 6.83 \text{ cms}^2$.

Therefore the area of the specimen = 6.83 cm^2.

(e) Calculation of Weight Losses from Polarisation Data.

The relationship $K = C/\left(\frac{\partial E}{\partial i}\right)_{E_{corr.}}$ was used to determine the theoretical values.

To determine the constant, C --

From experimental weight loss data, it is known that at a concentration of 0.05% benzotriazole the weight loss of copper was 0.0415 mg/d.cms.. From the polarisation curve for untreated copper in acid containing 0.05% benzotriazole,

$$\left(\frac{\partial E}{\partial i}\right)_{E_{corr}} = \frac{10}{0.0009} \quad \frac{mV}{mA/cms.}$$

$$C = \frac{0.0415 \times 10}{0.0009} \quad \frac{mg.mV}{d.mA}$$

$$C = 445 \ \frac{mg.mV}{d.mA}$$

$$\text{Corrosion Rate} = \frac{445}{\left(\partial E/\partial i\right)_{E_{corr.}}} \text{ mg/d.cms.}$$

APPENDIX 3

The Nitrogen Gas, used for de-oxygenating the acid media, had the following composition:-

Nitrogen	99.9% dry gas.
Oxygen	not less than 10 vpm., but less than 20 vpm.
Carbon Dioxide	up to 20 vpm..
Carbon Monoxide	nil.
Other Carbon Compounds	are less than 15 vpm..
Hydrogen	maximum of 20 vpm..
Neon	160 vpm..
Argon	less than 50 vpm..
Water Vapour	0.01 to 0.02 grams per cubic metre.

The composition of the Analar sulphuric acid (S.G. = 1.84) before dilution was:-

Acid	not less than 98.0%
Non-Volatile Matter	0.0025%
Chloride	0.0002%
Nitrate	0.00002%
Selenium	0.001%
Iron	0.0001%
Heavy Metals	0.0002%
Ammonia	0.0005%
Oxygen	0.00015%
Arsenic	0.00001%

APPENDIX 4

Design of the Packed Tower.

Assume that the acid initially is saturated with air at 25°C.

The maximum concentration for oxygen in white spot nitrogen = 20 ppm.

$= 2 \times 10^{-5}$

Henry's constant for oxygen at 25° C. = 4.01×10^{-4}

Therefore the oxygen concentration in the acid can be reduced, by scrubbing with white spot nitrogen to:-

$4.01 \times 10^{-4} \times 2 \times 10^{-5} = 8.02 \times 10^{-9}$.

Assume that the oxygen concentration is reduced to 1×10^{-8}.

Due to Norman (130)

$$Z = \frac{Gm\,(y_1 - y_2)}{K_L a.\, \rho.\, \Delta y_{LM}} \qquad \text{①}$$

where Z = height of the tower.

Gm = liquid flow rate.

y_1 and y_2 = initial and final oxygen concentrations.

ρ = density of liquid.

Δy_{LM} = logarithmic mean of y_1 and y_2.

$$= \frac{y_1 - y_2}{\ln y_1 / y_2}$$

Therefore $$Z = \frac{Gm.\ \ln y_1/y_2}{K_L a.\, \rho.} \qquad \text{②}$$

Due to Sherwood, Holloway, and Molstead (I30), the value of K a for ring packings within a 20% deviation either way is given by:-

$$K_L a = \frac{I20}{D}\left(\frac{L}{\mu}\right)^{0.75}\left(\frac{\mu}{\rho D}\right)^{0.5} \qquad \text{③}$$

where $K_L a$ = liquid-phase transfer coefficient of the tower

D = diffusivity = $4.33 \times I0^{-1}$ cms/hr.

μ = viscosity = I.0909 centipoise $I.09 \times 10^{-2}$ poise.

ρ = density = I.III grms/ml..

L = Gm = liquid flow rate $I8.7 \times I0^{3}$ grms/hr.

(Assuming only I liquid pass per hour.)

Substituting the above values in ③ -

$$K_L a = I20 \times 4.33 \times I0 \left(\frac{I8.7 \times I0}{I.09 \times I0}\right)^{0.75}\left(\frac{I.09 \times I0}{4.33 \times I0 \times I.III}\right)^{0.5}$$

$$= \frac{5I \times 4.4738 \times I0 \times 0.46.}{III.2 \times I0}.$$

Substituting this value in ② -

$$\ln {}^{y_1}/_{y_2} = \frac{2 \times 30.48 \times III.2 \times I0 \times I.III}{I8.7 \times I0}$$

Therefore $\ln {}^{y_1}/_{y_2} = 500.$

As can be seen the value of oxygen concentration estimated ($I \times I0^{-8}$) can easily be reached. The practical evidence, as given by the Beckman Oxygen Analyser, confirms that the oxygen concentration in the acid can be almost reduced to zero - as a maximum it was found to be 0.0I ppm..

References.

(I) J.Garside	Anticorrosion - Jan.I966.
(2) West	Electrochem. Principles.
(3) J.Sterling	Corr. I7(I945) March.
(4) U.R.Evans	Corr.& Oxid. of Metals. Arnold. London.I960.
(5) L.L.Shreir	Corr. Vols.I & 2. Newnes. London. I963.
(6) H.H.Uhlig	Corr.& Corr. Control. Wiley & Sons. I963.
(7) S.Glasstone	Principles of Electrochem. Van Nostrand N.Y. I942.
(8) J.Scully	Fundamentals of Corrosion.
(9) Putilova,Balezin,Barannik	Metallic Corr. Inhibitor.
(I0)Baldwin	Brit. Pat. 2327.
(II)Marangoni & Stephenelli	J.Chem. Soc. I872. 25. II6.
(I2)Evans U.R.	Metallic Corr.,Passivity, & Protection.
(I3)N.Hackerman	Corrosion. I8(I952) I43.
(I4)Sieverts & Lueg	Zanorg. Chem. I26. I93(I923)
(I5)D.Jones	Ph.D. Thesis M/C.I96I.
(I6)M.N.Desai & S.S.Rana	2nd. European Symposium I965.
(I7)Schunbert	Z.phys. Chem.A. I67.I9 (I923).
(I8)Hackerman & Schmidt	Corr. 5.7.23(I949).

(I9) Hackerman & Sudbury	J.Electrochem. soc. 97(I950) 4.
(20) H.H.Uhlig	Chem. & Eng. News - 24(I946) 3I54.
(2I) N.G.Chen	J.App. Chem. U.S.S.R. (I964)P.I942.
(22) Chappell, Roetheli,& McCarthy	Ind. Eng. Chem. 20(I928)582
(23) Mann, Lauer, & Hultin	Ind. Eng. Chem.28(I936) I59
(24) Mann, Lauer, & Hultin	Ind. Eng. Chem.28(I936) I066
(25) Mann	Trans. Electrochem. Soc. 69 (I936) II5.
(26) Machu	Trans. Electrochem. Soc. 72 (I937) 333.
(27) Rhodes & Kuhn	Ind. Eng. Chem. 2I(I929) I066.
(28) Bockris & Conway	J.Phys. & Coll. Chem. 53. 527 (I949).
(29) T.P.Hoar	2nd. International Congress on Surf. Act. I953 London.
(30) Mears	Ind. Eng. Chem. 37(I945) 736.
(3I) Mazzuchelli	Atti. Accad. Lincei. I9I4. 23II. 626.
(32) Cavallaro	Ferrara. I946.
(33) Makrides & Hackerman	J. Phys. Chem. 59(I955) 707.

(34) Mackrides & Hackerman — Ind. Eng. Chem. I954. 523.

(35) Bockris & Conway — J. Phys. Chem. I949. 53. 583.

(36) Fischer & Elze — J. Electrochem. Soc. 99(I952) 259.

(37) Kuznetsov & Iofa — Zh. fiz. khim. 2I. 20I. (I947)

(38) Hackerman & Makrides — Ind. Eng. Chem. I955. 47. I773.

(39) Hackerman & Cook — J. Electrochem. Soc. 97(I950)I.

(40) Hackerman & Finlay — Ibid. I05(I958) I9I.

(4I) Hackerman & Bordeaux — J. Phys. Chem. 6I(I957) I323.

(42) Hackerman — European Symposium Ferrera I960.

(43) Hoar — European Symposium Ferrera. I960.

(44) Hackerman & Hurd — Metallic Corr. Symp. London I96I.

(45) Frumkin — Moscow State Univ. I952.

(46) Antropov — Corr. Symp. London. I96I.

(47) Brasher — Ibid.

(48) De. — Nature London I957. I80. 803.

(49) Grahame D.C. Chem. Rev. 41(1947) 441.

(50) L.I.Antropov 2nd. European Symp. Ferrara. 1965.

(51) Pandey S.W. & Sanyal B. Labdev (India) 2(4) 1964. 213.

(52) Zwierzykowska Zeszyty. Nank. Politech. Gdansk Chem.7.3-14.(1964)

(53) H.C.Gatos J.Electrochem. Soc. 101 (1954) 433.

(54) K.Ariz & A.M.Din Corr. Sci. 5(7) 489.(1965)

(55) L.I.Antropov J. App. Chem. U.S.S.R. (1958) p.1839.

(56) Z.A.Foroulis 2nd. European Symp. Ferrara. 1965.

(57) S.A.Balezin J.App.Chem. U.S.S.R. (1961) p.2329.

(58) L.R.Snyder J.Phys. Chem. 67(1963) 2344.

(59) Y.Yao J.Phys. Chem. 68(1964) 101.

(60) A.H.Roebuck & T.R.Pritchett Mat. Prot. 5(1966) July.

(61) Duwell, Todd, & Butzke Corr. Sci. 4(1964) 435.

(62) Murakawa & Hackerman Corr. Sci. 4(1964) 389.

(63) Hackerman & Snavely J.Electrochem. Soc. 113 (1966) 7.677.

(64) Iofa Z.A. Electrochem. Acta. 9(1964) 1645.

(65) Iofa Z.A. — 2nd. European Symp. Ferrara I965.

(66) J.P.Barratt — Mat. Prot. 5(I966) 7.43.

(67) O.Reynolds — Phil. Trans. Royal Soc. Part 3 I883.

(68) J.O.Hinze — Turbulence. McGraw-Hill.

(69) L.Prandlt — Fluid Dynamics (Authorised Translation)

(70) Coulsen & Richardson — Chem. Eng. Vols.I & 2.

(7I) H.R.Copson — Ind. Eng. Chem. 44(I952) August.

(72) M.Stern — Corrosion I3(I957) II.

(73) Heyn.E. & Bauer — Mitt. Nat.Amt. Berlin 28. I00.I9I0.

(74) Friend — J.Chem. Soc. II9(I92I) 932.

(75) Speller & Kendell — Ind. Eng. Chem. I5(I923)I34

(76) Russel R.P.,Chappell E.L. & White. — Ind. Eng. Chem. I9(I927)65.

(77) B.E.Roethell & R.H.Brown — Ind. Eng. Chem. 23(I93I) September.

(78) R.E.Wilson — Ind. Eng. Chem. I5(I928)I28

(79) Wormwell F.J. — J.App.Chem. (London)3(I953) I64 & 276.

(80) Wormwell F.J.& Ison C. — Chem. & Ind. I950. July.

(8I) Hatch G.B. & Rice O. — Ind. Eng. Chem.37(I945)752.

(82) Romeo A.J. et al — Proc. Am. Soc. Civ. Eng. I958.

(83) Whitman — Ind. Eng. Chem. I5(I923) 672.

(84) Ross T.K.& Hitchen B.P.L. — Corr. Sci. I(I965) 6I.

(85) Ross T.K.& Jones — J.App. Chem. I2(I962) 3I6.

(86) Makrides A.C.& Stern M. — J.Electrochem. Soc. I07(I960) 877.

(87) J.Venzcel,L.Knutsson, & G.Wranglen. — Corr. Sci. 4(I964) I.

(88) G.Butler & E.G.Stroud — Brit.Corr.J. I(I965) Nov.

(89) Z.A.Foroulis & H.H.Uhlig — J.Electrochem. Soc. III(I964) Jan.

(90) S.A.Balezin — 2nd. European Symp. Ferrara I965.

(9I) G.Chufarov — Ural'skiia Metallurgia. I(I936) 42.

(92) Beck & Hessert — Z.Electrochem. II(I93I)37.

(93) N.Hackerman & R.Hurd — Congress Metallic Corr. I96I.

(94) V.L.Stromberg — Mat. Prot. 4(I965) 4.60.

(95) Prelog — J.Chem. Soc. I950.420.

(96) R.F.Bryan & J.D.Dunitz — Helv. Chem. Acta. I960.43.

(97) R.Ayers & N.Hackerman — J.Electrochem. Soc. II0(I963) 6.

(98) Hackerman, Hurd & Annand — Corr.

(99) Hackerman — II8th Electrochem. Soc. Meeting Texas.

(I00) Hackerman, Hurd & Annand — J.Electrochem. Soc. II2 (I965) I38.

(I0I) Cox. — Corr. 20. I964. 9.

(I02) Szlarska-Smialowska Z. & Dus B. — Corr. 23(I967) May.

(I03) Aramaki & Fujii — Boskudo Gijutzu I3(I964) 5.

(I04) Foster, Oakes & Kucera — Ind. Eng. Chem. 5I(I959) 825

(I05) Blomgren, Bockris & Jesch — J.Phys. Chem. 65(I96I) 2007.

(I06) Balezin S.A. — J.App. Chem. U.S.S.R. (I960) I094.

(I07) Jensen & Friediger — Chem. Zentr I944. I. 4I6.

(I08) Heathfield & Hunter — J.Chem. Soc. I942.

(I09) I.R.Scholes & J.B.Cotton — Brit. Corr. J. 2(I) I967.I-5

(II0) J.B.Cotton — Corr. Symp. I963.

(III) Cotton J.B. & I.Dugdale — Corr. Sci. 3(2) I963.69.

(II2) Cotton J.B. — I.C.I. Brit. Pat. 933,979.

(II3) Barannik — J.App. Chem. U.S.S.R. (I965) p. 2346.

(II4) Hatch & Hagan — Chem. & Control Inc. June I96I.

(II5) K.H.Wall & I.Davies — J.App. Chem. I965. 385.

(II6) Private Communication — Gas Council Solihull.

(II7) Liddell & Birdeye — Chem. & Control Inc. Dec. I958.

(II8) Schaeffer to Procter & Gamble Ltd. (I952)

(II9) J.G.Kennedy — Anticorrosion April I967.

(I20) S.O. & Eng. Co. Pat. 984,488.

(I2I) Geigy Co. Ltd. Pat. 994,409.

(I22) Germ. Pat. I,I82,503.

(I23) Piontelli Z.Elektrochem. I955.59. 778

(I24) N.Ibl Study of Diffusion Layer. C.I.T.C.E. I955.

(I25) Murakawa, Nagaura & Hackerman. Corr. Sci. Feb. I967.

(I26) G.Soltz Ph.D. Thesis M/C. I965.

(I27) M.Stern & A.L.Geary J.Electrochem.Soc.I04,56(I957)

(I28) J.C.Reeve Current Corr. Res.Scan.I964.

(I29) Prall & Shreir Trans. Inst. Met. Fin.I964.

(I30) Norman Absorption,Distallaion,& Distallation Towers.

(I3I) J.A.Richardson. Unpublished Work.

(I32) Nikuradse Ing.Archiv.I3,377(I868).